INTEGRATED SOLAR ELECTROKINETIC REMEDIATION OF SOIL CONTAMINATED WITH COPPER

By

Ikrema Abdalla Hassan

Master of Science in Engineering in Environmental Engineering (MSc Eng)

This thesis is submitted in partial fulfillment of the requirements for the degree of

Master of Science in Engineering in Environmental Engineering (MSc Eng)

Faculty of Graduate Studies

Lakehead University

Thunder Bay, Ontario

November 2011

ABSTRACT

Electrokinetic remediation is an emerging in-situ technology for cleaning contaminated soil. The contaminants are mobilized by passing a low-level direct current between a row of positively charged electrodes (anode) and negatively charged electrodes (cathode). Due to the low electric current required by the technology, solar power can be an excellent option for providing the electric field. Along with the environmental benefits of solar power, solar cells can provide electricity in remote sites with no access to power lines. The electrolysis reactions in electrokinetic process generate an acid front at the anode and a base front near the cathode. The acid front travels by electroosmosis and electromigration towards the cathode, while the base front moves by electromigration to the anode. The base front reacts with the cations in the soil pore fluid causing premature precipitation of the cations as heavy metal hydroxides at a distance from the cathode equal 0.3 to 0.5 times the distance between the electrodes.

In this study, a three phase experimental program was performed using solar power to investigate electrokinetic remediation of soil contaminated with copper. In phase one, the effectiveness of electric field by solar cells in electrokinetic remediation was studied. The results showed that solar cells can generate electric field sufficient for electrokinetic remediation of the soil and the optimum voltage gradient was identified. In phase two, the effect of soil heterogeneity in electrokinetic remediation was explored. The results show that the general trends of the water content, pH, and copper removal after the remediation of heterogeneous soils are comparable to that of a homogeneous soil. However, the copper removal from most of the soil specimen was higher in the homogeneous soil. Phase three included tests comparing effectiveness of a novel electrode configuration, Two Anodes Technique (TAT), to combat the advancement of the base front and enhance the removal of copper from the soil with the effectiveness of innovative and conventional electrode configurations. Moreover, TAT configuration was optimized for electric current and location of secondary anode. The results showed that TAT was effective in hindering the movement of the base front and the copper removal was superior to that with innovative and conventional electrode configurations tests. The optimum TAT configuration and subsequently the highest copper removal, was in tests with current intermittence and the secondary anodes placed

closer to the cathode. In the optimum test, 80-92% of initial concentration was removed from 75% of the soil.

KEYWORDS: Electrokinetic remediation, electroosmosis, electromigration, electrolysis reactions, homogeneous and heterogeneous soils, solar cells, Two Anode Technique

ACKNOWLEDGMENTS

Firstly, I would like to thank the almighty Allah, my Lord and God, for His spiritual strength and guidance.

Then, I would like to express my sincere gratitude and appreciation to my helpful supervisor, Dr. Eltayeb Mohamedelhassan. He has overwhelmed me with his constructive ideas, substantial assistance and continuous support through the research program.

My thanks extend to my dear parents for their continuous prayers to Almighty Allah to bless and give me effort to carry on to do my research at best.

I will never forget my elder brother Mohamed who encouraged me and volunteered to bear the burden and beat the time to complete my registration papers and was eager and fully soldiered to render more help.

My esteemed Osaima was my backbone who supported and kept my momentum at high. I owe her my success in this program.

Also I would like to appreciate my colleagues Taylor, Ahmed, and Hassan help. I wish to express my gratitude to Conrad Hagstrom, Jason Servais, and Ain Raitsakas for their assistance.

DEDICATION

This thesis is dedicated to my father Abdalla and my mother Aisha. Also I want to dedicate this thesis to my wife Osaima, my son Abdalla, and my daughter Talia.

TABLE OF CONTENT

LIST OF TABLES

TABLE DESCRIPTION PAGE

CHAPTER TWO

CHAPTER THREE

CHAPTER FIVE

CHAPTER SIX

CHAPTER SEVEN

CHAPTER EIGHT

CHAPTER NINE

LIST OF FIGURES

FIGURE DESCRIPTION PAGE

CHAPTER TWO

CHAPTER THREE

CHAPTER FOUR

CHAPTER FIVE

CHAPTER SIX

CHAPTER SEVEN

CHAPTER EIGHT

FIGURE DESCRIPTION PAGE

FIGURE DESCRIPTION PAGE

FIGURE DESCRIPTION PAGE

CHAPTER ONE

INTRODUCTION

1.0 GENERAL

Improper mine tailings and industrial waste management is a major threat to the environment. Mine tailings usually contain substantial amount of heavy metals, which can cause soil contamination and consequently surface and ground water pollution. The spread of contaminants in the soil and water pose threat to human and animal life, soil fertility, and use of properties. There exist numerous efficient methods and techniques for the removal of contaminants from soil. It is very difficult to nominate a single method suitable for all contaminated sites. The appropriate remediation method depends on the contaminants, soil properties, and in-situ conditions. Electrokinetic remediation possesses an outstanding potential to effectively remove pollutants from soils. The main advantages of electrokinetic remediation treatment over conventional soil treatment methods such as thermal desorption, and soil vapour extraction, are that it is effective in mobilizing heavy metals and it suitable for remediating fine-grained soils with low hydraulic permeability (Vane and Zang, 1997; Page and Page, 2002). Additional advantages include close control over the direction of movement of water/flushing solution and dissolved contaminants, retention of the contaminants within a confined zone with higher adsorption capacity, reduced risk of exposure to personnel, and lower power consumption (West and Stewart, 1995; Page and Page, 2002).

In the last century some researchers including Puri and Anand (1936), Gibbs (1966) and Vadyunina (1968) started to use electrokinetics to remove salt or alkalis from soils. The application of electrokinetic phenomenon in removing heavy metals was started in the early 1980s (Segall et al., 1980). Since then, successful transport of contaminants has been reported in several studies (Acar and Alshawabkeh, 1993; Acar et al., 1994; Alshawabkeh and Acar, 1994; Acar et al., 1995; Acar and Alshawabkeh, 1996; Alshawabkeh et al., 1997; Hansen and Rojo, 2007; Yuan et al., 2009).

As electrokinetic remediation requires direct current (DC), alternating current (AC) from the electrical grid is altered to DC using electric transformers (DC power supply). The transformers capital costs and maintenance expenditures impose additional expenses to the cost of power. In addition to the obvious environmental benefits, solar cells generate DC electric field, which is directly used in the electrokinetics. This is a significant benefit as solar cells can be used in remote sites without active power lines. Over the last decade, the cost of a solar power system is declining and this trend is expected to continue as the price of solar cells is decreasing and the efficiency is increasing.

1.1 OBJECTIVES OF THE STUDY

This research was carried out to enhance the electrokinetic remediation of contaminated soil. The designated objectives are to:

- Investigate the potential use of solar power in electrokinetic remediation of soil.

- Examine the effectiveness of removing heavy metals from heterogeneous soils by electrokinetics.
- Propose, test, and verify a novel electrode configuration to retard the advancement of the base front.

Electrokinetic cells capable of testing under one- and two-dimensional electrode configurations were designed and manufactured for this study. Solar cell panels with maximum output of 41 V and 4.27 A were used as the power source. Copper was the heavy metal selected to artificially contaminate homogeneous and heterogeneous soils in the study.

1.2 THESIS OUTLINE

The thesis contains nine chapters. Chapter two presents the literature review of the principles of electrokinetic remediation. The theoretical models proposed to explain the electrokinetic phenomena are reviewed. Chapter two also discusses the influence of soil physiochemical properties and electric field parameters on electrokinetic remediation. Moreover, chapter two discusses the challenges facing electrokinetic remediation.

Chapter three presents the preliminary experimental work conducted on the soil used for this research. The chapter consists of two parts. Part one presents the results of the geotechnical analysis on the soil, while in part two the results of adsorption and desorption tests are reported and discussed.

Chapter four describes the experimental program undertaken in this research. The chapter discusses the soil preparation procedure, electrode configurations (one- and two-dimensional), and the proposed novel technique to hinder the advancement of the base front and improve the remediation process.

The effects of the applied electric field generated by solar cell panels on electrokinetic remediation are presented in chapter five. The chapter reports and discusses the results of volume of water collected, water content, pH, and copper removal for test carried out with varying applied voltages.

Chapter six discusses the effects of soil heterogeneity on electrokinetics. In this chapter, electrokinetic remediation tests with one- and two-dimensional electrode configurations were conducted for three heterogeneous soils and a homogeneous clay. The chapter discusses the results of the applied voltage, accumulated volume of water, water content, pH, and copper removal.

The results of electrokinetic remediation with a novel electrode configuration are presented in chapter seven. In this chapter, three electrode configurations are investigated including Conventional Anode-Cathode (CAC), Stepwise Moving Anode (SMA), and the novel Two Anodes Technique (TAT). The results of applied voltage, electric current, water content, pH, and copper removal are presented and discussed.

Chapter eight presents the tests carried out to optimize TAT for electric current and secondary anode location. The results for electrical current, pH, and copper removal are reported and discussed. Moreover, possible differential setups for Two Anodes Technique are investigated.

Chapter nine includes summary, conclusions and recommendations for future research.

CHAPTER TWO

LITERATURE REVIEW

2.0 INTRODUCTION

Electrokinetic remediation is an emerging innovative in-situ technology for remediating contaminated soil. It is implemented by applying a low–level direct current (DC) through the contaminated soil via pair(s) of electrodes placed horizontally or vertically at the ends of the soil (see Figure 2.1). Due to the applied DC electric field, one of the electrodes becomes positively charged (anode) and the other negatively charged (cathode). The electric field results in electrolysis reactions at the electrodes. As a result, oxidation of water occurs at the anode and reduction takes place at the cathode. The oxidation reactions at the anode produce hydrogen ions (H^+), which create acidic environment suitable for dissolving various heavy metals adsorbed in the soil matrix. The reduction reactions at the cathode generate hydroxyl ions (OH^-) and consequently create an alkaline medium in the vicinity of the cathode.

The primary objective of the electric field in an electrokinetic treatment process is to incite contaminant transport mechanisms. Namely; electroosmosis, electromigration, and electrophoreses. Electroosmosis and electromigration along with the electrolysis reactions are the components of electrokinetic remediation. Electrophoresis is only important in soil slurries and has negligible impact in compacted soil. The degree of success of an electrokinetic remediation process is a function of the characteristics and interaction of the individual

components of the technology as well as the physiochemical and geotechnical properties of the contaminated soil and the type and concentration of the contaminant.

In this chapter, the components of electrokinetics are defined and the associated chemical and physical properties interactions of the soil and soil pore fluid system are reviewed to point out the effects and contributions of these elements in an electrokinetic process. In section 2.1 electroosmosis flow is reviewed. Electromigration is presented in section 2.2. Electrolysis reactions are discussed in section 2.3. Section 2.4 discusses the soil properties and electrokinetics. The influence of the applied-electric-field parameters is presented in section 2.5. The effects of pH in electrokinetic remediation processes are reviewed in section 2.6. The solar energy is discussed in section 2.7 and section 2.8 contains the conclusions.

2.1 ELECTROOSMOSIS FLOW

Electroosmosis flow is defined as the movement of water in soil pores from positively charged electrode (anode) towards negatively charged electrode (cathode) that results from an applied electric field gradient (see Figure 2.2). In the following paragraph, a historical review of this phenomenon is presented. In the subsequent sections the well-known theories that are used to define and measure electroosmosis flow will be discussed including Helmholtz-Smoluchowski and Schmid models. Also, Gray-Mitchell approach for electroosmosis flow efficiency is reviewed.

The first attempt to study electroosmosis phenomenon was by Reuss in 1809. In his experiment, Reuss applied electrical potential across a soil sample and due to the voltage difference water was pumped from the anode side to the cathode side (Yeung, 1994). Between 1852-1856, Wiedemann performed some experiments and stated that the water flow depends on the magnitude of the applied electric field and not on the capillary dimensions. In 1861 Quincke performed experiments to study the electroosmosis flow phenomena (Yeung, 1994). He was the first to suggest the existence of layer of opposite charges at the interface between the soil and liquid (the theory of double layer). The clay particles are negatively charged due to the isomorphous substitution and the presence of the broken bonds (Mitchell and Soga, 2005). Thus, according to the theory of double layer, the cations must be tightly held to the negatively charged particles (see Figure 2.3) so as to neutralize the electronegativity in the clay. The extra cations, not needed for the neutralization of clay, should go into the solution (Mitchell and Soga, 2005). Therefore, Quincke concluded that electroosmosis flow direction depends on the polarity of charges in the liquid and not on the direction of the electric current. At that time in the history, many researchers started to develop theories to explain the electroosmosis phenomenon and equations to estimate the electroosmosis flow rate.

2.1.1 Helmholtz-Smoluchowski model

Based on the concept of the electrical double layer, Helmholtz developed a mathematical model to describe electroosmosis phenomenon. The model was refined by Smoluchowski in 1914 (Mitchell and Soga, 2005). In the model, a liquid-filled capillary is treated as an electrical condenser with ions of one sign near to or on the wall surface and mobile ions of opposite sign

in the liquid accumulated in a layer at a very small distance from the wall surface (see Figure 2.4). Therefore, for negatively charged surface (e.g. clay soil), the cations will accumulate on the soil surface and the excess cations will form the mobile phase in the liquid. Under an applied electric field, the cations travel towards the oppositely charged electrode (cathode). As a result, the cations drag the liquid through the capillary from the anode to the cathode. The flow rate of the liquid is governed by the balance between the applied electric field moving the liquid and the frictional force between the liquid and the wall. This theory is suitable for clayey soils with large pores. The following equations illustrate the mathematical model. The velocity gradient, vg (1/s), between the wall and the center of the positive charge is given by (Mitchell and Soga, 2005)

$$vg = \frac{v}{\delta} \qquad [2.1]$$

where;

v (m/s) is the velocity of the flow, and δ (m) is the distance from the solid surface to the center of the mobile charge.

Therefore, the drag force, F_d (N/m), per unit area is given by:

$$F_d = \frac{\eta v}{\delta} \qquad [2.2]$$

where;

η (N·s/m^2) is the dynamic viscosity of the liquid.

The electrical force, F_e, per unit area is given by:

$$F_e = -\sigma \frac{\Delta V}{\Delta L} = \sigma E \qquad [2.3]$$

where;

σ (C/m^2) is the surface charge density, C is coulomb, ΔV (V) is the voltage, ΔL (m) is the distance between the electrodes, and E (V/m) is the electric field intensity $=-\frac{\Delta V}{\Delta L}$

The negative sign in Eq. [2.3] is used to indicate that the electrical forces on the cations act in the direction of decreasing electrical gradient. At equilibrium, the drag force equals the electrical field force (Eq. [2.2] equals Eq. [2.3]). Thus;

$$\eta \frac{\nu}{\delta} = \sigma E \qquad [2.4]$$

rearrangement of Eq. [2.4] yields

$$\nu = \frac{\sigma \delta}{\eta} E \qquad [2.5]$$

The zeta potential, ζ (V), the electrical potential at the junction between the fixed and mobile part of the double layer, is opposite to the sign of the mobile ions in the soil pores fluid and is given by:

$$\zeta = -\frac{\sigma \delta}{\varepsilon} \qquad [2.6]$$

where;

ε(F/m) is the permittivity (a measure of the ease with which molecules can be polarized and oriented) of the pore fluid (Page and Page, 2002).

The substitution of the mathematical expression of ζ from Eq. [2.6] into Eq. [2.5] yields:

$$v = -\frac{\zeta \varepsilon}{\eta} E \qquad [2.7]$$

The flow rate, q_a (m^3/s), in a capillary of a radius r (m) and area, a (m^2), $a = \pi r^2$ is given by

$$q_a = v \cdot a = v \pi r^2 \qquad [2.8]$$

By substitution of v from Eq. [2.7] in Eq. [2.8]

$$q_a = v \cdot a = \frac{\zeta \varepsilon}{\eta} E \pi r^2 \qquad [2.9]$$

For a bundle of N capillaries of radius r (m), the general form of Eq. [2.9] should include the area of all capillaries, $N\pi r^2$, within the entire cross-section area, A (m^2), normal to the flow. For a porous medium with porosity, n, the cross-sectional area of the voids is $nA = N\pi r^2$. Therefore, the total electroosmosis flow rate, q_A (m^3/s), is given by:

$$q_A = \frac{\zeta \varepsilon}{\eta} E (N \pi r^2) = \frac{\zeta \varepsilon}{\eta} E (n A) \qquad [2.10]$$

To calculate the electroosmosis flow, Casagrande (1949) developed an empirical formula, similar to Darcy's law of hydraulic flow rate

$$q_A = k_e E A \qquad [2.11]$$

where;

k_e(m^2/sV) is coefficient of electroosmosis permeability.

By comparing the Helmholtz-Smoluchowski model (Eq.[2.10]) and the empirical relationship (Eq.[2.11]) the coefficient of electroosmosis permeability, k_e, given by Helmholtz-Smoluchowski model is;

$$k_e = -\frac{\zeta \varepsilon n}{\eta} \qquad [2.12]$$

Helmholtz-Smoluchowski model does not account for the counterions in the pores and assumes that the free ions and the liquid travel with the same velocity. Some researchers found the results by the Helmholtz-Smoluchowski model in agreement with the experimental results for soils with pore diameter greater than 0.1 μm (i.e. D_{10} > 0.5 μm) and dilute electrolyte solution (Mitchell and Soga, 2005).

2.1.2 Schmid model

This theory accounts for the existence of counterions in the pores which was not accommodated by the Helmholtz-Smoluchowski model. To account for the counterions, Schmid (1950, 1951) assumed uniform distribution of counterions in the bulk fluid (see Figure 2.5). To develop a new formula for calculation of the volumetric flow rate, q_a (m^3/s), in a capillary of a radius r (m), Schmid used Hagen-Poiseuille equation (see Eq.[2.13]) and replaced the hydraulic pressure gradient, $\frac{\Delta P}{\Delta L}$ (N/m^3), by hydraulic force, F_h (N/m), per unit length. Since the electrical force is the driving force for the electroosmosis flow and not the hydraulic force Schmid substituted the hydraulic force per unit length, F_h (N/m), by the electric force, F_e (N/m), per unit length. The steps to drive Schmid equation are:

$$q_a = \frac{\pi r^4}{8\eta}(-\frac{\Delta P}{\Delta L}) \quad [2.13]$$

η is the dynamic viscosity of the liquid in (Ns/m^2).

The hydraulic force, F_h (N/m), per unit length causing the flow is given by

$$F_h = \pi r^2(-\frac{\Delta P}{\Delta L}) \quad [2.14]$$

By substituting Eq.[2.14] into Eq.[2.13]

$$q_a = \frac{r^2}{8\eta}F_h \quad [2.15]$$

The electrical force, F_e (N/m), per unit length is given by the following equation

$$F_e = A_o F \pi r^2(-\frac{\Delta V}{\Delta L}) \quad [2.16]$$

where;

A_o (equivalent/m^3) is concentration of surface charges in ionic equivalents per unit volume of pore fluid, ΔV (V) is the voltage, ΔL (m) is the distance between the electrodes, and F (96485 C/equivalent) is the Faraday's constant.

By substituting F_e (N/m) from Eq.[2.16] for F_h (N/m) in Eq.[2.16]

$$q_a = \frac{\pi r^4}{8\eta}A_o F(-\frac{\Delta V}{\Delta L}) \quad [2.17]$$

For a cross-sectional area, A, perpendicular to the flow with a bundle of N capillaries, and porosity n, the cross-sectional area of the voids is $nA = N\pi r^2$. Therefore, the total volumetric flow rate, q_A (m^3/s), is given by:

$$q_A = \frac{A_o F r^2 n}{8\eta}(-\frac{\Delta V}{\Delta L})A \qquad [2.18]$$

From Eq. [2.18], k_e, coefficient of electroosmosis permeability, can be calculated using the following equation

$$k_e = \frac{A_o F r^2 n}{8\eta} \qquad [2.19]$$

As indicated by Eq. [2.18], the volume of flow rate is sensitive to pore size and proportional to the power of porosity of the medium as A_o is always a function of porosity.

2.1.4 Gray-Mitchell approach

Gray and Mitchell (1967) reported that the efficiency of electroosmosis flow depends on the transported amount of water per unit electrical charge passing through the soil. Soil type, water content, ionic concentration, and cations and anions distribution in the soil pores affect the amount of transported water. Gray and Mitchell (1967) developed a rational approach to evaluate the influence of these factors on the efficiency of electroosmosis. This approach was developed on the basis of Donnan's theory of membrane equilibria. As shown in Figure 2.3, cations are attracted by the negative charge on the surface of the clay particles, while anions are accumulated in the bulk solution. Donnan's theory suggests that at equilibrium the chemical

potentials of the internal and external phases are equal and electroneutrality is maintained in both phases (Yeung, 1994).

Gray and Mitchell (1967) introduced a distribution coefficient, R_D, defined as the ratio of cations to anions in the internal phase for a symmetrical electrolyte. R_D is given by

$$R_D = \frac{C^+}{C^-} = \frac{1+\sqrt{1+y^2}}{-1+\sqrt{1+y^2}} \qquad [2.20]$$

and

$$y = \frac{2C_o\gamma\pm}{A_o\,\bar{\gamma}\pm} \qquad [2.21]$$

where;

C_o (equivalent/m^3) is the concentration in external solution, $\gamma\pm$ is the mean molar activity coefficient in external solution, $\bar{\gamma}\pm$ is the mean molar activity coefficient in double layer, and

A_o (equivalent/m^3) is concentration of surface charges in ionic equivalents per unit volume of pore fluid. A_o is proportional to the cation exchange capacity of the soil by the expression (Gray and Mitchell, 1967):

$$A_o = \frac{(CEC)\rho_W}{w}\times 100 \qquad [2.22]$$

where;

CEC (equivalent/kg soil) is the exchange capacity of the soil, w (%) is the water content of the soil, and ρ_W (1000 kg/m^3) is the density of water.

All other factors being equal, the higher the distribution coefficient, R_D, the greater the electroosmosis water transport (Mitchell and Soga, 2005). Higher R_D values indicate higher exclusion of co-ions. In such case, electroosmosis flow is less affected by an increase in the pore water chemistry. Figure 2.6 shows that soils with low cation exchange capacities (e.g. kaolinite clay) exhibit a very high electroosmosis water transport per charge when they are saturated by dilute electrolyte solutions while the transport rate significantly decreases at concentrated electrolyte solutions. This may be due to high water-counterion ratio in the internal phase. On the other hand, soils with high cation exchange capacities such as illitic and bentonitic soils exhibit very low electroosmosis water transport due to low water-counterion ratio in the internal phase, but this flow is relatively un-affected by the increase of salinity in the pore water because of good co-ion exclusion (Yeung, 1994).

2.2 ELECTROMIGRATION

The application of an electric field in electrokinetic remediation processes exploits ions transport through electromigration phenomenon. Electromigration, also known as ionic migration, is the movement of ions towards the oppositely charged electrodes (Koryta, 1982). The movement of the ionic species in the aqueous pore solution depends on the electromigration together with other effects including diffusion, adsorption, and complexation

and precipitation reactions (Probstein et al., 1994; Page and Page, 2002). One of the practical applications of electromigration in our daily life is the use of electrolytic cell in metal plating process. The rate of ionic movement towards the oppositely charged electrode in soil pore fluid is quantified by the effective ion mobility, u_j (m^2/ s·V), which is defined as the velocity of the ion in the soil under influence of a unit electric field gradient and can be evaluated by (Koryta, 1982):

$$u_j = \frac{D_j z_j F}{RT} \tau n \qquad [2.23]$$

where;

D_j (m^2/s) is the diffusion coefficient of ion species j in dilute solution, z, is the valence of ion species j, F (96487 C/mol) is the Faraday's constant, R (8.314 J/mol·K) is the universal gas constant, T (K) is the absolute temperature, τ is the tortuosity factor, and n is the porosity of the soil.

Various factors contribute to the efficiency of ion migration in an electrokinetic process. The electromigration of a certain ion depends on the conductivity of the soil, porosity, pH, applied electric field, concentration of the given ion, and presence of competitive ions (Reddy and Cameselle, 2009). The existing cations (positive charge) and anions (negative charge) adsorbed by the soil or dissolved in the pore fluid will be under the influence of the generated electric field. Therefore, the cations and anions in the system move towards the oppositely charged electrode. Depending on the buffering capacity (the amount of protons or hydroxide ions the

soil can absorb without a significant change in its pH), the advancement of the acid medium generated by electrolysis reactions at the anode through the soil can lower the pH of the system and consequently help the disassociation of heavy metals from the soil. Heavy metals in the soil can be bound to ion exchange sites forming complexes such as hydroxide, carbonate or sulfate. Also the heavy metals can react with the humic and fulvic materials in the soil to form complexes with the organic ligands. The hydrogen (H^+) ions react with heavy metal precipitated in the soil as follows:

$$2M(OH)_2(s) + 4H^+ \rightarrow 2M^{2+} + 4H_2O \qquad [2.24]$$

where;

M is the heavy metal.

The cations, M^{2+}, resulted from this reaction move by ion migration, as discussed above, towards the cathode. Thus, the dissolved cations can be effectively removed by the combined actions of electroosmosis and electromigration (Karim and Khan, 2001).

Acar and Alshawabkeh (1993) introduce λ_e (the ratio of ionic mobility of a species to electroosmosis coefficient of permeability of a soil) as transport number which provides a sense of the mass flux of species by ionic migration under electric field with respect to electroosmosis. Acar et al. (1992) had demonstrated the efficient removal of cadmium even when there is no electroosmosis flow, validating the hypothesis that electromigration is as significant a species transport mechanism in electrokinetic remediation as electroosmosis. Figure 2.7 shows that at maximum values of k_e, the mass flux by electroosmosis is approximately equal to the mass flux

by electromigration for most ionic species. However, at lower K_e values, Figure 2.7 shows the flux by electromigration to be one to three orders of magnitude higher than the flux by electroosmosis (Acar and Alshawabkeh, 1993; Acar et al., 1995).

2.3 ELECTROLYSIS REACTIONS

Electrolysis reactions occur at the electrodes in an electrokinetic process and result in oxidation-reduction reactions. Oxidation takes place at the anode, which generates hydrogen ions (H^+) and liberates oxygen gas. On the other hand, reduction occurs at the cathode produces hydroxyl ions (OH^-) and disperses hydrogen gas.

Oxidation reaction at the anode:

$$2H_2O - 4e^- \rightarrow O_2 \uparrow + 4H^+ \qquad [2.25]$$

Reduction reaction at the cathode:

$$2H_2O + 2e^- \rightarrow H_2 \uparrow + 2OH^- \qquad [2.26]$$

These reactions play a very important role in the outcome of an electrokinetic remediation process. Most of the heavy metals tend to desorb from soil at low pH values (see Eq. [2.24]). Therefore, the acidic environment near the anode can cause dissolution of heavy metals from the contaminated soil. On the other hand, the propagated alkaline front (OH^-) results in the precipitation of various heavy metals hydroxides in the soil. The alkaline medium is also effective in desorbing anions and certain organic molecules.

2.4 SOIL PROPERTIES

The soil matrix at the contaminated site has a significant influence on the electrokinetic remediation technology. For instance, the presence of large objects such as cobblestones and boulders in the contaminated soil may affect the field application of the technology. The soil composition can also retard the electrokinetic remediation success. For example, conductive materials, metal objects, resistive materials, and concrete debris can disrupt the current during an electrokinetic process. Electrokinetic remediation technology is suitable for soils with high surface charge and low hydraulic permeability (Gary and Olsen, 1986). Nevertheless, the technology can be used alone to treat sandy/silty soils or in conjunction with other remediation techniques. The efficiency of the treatment process however is affected by many contributors including; cation exchange capacity, porosity, pH, moisture content, and pore fluid chemistry.

In the following section 2.4.1 soil physicochemical properties are reviewed. Section 2.4.2 discusses clay mineralogy. The soil cation exchange capacity is reviewed in section 2.4.3. Section 2.4.4 illustrates zeta potential effect in electrokinetic remediation processes. Section 2.4.5 reviews the effect of soil pH. Soil electrical conductivity is discussed in section 2.4.6.

2.4.1 Physicochemical properties of soil

It has been reported that the physicochemical properties of soil have great potential in altering the efficiency of the remediation process due to changes in pH caused by the oxidation and reduction reactions at the electrodes. The essential components of soil are inorganic minerals, organic matters, water and dissolved salts, and air in the soil pores. The inorganic minerals

widely occur in the soil are oxygen, silicon, and aluminum. Organic matters are generally made up of carbon, oxygen, and hydrogen. The soil adsorption, transformation, and desorption to contaminants are largely dependent on the electrochemical properties of the major soil constituents; such as aluminosilicates, oxides, and organic matter (Evangelou, 1998). Therefore, the success of the electrokinetic remediation process is a function of the properties of the soil composition. The adsorption and desorption are directly related to the pH of the soil, which can be controlled during an electrokinetic processes by the addition of the chemical compounds.

2.4.2 Clay mineralogy

The conventional term clay generally refers to either all soil particles with size less than 2 μm or clay minerals with specific characteristics; such as small particle size, high surface area to mass ratio, net negative electrical charge, plasticity when mixed with water, and high weathering resistance. The common clay minerals in the soils of engineering interests are kaolinite, illite, and montmorillonite (Mitchell and Soga, 2005). The structure of clays is formed in layers composed of sheets of silica tetarhedra cross-linked, by sharing oxygen atoms, with sheets of alumina octahedra. Some types of intersheet and interlayer bonding in the clay minerals are:

1- Van der Waals forces (weak bond)

2- Hydrogen bonding (strong bond)

3- Cations between the layers needed for electrical neutrality (strong bond)

The tetrahedral sheets and octahedral sheets in the clay soils can be found linked together at different ratios 1:1 (e.g. kaolinite), 2:1 (e.g. illite), and 2:1:1 (e.g. chlorite) (Evangelou, 1998). Replacement of silicon by aluminum or the replacement of aluminum by divalent cation such as

magnesium can be observed in most of the clay soils. This substitution is known as isomorphous substitution which causes permanent surface charge to occur on the clay minerals. For instance, the surface charge can be negative when an aluminum atom is substituted for a silicon atom during the formation of lattice (American Water Works, 1990). The clay soil has very small pore size and long tortuous path and subsequently low hydraulic permeability. Thus, it is extremely difficult to perform in-situ remediation for contaminated clay soil using the traditional remediation methods such as soil flushing. The transport of fluids by electrokinetics is largely independent on the size of the pores and therefore electrokinetic remediation has the capacity to remediate contaminated clay soils.

2.4.3 Cation exchange capacity (CEC)

Under certain environmental conditions the clay soil adsorbs cations to balance the negative charge. If these conditions are altered, a replacement (exchange reactions) to the adsorbed ions may occur. These exchange reactions are normally accompanied by important changes in physical and physicochemical properties of the soil. The sources of soil exchange capacity include isomorphous substitution, broken bonds, and replacement (Mitchell and Soga, 2005). The isomorphous substitution is the major source of clay exchange capacity, except for kaolin minerals. The broken bonds provide exchange sites along the clay particle edges mainly on kaolinite soil. The replacement occurs when the hydrogen of an exposed hydroxyl is replaced by another type of cation. The contributions of these sources in the total amount of soil exchange capacity depend on different environmental and compositional factors. As a result, there is no

single value for clay soil exchange capacity but a range of exchange capacity for each clay type. Table 2.1 shows the range of cation exchange capacity (CEC) for common clay minerals.

Soils which have high CECs, e.g. illitic and bentonitic clays, adsorb considerable amount of contaminants and are more difficult to decontaminate compared with soils that have low CECs such as kaolin(Page and Page, 2002). The removal rate of contaminant cations from soil with high CEC with conventional methods such as soil flushing is very limited due to the strong bond between the contaminant and the soil. On the contrary, electrokinetic remediation is more effective with such soil.

2.4.4 Zeta potential

Zeta potential, ζ, is defined as the electrical potential at the junction between the fixed and mobile parts of the electrical double layer (West and Stewart, 1995) (see Figure 2.8). As per Helmholtz-Smoluchowski model (Eq. [2.6]), ζ sign coincides with the charge sign on the soil particle surfaces. It has been observed that the magnitude and the sign of ζ are dependent on the pH and ionic strength of the pore fluid. The alkaline environment at the cathode in the electrokinetic remediation processes results in high ζ values near the cathode. The observed high flow rate near the cathode is attributed to the high ζ (Eykholt and Daniel, 1994). On the other hand, the acidic medium near the anode results in low or even positive ζ. Consequently, the low flow rate near the anode is explained by the existence of low ζ. In agreement with the

Helmholtz-Smoluchowski model, it has been observed that the electroosmosis flow increases at high negative values of ζ and decreases or cease at low negative or positive values of ζ.

From the theory of the double layer, the increase in ionic strength decreases the thickness of the electrical double layer. The decrease in the double layer thickness results in reduction of the dragging force, which is responsible for moving the bulk solution in electroosmosis flow (see Figure 2.4 (a)). This may explain the observed low values of ζ when the ionic strength of the pore solution increases. Also, a number of investigators have observed that adsorption of cationic species under neutral to alkaline conditions can causes ζ reversal (James and Healy, 1972). As the concentration of hydrolysable metal ions increases, ζ become less negative at all pH values, but the effect is largest with pH values slightly above pH at which precipitation of metal hydroxide would be expected to occur in the bulk solution (Hunter and James, 1992). Under acidic conditions the effect of hydrolysable metal ions is smaller and insufficient to cause ζ reversal (West and Stewart, 1995).

2.4.5 Soil pH

In electrokinetic remediation processes, the pH of the soil is crucial in desorption and adsorption of contaminants. At high pH values charged metal ions (M^+ of charge n) have tendency to react with hydroxyl and precipitate as metal hydroxide as follow:

$$M^{n+} + n(OH)^- \rightarrow M(OH)_n \downarrow \qquad [2.27]$$

The mineral solubility can be predicted using the solubility product constant K^0_{so}, which is equal to the product of the activities of the chemical species in solution. Figure 2.9 shows the activity of metal-hydroxides is directly influenced by the pH value of the solution. Thus, the basic medium at the vicinity of the cathode promotes the precipitation of heavy metals. The premature precipitation near the cathode is the major drawback of electrokinetic remediation processes. An extensive review of the proposed solution to this problem is presented in this chapter. The high pH values may result in the formation of heavy metals negative complexation, which migrate towards the zone of acid-base junction and eventually precipitating in this zone as insoluble hydroxides (Acar and Alshawabkeh, 1993; Probstein and Hicks, 1993).

A low pH results in dissolution of the contaminants from the soil, which favor the contaminant removal, but it also decreases the zeta potential and consequently reduces or in some cases reverses the electroosmosis flow (Shapiro and Probstein, 1993; West and Stewart, 1995; Yang and Lin, 1998). The optimum pH value for efficient remediation should be as low as possible to maintain the solubility of the metal contaminants and as high as required to keep the zeta potential negative (Virkutyte et al., 2002). The previous combination, negative zeta potential and dissolved metal requirements, is the greatest challenge hindering the effectiveness of electrokinetic remediation.

2.4.6 Soil electrical conductivity

The soil conductivity is a material property that mainly depends on the water content, soil type, and pore fluid chemistry. The bulk soil electrical conductivity, λ (S/m), is composed of the

electrical conductivity of the soil solids and the electrical conductivity of the pore fluid. In general, the electrical conductivity of the soil solids is much lower than that of the pore fluid. Thus, in the electrokinetic process the bulk electrical conductivity in general decreases as the fluid drained by the electroosmosis flow. Electrical conductivity can be measured in-situ or in the laboratory by testing undisturbed samples using American Society of Testing and Materials Standards procedure G57-95a (ASTM, 2001). The bulk soil electrical conductivity plays dominant role in the determination of the efficiency of the electroosmosis flow. The efficiency of the electroosmosis flow is determined by measuring the volume of water removed from the soil per unit electrical charge through the soil (m^3/C). For soil with high electrical conductivity the resistance to the current is low, which results in a high current and consequently a high energy consumption. Thus, the efficiency of electroosmosis process decreases as the electrical conductivity increases.

2.5 ELECTRIC FIELD PARAMETERS

The effectiveness of an electrokinetic remediation process is influenced by electrical field parameters including electrode materials, current intermittence, and applied electric field. Section 2.5.1 discusses the electrode materials effect. The current intermittence is presented in section 2.5.2. The applied electric field is reviewed in section 2.5.3.

2.5.1 Electrode materials

Various electrode materials are used in electrokinetic applications. Two main factors should be taken into consideration when selecting the material for an electrokinetic remediation process.

First, the electrode material should be properly selected to avoid or minimize the adverse reactions by-products of the material with the hydrogen and hydroxyl ions propagated at the electrodes. Second, the material should be selected to minimize the voltage loss at the soil-electrode interfaces. Often, it is very difficult to achieve both. For example, the use of non-metallic electrodes will not produce unwanted by-products compared with metallic electrodes. However, the voltage loss at the soil-electrode interface is higher with non-metallic electrodes as reported by previous researchers (e.g. Lockhart, 1983; Mohamedelhassan and Shang, 2001).

For kaolinite (the subject of this research), Segall and Bruell (1992) performed a study to compare iron and graphite electrodes on the basis of generated electroosmosis flow rate, pH of effluent and pore fluid, and the power consumption. The results showed that the flow rate for the iron electrode was twice that of the graphite electrode for the same power consumption. The pH throughout the soil tested with graphite electrodes was lower than that tested with iron electrodes.

2.5.2 Current intermittence

Current intermittence is the use of on and off cycles for the applied electric field during an electrokinetic application. It can improve the electrokinetic remediation process by altering the polarization process of the ions of opposite signs in the double layer. In the diffuse double layer, the stationary clay particles (negatively charged) are surrounded by the mobile cations (positively charged). The applied DC electric field results in redistribution of charges (polarization) in the double layer, which is against the applied electric field. As a result, the

polarization decreases the efficiency of electrokinetic remediation by reducing the electroosmosis flow. The intermittence allows the double layer to restore its original charge distribution and thereby increase the efficiency of the electroosmosis process (Mohamedelhassan and shange, 2001). Many researchers had reported a significant increase in electroosmosis flow rate by intermittent current (e.g. Sprute and Kelsh, 1976; Yankovskii et al., 1989; Mohammedelhassan and Shang, 2001), while few studies showed that current intermittence has no influence on the flow rate (Lockhart and Hart, 1988).

2.5.3 Applied electric field

The applied electric field in electrokinetic remediation processes affects both the electroosmosis flow and electromigration. The stronger the electric field, the higher the electroosmosis flow and electromigration as per Eq. [2.11] and [2.23] and subsequently high removal rate of the contaminant. However, the rate of increase is not linear and the efficiency of the removal reaches a plateau at higher electric field as noted by previous researchers (Lockhart, 1983; Shang, 1997). Furthermore, at high electric field, significant energy is lost in heating which is not beneficial to the process.

Shang et al. (1996) performed a series of tests to investigate the effect of voltage gradient in electroosmosis consolidation. The coefficient of electroosmosis permeability, an indicator for the rate of consolidation, was evaluated for each voltage gradient. It was concluded that the coefficient of electroosmosis permeability was decreased as the voltage gradient increased.

Mohamedelhassan and Shang (2001) studied the effect of applied voltage on the magnitude of the voltage drop at the soil-electrode interfaces. The test was conducted for a range of applied voltage and the voltage loss at the soil-electrode interfaces was measured. To quantify the voltage drop, an efficiency factor, β, is introduced as:

$$\beta(\%) = \frac{V_e}{V_o} \times 100 = \frac{V_o - (\Delta V_a + \Delta V_c)}{V_o} \times 100 \qquad [2.28]$$

where;

V_e(V) is effective voltage, V_o (V) is the applied voltage, ΔV_a (V) is the voltage loss at soil-anode interface, and ΔV_c (V) is the voltage loss at soil-cathode interface.

They suggest that due to voltage loss at the soil-electrode interfaces, the electric field that contributes to electroosmosis and electromigration is the effective electric field intensity, E_e (V/m), defined as:

$$E_e = \frac{\beta E_o}{100} \qquad [2.29]$$

where;

E_o (V/m) is the applied electric field intensity.

2.6 MITIGATING THE pH EFFECTS IN ELECTROKINETIC REMEDIATION

The removal of heavy metals from contaminated soil by electrokinetic remediation is affected by the following factors: (1) contaminant concentration, (2) mobility of contaminant ions, (3)

soil type and structure, (4) soil chemistry, and (5) electrical conductivity of soil. Although all these factors contribute to the effectiveness of the electrokinetic remediation process, an optimum pH value is the dominant factor for the success of the process. The pH of the pore fluid controls desorption of the heavy metals from the soil particles to pore solution, which is a prerequisite for contaminant removal (Virkutyte et al., 2002; Yuan et al., 2009). In electrokinetic remediation, the acid front (i.e. H^+) is generated at the anode and moves towards the cathode via electroosmosis and electromigration and decreases the pH of the soil along its path. The base front (i.e. OH^-) is produced at the cathode and travels towards the anode by electromigration. The base front increases the pH of the soil as it travels. The created alkaline environment is suitable for formation and consequent precipitation of metal hydroxides (see Eq. [2.27]) and consequently decreasing the effectiveness of electrokinetic remediation. The acid front and the base front meet approximately at 0.3 to 0.5 the distance between the electrodes from the cathode (see Figure 2.10). The distance travelled by the acid front is larger than the distance traveled by the base front because the hydrogen ions are smaller than the hydroxyl ions. Furthermore, while electroosmosis and electromigration contribute to the movement of the H^+ ions, OH^- ions are transported by electromigration alone. As the acid and base fronts meet, they form water. The dissolved cations that are transported through the pore fluid precipitate as a result of the change in the soil chemistry at the junction of acid and base fronts.

The high pH environment produced by the base front is the major hindrance for electrokinetic remediation applications (Pazos et al., 2006). To overcome this limitation, researches have

previously implemented conventional and innovative solutions. The conventional methods include the use of ion selective membrane (Hansen et al., 1997), enhancement by addition of chemical conditioning agents such as ethylenediaminetetraacetic (EDTA) (Reed et al., 1995; Wong et al., 1997), Acetic acid (Acar and Alshawabkeh, 1993), and Nitric acid (Denisov et al., 1996). Innovative techniques on the other hand including stepwise moving anode (Chen et al.2005) and polarity exchange (Pazos et al., 2006) were implemented in recent years to control the negative impact of the alkaline medium. The conventional methods are discussed in section 2.6.1. The innovative techniques for improving electrokinetic treatment are presented in section 2.6.2.

2.6.1 Conventional methods

2.6.1.1 Enhancement fluids

The negative impact of the base front can be controlled by the addition of acids in the vicinity of the cathode to lower the pH of the basic environment. Both organic (e.g. acetic acid) and inorganic (e.g. hydrochloric acid) acids can be used. It is safe to use acetic acid for the enhancement of electrokinetic processes because it does not fully dissociate and most of its salts are soluble (Virkutyte et al., 2002). In contrast, the hydrochloric acid can increase soil as well as ground water contamination (e.g. formation of chlorine gas). To enhance electrokinetic remediation efficacy, it is recommended to use calcium hydroxide at the anode and low concentration hydrochloric acid at the cathode. The use of improper enhancement fluids may result in production of secondary contaminant(s) in the subsurface, propagation of waste products due to electrochemical reactions, and making the existing contaminant impacts more

troublesome. Several techniques have been proposed to deal with basic solution formed in the vicinity of the cathode, such as:

- The implementation of selective membranes to control the ions stream movement into and out of the soil (Ottosen et al., 2003).
- Addition of reagent, such as complexing agents, which improves the metal solubility forming stable complexes in a wide range of pH (Reed et al., 1995; Yang and Lin, 1998).
- Control pH in the cathode chamber so as to avoid the formation of an alkaline solution (Puppala et al., 1997; Li and Li, 2000).

A Group of researchers suggest the use of conductive solution, which simulates the ground water condition, between the cathode and the soil under treatment (Li et al., 1997; Li et al., 1998; Li and Li, 2000). The conducted laboratory experiments showed the required horizontal length of the conductive solution must be double the length of contaminated soil and the solution should be confined in a container. In field applications, this approach is costly and impractical. The alternative, the selective membrane, was introduced to address these problems. In this approach, the membrane is immersed in the conductive solution in front of the cathode. From an experimental works, it was found that the use of selective membrane had significantly reduced the length of the conductive solution. However, the reduction in the volume of conductive solution results in high pH and leakage of anions through the membrane.

A different attempt to control the pH was tried by Saichek and Reddy (2005). In their laboratory tests they used surfactant flushing solution (5% Igepal CA-720) to remediate sand soil, clay soil and heterogonous soils containing clay and sand. The surfactant flushing solution under the hydraulic flow alone was found to be effective in cleaning the sand soil, whereas for the clay electroosmosis flow was required to successfully remove the pollutants. It was found that along with the electroosmosis flow, control of solution pH was required to enhance the removal of the contaminants from homogeneous and heterogamous soils containing clay.

The enhancement to electrokinetic remediation by adding acids has drawn the attention of many researchers. For instance, Giannis and Gidarakos (2005) conducted two sets of laboratory tests to evaluate the combination of electrokinetic remediation and soil washing technology in order to remove cadmium from contaminated soil. In the first set of test, the soil was saturated with water, while acetic, hydrochloric, and EDTA acids were used as purging solutions. In the second set of tests, the citric, nitric and acetic acids were used for soil saturation as well as purging solutions. In the first test, the removed cadmium from soil was < 24% of the initial amount. When acids were used for soil washing, in the second set of tests, 85%, 70%, 25% of the initial cadmium was removed by citric, nitric, and acetic acids, respectively. Thus, it was concluded that citric and nitric acids are suitable for removing metals bound to soils.

As in the previous discussion, chemicals can be added to overcome the premature precipitation problem. Instead of using external chemicals, electrokinetics can be used to generate acidic medium which is then pumped through the contaminated soil in order to decrease the soil pH

and consequently dissolve the cations (Karim and Khan, 2001). The effluent from the soil can be passed through sorptive/desorptive ion-exchange heavy metal selective membranes to capture the cations. This method can be effective in soils with high permeability, such as sandy/silty soils. The technique by Karin and Khan (2001) eliminates the base front without the need to induce external chemicals. Moreover, the heavy metal cations are not precipitated inside the soil under treatment; rather they are recovered in the ion exchange medium outside the contaminated soil.

The main disadvantages of the addition of chemical compounds are discussed in the following points:

- First, the addition of acids (e.g. HNO_3) may cause excessive acidification for the soil and as a consequent the soil may become infertile.
- Second, the formation of by-products which may exacerbate the contamination problem, such as the formation of chlorine gas when HCL is used.
- Third, the chemical compounds may form strong complexes with variety of metals in soil and no longer be available for the removal of the contaminants (e.g. EDTA).
- Fourth, the use of inappropriate enhancement fluid may aggravate the existing contamination problem (Virkutyte et al., 2002; Giannis and Gidarakos, 2005).

2.6.2 INNOVATIVE TECHNIQUES

2.6.2.1 Stepwise Moving Anode

Chen et al. (2006) suggested Stepwise Moving Anode (SMA) approach to enhance the electrokinetic remediation process of soil contaminated with heavy metals. The concept used in this approach is to move the anode towards the cathode in steps. The step length and the treatment duration depend on the soil type and the contaminant and can be determined in the laboratory prior to the field application. Because the electrolysis reactions cause low pH in the vicinity of the anode, the anode advancement towards the cathode develops low pH environment through most of the soil and thereby promotes the disassociation of heavy metals from soil. The dissolved ions are then transported by electroosmosis and electromigration towards the cathode. Therefore, SMA can be successful in enhancing an electrokinetic remediation of soil contaminated with heavy metals.

In a laboratory test, Chen et al. (2006) investigated the effectiveness of SMA in the remediation of soil contaminated with cadmium. The results showed that SMA was effective in enhancing cadmium desorption from the soil and the dissolved cadmium was effectively transported towards the cathode by electromigration and electroosmosis flow. Chen et al. (2006) used cation-exchange membrane to prevent the advancement of the base front (see Figure 2.11). The use of the membrane; however, increases the total cost of the process. Thus, the existence of the membrane may affect the method efficiency (Chen et al., 2006). On the other hand, relocating the anode involves high risk of electrode damage each time the anode is pulled out or pushed into the soil. This also will be reflected on the overall cost of the process.

2.6.2.2 Polarity exchange technique

The polarity exchange technique was suggested to avoid the negative effect of OH^- on metal transportation. In this technique, the chemical species are directed to one side or the other by reversing the polarity of the electrodes. In a laboratory test, Pazos et al. (2006) implemented this technique to remove manganese (Mn) from clay soil. The results showed that significant amount of Mn was removed from the soil to the cathode chamber. The technique succeeded in neutralizing the base front without the addition of chemicals, complexing agents, or selective membrane. It relies mainly on the preciseness of pH measurement during the treatment and the current intensity. The major concern over the polarity exchange technique is the possibility of the heavy metals movement towards the initial anode when the polarity is reversed.

2.7 Solar energy

Electrokinetic remediation technique is aimed to remove inorganic and organic pollutants such as heavy metals and hydrocarbons from contaminated low permeability soils using DC electric field (Virkutyte et al., 2002). According to Page and Page (2002), the low current is used in electrokinetic remediation processes for the workers safety and to avoid adverse heating effects. The energy consumption is a major contributor to the total cost of the electrokinetic remediation. High energy consumption increases the overall expenditure of the remediation process and may become a major issue restricting the field applications of this technology. Very few projects have been conducted to resolve the high energy cost that can be associated with electrokinetic remediation (e.g. Yuan et al., 2009).

In the last decade solar energy has gained the attention of scientists and the general public, leading to a multitude of beneficial applications. Although, a solar cell can be an excellent candidate for power supply in electrokinetic remediation, very few researchers attempted to investigate its use. The use of solar cells as a source of power can cut the electricity transmission expenses and eliminate power losses in the transmission lines. Furthermore, the power produced by solar cell is environmentally friendly and can be used in sites located in remote areas without active power lines. Also, solar panel produces DC electric field that is usable in electrokinetic applications without alteration (i.e. without DC transformer). The expected reduction in solar cell prices as the technology continues to improve can significantly reduce the initial cost of a solar power system.

The power generated by solar cell panel depends on the duration of the day and the weather conditions. This can cause fluctuation in the power supply during the day and intervals of zero voltage at night. As discussed before, current intermittence can be beneficial to the outcome of an electrokinetic process (Mohamedelhassan and Shang, 2001; Hansen and Rojo, 2007). Thus, electrokinetic remediation with solar cells can improve the process by the intermittent resulting from periods of zero voltage during nights.

Yuan et al. (2009) investigated the use of solar cell in electrokinetic remediation of kaolinite clay contaminated with cadmium. Three set of laboratory experiments were carried out; the first one on a cloudy rainy day, the second one in a sunny day, the third set as a control experiment conducted with DC power supply. It was found that the output potential generated from the

power supply was the highest and for solar cell the potential generated on the sunny day is higher than that on cloudy and rainy days. It was found that although the potentials generated were different, the efficiency of cadmium removal in the tests were comparable. This could be attributed to the fact that the pH profiles and the contaminant removal graphs showed that desorption, caused by low pH, not the electric potential was the dominant factor in cadmium removal. Yuan et al. (2009) reported that in China the cost of electrokinetic remediation with solar cell panel was 40% of that carried by electric power from the grid.

2.8 CONCLUSIONS

In the last decade electrokinetic remediation has gained increasing attention of researchers and scientists. Electrokinetic remediation has the capacity to remove contaminants form soils with low hydraulic permeability, which are difficult to remediate by conventional methods. The predominant soil type used in the previous laboratory investigations was homogeneous clay and the results have shown that electrokinetic remediation can be effective in heavy metal removal from such soils (Hansen et al., 1997; Reddy and Parupudi, 1997; Reddy et al., 1997; Ribeiro and Mexia, 1997; Sah and Che, 1998). In the published literature, very few studies have been conducted to investigate the effect of soil heterogeneity in electrokinetic remediation (e.g. Saichek and Reddy, 2005). The conventional methods such as soil flushing are incapable of removing contaminants from heterogeneous soil because the solution will move through the shortest path, whereas electrokinetics has the capacity to control the direction of flow via electrodes orientation.

In electrokinetic remediation, the recommended voltage gradient generated across the soil under treatment is in the range 20-200 V/m (Probstein and Hicks, 1993). The DC power supply required for electrokinetic remediation is obtained by converting the alternating current (AC) to DC by using electric transformers. The need for the DC transformers increases the overhead cost of the electrokinetic. In addition, the relatively longer remediation time required for electrokinetic treatment raises the issue of the energy expenditure in the possible field application of this technology. Therefore, low energy cost is essential for cost-effective electrokinetic remediation process. The solar cells generate DC electric field which can be used in electrokinetic remediation without the need for electric transformers. Despite the high capital cost, the running cost of solar system is low compared with the maintenance cost required for the electric devices and electric grid. The power generated from solar cell is a promising technology and can be integrated with electrokinetic remediation. In a recent study, Yuan et al. (2009) successfully implemented the power generated form solar cell as an alternative source of power for electrokinetic remediation.

Numerous previous investigations in electrokinetic remediation were conducted to improve and enhance the effectiveness of the technology. Compactness of the negative effect of the base front was the center focus for majority of the researches. Considerable amount of effort and time was directed to control the advancement of the base front. Many conventional enhancement approaches have been implemented including controlling pH of cathode and anode compartments (Saichek and Reddy, 2003), introducing ionic exchange membrane (Li et al., 1998), and electrode solution circulation (Lee and Yang, 2000). On the other hand,

innovative enhancement techniques have been implemented including Stepwise Moving Anode (Chen et al., 2006), and polarity exchange technique (Pazos et al., 2006). The conventional enhancement techniques involve the addition of chemical compounds which increase the overall cost of the process and may cause new contamination problems. Despite to the encouraging results achieved by implementation of innovative enhancement techniques, the cost of the remediation can be high due to the extra field work involved. Therefore, further work is needed in order to incorporate the effectiveness of the enhancement methodology with the overall cost.

Table 2.1 Cation exchange capacity for common clay minerals (Mitchell and Soga 2005)

Clay mineral	Cation Exchange Capacity (meq /100 g of soil)
Kaolinite	3-15
Montmorillonite	80-150
Illite	10-40

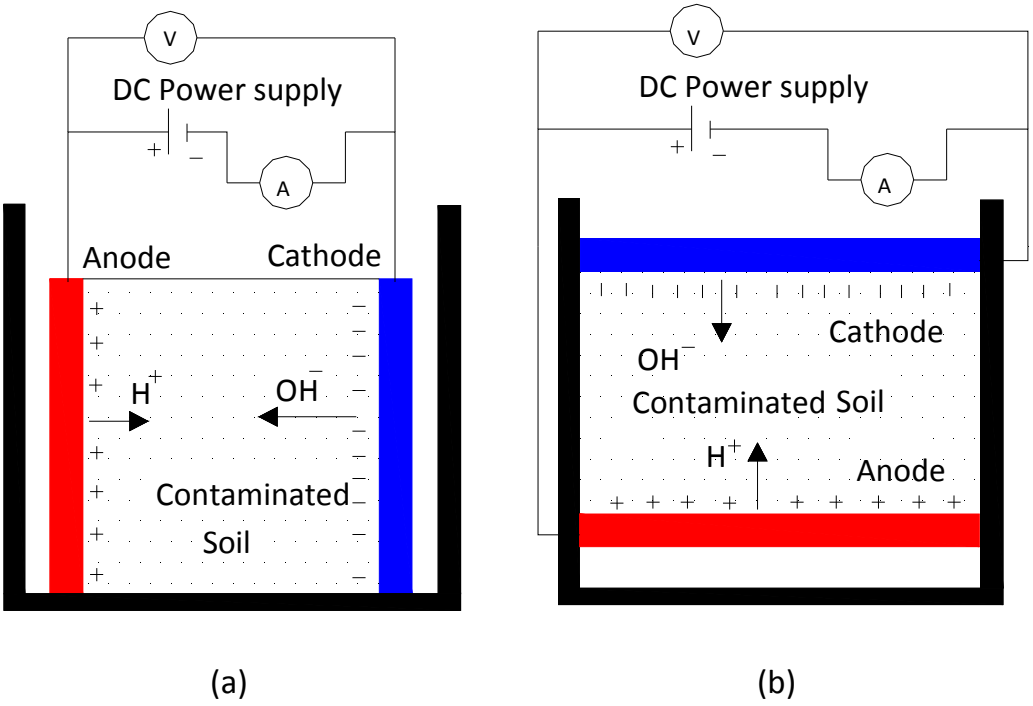

Figure 2.1 Typical electrokinetic remediation configurations; (a) Vertical electrodes orientation (b) Horizontal electrodes orientation.

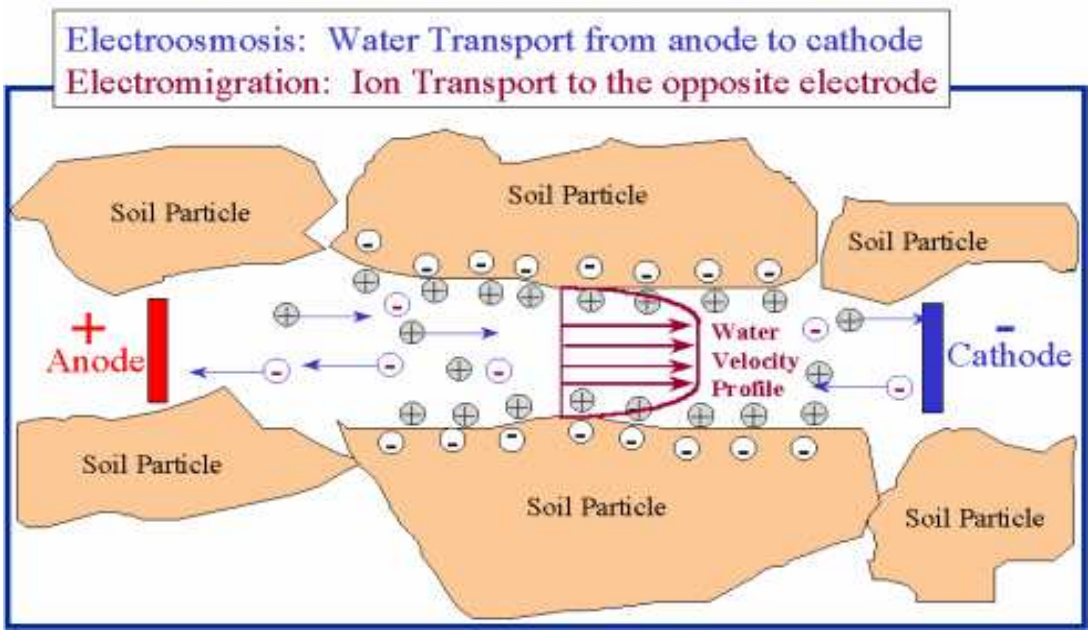

Figure 2.2 Schematic of electroosmosis flow and electromigration.

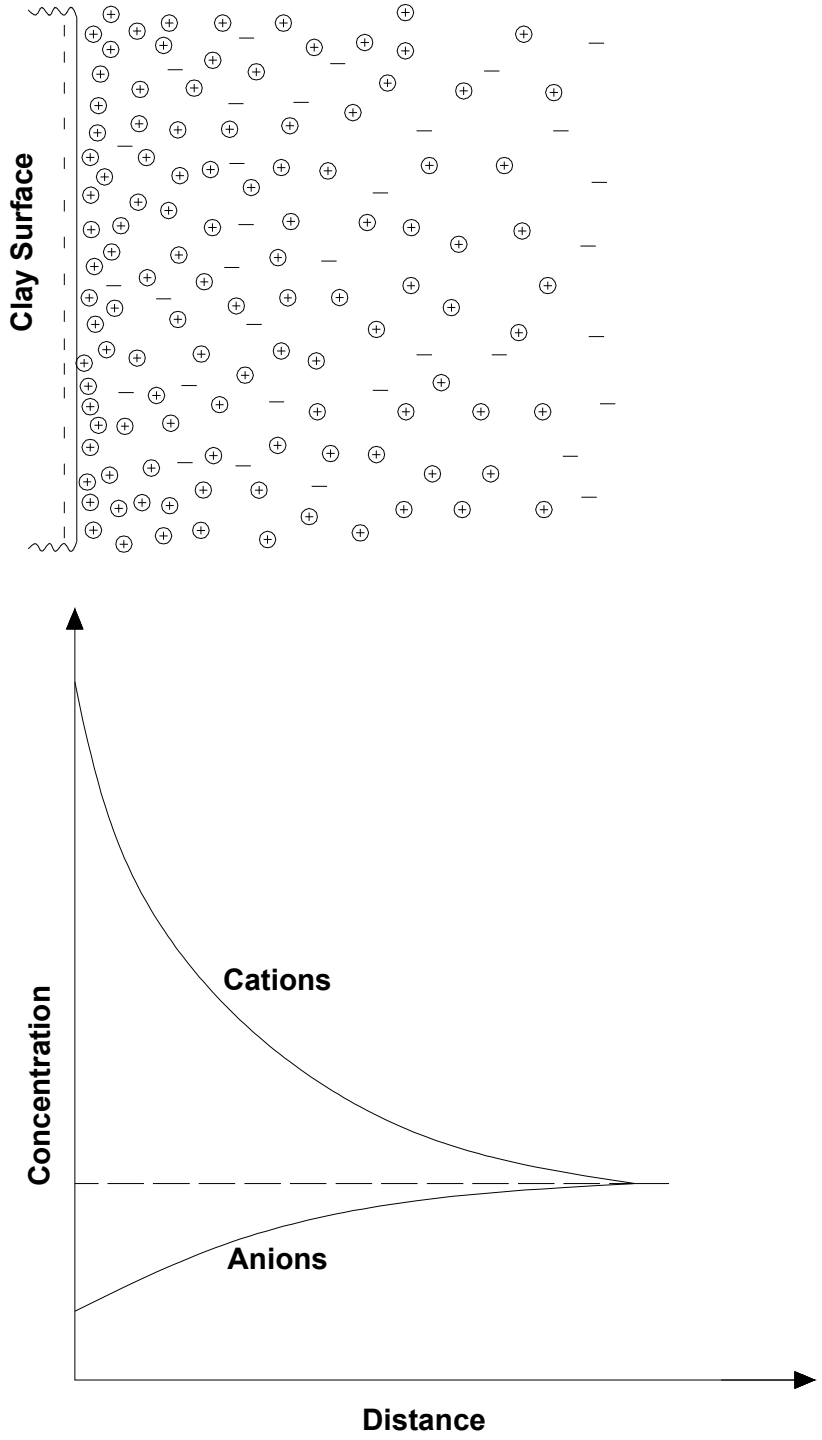

Figure 2.3 Distribution of ions adjacent to a clay surface according to the concept of diffuse double layer (after Mitchell and Soga, 2005).

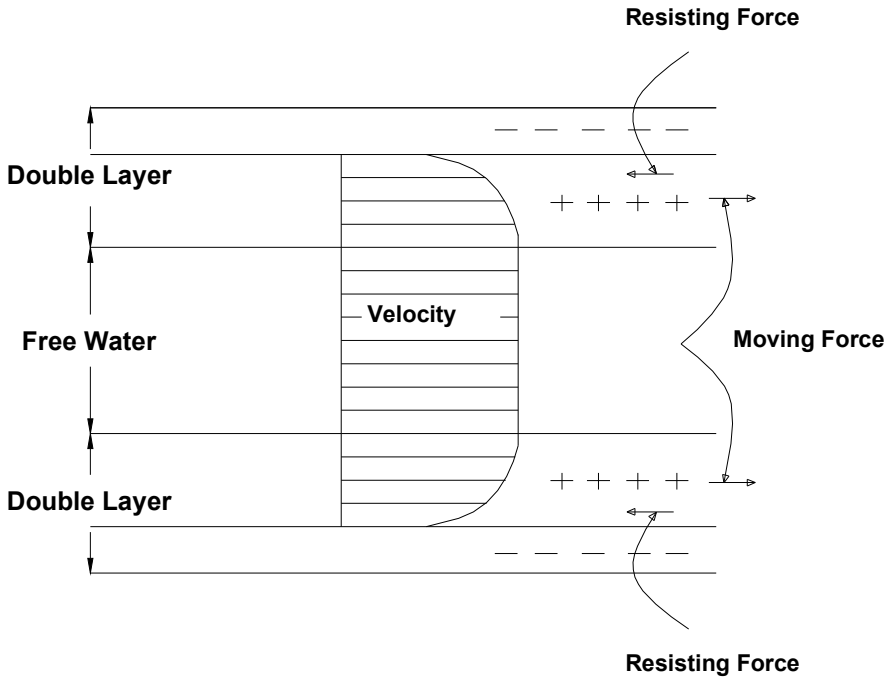

(a) ELECTROOMOSIS FLOW

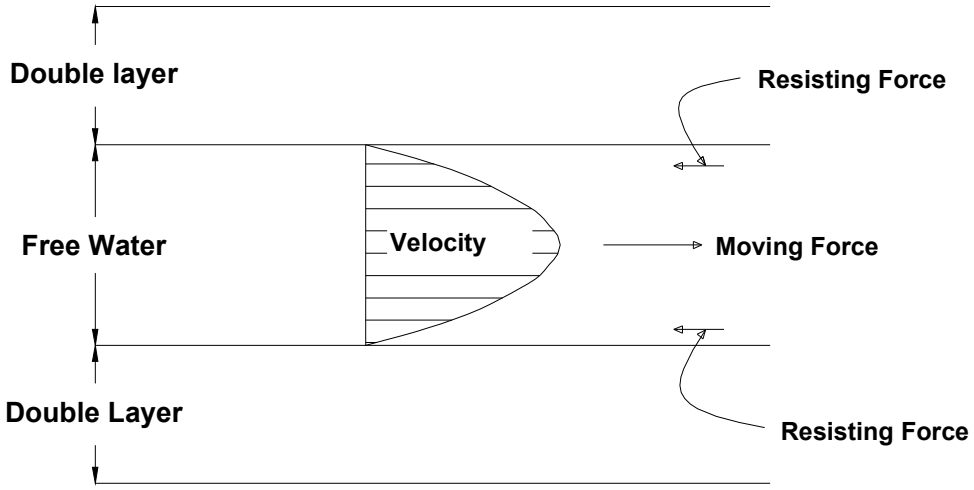

(b)HYDRAULIC FLOW

Figure 2.4 Comparison of electroosmosis flow with hydraulic flow in a capillary; (a) Helmholtz-Smoluchowski model for electroosmosis (b) Hydraulic flow (after Casagrande, 1953).

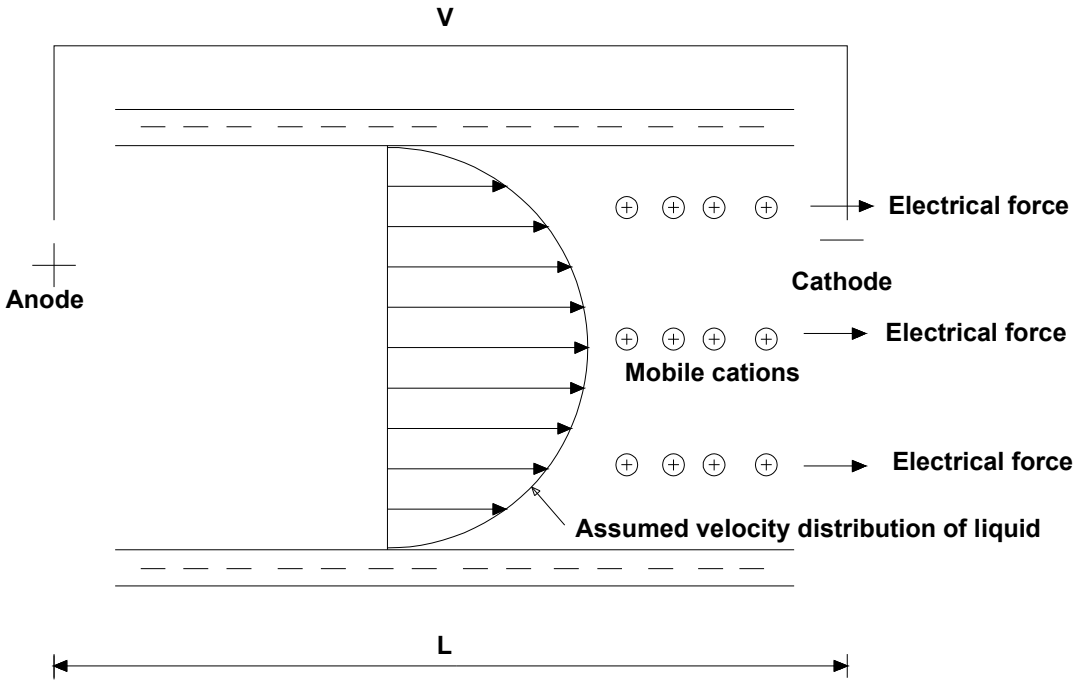

Figure 2.5 Schmid model for electroosmosis (after Yeung, 1994).

Where,

V is the applied voltage between the anode and the cathode.

L is the distance between the anode and cathode.

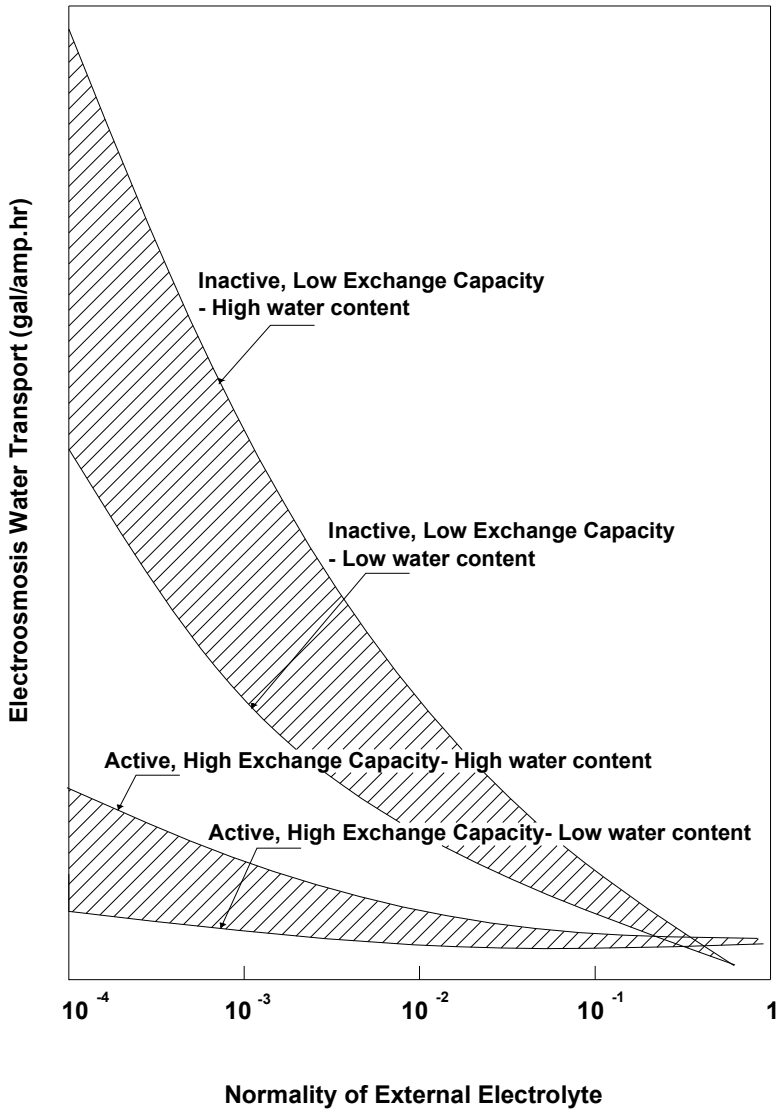

Figure 2.6 Schematic prediction of water transport by electroosmosis in various clays according to the Donnan Concept (after Mitchell and Soga, 2005).

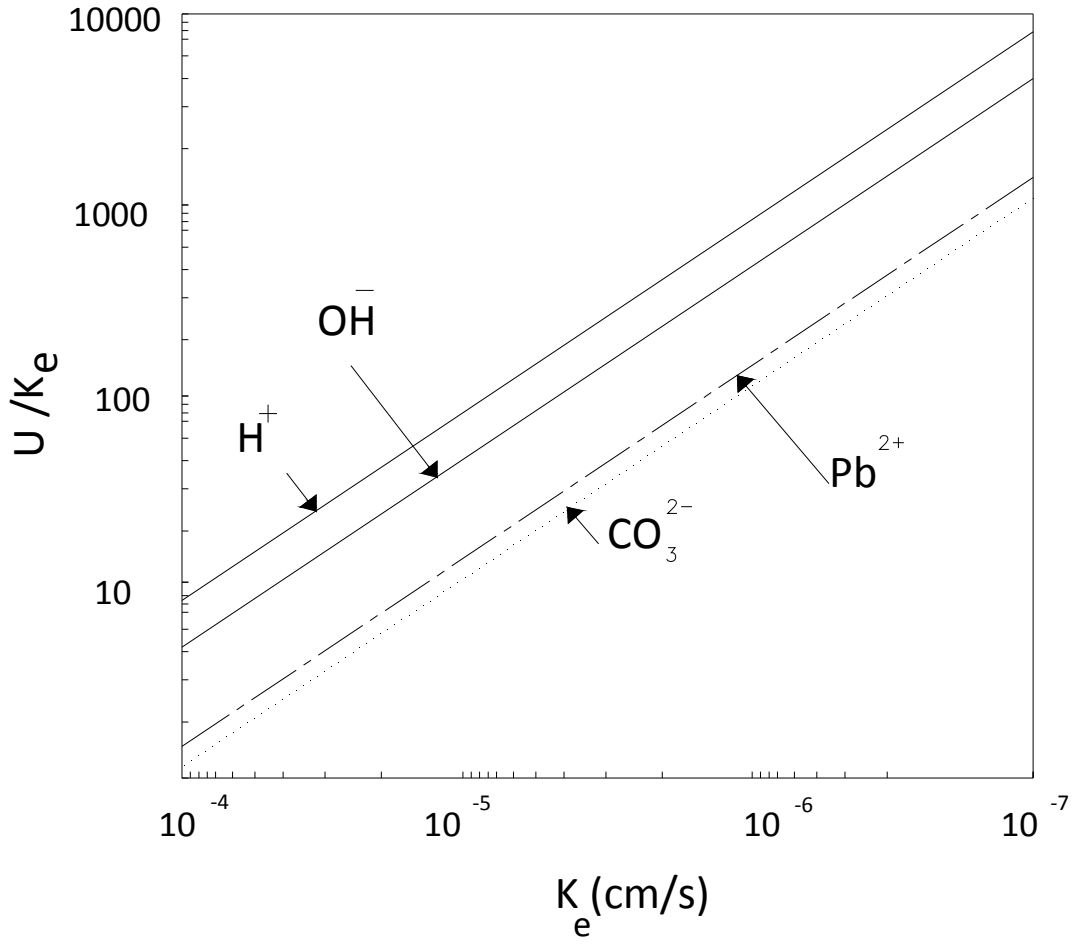

Figure 2.7 The ratio of the effective ionic mobility to coefficient of electroosmosis permeability, u/k_e, vs. the coefficient of electroosmosis permeability, K_e (after Acar et al., 1995).

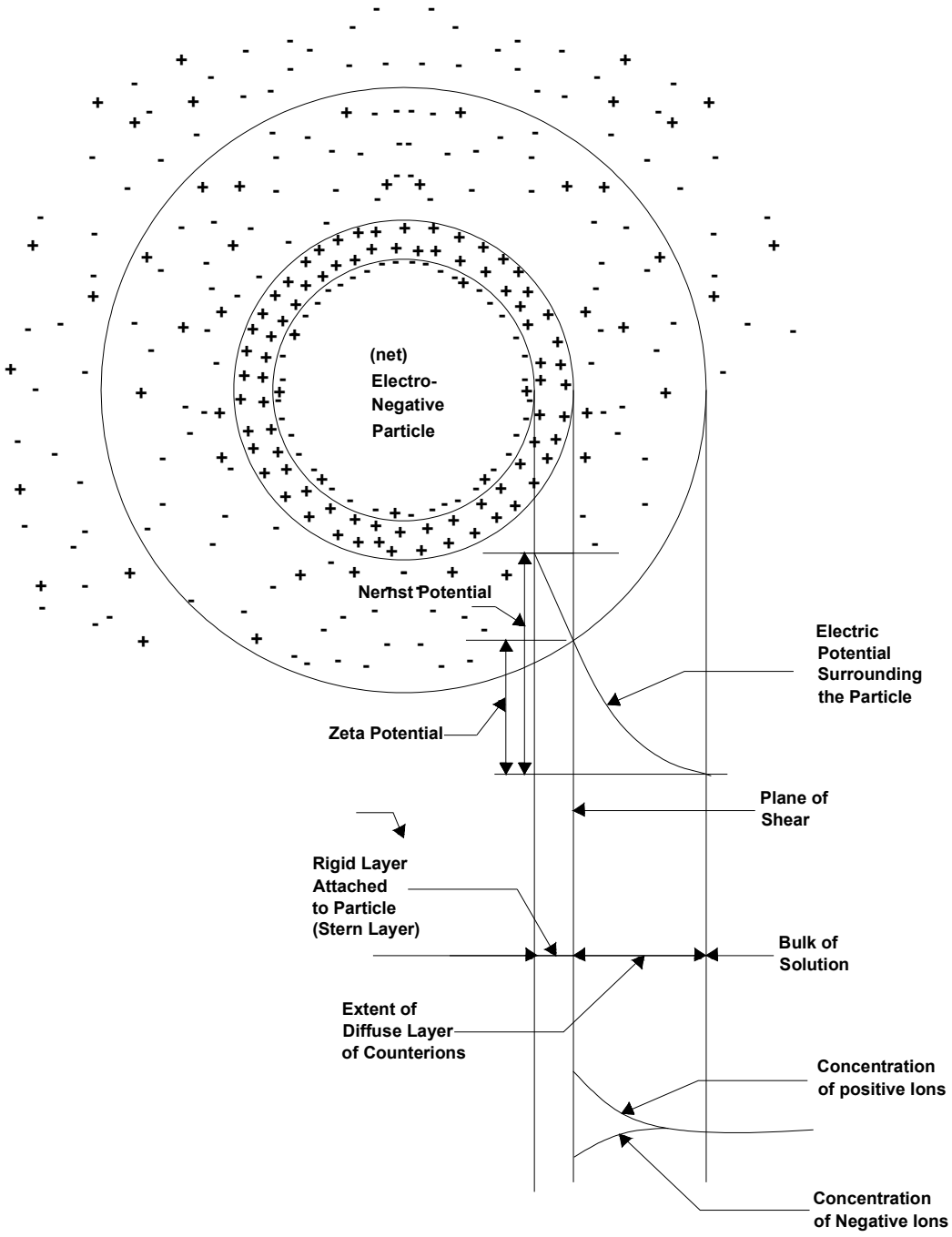

Figure 2.8 Negatively charged particle, the diffuse double layer, and the location of zeta potential (Water Quality and Treatment, 1999).

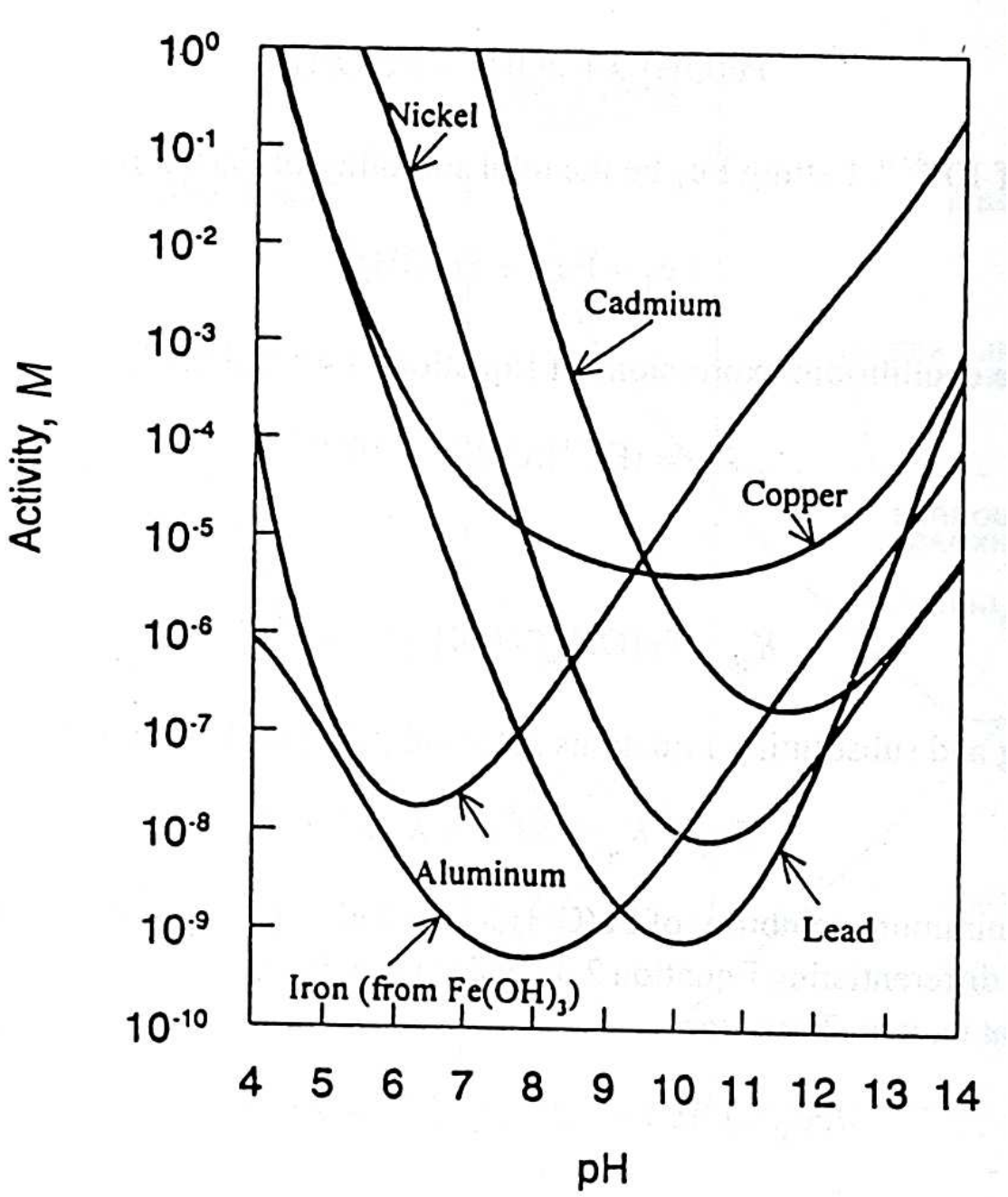

Figure 2.9 Solubility of various metal-hydroxides as a function of pH (after Evengelou, 1998).

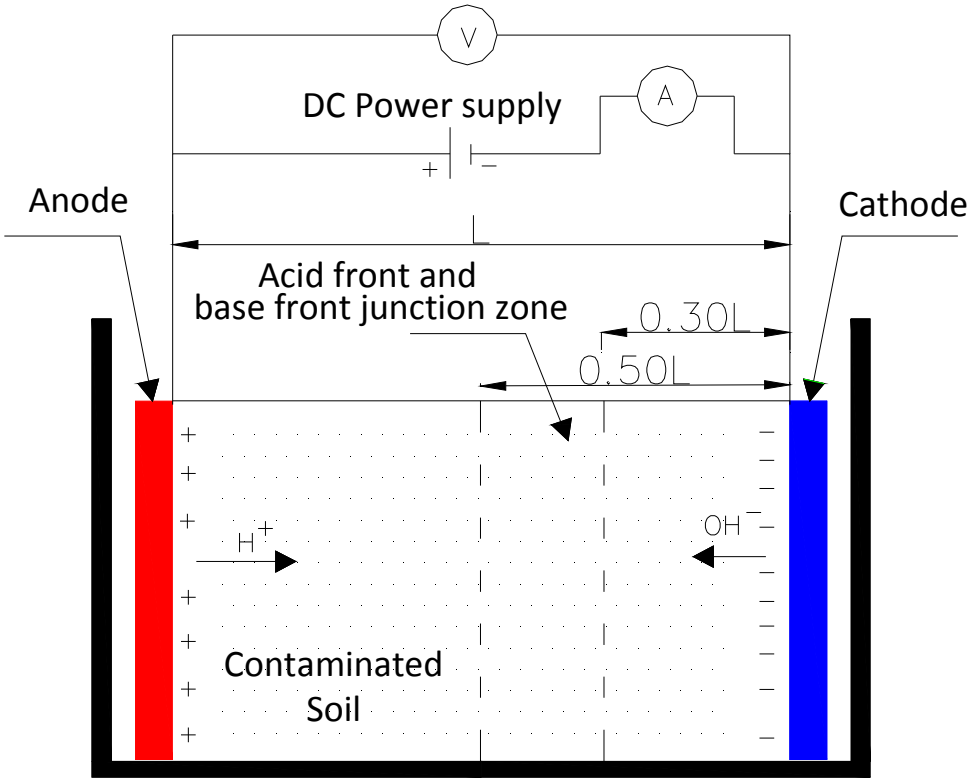

Figure 2.10 Typical acid front and base front junction zone in electrokinetic remediation.

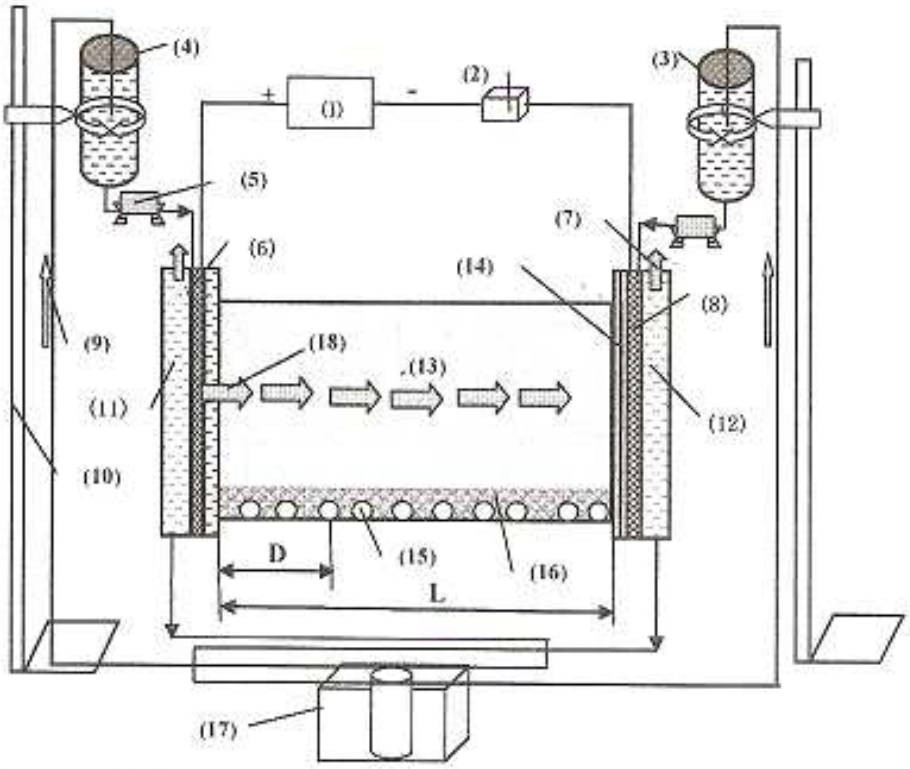

Schematic diagram of the electrokinetic laboratory apparatus. (1) DC power; (2) Multimeter; (3) Cathode reservoir; (4) Anode reservoir; (5) Flux controller; (6) Anode electrode; (7) Air vent; (8) Cathode electrode; (9) Cycling direction; (10) Stand; (11) Anode compartment solution; (12) Cathode compartment solution; (13) Soil; (14) Cation-exchange membrane; (15) Porous pipe; (16) Quartz sand; (17) Peristaltic pump; (18) Anode moving direction. *Note: D-distance from the anode; L-length of the soil bed.

Figure 2.11 Schematic diagram of the electrokinetic laboratory apparatus (Chen et al. 2006).

CHAPTER THREE

MATERIAL PROPERTIES AND CHARACTERIZATION

3.0 INTRODUCTION

Clay and sand were used to prepare the soil specimens used throughout this research. The clay soil was obtained from Plainsman Clay in Medicine Hat, Alberta. The sand was procured from a pile of natural sand in Thunder Bay, Ontario. Geotechnical and mineralogical tests were carried out on the clay soil. Grain size distribution analysis was performed on the sand. The results of the tests are presented in section 3.1. Adsorption and desorption properties of the clay soil are discussed in section 3.2.

3.1 GEOTECHNICAL ANALYSIS

3.1.1 Clay soil

Tests were carried out to determine the chemical and physical properties of the clay soil used in the experiments conducted in this research. The following subsections present the results of the tests carried out in the clay soil including particle-size analysis, Atterberg limits, specific gravity, soil classification, cation exchange capacity, and X-ray diffraction. Most of the tests were carried out in triplicate and the results were consistent. The results are summarized in Table 3.1.

Particle-size analysis: Sieve analysis on the clay soil revealed that all the particle sizes are less than 0.075 mm (passed No. 200 sieve). Therefore hydrometer analysis was conducted to estimate the distribution of soil particle sizes in accordance with the American Society of Testing and Materials Standards procedures D421 and D422 (ASTM, 2007). Figure 3.1 shows the grain size distribution curve for the soil (average of three tests).

Consistency of soil: Atterberg limits tests were performed in accordance with American Society of Testing and Materials Standards procedure D4318 (ASTM, 2005) to determine the liquid and plastic limits of the clay soil. The results were used to classify the soil and select the appropriate water content to prepare the soil specimen. The Atterberg limits results are shown in Table 3.1.

Specific gravity: The specific gravity of the clay soil was determined in accordance with American Society of Testing and Materials Standards procedure D854 (ASTM, 2006).

Soil classification**:** According to the Unified Soil Classification System (USCS), the group symbol of clay soil is CL and the group name is lean clay.

Cation exchange capacity (CEC): The cation exchange capacity for the clay soil used in this study was obtained using effective cation exchange capacity method outlined in the four United

State regional soil test manual. The method is simple and provides a rapid means to estimate the CEC. The result is shown in Table 3.1.

Mineralogical Analysis: X-ray diffraction test was performed on the clay soil. The results, shown in Figure 3.2, concluded that the kaolinite is the dominant clay mineral. The test conducted was the powder pattern diffraction without crushing the soil. This can explain the low percentage of kaolinite reported by the test.

3.1.2 Sand soil characteristics

The sand was obtained from a pile of natural sand of fine to coarse particles. The fraction of the sand particles passing the No. 30 sieve (0.6 mm) and retained on the No. 40 sieve (0.425 mm) was used to prepare the soil specimens. The sand was washed prior to the test using No. 200 sieve (0.075 mm). According to the Unified Soil Classification System the group symbol of the sand is SP. The group name is poorly graded sand. The specific gravity of the sand is 2.70.

3.2 ADSORPTION AND DESORPTION

In the electrokinetic remediation processes, the electrolysis reactions at the anode and the cathode alter the pH of the soil. In these tests, the sorption and desorption of copper by the soil were determined in the pH range typically encountered in an electrokinetic remediation process. Sections 3.2.1 and 3.2.2 present and discuss the results of the adsorption and desorption tests. The procedure followed in the adsorption and desorption tests was in accordance with the previous work by Yuan et al., (2007).

3.2.1 Copper adsorption

The adsorption characteristics of a contaminated soil are crucial for better understanding the effectiveness of electrokinetic remediation. The adsorption capacity of the soil is of great importance to estimate the amount of contaminant in soil solids and that in the soil pore fluid. The adsorbed value is function of the pH. This section presents the experiments conducted to investigate the copper adsorption behavior in the clay soil used in this study. In the following subsections, the procedure followed for the adsorption test is illustrated in detail and the results are presented and discussed.

3.2.1.1 Adsorption test procedure

In these tests the adsorption experiments were conducted in triplicate. A mass of 0.85 g of $NaNO_3$ (molecular weight of 84.99 g/mole) was weighed using a sensitive scale. One liter of deionized water was measured and placed in a graduated cylinder. To obtain one liter of 0.01 M $NaNO_3$ solution, the deionized water in the graduated cylinder was mixed with the 0.85 g of $NaNO_3$. The mixture was thoroughly shaken until a homogeneous solution was obtained. The 0.01 M $NaNO_3$ solution was used as background electrolyte in the adsorption tests. Copper (II) chloride dihydrate, $CuCl_2 \cdot 2H_2O$ (molecular weight of 170.48 g/mole), was used as the source of copper in the tests. Copper solution of concentration 1 g of copper per liter was prepared by mixing 0.268 g of $CuCl_2$ $2H_2O$ and 100 mL of the previously prepared 0.01 M $NaNO_3$ solution in 250 mL Erlenmeyer flask. Six additional solutions with lower copper concentrations (0.5 g/L, 0.25 g/L, 0.1 g/L, 0.05 g/L, 0.02 g/L, and 0.005 g/L) were prepared by successive dilution of the prepared copper solution (1 g/L) using the 0.01 M $NaNO_3$ solution. The concentrations of

copper solution were selected to copper wide range of copper adsorption (60 to 3720 mg of copper per kg of dry soil).

Seven stopper 50 mL Erlenmeyer flasks and seven Centrifuge tubes (50 mL) were used in this experiment. Soil sample of 1 g was weighed into each flask. From each of the prepared copper solution, 14 mL was measured into a Centrifuge tube. Each of the 14 mL copper solutions was added to one of the seven soil samples in the Erlenmeyer flasks. The soil-solution mixtures were equilibrated at room temperature (21 ± 1 C^{o}) for 24 hr in a shaking table at 120 rpm. The pH of the soil-solution suspensions was adjusted to 5.75 ± 0.25 with nitric acid (HNO_3) and/or sodium hydroxide (NaOH). The pH was measured every two to three hours and readjusted when needed. pH-Electrode Sentix 41-3 (WTW-Multi 340i/set) was used to measure the pH. The soil and solutions were then transferred to 20 mL centrifuge tubes. The tubes with the soil and equilibrated suspensions were placed in centrifuge (Clinical 50 centrifuge 82012-800 VWR) and rotated at 4000 rpm for 10 min. After that, 1 mL of the supernatant from each tube was drawn and placed in 20 mL plastic tube. The solution in each tube was diluted by adding 9 mL deionized water. The concentrations of the diluted solutions were determined using the Inductivity Coupled Plasma-Optical Emission Spectroscopy (ICP-OES).

3.2.1.2 Results

Adsorbed copper was calculated as the difference between the amount initially present in the solution and the amount remaining in solution after equilibration. The results were used to determine the parameters for both Langmuir and Freundlich sorption models. The Langmuir

isotherm was found to best represent the data. Langmuir equation is given by (Atanassova and Okazaki, 1997):

$$\frac{C_e}{S} = \frac{1}{K_L M_L} + \frac{C_e}{M_L} \qquad [3.1]$$

where;

C_e (mg/L) is the equilibrium copper concentration in the supernatant, S (mg/g) is the amount of copper adsorbed per g of soil, K_L (L/mg) is the Langmuir constant, and M_L (mg/g) is the Langmuir adsorption maximum (maximum adsorption capacity of the soil).

$$C_e = C_{ave} = \frac{(C_{e1} + C_{e2} + C_{e3})}{3} \qquad [3.2]$$

$$S = \frac{C_e - C_i}{(g \cdot of \cdot soil)} \times (14\ mL) \times (\frac{1L}{1000\ mL}) \qquad [3.3]$$

where;

C_i (mg/L) is the initial copper concentration in solution, C_{ave} (mg/L) is the average equilibrium copper concentration, and C_{e1}, C_{e2}, and C_{e3} (mg/L) are equilibrium copper concentrations obtained after tests 1, 2, and 3.

The initial copper concentration (C_i), average equilibrium copper concentration (C_{ave}), equilibrium copper concentrations obtained after tests (C_{e1},C_{e2},C_{e3}), amount of copper adsorbed per g of soil (S), and the ratio (C_e/S) for the three tests are presented on table 3.2.

Table 3.3 presents Langmuir equation, Langmuir constant (K_L), and the maximum adsorption capacity of the soil (M_L). From the results of the adsorption test, the Langmuir equation for the soil is given by:

$$\frac{C_e}{S} = 19.22 + 0.2508 C_e \qquad [3.4]$$

Figure 3.3 shows that the adsorbed amount of copper increased with the increase of the aqueous equilibrium concentration. The results obtained from this test show similar adsorption behavior to that reported by Yaun et al.(2007) who used kaolin clay.

3.2.2 Copper desorption

Optimum application of electrokinetic remediation of soil contaminated with copper requires a thorough understanding of copper desorption for a range of pHs and concentrations. The pH is known to be a dominant factor on the adsorption/desorption behavior of heavy metals on soils (Yuan et al., 2007). In electrokinetic remediation, electrolysis reactions change the soil pH. Two sets of tests were conducted to investigate copper desorption behavior from the soil under various conditions. In the first set, the effects of initial copper concentration on desorption was studied under similar pH. The second set investigated the effects of different pH values on desorption of copper from soil samples with equal initial copper concentration. The selected pH values cover the range encountered in an electrokinetic process. Section 3.2.2.1 discusses the effects of concentration in adsorption. The effect of pH is presented in section 3.2.2.2.

3.2.2.1 Effects of concentration

In this experiment, desorption tests were conducted using soil samples containing different amount of adsorbed copper per g of dry soil. The amount of copper desorbed in each test was obtained and compared with the initial amount of copper adsorbed into the soil sample. The following subsections discuss the test procedure and the results.

3.2.2.1.1 Test procedure

After decanting the solutions from the centrifuge tubes in the adsorption tests as discussed in section 3.2.1.1, the soil samples were used for desorption tests. For each soil sample (1 g of soil), 14 mL of 0.01 M $NaNO_3$ solution was added and then the soil and the solution were equilibrated for 24 hr in a shaking table (120 rpm) at room temperature (21 ± 1 C^o). The pH of the soil-solution suspensions was adjusted to 5.75 ± 0.25 with nitric acid (HNO_3) and/or sodium hydroxide (NaOH). The pH was measured and readjusted every two to three hours. After 24 hr, the tubes with the soil and the solution mixture were centrifuged at 4000 rpm for 10 min. From each tube, 1 mL from the supernatant was drawn and poured in a 20 mL plastic tube. The solution in the tube was diluted by adding 9 mL deionized water. The concentrations of copper in the diluted solutions were then determined using ICP-OES.

3.2.2.1.2 Results

The amount of copper desorbed per g of soil was calculated as follows:

$$D_{ave} = \frac{\left(D_{c1} + D_{c2} + D_{c3}\right)}{3} \qquad [3.5]$$

$$D_e = \frac{(D_{ave} - C_o) \times Vl}{(g \cdot of \cdot soil)} \times \frac{1000g}{kg} \quad [3.6]$$

where;

D_{ave} (mg/L) is the average desorption equilibrium copper concentrations, D_{c1}, D_{c2}, and D_{c3} (mg/L) are desorption equilibrium copper concentrations obtained after tests, D_e (mg/kg) is the desorbed amount of copper, C_o (mg/L) is the initial copper concentration (initial copper concentration in the sodium nitrate solution was zero), and Vl (L) is the volume of sodium nitrate solution added to each soil sample (Vl = 0.0 14 L).

Table 3.4 shows the data obtained from the experiments. The amount of copper adsorbed (S) was calculated as in the section 3.2.1.2 and reported in Table 3.2. The copper desorbed was plotted against the initial adsorbed copper (see Figure 3.4). These experiments covered the range of the adsorbed copper between 60 and 3700 mg per kg of dry clay soil. For the range tested, Figure 3.4 shows that the desorbed copper increases with the increase of the initial adsorbed copper. The highest copper desorbed (670 mg/kg) was obtained for the adsorbed amount of 3700 mg/kg. For the low initial adsorbed copper (< 1000 mg/kg of dry soil), the slope of desorption profile is somewhat flat whereas for initial adsorbed copper >1000 mg/kg of dry soil the profile slope is steep. The percentage of desorbed copper (D_e) to the initial adsorbed copper (S) was calculated. Figure 3.5 shows the ratio (D_e/S) vs. S. As seen in the figure in general, D_e/S increases with the increase of S. The highest D_e/S reported was 16.5% in the test with initial adsorbed copper of 3700 mg/kg of dry soil.

3.2.2.2 Effects of pH on desorption

In this experiment, desorption tests were conducted using soil samples with the same copper concentrations. The amount of copper desorbed at different pH values was obtained in each test and compared with the initial copper concentration. The following subsections discuss the procedure followed in these tests and present the results.

3.2.2.2.1 Test procedure

The clay soil sample was initially contaminated with 355 mg of copper per kg of dry soil with water content 41% (the same concentration and water content of soil sample to be used later in the electrokinetic tests). The soil sample was air-dried for 72 hr and then ground. Five soil samples of 1 g each were weighted into 5 Erlenmeyer flasks of 50 mL volume. 14 mL of 0.01 M sodium nitrate ($NaNO_3$) solution was added to each soil sample in the Erlenmeyer flasks. The soil samples with the solution were equilibrated for 24 hr in a shaking table (120 rpm) at room temperature (21 ± 1 C^o). The pH of the soil-solution suspensions in each flask was controlled at one of the following pH values 2, 4, 6, 8, and 10 with the addition of nitric acid (HNO_3) and/or sodium hydroxide (NaOH). The pH was measured every two to three hours and readjusted when needed. Then the soil and solutions were transferred to 20 mL plastic centrifuge tubes. The tubes with the soil and solution mixture were then centrifuged at 4000 rpm for 10 min. After that, 1 mL of the supernatant from each tube was drawn and placed in 20 mL plastic tube. Then the solution in each tube was diluted by adding 9 mL deionized water. The concentrations of the diluted solutions were determined using ICP-OES. The experiments were conducted in triplicate.

3.2.2.2.2 Results

The amount of copper, D_{Cu} (mg/kg), desorbed was calculated as follows:

$$D_{epH} = \frac{\left(D_{t1} + D_{t2} + D_{t3}\right)}{3} \quad [3.7]$$

$$D_{cu} = \frac{\left(D_{epH}\right) \times Vl}{(g \cdot of \cdot soil)} \times \frac{1000g}{kg} \quad [3.8]$$

where;

D_{epH} (mg/L) is the average desorption equilibrium copper concentrations (pH effects tests), D_{t1}, $D_{t2,}$ and D_{t3} (mg/L) are desorption equilibrium copper concentrations obtained after the tests, D_{Cu} (mg/kg) is the desorbed amount of copper (pH effects tests), and Vl (L) is volume of sodium nitrate solution add to each soil sample (Vl = 0.0 14 L).

Table 3.5 shows the data obtained from the experiments as well as the calculated amount of desorbed copper at pH values 2, 4, 6, 8, and 10. Figure 3.6 shows the amount of desorbed copper at different pH values. Figure 3.6 shows that the amount of desorbed copper decreases as the pH increases. For instance, the figure shows that at pH of 2, the amount of desorbed copper was about 270 mg/kg of dry soil compared with 180 mg/kg dry soil at pH of 4. Figure 3.6 shows that very little or no copper was desorbed at pH ≥8. Figure 3.7 shows the ratio in percentages of copper desorbed to the initial copper in the soil (355 mg/kg of dry soil) at different pH values. At low pH values (i.e. pH of 2 and 4) the percentages of copper desorption were 81% and 50%, while at pH values > 8 (alkaline medium) no copper was desorbed from the soil. It has been reported in the literature that the rise of pH results in more adsorption of

heavy metals on soils (Phillips et al., 2004; Oren and Kaya, 2006; Yuan et al., 2007). Therefore, it can be concluded that for the clay soil and copper concentration tested, desorption of copper increases with the decrease of pH. The maximum desorbed copper was 81% of the initial copper reported in the test with solution of pH of 2. The desorbed copper will be free in the solution and available to be removed by electroosmosis flow through electrokinetic remediation. Therefore, any copper removal higher than 81% achieved by electrokinetic remediation can be attributed to removal by electromigration. As per the results of these tests, for clay soil contaminated with copper at 355 mg/kg of dry soil, the use of conventional soil flushing technique with flushing solution 14 times the mass of the soil and pH of 2, after 24 hr of agitation, can result in removal of 81% of the initial copper. Obviously, it will be a very expensive process to remove such amount from the soil.

Table 3.1 Characteristic of clay soil

Parameter	Value
Liquid limit	41
Plastic limit	19
Sand (%)	0
Silt (%)	58
Clay (%)	42
Specific gravity	2.64
Cation Exchange Capacity	8.9 meq/100g of soil

Table 3.2 Adsorption tests results- Langmuir isotherm

Initial Cu concentration (mg/L)	Equilibrium Cu concentration (mg/L)			Average Equilibrium Cu concentration (mg/L)	Amount adsorbed (mg/g)	C_e/S (g/L)
	Test No.1	Test No.2	Test No.3			
C_i	C_{e1}	C_{e2}	C_{e3}	$C_{ave} = C_e$	S	C_e/S
1001.00	690.80	735.60	780.70	735.70	3.71	198.08
511.20	286.80	316.70	308.80	304.10	2.90	104.88
274.50	126.80	127.70	126.00	126.83	2.07	61.35
96.21	24.53	25.40	30.37	26.76	0.97	27.53
48.43	20.12	9.802	2.95	10.96	0.52	20.89
21.70	7.49	0.5245	1.54	3.19	0.26	12.29
5.33	0.766	0.7329	0.89	0.80	0.06	12.58

Table 3.3 Langmuir isotherm equation.

Regression equation	Coefficient (R^2)	K_L (L/mg)	M_L (mg/g)
$C_e/S=0.2508\ C_e+19.22$	$R^2= 0.988$	$1.3x10^{-2}$	3.98

Table 3.4 Effects of concentration on desorption tests results

Amount adsorbed (mg/kg)	Desorption equilibrium Cu concentration (mg/L)			Average (D_c) (mg/L)	Amount desorbed (mg/kg)	% desorbed (D_e/S)
	Test1	Test2	Test3			
S	D_{c1}	D_{c2}	D_{c3}	D_{ave}	D_e	(D_e/S)
3714	41.85	41.55	47.93	43.78	613	16.52
2899	29.44	30.12	32.00	30.52	427	14.73
2079	15.03	15.75	14.67	15.15	212	10.25
972	4.28	4.21	5.03	4.51	63.1	6.50
525	3.34	3.05	1.86	2.75	38.5	7.40
259	1.22	0.25	0.31	0.60	8.4	3.21
63.42	0.09	0.30	0.15	0.18	2.52	4.18

Table 3.5 Effects of pH on desorption tests results.

pH	Initial Cu per kg of soil (mg of Cu/kg of soil)	Desorption Cu equilibrium concentration (mg/L)			Average concentration (mg/L)	Desorbed Cu from soil (mg/kg)	Percentage desorbed (%)
		Test No.1	Test No.2	Test No.3			
pH	S_i	D_{t1}	D_{t2}	D_{t3}	D_{epH}	D_{cu}	(D_{cu}/S_i)
2.00	355.00	20.55	18.27	19.42	19.41	271.79	76.56
4.00	355.00	14.81	13.99	10.42	13.07	183.03	51.56
6.00	355.00	1.56	3.09	2.24	2.30	32.18	9.06
8.00	355.00	0.13	0.14	0.09	0.12	1.70	0.48
10.00	355.00	0.09	0.05	0.05	0.06	0.89	0.25

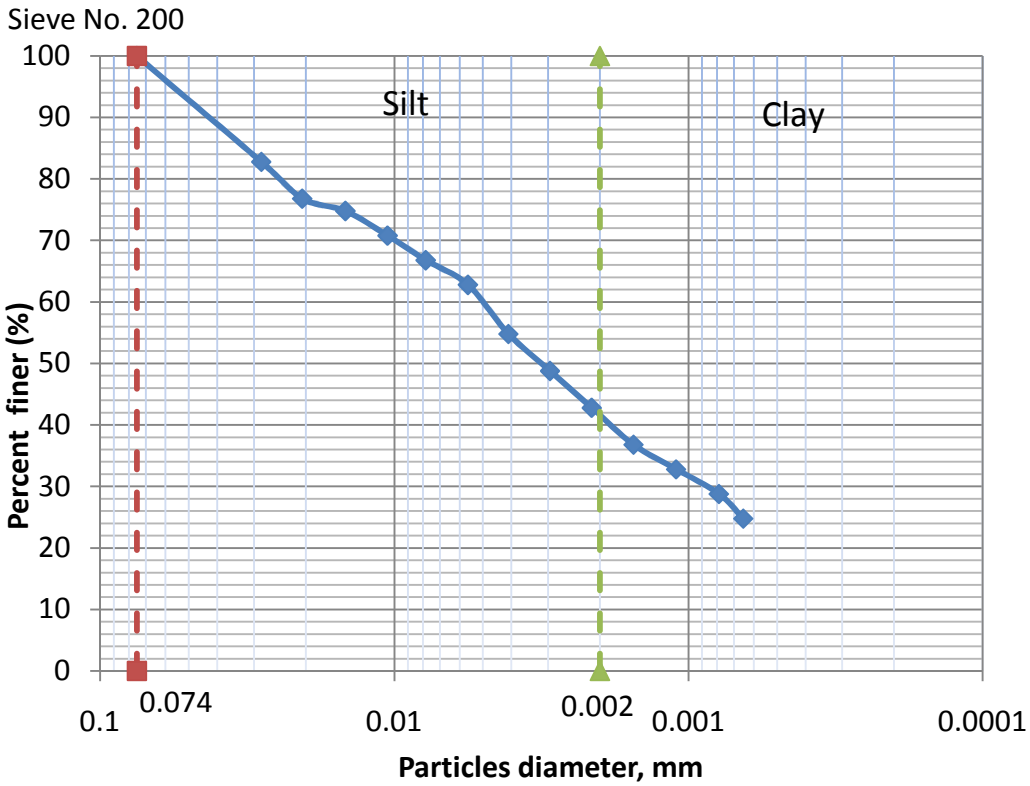

Figure 3.1 Soil grain size distribution curve for the clay soil.

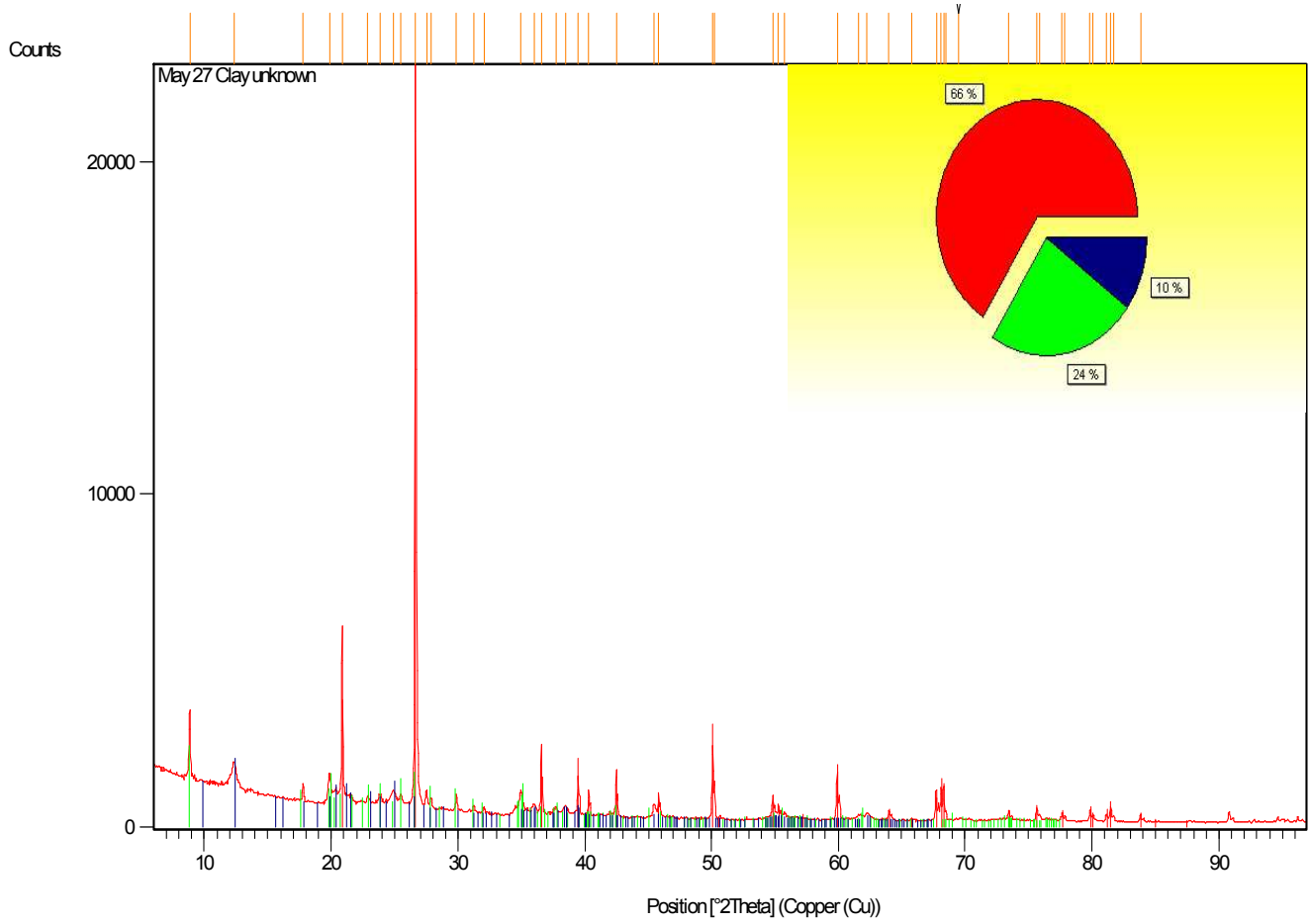

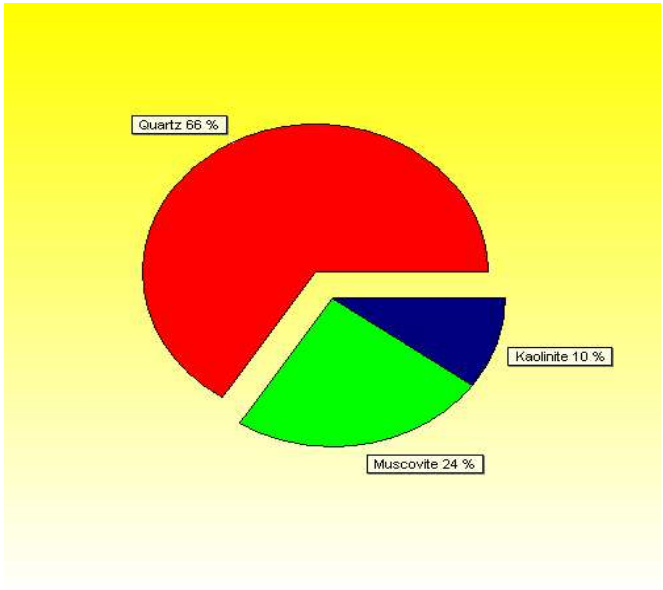

Figure 3.2 X-ray diffraction pattern for clay soil.

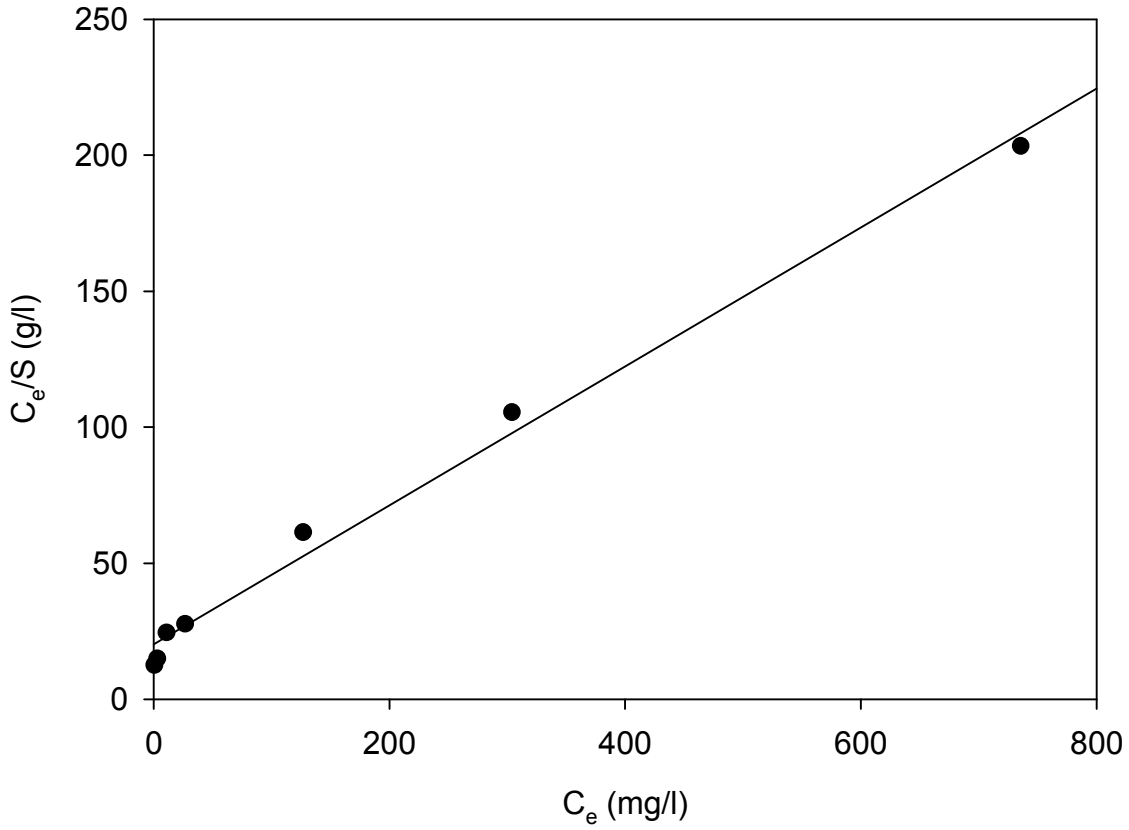

Figure 3.3 Copper adsorption Langmuir isotherm.

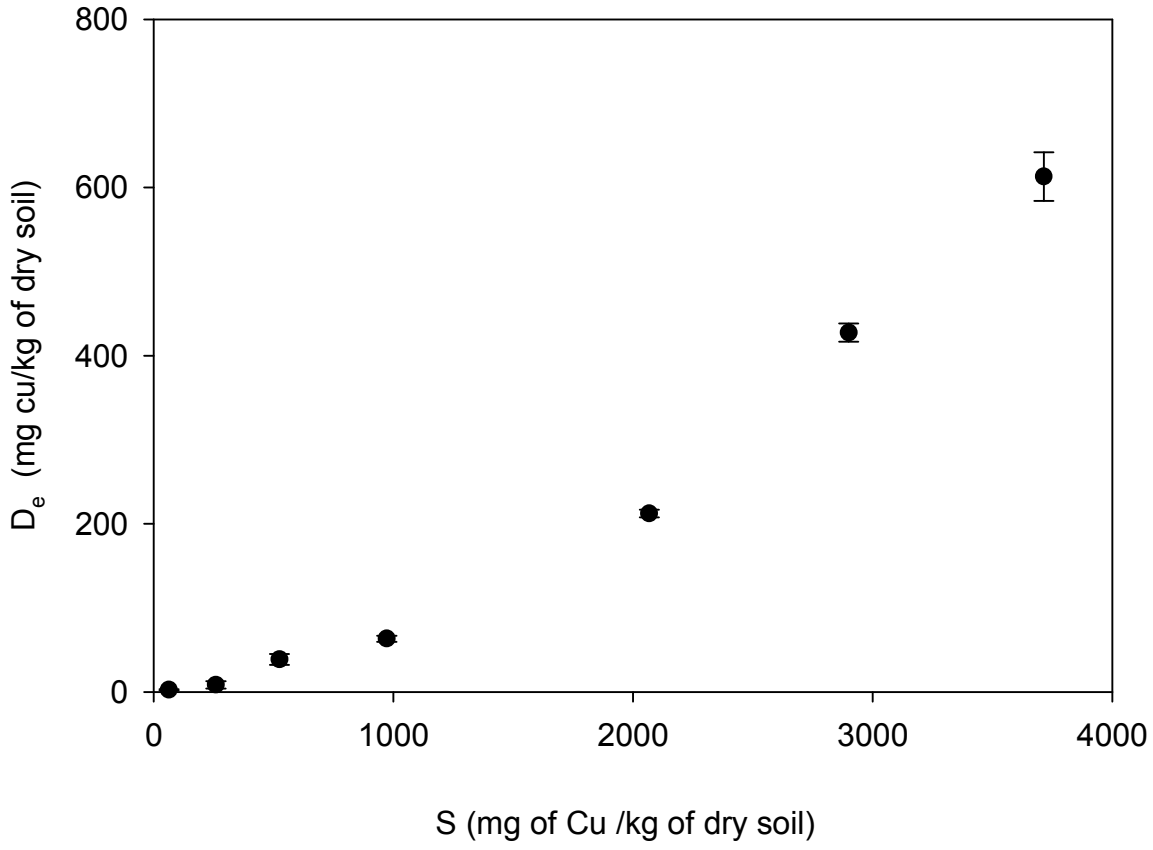

Figure 3.4 Amount of desorbed copper (D_e) vs. initial adsorbed copper (S) at pH of 5.75 ± 0.25.

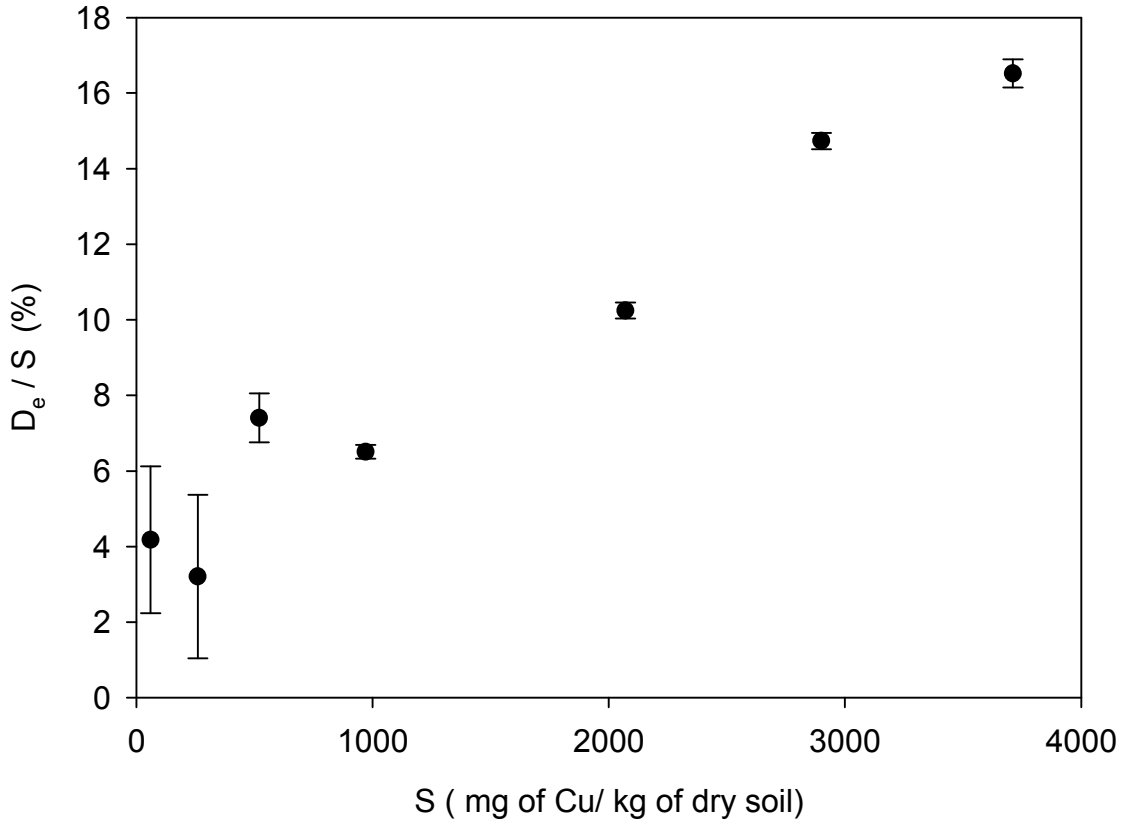

Figure 3.5 The ratio of desorbed copper to the initial adsorbed copper (D_e/S) vs. initial adsorbed copper(S) at pH of 5.75 ± 0.25.

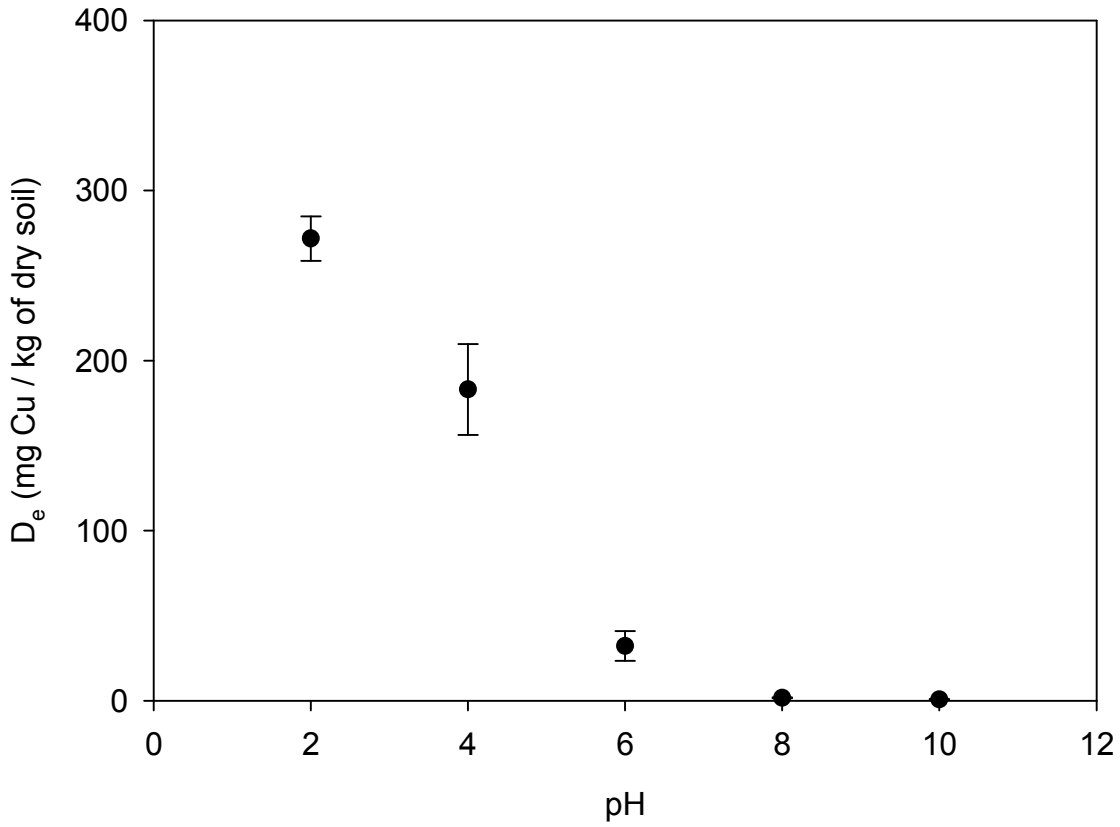

Figure 3.6 Desorbed copper (D_e) vs. pH for soil with initial copper concentration of 355 mg/ kg of dry soil.

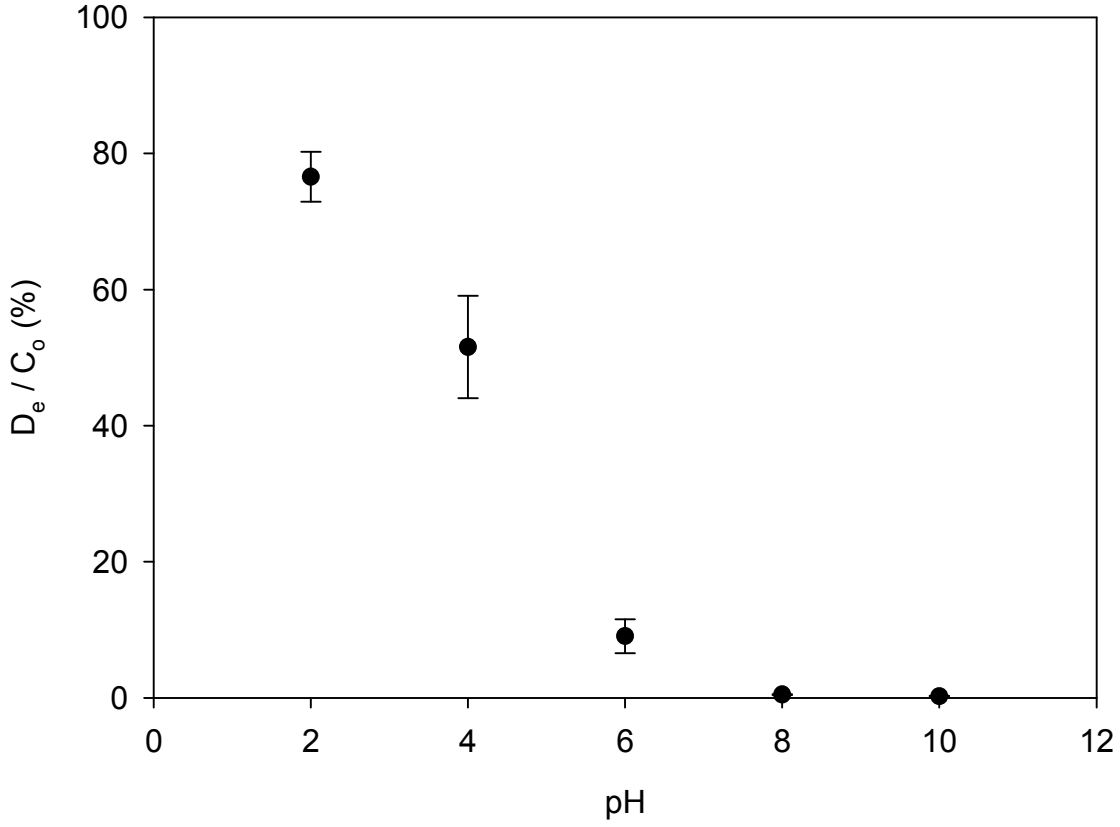

Figure 3.7 The ratio (D_e/C_o) of copper desorbed (D_e) to initial copper (C_o) in soil vs. pH for soil with initial (C_o) of 355 mg Cu/kg of dry soil.

CHAPTER FOUR

EXPERIMENTAL APPARATUS, METHODOLOGY, AND INNOVATIONS

4.0 INTRODUCTION

This research was carried out to investigate the use of power generated by solar cells in electrokinetics, the effects of soil heterogeneity in electrokinetic remediation, and the effectiveness of a novel technique to retard the base front movement. Section 4.1 of this chapter describes the apparatus used in the research. The methodologies are described in section 4.2. The novel technique to combat the base front movement is presented in section 4.3.

4.1 EXPERIMENTAL APPARATUS

4.1.1 Electrokinetic cell

Electrokinetic cells were designed and fabricated to perform the soil remediation tests in this research. The general design considerations of the cell were:

i. Vertical electrodes configuration. The vertical electrodes layout was selected for its practicality in field installation and the ease of replacing electrodes.

ii. Capability to apply a surcharge load to the soil specimen. The surcharge load can be used to simulate in-situ stress conditions, and to produce soil samples with different void ratios.

iii. Capacity to test with one-and two-dimensional electrode configurations.

The electrokinetic cell, constructed of clear Plexiglas plates 15 mm in thickness, has inner dimensions of 385×125×250 mm (length × width × height). The cell is composed of upper part, base, and two movable rectangular perforated Plexiglas plates (250 mm length × 125 mm width). The upper part forms an outer boundary to accommodate the soil sample. The rectangular perforated Plexiglas can be used to adjust the soil sample length between 200 and 320 mm. The base of the cell is detachable to allow for easy recovery and minimum disturbance for the soil samples that are to be used for subsequent parametric studies. At the base far ends, two drainage valves were installed and used to collect water during the remediation process. The voltage across the soil specimen is monitored via four voltage probes installed along the base of the cell. Figure 4.1 shows the schematic of the electrokinetic remediation cell.

4.1.2 Soil pore fluid squeezer

Soil pore fluid squeezer cell was specially designed and manufactured to recover pore fluid from soil specimens for subsequent testing. It is compose of steel chamber to host the soil specimen, steel piston to exert pressure on the soil sample and a base. A porous plate is placed on the upper portion of the base and underlain by a drainage line grove through the base. The chamber inner dimensions are 50 mm in diameter and 100 mm long. Figure 4.2 shows the schematic of the soil pore fluid squeezer cell.

4.1.3 Solar cell panel

Three solar cell panels (NT-175U1) were used as power source. Cell dimensions are 1590 mm × 820 mm (Figure 4.3). The open circuit voltage, maximum current, and maximum power of the

cell are 41 V, 4.27 A, and 175 Whr, respectively. The longitude and latitude of Thunder Bay, Ontario, where the experiments were performed, are $89^{o}14'$ W and $48^{o}24'$ N, respectively. During the tests, the solar cell panels were placed in a yard open to the sky and mounted on wooden frames at an angle of 48^{o} to the horizontal for maximum exposure with the bottom of the cell elevated 250 mm from the ground. The solar panels were connected to the electrokinetic cells placed in a basement-floor laboratory about 100 m from the yard.

4.1.4 Laboratory devices

Standard operating procedures were followed using modern laboratory equipment for testing and analysis. A heavy duty mechanical paddle mixer was used for stirring the soil sample with contaminated solution. The pH and electrical conductivity were measured using a pH-Electrode sentix 41-3 and TetraCon 325 (Multi 340i/set WTW). Digital table shaker with rate of 0-500 rpm was used for proper mixing of soil-fluid mixture. A centrifuge (Clinical 50) with maximum speed of 4000 rpm was used to separate fluid from soil. The concentration of copper in the supernatant was determined using an Inductive Couple Plasma-Optical Emission Spectroscopy (ICP-OES).

4.2 METHODOLOGY

Copper was selected to artificially contaminate the soil and represent common heavy metal pollution. The selection was based on the abundance of sites contaminated by copper and the ease of handling. The copper salt was copper (II) chloride dihydrate ($CuCl_2 \cdot 2(H_2O)$). Graphite was selected to be used in the electrode materials so as to avoid the adverse reactions by-

products (see section 2.5.1). The soil was prepared in batches of 5 kg of soil in order to fit the size of the mechanical mixer. Homogeneous and heterogeneous samples were used in the experiments throughout this research. One- and two-dimensional electrode configurations were implemented in the research. Section 4.2.1 describes the procedure followed to prepare and artificially contaminate the homogeneous soil. The heterogeneous soils preparation is presented in section 4.2.2. Electrode configurations are presented in section 4.2.3 and 4.2.4. Section 4.2.5 discusses the testing procedure followed during and at the end of the test.

4.2.1 Homogeneous soil

The homogeneous soil used in this research was clay. For each batch, 5 kg of dry soil was weighed into a plastic pail. 2050 mL of tap water (required for water content of 41% similar to the liquid limit of the soil sample) was measured and poured into a container. There are numerous sorption sites on the soils having a range of binding energies (Reed et al., 1996). To investigate the effectiveness of electrokinetics in remediating soil contaminated with varying heavy metal concentrations, copper concentrations of 150 and 355 mg of copper per kg of dry soil were used to contaminate the soil. At low copper concentration (150 mg/kg), the high-energy binding sites are occupied first. At higher copper concentrations (355 mg/kg), the high-energy binding sites are completely occupied and the lower-energy binding sites begin to fill, resulting in a decrease in the average metal-soil binding energy. Therefore, it is ease to remove copper from the highly contaminated soil compared with the low contaminated soil. Copper (II) chloride dihydrate to achieve the required concentration was weighed and then added to the water in the container. The dry soil and the copper solution were mixed using the mechanical mixer. Additional batches were similarly prepared. The soft contaminated soil was poured in

heavy duty plastic bags and placed in pails with airtight covers. The soil was stored to allow for copper adsorption by soil to take place and reach equilibrium. Seventy-two hours after preparing the pre-contaminated soil, the soil was placed into the electrokinetic cell in three layers for a total height of 165 mm. Each layer was rodded 25 times using steel rod, 16 mm in diameter and 600 mm long with a hemispherically shaped tip, to prevent the entrapment of air pockets. The high water content of the soil and the thorough rodding during placement insured that the soil specimen was nearly, if not fully, saturated. A surcharge load of 12.8 kg (corresponding to a pressure of 5 kPa) was applied to the soil via the loading plate (Figure 4.1) in four increments over a period of four days. The first surcharge load was 0.6 kg, followed by 3, 5, 7.8, and 12.8 kg.

4.2.2 Heterogeneous soil

Three heterogeneous soils were laboratory-prepared using clay and sand. The heterogeneous soils were clay-sand mixture, clay with sand pockets, and clay-sand layers consisting of two layers of clay sandwiching a sand layer. The ratio of the clay to the sand in the three soils was 2:1 (mass/mass). For each batch of the clay sand mixture, 3.33 kg of dry clay and 1.67 kg of dry sand were weighted and placed in a plastic pail. Two thousand and fifty mL of water was measured and poured in a container. Copper (II) chloride dihydrate (2.01 g) was then added to the container to achieve a concentration of 150 mg Cu per kg of dry soil. The soil batch was prepared by thoroughly mixing the clay and sand mixture with the copper solution using the mechanical mixer. Additional batches were prepared in similar manner. Clay and sand soils were separately prepared for clay-sand layers and the clay with sand pockets specimens.

Copper solution was thoroughly mixed with clay to water content of 52% and with sand to water content of 19%. Thus, the average water content and copper concentration of the soil specimens were 41% and 150 mg per kg of dry soil. From observations, nineteen-percent was found to be the maximum water content that can be retained by the sand. The contaminated clay and sand were poured in separate heavy duty plastic bags and stored for seventy two hours in pails with airtight covers to allow for copper adsorption by the soil to take place and reach equilibrium.

The clay sand mixture soil was placed in the electrokinetic cell in similar manner to the homogeneous clay described in section 4.2.1. In the clay-sand layers, a layer of clay of 55 mm thickness was laid first and then overlain by a similar layer of sand. A second layer of clay 55 mm thick was placed over the sand. The layers were rodded and a surcharge load was applied as described in section 4.2.1. The clay with sand pockets was prepared in three layers. The first clay layer, 55 mm, was laid and rodded as described in section 4.2.1. Hollow plastic cylinders were then inserted at arbitrary locations into the clay layer and filled with sand. The similar procedure was repeated for the second and third layers. Each layer was rodded and a surcharge load was applied as described in section 4.2.1.

4.2.3 One-dimensional configuration

Graphite (nonmetallic) was selected as electrode material to avoid/minimize adverse reactions by-products of metallic electrode (see section 2.5.1). Two perforated graphite electrodes, one serving as anode and the other as cathode with dimension of 200 x 125 x 3 mm

(height × width × thickness) were placed in direct contact with the soil. The length of the soil between the two electrodes was 200 mm. The surface area of the electrode and the cross-sectional area of the soil are identical (See Figure 4.4). Thus, the electric field was uniform across the area and the soil was subjected to one dimensional electric field. A geotextile filter was wetted by tap water and placed between the electrode and the Plexiglas. The soil was then placed in the cell as described in previous section and the electrodes were connected to solar cells panel.

4.2.4 Two-dimensional configuration

The difference between one- and two-dimensional configurations is the electrodes size and placement with respect to the cross-sectional area of the soil. In one-dimensional configuration the electrode sheet cover the entire cross-section of the soil as shown in Figure 4.4, whereas in the two-dimensional configuration the electrodes were made of strip and cover about 24% of the soil (see Figure 4.5). In two-dimensional configuration, four graphite electrodes with dimensions 200x15x6 mm (height × width × thickness) serving as pair of anodes and pair of cathodes were placed in electrokinetic cell in direct contact with the soil specimen. As shown in Figure 4.5, the pair of electrodes was placed 31.6 mm apart. A geotextile filter was wetted by tap water and placed between the electrode and the Plexiglas. The soil was placed in the cell as described in previous section and the electrodes were then connected to the solar cell.

4.2.5 Data collection and subsequent testing

The following procedure was followed in all tests. Electric current, voltage across the soil, and water collected in the graduated cylinder (Figure 4.1) were monitored and reported every three to four hours during the test. At the end of the test, the soil was extruded from the cell and divided into five or four equal sections (S1 to S5 or S1 to S4) as shown in Figures 4.6 and 4.7. For the heterogeneous soils, the clay/sand ratio was kept at 2/1 for the samples used for the water content, pH, and copper concentration. The soil in each section was tested for water content, pH, and copper concentration. Part of the soil in the section was squeezed for pore fluid using the soil pore fluid squeezer described in section 4.1.2. The pH and electrical conductivity of the pore fluid were obtained using pH-Electrode sentix 41-3 and TetraCon 325. The copper concentration was determined using ICP-OES. To determine the total copper and pH in each soil section, approximately 30-40 g of the soil sample was air-dried for 48-72 hr and then ground. For pH measurement, 5 g of dry soil was mixed with 10 mL of deionized water and the pH of the mixture was determined by pH-Electrode. For the copper concentration, 2.2 g of dry soil was mixed with 11 mL of concentrated nitric acid. The mixture was agitated in a shaking table for 12 hr at 150 rpm. Afterward, the mixture was centrifuge for 20 min at 4000 rpm. The supernatant was drawn and the concentration of copper in the supernatant was then determined using ICP-OES. The detection limit for Cu was about 10 ppb w/v (ug/mL).

4.2.6 Copper removal calculations

The copper removal from soil section was calculated as follows:

$$\text{Copper removal (\%)} = \left(1 - \frac{C}{C_o}\right) \times 100 \qquad [4.1]$$

where;

C (mg/kg of dry soil) is the copper concentration after the test, and C_0 (mg/kg of dry soil) is the initial copper concentration. A calculated negative copper removal from Eq. [4] means copper had accumulated in the section.

4.3 INNOVATIONS

During the electrokinetic remediation processes, the acid front travels towards the cathode by electromigration and electroosmosis flow, while the base front moves towards the anode by electromigration and the two fronts meet at a distance closer to the cathode (see Figure 2.10). For soil contaminated with heavy metals, the base front reacts with the cations in the soil pore fluid causing premature precipitation of the heavy metals as hydroxides (Giannis and Gidarakos, 2005). The precipitation of heavy metals is considered as a major drawback for electrokinetic remediation (Pazos, 2006). Numerous attempts, conventional and innovative, have been carried out to suppress the base front advancement and the subsequent premature precipitation of ionic species. The conventional approaches rely solely on the addition of chemical compounds. On the other hand, the innovative techniques including Stepwise Moving Anode (SMA) and polarity exchange utilize electrode and electric field re-configuration and consequently require additional field work and setup.

The following section discusses our novel approach, Two Anodes Technique (TAT), to retard the advancement of the base front in electrokinetic remediation applications. As per the current published literature, this research illustrates the first application of TAT.

4.3.1 Two Anodes Technique (TAT)

In the conventional anode cathode electrokinetic application, the anode directly faces the cathode (see Figures 4.4 and 4.5). The anode and the cathode are connected to the positive and negative ends of the DC power source and the soil is under the effects of one electric circuit. The electrode configuration in the novel Two Anode Technique (TAT) is somewhat different. In TAT, there are primary and secondary anodes and a cathode forming main and secondary electric circuits. As shown in Figure 4.8, the primary anode and the cathode are placed at the boundaries of the soil, while the secondary anode is placed between them in close proximity to the cathode. The secondary anode is connected to the positive end of a separate power supply, while the negative end is connected to the cathode. As shown in Figure 4.8, the primary anode together with cathode forms the main electric circuit, while the secondary electric circuit is made by the secondary anode and the cathode. To generate current through the secondary electric circuit, the applied voltage through the secondary electric circuit should be higher than the voltage at the position of the secondary anode prior to the secondary electric circuit. Due to the presence of the secondary circuit, the initial voltage gradient (see Figure 4.9) resulted from the main electric circuit across the soil is altered (see Figure 4.10). Application of TAT in electrokinetic remediation causes three unique electric currents:

- Main electric circuit current, that between the primary and secondary anode.

- Secondary electric circuit current, that between the secondary anode and the cathode.
- Total current on the secondary electric circuit, that between the secondary anode and the cathode.

The sole purpose of the secondary anode is to produce hydrogen ions (H^+) via electrolysis reactions. Thus, additional acid front will be generated at the secondary anode in close proximity to the cathode. This acid front will travel by electroosmosis and electromigration towards the cathode and meet the base front at a very close distance from the cathode (see Figure 4.11). As a result, the base front advancement will be significantly reduced. Moreover, H^+ ions will lower the soil pH in the vicinity of the cathode promoting desorption of heavy metals from the soil closer to the cathode

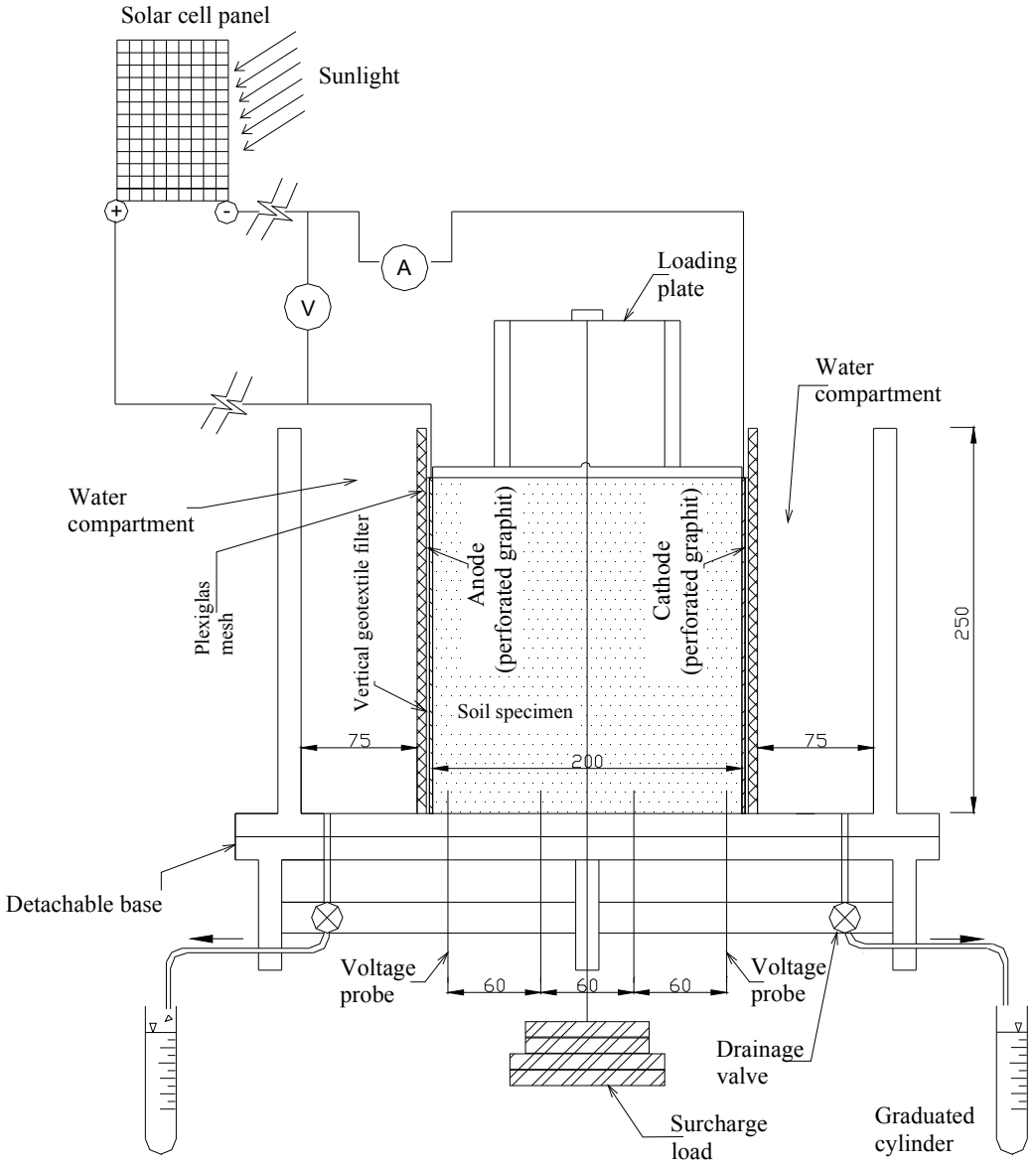

Figure 4.1 Elevation view of electrokinetic remediation cell (dimensions in mm).

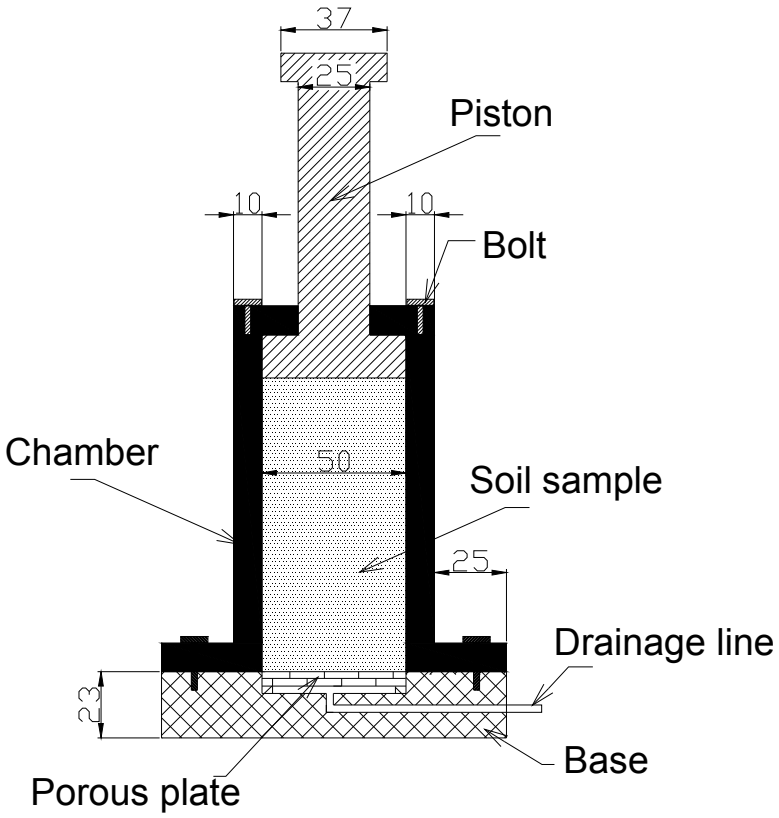

Figure 4.2 Section view through the soil pore fluid squeezer (dimensions in mm).

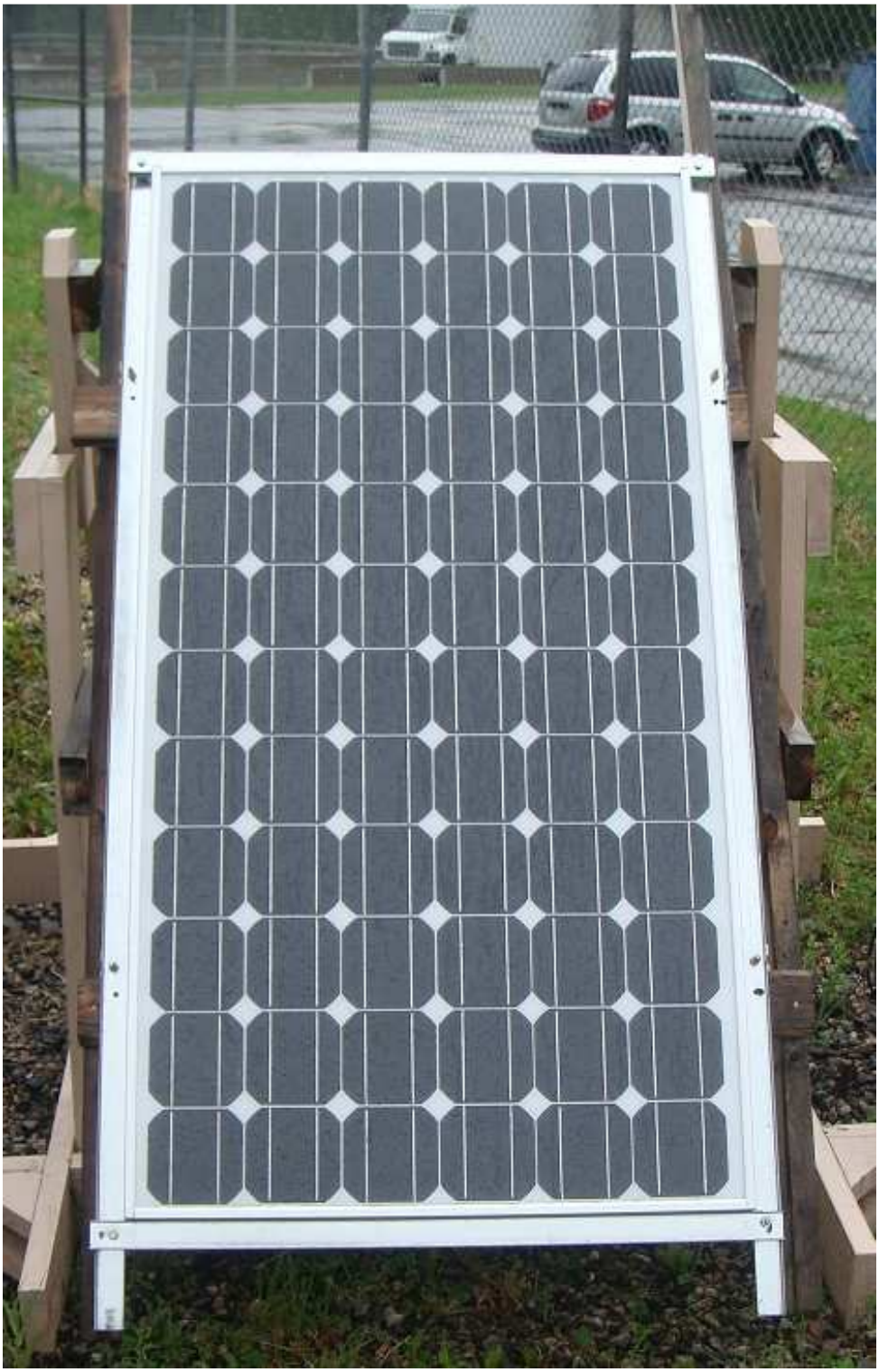

Figure 4.3 Solar cells panel.

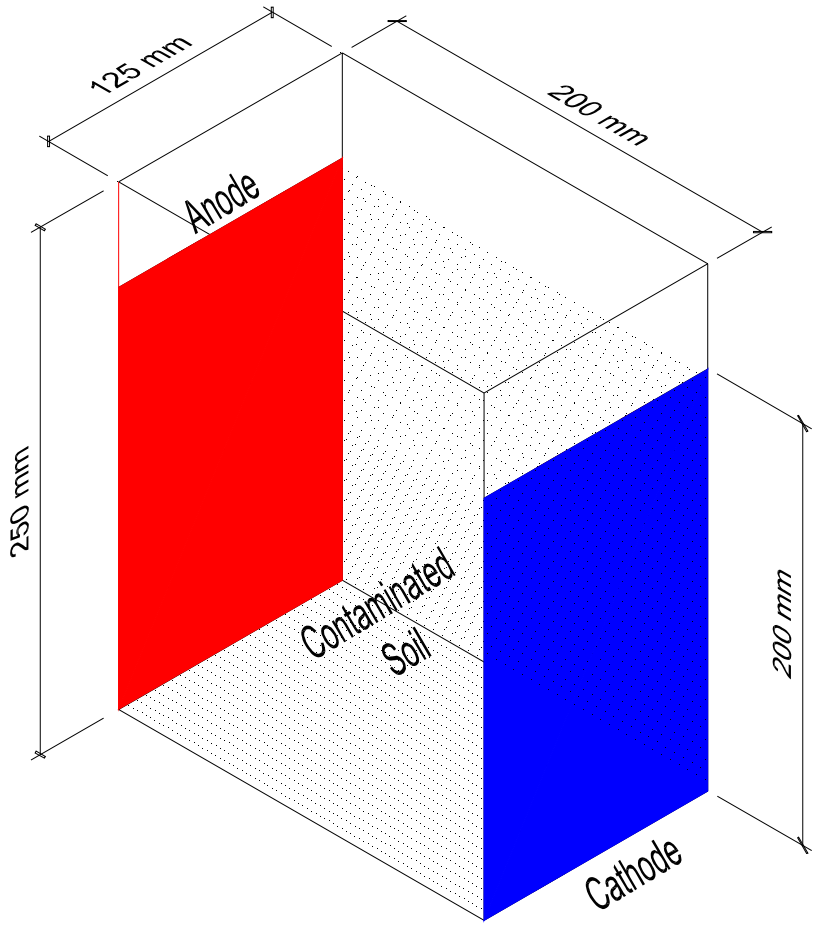

Figure 4.4 Electrode placement in one-dimensional configuration.

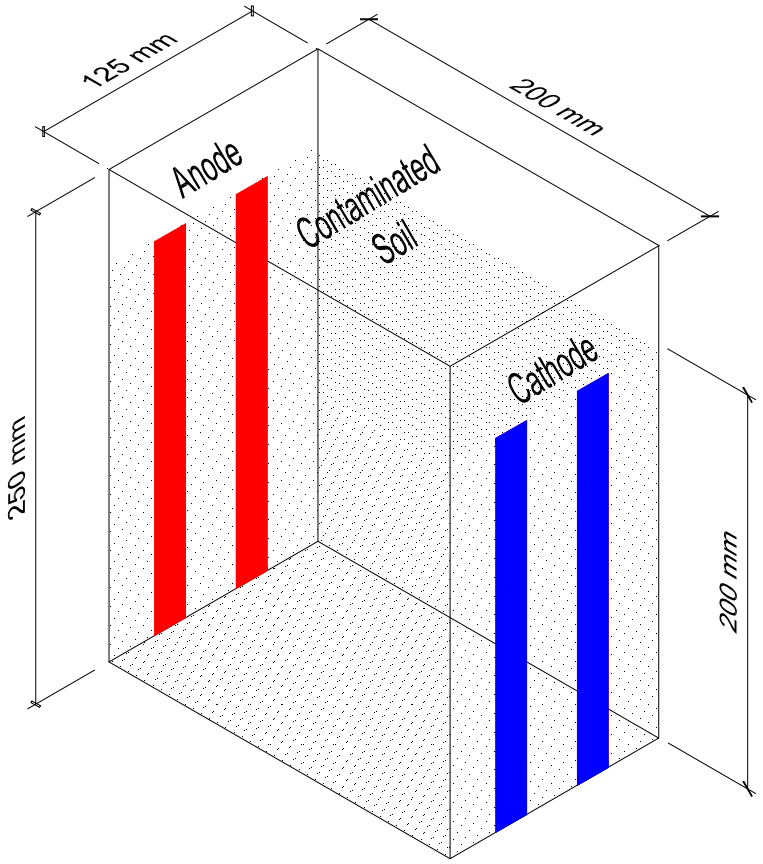

Figure 4.5 Electrode placement in two-dimensional configuration.

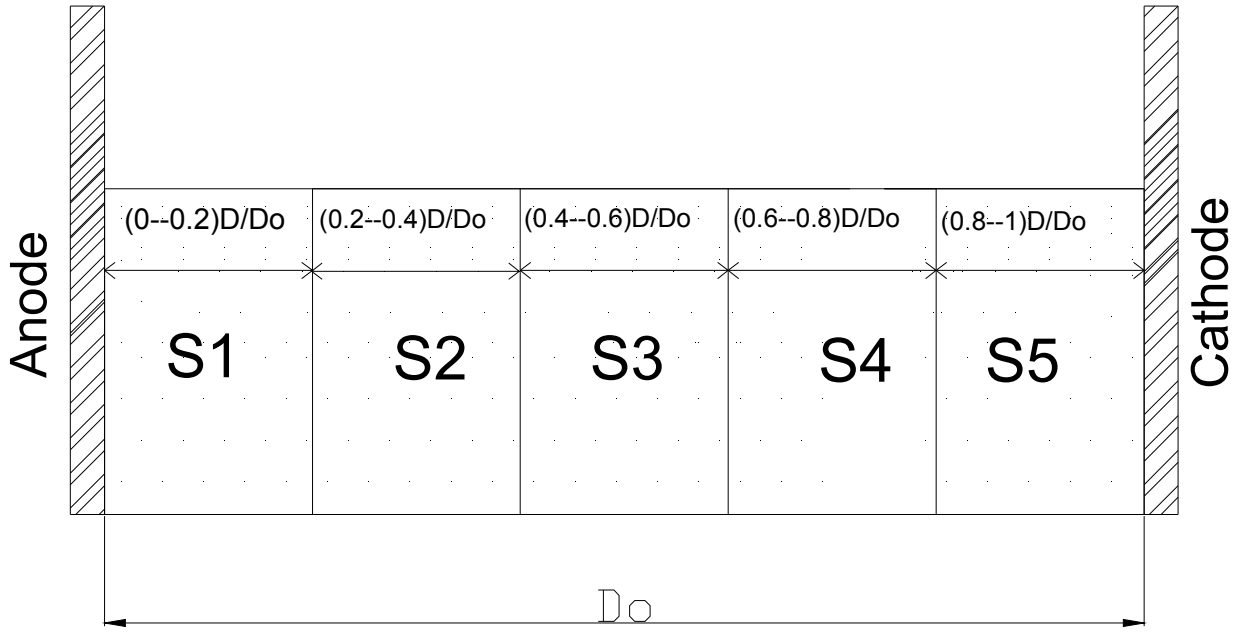

Figure 4.6 Sections (S1-S5) along the cell from anode to cathode.

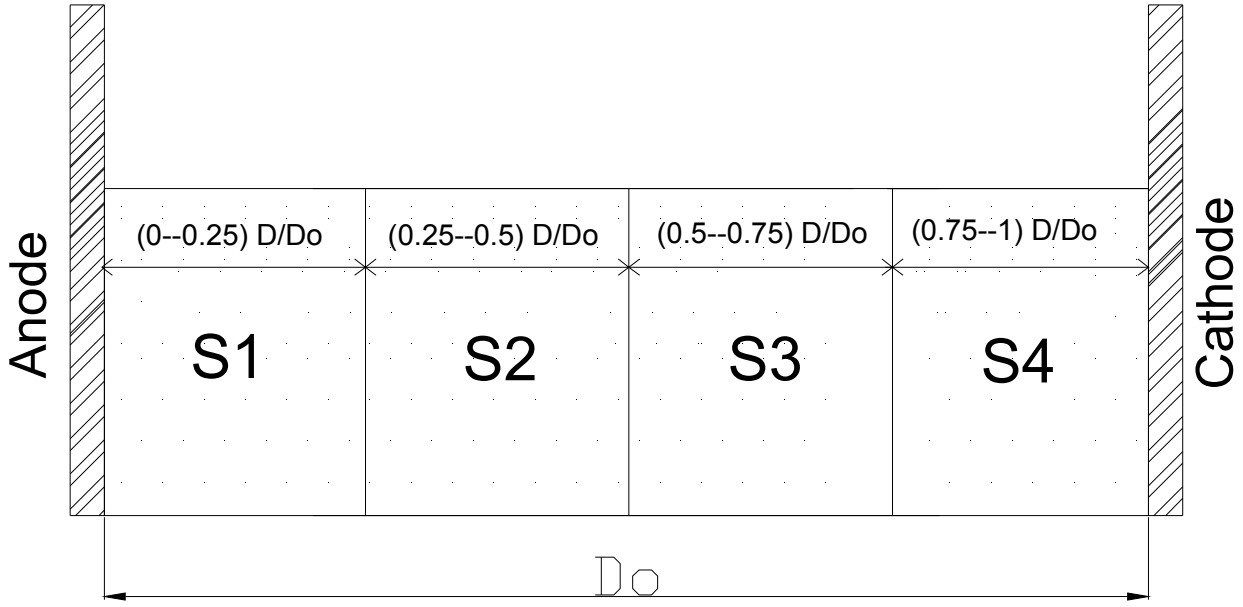

Figure 4.7 Sections (S1-S4) along the cell from anode to cathode.

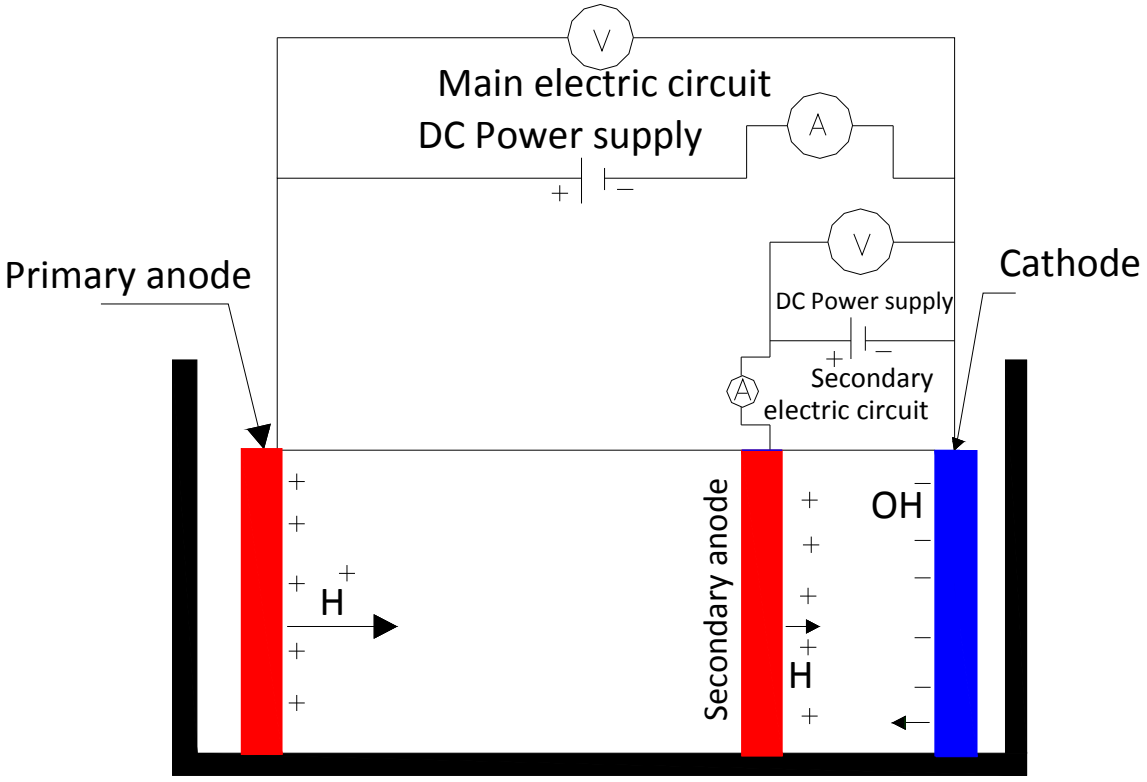

Figure 4.8 Electrode configuration and the main and secondary electric circuits in Two Anodes Technique (TAT).

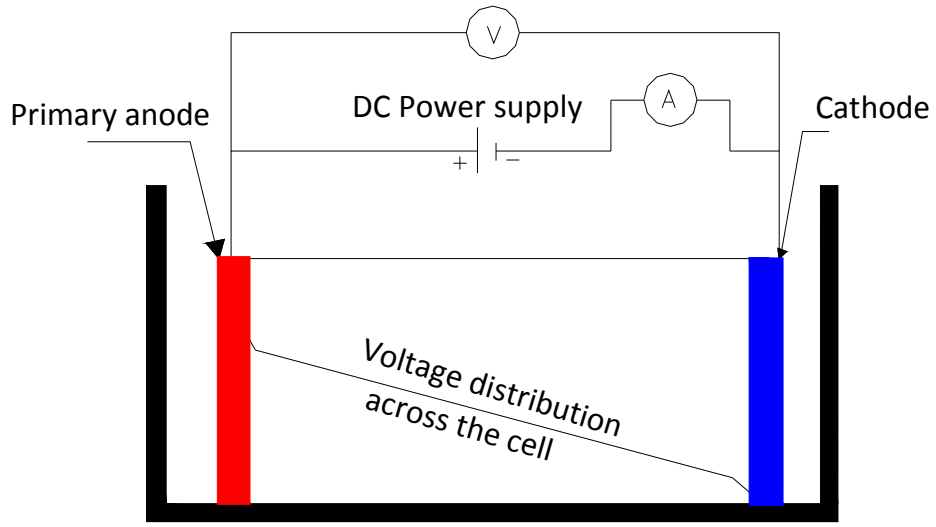

Figure 4.9 Typical voltage distribution in conventional electrokinetic remediation cell.

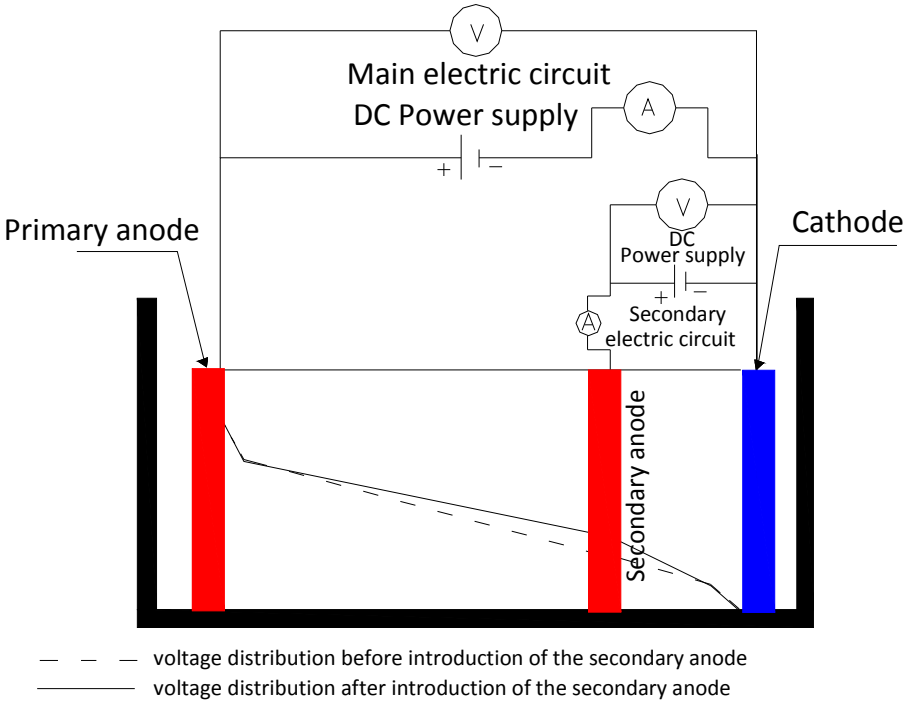

Figure 4.10 Voltage distribution before and after introducing the secondary anode.

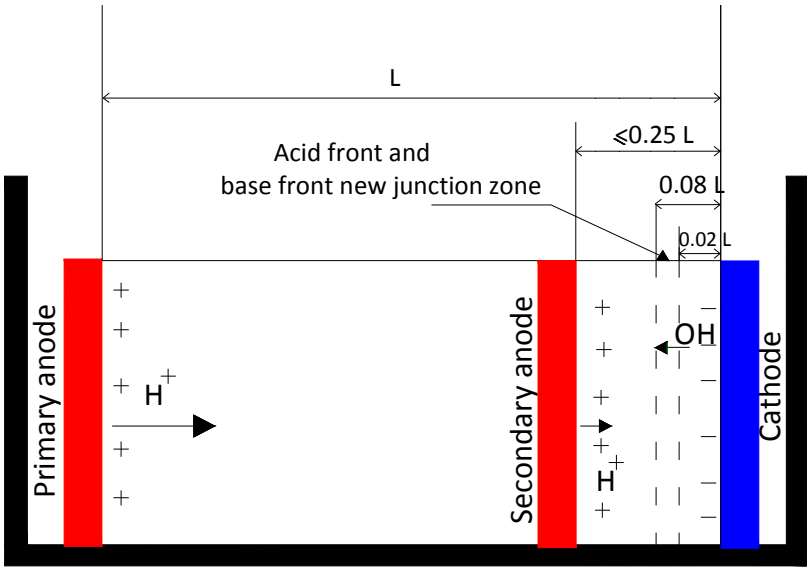

Figure 4. 11 Acid front and base front junction zone in Two Anodes Technique.

CHAPTER FIVE

EFFECTS OF APPLIED VOLTAGE ON INTEGRATED SOLAR ELECTROKINETIC REMEDIATION OF CLAY CONTAMINATED WITH COPPER

5.0 INTRODUCTION

Electric energy is required in an electrokinetic remediation process. The period needed for successful remediation depends on the contaminant type and concentration, the soil properties, and the strength of the electric field. For long periods of remediation, the energy expenditure can be the major factor impacting economic viability of the process. Therefore, cost-effective remediation may require power of low cost. A previous study by Yaun et al. (2009) showed that in China, the cost of the power generated by solar cells for electrokinetic applications is substantially lower than the cost of power from the electric grid. In this research, solar cell panels were proposed as an alternative power source to generate the electric field required for the electrokinetic remediation. This chapter will discuss the effectiveness of solar cells in generating electric field sufficient for electrokinetic treatment of a soft clay soil contaminated with copper.

5.1 TEST PROCEDURE

Electrokinetic remediation tests with one-dimensional configuration were conducted using homogeneous clay soil artificially contaminated with copper. The procedures described in sections 4.2.1 and 4.2.3 were followed from soil sample preparation and placement in the

electrokinetic cell. Three solar cell panels with peak outputs of 13.5, 27, and 41 V were connected to identical electrokinetic cells Cell A, B, and C. A control test (Cell D) was carried without electric field to provide baseline data for comparison. Each of the three solar cell panels was connected to the graphite electrodes in the three electrokinetic cells, Cell A, Cell B, and Cell C. The solar cell panels connected to Cell A and Cell B were partially covered to maintain peak voltages of 13.5 V and 27 V, respectively. The corresponding maximum voltage gradients across Cell A, Cell B, and Cell C were 67.5, 135, and 205 V/m, respectively. The experiments were carried out in July 3, 2010 for a period of seven days. At the end of each test, the soil was extruded from the cell and the procedure described in section 4.2.5 was followed for data collection and subsequent testing. For ICP-OES analysis, 5 mL of each copper solution was diluted by adding 15 mL of deionized water.

5.3 RESULTS AND DISCUSSION

Tables 5.1 to 5.4 summarize the test results (water content, pore fluid pH and electrical conductivity, dry soil pH, copper in soil pore fluid, copper in soil solids, and total copper in soil) for Cell A, Cell B, Cell C, and Cell D, respectively. The following subsections will present and discuss the results.

5.3.1 Applied voltage and electric current

Figures 5.1 and 5.2 show the applied voltage and electric current during the electrokinetic remediation tests for Cells A, B, and C. The zero values correspond to night time. The applied voltage and electric current vary during the daytime according to the degree of sunshine and

exposure. As seen in the figures, for the three cells, the applied voltage and current had rapidly increased in the morning shortly after the sunrise (6 am), and peak values were reached between 10 am and 4 pm and then decreased towards the end of the daytime. The output potential of solar cells was zero in darkness and therefore the voltages and the currents diminished. From Figure 5.1, the peak applied voltages were 13.5 V for Cell A, 27 V for Cell B, and 41 V for Cell C and were consistent during the seven days of remediation. At the period of maximum voltages, the corresponding maximum current values (0.12, 0.34, and 0.59 A for Cells A, B, and C, respectively) were found to be on the first day of the test while the minimum values (0.06, 0.1, and 0.15 A) were reported on the last day. The electric current range produced by the solar cells is sufficient for electrokinetic remediation as per previous effective electrokinetic applications. For example, Lageman et al. (1989) successfully used similar current values to remove copper from contaminated clayey soil. Thus, the solar cells were able to generate voltage gradients and current densities enough for the electrokinetic remediation.

The decrease in current resulted from the decrease in electrical conductivity of the soil during the remediation process. The change in the conductivity of soil during an electrokinetic process is a result of two opposing mechanisms. The bulk electrical conductivity of a soil is a product of the electrical conductivity of the two components of the soil, namely, the soil pore fluid (water) and soil solids. In general, the electrical conductivity of the pore fluid is much higher than that of the soil solids and thereby dominates the bulk conductivity of the soil. Therefore, as water is drained out during an electrokinetic remediation process, the bulk electrical conductivity of the soil decreases. However, for water still remaining inside the soil pores, the electrical

conductivity increases with the remediation time as a result of electrolysis reactions associated with electrokinetics (Narasimhan and Ranjan, 2000; Mohamedelhassan and Shang, 2003). Therefore, as the drainage of water during an electrokinetic remediation deceases with time, the increase in the electrical conductivity of the pore fluid by the electrolysis reactions may become more dominant than the decrease in soil conductivity resulting from the draining of water. Thus, the bulk conductivity of the soil and thereby the electric current through the soil may sometimes increase during the remediation process. The electrical conductivity of the pore fluid is also influenced by the dissolution of cations as discussed in section 5.3.3.

The loss in voltage at the interface between the electrodes and the soil was studied. To quantify the voltage loss at the soil-electrode interfaces, the electric field efficiency factor (β) was calculated using Eq.[2.28]. Figures 5.3, 5.4, and 5.5 show the applied voltages and β for the first day of the remediation for Cell A, Cell B, and Cell C. For Cell A, the lower the applied voltage the higher was the percentage in voltage drop at the interface between the anode (graphite) and the soil. The efficiency factors varied between 5% in the morning to 79% at the peak hours. At the cathode soil interface, the drop in voltage was found to be independent of the applied voltage. Cell A (13.5 V), the voltage drop at soil and the anode and cathode interface for is in agreement with a previous study by Mohammedelhassan and Shang (2001). For Cell B (27 V), the efficiency factors varied between 72% in the morning to 89% at the peak hours. For Cell C (41 V), efficiency factors ranged between 76% in the morning to 90% at the peak hours. For Cell B (27 V) and Cell C (41 V), the voltage drop near the anode had decreased as the applied

voltage increased. Similar to Cell A the voltage drop near the cathode for Cell B and Cell C was independent of the applied voltage.

5.3.2 Water collected and water content

The water collected before the application of the electrical field from Cells A, B, C, and D were 89, 143, 101, 124 mL, respectively. The cumulative volume of water drained from the soil during the electrokinetic remediation tests is shown in Figure 5.6. As seen in the figure, cumulative volumes of 493, 960, and 1024 mL were collected by the end of the test from Cells A, B, and C, respectively, with volume increasing with the increase in voltage. The much larger volumes collected in the electrokinetic tests were due to electroosmosis flow. The volume of water collected in the control test was due to soil consolidation by the surcharge pressure (5 kPa) exerted on the soil, while the water collected in the electrokinetic tests was due to the electroosmosis along with the consolidation. Figure 5.6 shows the volume of water collected during the early hours of the remediation, i.e. immediately following the 72 hr of loading, to be higher than that during the late hours of the remediation. This is to be expected as more water was available at the start of the remediation process. At the end of the tests, the difference between the volumes of water collected in Cells B and A was 467 mL compared with difference of only 64 mL between Cells C and B. The results showed that the voltage increase of 100% (from 13.5 to 27 V) increased the volume of water drained by electroosmosis by 95% (from 493 to 960 mL). However, increasing the voltage from 27 V to 41 V (52%) had resulted in an increase of 6% only in the collected volume of water. The concentrations of the copper in water collected during electrokinetic remediation in Cells A, B, and C were 43.8 μg/l, 40.1μg/l, and

28.7 μg/l, respectively, representing a negligible amount (< 0.01%) of the initial mass of the metal. This means while electroosmosis was effective in draining water from the contaminated soil, the concentration of copper in the drained water was negligible.

Prior to the application of the electric field the average value water content of Cells A, B, C, and D were 39%, 38%, 39%, 39%, respectively. Figure 5.7 shows the water content in sections S1 to S5 along the soil specimens (see Figure 4.6). D is the horizontal distance between the mid of the soil section and the anode. D_o is the total length of the soil samples (200 mm). Thus, the water content at 0.1 D/D_o is for the section near the anode (S1), while 0.9 D/D_o represents the section near cathode (S5). Consistent with the higher volume of water drained by electroosmosis, lower water contents were observed after electrokinetic remediation as compared with the control test which demonstrated the effectiveness of electrokinetic remediation in dewatering contaminated clayey soil. Figure 5.7 shows that after electrokinetic remediation, the water contents along the soil specimen in Cells C and B were lower than the water contents in Cell A. This was to be expected as more water was drained in Cells C and B (see Figure 5.6). Contrary to the general water content trend, Figure 5.7 shows the water content at 0.7 D/D_o (S4, 60 mm from the cathode) remained relatively high and similar to that at 0.9 D/D_o (S5, 20 mm from the cathode). The high water content at 0.7 D/D_o was a result of the water produced where the acid and base fronts, generated by electrolysis reactions at the electrodes, meet (see Figure 5.8). The H^+ ions have smaller size than OH^- ions and accordingly by electromigration transport H^+ ions travel a longer distance than OH^- ions. Further, H^+ ions also travel by electroosmosis towards the cathode resulting in an acid-base meeting closer to the cathode. The formation of

water at the acid-base front junction in this study is in agreement with results by previous researchers (e.g. Narasimhan and Ranjan, 2000; Mohamedelhassan and Shang, 2003).

5.3.3 pH and electrical conductivity

Figure 5.8 shows the pH along the soil specimen after the tests. The pH of the soil prior to the test was 7.6. The figure shows that for the control test (Cell D) the pH remained at 7.6 to 7.7. For Cell A (13.5 V), the pH was < 7 for S1 and S2, and > 7 for the rest of the soil. As shown in the figure, the pH profile for Cell B (27 V) and Cell C (41 V) coincided and 60% of the soil (S1, S2, and S3) reported pH < 3.5 (i.e. acidic) with the lowest pH near the anode (2.1 and 2.2). The remaining 40 % of the soil (S4 and S5) reported pH > 7 and the highest pH was 8.9 reported near the cathode (S5) in Cell C. The pH profiles are in agreement with the electrolysis reactions at the electrodes and the distance travelled by the H^+ and OH^- ions. It is observed that at higher applied voltages (27 and 41 V) most of the soil sample becomes acidic, while at voltage of 13.5 V the largest portion remained neutral or become slightly alkaline. Heavy metals in soil are more soluble in acidic environment and thereby easier to remove. The pH of the accumulated water during the test for Cells A, B, and C were 9.1, 11, and 11.5, respectively. This can explain the low copper concentration in the water collected during the test.

The electrical conductivity of the soil pore fluid of the tests is shown in Table 5.1 to 5.4. As shown in the tables, the electrical conductivities of the pore fluid in the sections in the vicinity of the anode (S1 and S2) were in general higher than the conductivities in the sections closer to the cathode (S4 and S5). The low pH near the anode causes dissociation of cations (copper) from the contaminated soil to the pore fluid whereas the high pH in the vicinity of the cathode

results in precipitation of the copper ions in the soil pores. Also, water formed at the acid-base front junction closer to the cathode as discussed before contributing to dilution of the pore fluid near the cathode. This explains the higher and lower electrical conductivity of the pore fluid near the anode and the cathode, respectively.

5.3.4 Copper concentration

Figures 5.9 to 5.11 show the ratio (in percentage) of the copper concentration after the test (C) to the initial concentration (C_o = 150 mg Cu/kg of dry soil). The concentrations are presented for the total copper in the soil, copper in soil solids, and copper in pore fluid. The figures clearly show that the electric field generated by the solar cells was in general effective in moving copper from the anode towards the cathode. The movement however, was proportional to the applied voltage. The heavy metal migration from contaminated soil by electrokinetics is due to combine effects of electroosmosis and electromigration along with the change in the soil pH during the process. As discussed before, the concentration of copper in the water drained by electroosmosis in Cell B (27 V) and Cell C (41 V) were equally negligible. The collected volumes of water in the two tests were approximately the same and the pH profiles were almost identical (see Figure 5.8). Thus, higher copper removal from Cell C can be attributed to electromigration. The dominance role of electromigration is in agreement with previous studies by Page and Page (2002) and Probstein (1994). Acar et al., (1992) had successfully removed cadmium without electroosmosis flow.

In Cell C (41 V), 14% was the lowest ratio of the copper concentration after the test to the initial concentration, which was observed at S1 near the anode (0.1 D/D_o). Thus, 86% of the initial copper was removed from S1 of the soil specimen. This removal is greater than that achieved by the desorption test (81%) discussed in section 3.2.2.2.2. The copper concentration increases toward the cathode with the maximum concentration of 256% at S4 (the location where acid and base fronts meet). As seen in Figures 5.9 to 5.11, the highest ratio of copper in soil pore fluid was observed near the anode and the ratio decreased towards the cathode. This is a result of the low pH near the anode which promotes copper dissolution and the high pH at the cathode which results in copper precipitation.

Refer to Appendix A for ICP-OES results.

5.4 CONCLUSIONS

The electric power generated by solar cells was sufficient for electrokinetic remediation of homogeneous clay contaminated with 150 mg copper per kg dry soil. The highest copper removal was reported in soil section near anode (S1) in Cell C (41 V). The efficiency of the applied voltage increased with the increase in voltage with maximum efficiency of 79% at 13.5 V and 90% at 41 V. The voltage and current generated by the solar cell flocculated during the day time and diminished at night. The highest electric currents were reported at the start of the tests. The copper concentration in the water drained by electroosmosis was negligible in all tests. The volume of water drained by electroosmosis and the change of soil pH were almost identical for applied voltages of 27 V and 41 V. Therefore, the significant amount

of copper removed from part of Cell C (41 V) in particular near the anode was due to electromigration. The copper removal was found to be proportional to close proximity from the anode and the magnitude of the applied voltage.

Table 5.1 Results summary for Cell A (13.5 V) after the test.

	Distance from Anode					
	20 mm	60 mm	100 mm	140 mm	180 mm	
	S1	S2	S3	S4	S5	
	Water content (%)					
	29.6	27.6	28.2	29.0	30.0	
	Soil pore fluid pH					
	1.8	3.7	7.3	7.5	8.6	
Anode	Dry soil pH					
	2.3	6.0	7.9	8.0	8.8	
(+)	Soil pore fluid electrical conductivity (µS/cm)					Cathode
	18080	2660	1128	686	288	
	Copper in soil pore fluid (C_f /C_0)*%					(-)
	16.35	1.18	0.045	0.021	0.076	
	Copper in soil solids (C_s/C_0)**%					
	54.22	73.49	78.72	135.36	80.71	
	Total copper in dry soil (C_d/C_0)***%					
	70.58	74.67	78.76	135.38	80.79	

Table 5.2 Results summary for Cell B (27 V) after the test.

	Distance from Anode				
	20 mm	60 mm	100 mm	140 mm	180 mm
	S1	S2	S3	S4	S5
	Water content (%)				
	19.8	20.7	22.4	26.3	29.2
	Soil pore fluid pH				
	1.6	3.9	4.8	7.0	10.6
Anode	Dry soil pH				Cathode
(+)	2.1	2.8	3.3	7.7	8.8
	Soil pore fluid electrical conductivity (µS/cm)				(-)
	29900	573	178	375	897
	Copper in soil pore fluid (C_f /C_0)*%				
	6.05	0.62	0.11	0.04	0.03
	Copper in soil solids (C_s/C_0)**%				
	21.52	53.05	127.66	153.33	83.19
	Total copper in dry soil (C_d/C_0)***%				
	27.57	53.67	127.77	153.37	83.22

*C_0 initial copper concentration in soil sample, C_f Copper concentration in soil pore fluid,

** C_s Copper concentration in soil solids, and *** C_d Copper concentration in dry soil.

Table 5.3 Results summary for Cell C (41 V) after the test.

	Distance from Anode					
	20 mm	60 mm	100 mm	140 mm	180 mm	
	S1	S2	S3	S4	S5	
	Water content (%)					
	18.1	18.7	18.7	24.0	27.3	
	Soil pore fluid pH					
	1.4	3.1	6.6	8.6	11.4	
Anode (+)	Dry soil pH					Cathode (-)
	2.2	2.9	3.3	7.8	8.9	
	Soil pore fluid electrical conductivity(µS/cm)					
	51700	2900	241	893	2560	
	Copper in soil pore fluid (C_f /C_0)*%					
	8.43	1.69	0.04	0.07	0.01	
	Copper in soil solids (C_s/C_0)**%					
	5.37	29.29	84.29	233.28	104.02	
	Total copper in dry soil (C_d/C_0)***%					
	13.8	30.98	84.33	233.35	104.03	

Table 5.4 Results summary for Cell D – control after the test.

	Distance from Anode					
	20 mm	60 mm	100 mm	140 mm	180 mm	
	S1	S2	S3	S4	S5	
	Water content (%)					
	39.6	39.8	39.8	39.8	39.6	
	Soil pore fluid pH					
	7.9	7.7	7.7	7.7	7.9	
Anode (+)	Dry soil pH					Cathode (-)
	8.1	8.0	8.0	8.0	8.1	
	Soil pore fluid electrical conductivity (µS/cm)					
	3740	3760	3750	3770	3740	
	Copper in soil pore fluid (C_f /C_0)*%					
	0.053	0.053	0.053	0.053	0.053	
	Copper in soil solids (C_s/C_0)**%					
	99.94	99.94	99.94	99.94	99.94	
	Total copper in dry soil (C_d/C_0)***%					
	100	100	100	100	100	

*C_0 initial copper concentration in soil sample, C_f Copper concentration in soil pore fluid.

** C_s Copper concentration in soil solids.

*** C_d Copper concentration in dry soil.

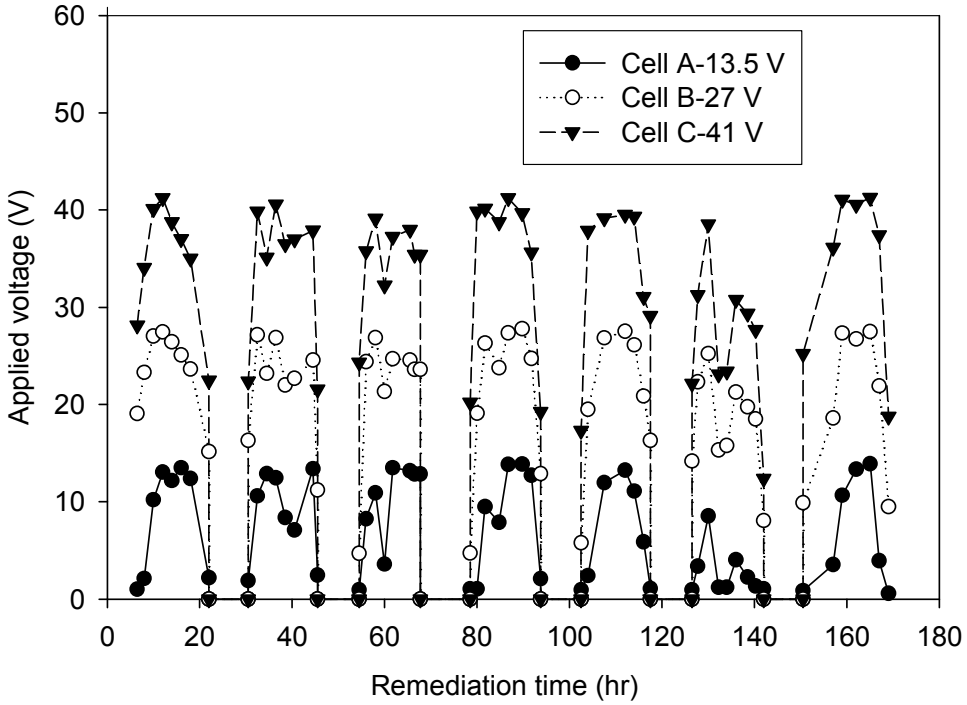

Figure 5.1 Applied voltage during the tests.

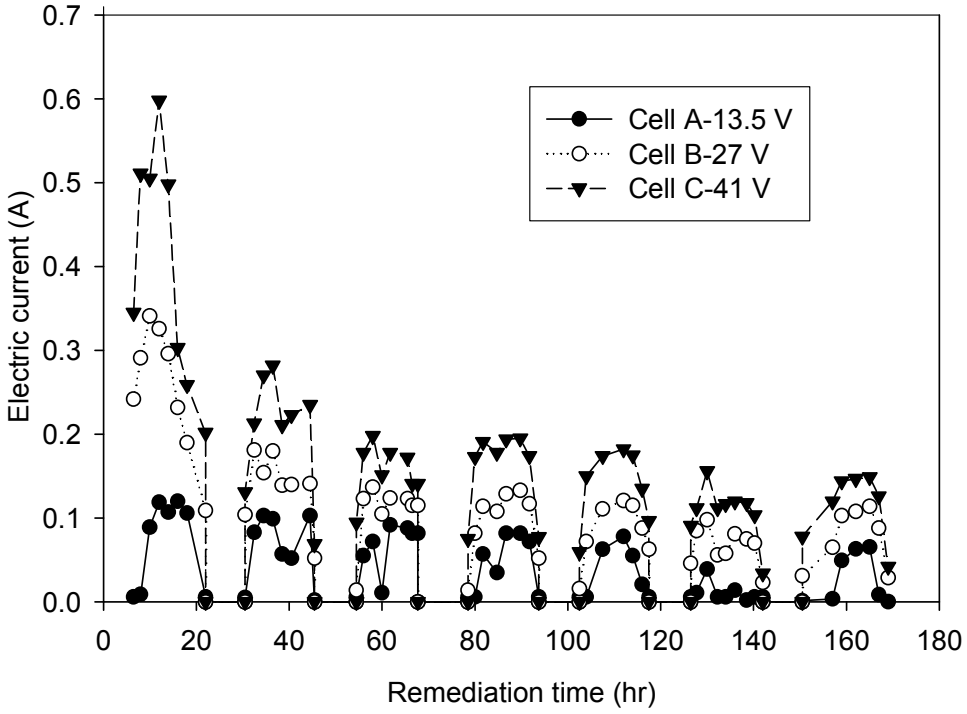

Figure 5.2 Electric current during the tests.

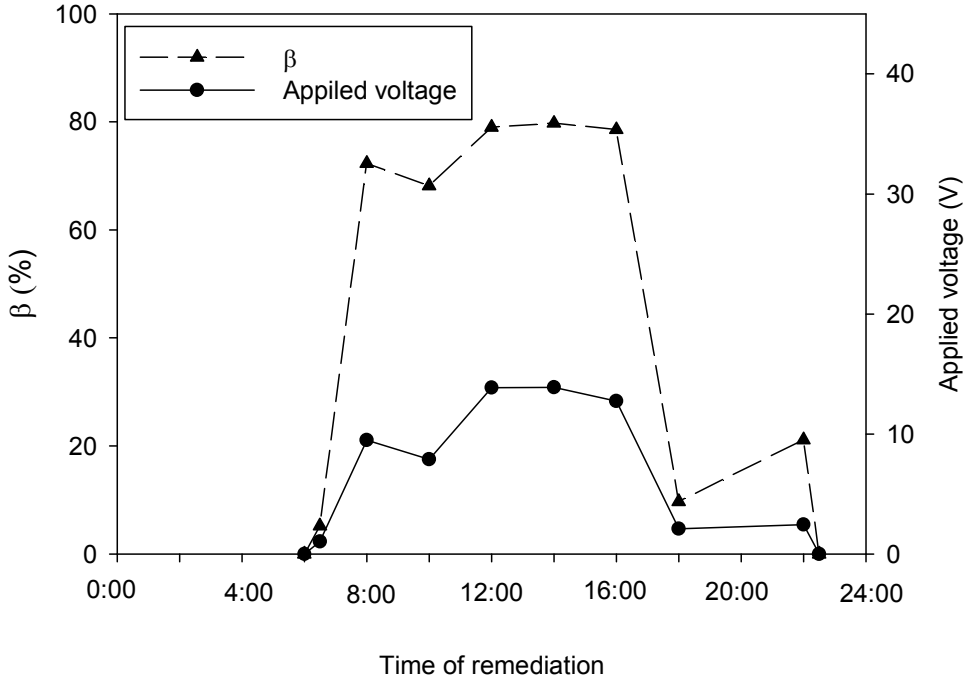

Figure 5.3 Efficiency factor (β) and applied voltage during the first day of remediation for Cell A (13.5 V).

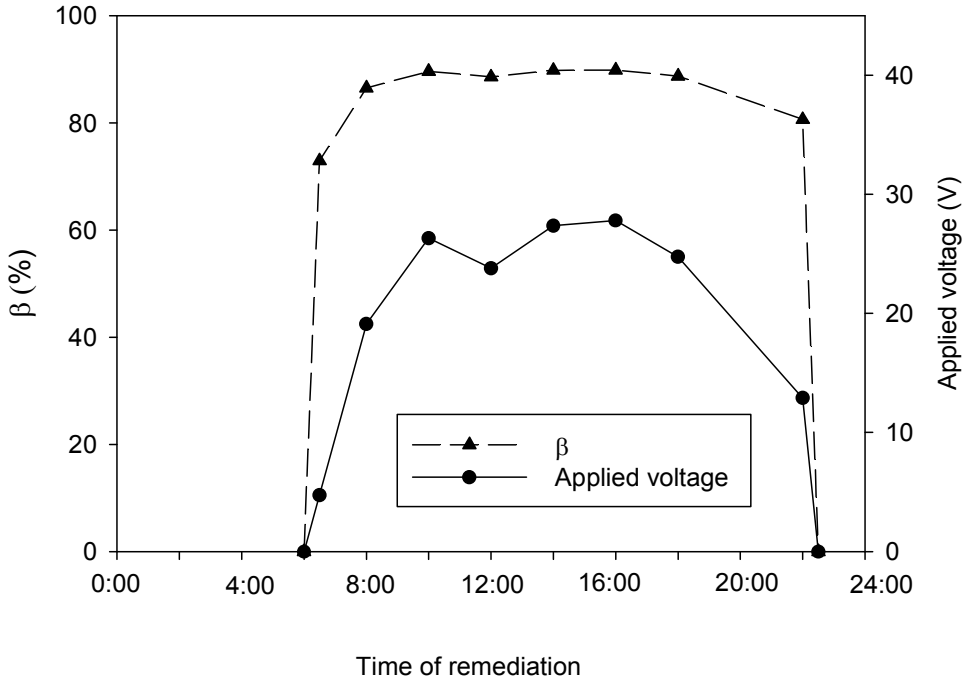

Figure 5.4 Efficiency factor (β) and applied voltage during the first day of remediation for Cell B (27 V).

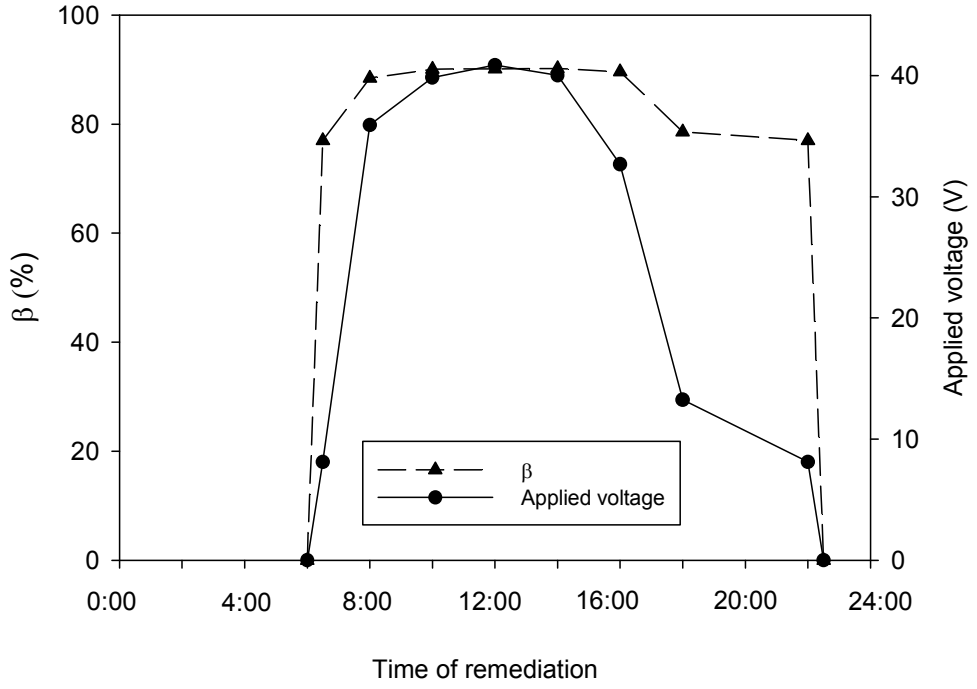

Figure 5.5 Efficiency factor (β) and applied voltage during the first day of remediation for Cell C (41 V).

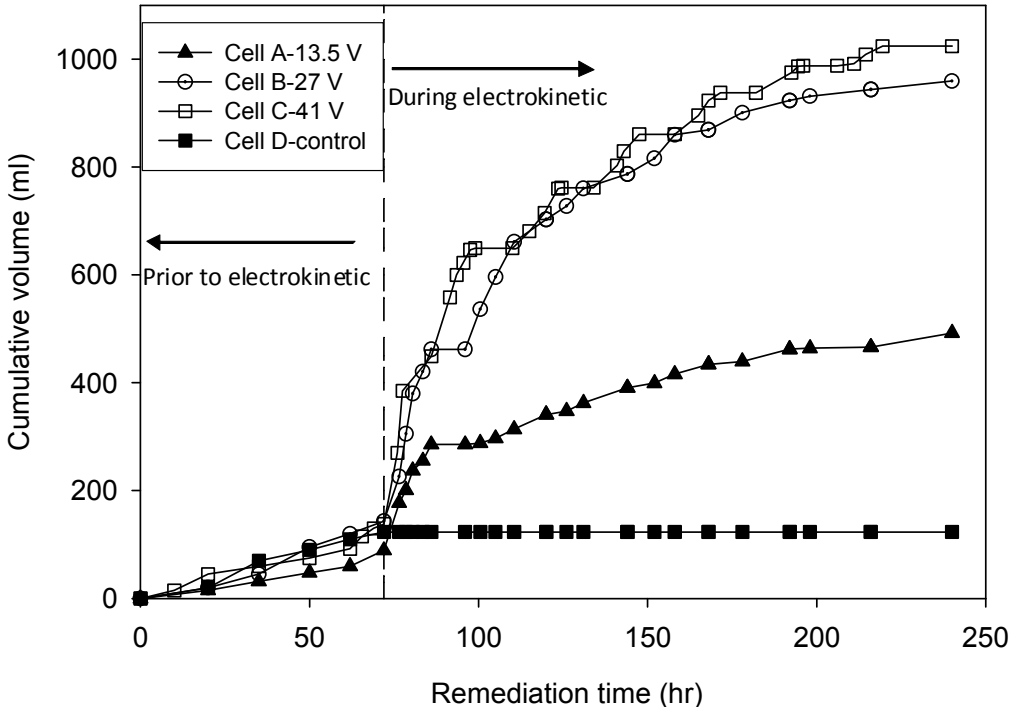

Figure 5.6 Cumulative volume of water collected during the tests.

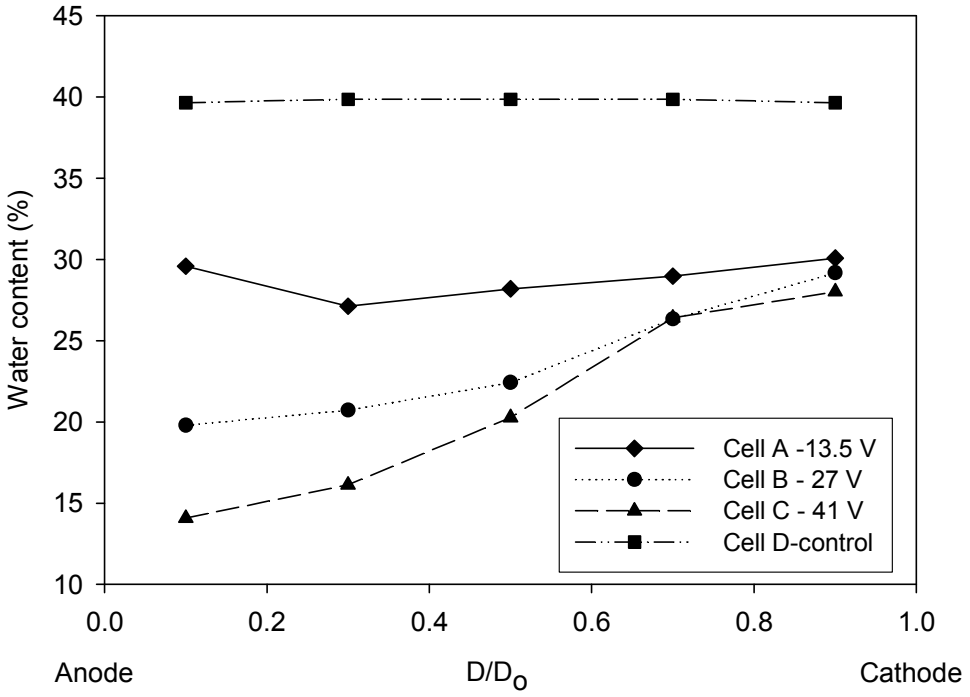

Figure 5.7 Water content after the tests.

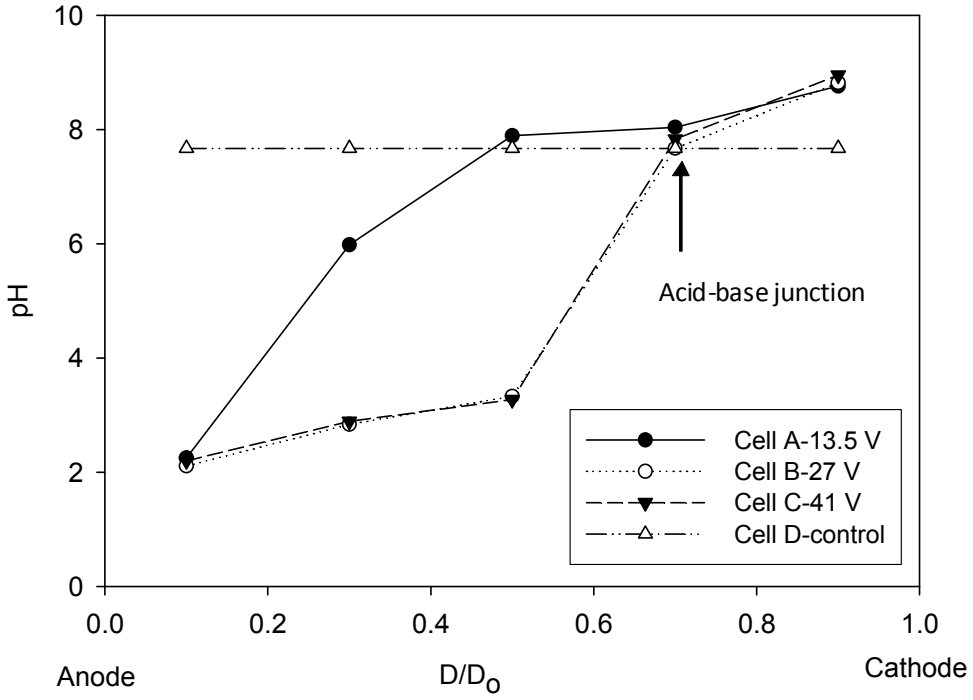

Figure 5.8 pH of the soil after the tests.

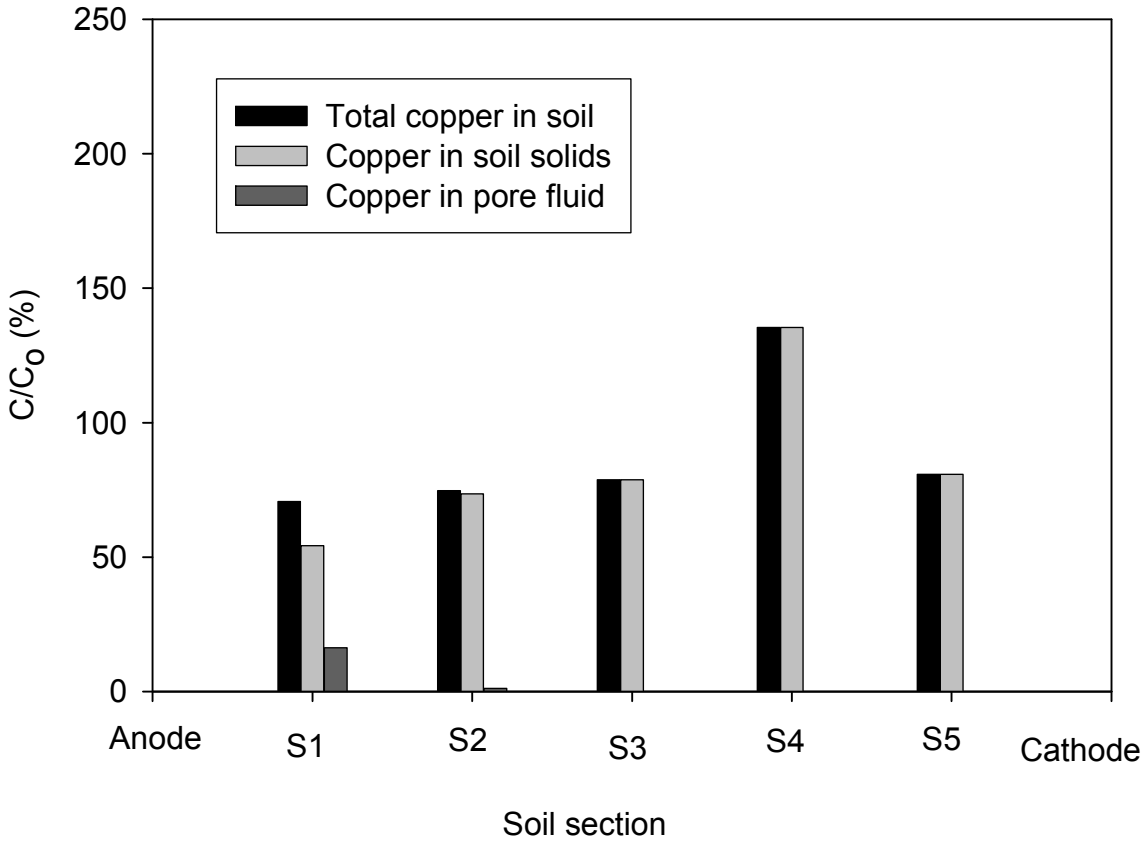

Figure 5.9 Copper concentration after the test in sections S1 to S5 for Cell A (13.5 V).

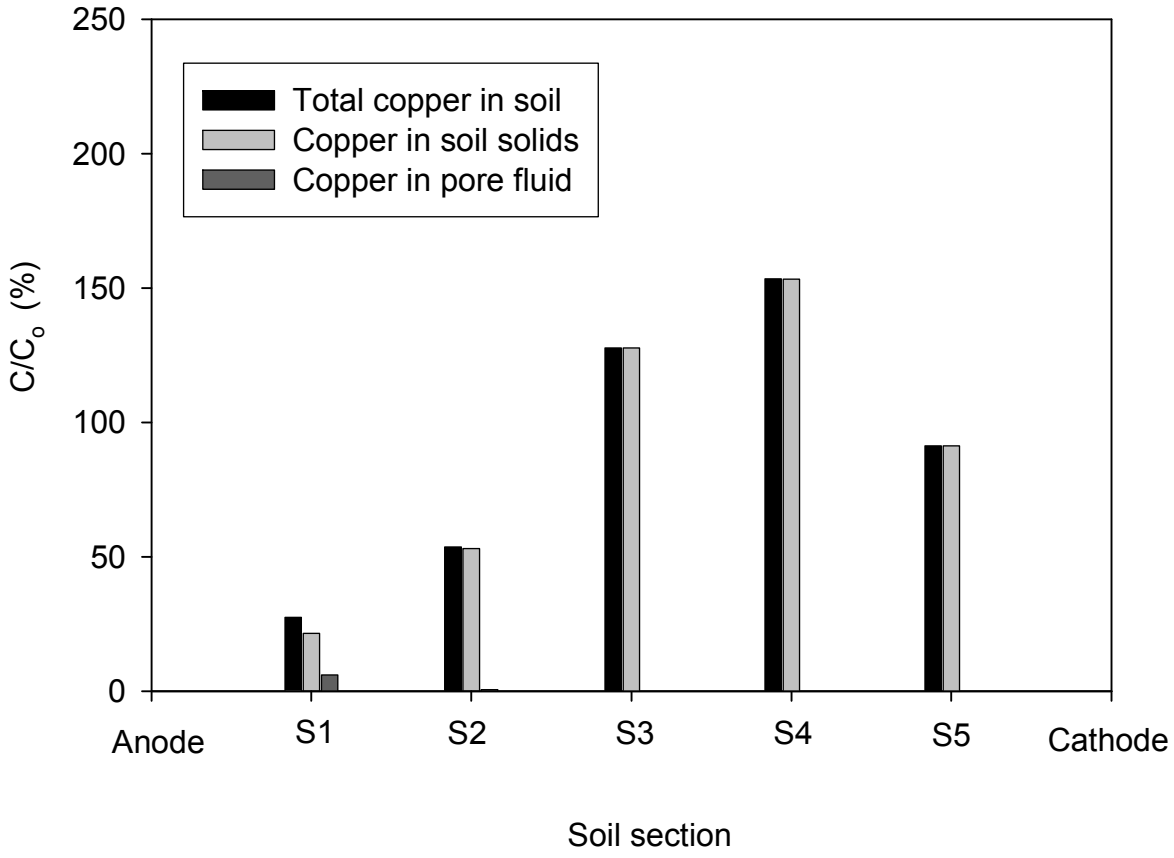

Figure 5.10 Copper cocnetration after the test in sections S1 to S5 for Cell B (27 V).

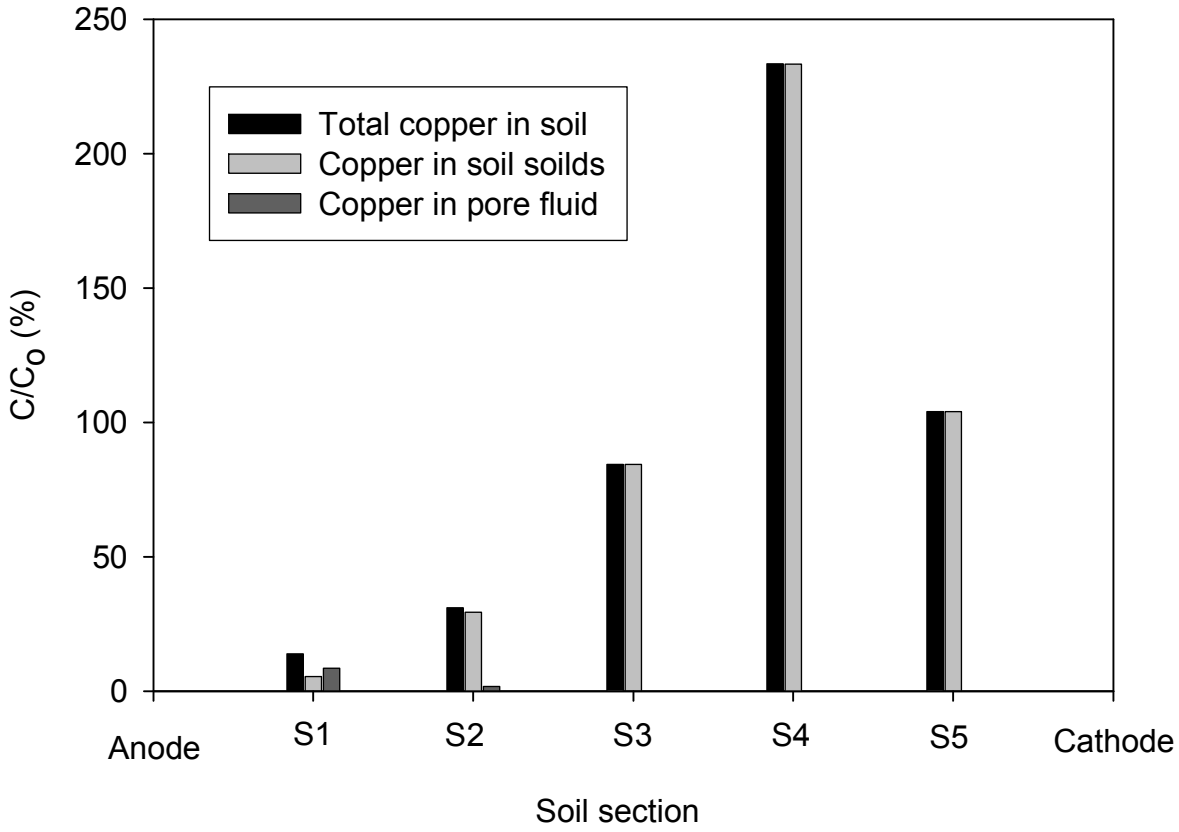

Figure 5.11 Copper concnetration after the test in sections S1 to S5 for Cell C (41 V).

CHAPTER SIX

EFFICACY OF ELECTROKINETIC REMEDIATION IN HETEROGENEOUS SOILS CONTAMINATED WITH COPPER

6.0 INTRODUCTION

Electrokinetic remediation can be effectively used in-situ for removal of contaminants from fine-grained soils with low hydraulic permeability, the most difficult to remediate by conventional methods (Vane and Zang, 1997; Page and Page, 2002). According to Buchireddy et al. (2009), among many factors the contaminated soil characteristic, either homogeneous or heterogeneous, plays dominant role in the selection of the appropriate remediation method. Due to the wide varieties in contaminated site conditions, environmental scientists believe that there will not be a single method suitable for all situations (Virkutyte et al., 2001). Rather implementation of integrated technologies can be efficient and cost-effective. Despite the numerous trials, the remediation of heterogeneous soils by conventional methods remains to be a great challenge. For instance, in-situ soil flushing process is ineffective for heterogeneous soils because the flushing fluid tends to flow through the soil with the higher permeability. This normally results in removal of the contaminant from the soil part with high permeability, whereas for the soil with low permeability only the limited diffusion mechanism will control the remediation process. On the other hand, electrokinetic remediation has a great control over the electric field distribution on the soil under treatment. The orientation of the electrodes directs the electrical current and consequently controls the contaminant transport in soil strata (Giannis and Gidarakos, 2005). This capability can make electrokinetic remediation a better alternative for heterogeneous soils. Although, most of the electrokinetic remediation

investigations were done on homogeneous soils, limited tests were carried out in heterogeneous soils (Saichek and Reddy, 2005).

This chapter discusses the effect of soil heterogeneities such as layers, pockets, and mixtures on the effectiveness of copper removal by electrokinetics. Solar cell panels were used to generate the electric field required for the remediation process. The heterogeneous soils were treated using one- and two-dimensional electrode configurations. Section 6.1.1 discusses the test procedure for one-dimensional configuration and the results are presented in section 6.2.1. The test setup and the results and discussion for the two-dimensional configuration are presented in section 6.1.2 and 6.2.2.

6.1 TEST PROCEDURES

6.1.1 One-dimensional electrode configuration

Four tests were performed with one-dimensional electrode configuration in the electrokinetic cells (see Figure 4.1). In one-dimensional configuration, the electrode covers the entire cross-sectional area of the soil perpendicular to the direction of treatment (see Figure 4.4). A homogeneous soil and three heterogeneous soils were laboratory-prepared for the tests using clay and sand. The homogeneous soil was clay. The procedure discussed in section 4.2.1 was followed to prepare and place the soil in the cell. The heterogeneous soils were clay-sand mixture, clay-sand layers, and clay with sand pockets. The heterogeneous soils were prepared and placed in the cells according to the procedure presented in section 4.2.2. In the tests, the

maximum applied voltage was 41 V, generated from one solar panel. The procedure discussed in section 4.2.5 was followed for data collection and soil sampling. For ICP-OES analysis, 5 mL of each copper solution was diluted by adding 15 mL of deionized water.

6.1.2 Two-dimensional electrode configuration

Four tests were carried out using two-dimensional electrode configuration in the electrokinetic cell shown in Figure 4.1. In two-dimensional electrode configuration, the electrode covers 24% of the area of soil (see Figure 4.5). A homogeneous clay soil and three heterogeneous soils were tested. The homogeneous clay soil was prepared as discussed in section 4.2.1. The heterogeneous soils were clay-sand mixture, clay-sand layers, and clay with sand pockets. The procedure discussed in section 4.22 was followed to prepare the soil specimens. The maximum applied voltage was 41 V generated from one solar cell panel. The procedure discussed in section 4.2.5 was followed for data collection and soil sampling. For ICP-OES analysis, 5 mL of each copper solution was diluted by adding 15 mL of deionized water.

6.2 RESULTS AND DISCUSSION

6.2.1 One-dimensional electrode configuration tests

Tables 6.1 to 6.4 summarize the results for one-dimensional configuration tests (water content, dry soil pH, soil pore fluid electrical conductivity and pH, and copper concentration) along the soil specimen. The following subsections will present and discuss the results.

6.2.1.1 Applied voltage and electric current

Figures 6.1 and 6.2 show the profile of applied voltage and electric current during the tests. The zero values were reported during the night. Figure 6.1 shows the voltage profile to be identical in the four tests. The test was started on July 26 and continued for 7 days. The applied voltage and electric current vary during the daytime according to the degree of sunshine and exposure. As seen in the figures, the applied voltage and current rapidly increased in the morning following sunrise (i.e. 6 am) and peaked between 10 am and 4 pm. The voltage and the current started to decrease towards the end of the daytime. The output potential of solar cells was zero in darkness. At the period of maximum voltages (41 V), the corresponding maximum current values (0.51, 0.4, 0.39, and 0.38 A, for the homogeneous clay, clay-sand layers, clay-sand mixture, and clay with sand pockets, respectively) were reported on the first day of remediation and the minimum values (0.15, 0.17, 0.06, and 0.11 A) were reported on the last day.

6.2.1.2 Water collected and water content

The cumulative volume of water drained from the soil during the electrokinetic remediation is shown in Figure 6.3. As seen in the figure, cumulative volumes of 1024, 875, 667, and 519 mL were collected by the end of the electrokinetic remediation from the homogeneous clay, clay-sand mixture, clay with sand pockets, and clay-sand layers, respectively. The largest volume collected in the homogeneous clay may be attributed to the higher electric current observed during the test and therefore the higher power consumption. It must be noted that the highest total volume was collected in the homogeneous clay test in spite of the lowest water collected in the test prior to the application of electric field (see Figure 6.3). This further illustrates the

effectiveness of electrokinetic in moving water in fine-grained soils. The least volume of water was collected from clay-sand layers test. This can be attributed to the low water content of the sand (19% at the beginning of the test compared with 41% in the homogeneous clay). As the sand layer had lost most of its water during the early hours of the test, the drained water was expected to be primarily from the clay layers (67% of the total area) during most of the test. As the sand layer lost its water in the early hours of the test, the electrical power consumption by the sand layer did not contribute to the collected water. Figure 6.3 shows the volume of water collected during the early hours of remediation (i.e. immediately following the 72 hr of loading) for the tests to be higher than that during the late hours of the remediation. This is to be expected as more water was available at the start of the remediation process.

At the end of remediation, the volumes of water collected in the three tests with heterogeneous soils were between 519 and 875 mL or 51% to 85% of the dewatering from homogeneous clay (1024 mL). Therefore, it can be concluded that an applied voltage of 41 V was somewhat effective in removing water from heterogeneous soils. The concentrations of the copper in water collected after electrokinetic remediation in the homogeneous clay, clay-sand mixture, clay-sand layers and clay with sand pockets were 28.7 μg/l, 25.2 μg/l, 44.5 μg/l, and 7.6 μg/l, respectively, which represent a negligible amount (< 0.01%) of the initial mass. This means while electroosmosis was effective in draining the contaminated soils from water, the amount of copper in the drained water was negligible.

Figure 6.4 shows the water content along the soil specimen after the test. For the heterogeneous soils, the clay/sand ratio was kept at 2/1 for the samples used for the water content, pH, and copper concentration. D is the horizontal distance between the centre of the layer and the anode and D_o is the total length of the soil samples. Thus, the water content at 0.1 D/D_o represents the soil section near the anode (S1), while 0.9 D/D_o represents the section near the cathode (S5) (see Figure 4.6). Although electroosmosis flow was responsible for dewatering the cells, the movement of H^+ and OH^- ions towards the oppositely charged electrode also affects the water content of the soil. Figure 6.4 shows an increase in water content in the sections close to the cathode in most of the tests. For distance up to 0.6 D/D_o, the water content in all the tests was consistent with the volume of water drained from the corresponding cell. On the other hand, the water contents between 0.6 D/D_o and 0.9 D/D_o were found to be independent on the volume of water drained. For example, while the least volume of water was drained in the clay-sand layers test, the lowest water content at 0.7 D/D_o (60 mm from the cathode) and 0.9 D/D_o (20 mm from the cathode) was found in the clay-sand mixture test. As seen in Figure 6.4, the water content at 0.7 D/D_o remained high and roughly similar or slightly higher to that at 0.9 D/D_o. The high water content at 0.7 D/D_o is a result of the water formed when the acid and base front meet as discussed in section 5.3.2.

6.2.1.3 pH and electrical conductivity

Figure 6.5 shows the pH along the soil specimen after the tests. The initial pH of the clay and sand soils were 7.6 and 6.1, respectively. In accordance with electrolysis reactions, the pH profiles for the soils after the tests were acidic near the anode (< 4) and basic in the area close

to cathode (> 7). The lowest pH values of 2.2 and 2.5 were reported in the homogeneous clay and the clay-sand mixture, respectively. The pH of section S1 in the clay-sand layers and clay with sand pockets specimens were slightly higher than the previous tests. In agreement with electrolysis reactions near the cathode, the highest pH values were observed at sections S5 and varied between 8.6 and 8.9. As expected, Figure 6.5 shows that the distance travelled by the H^+ ions to be greater than that traveled by OH^- ions. Figure 6.5 shows the pH profiles after electrokinetic remediation of heterogeneous soils to have the same general trend of that of homogeneous soil.

Tables 6.1 to 6.4 show the electrical conductivity of the pore fluid for the homogeneous and heterogeneous soils. As the soil sample composed of clay and sand, the sand tends to lose its moisture. The sand soil retains no or few cations as sand among all types of soils has the lowest total electrical charge per unit surface area (Acar et al., 1995). The hydrogen ions (H^+) generated by electrolysis reaction cause desorption of the cations from the clay soil. Therefore, the soil pore fluid electrical conductivity is influenced by the pH of clay soil and the amount of cations released into the soil pore fluid. The effects of the electroosmosis and electromigration flow on the electrical conductivity were discussed in section 5.3.1. The tables show that the electrical conductivity varied from the anode to cathode. The electrical conductivity near the anode and cathode were relatively high. The high electrical conductivity near the anode can be attributed to the low pH near the anode that results in high ionic concentration and dissolution of ions from the soil.

6.2.1.4 Copper concentration

Figures 6.6 to 6.9 show the ratio (in percentage) of copper concentration after remediation (C) to the initial copper concentration (C_o = 150 mg Cu /kg of dry soil) in the soil sections (refer to Figure 4.6). Figures 6.6 to 6.9 clearly show that the power generated by solar cell panel for electrokinetic remediation was effective in moving copper from the anode toward the cathode in homogeneous and heterogeneous soils. Figure 6.6 shows that substantial amounts of copper were removed from sections S1 (87%) and S2 (72%) of clay-sand mixture and precipitated at specimen S3. For clay-sand layers, shown in Figure 6.7, it was found that 57%, 33%, and 23% of the initial copper was removed from sections S1, S2, and S3, respectively. The removed copper precipitated in sections S4 and S5. In Figure 6.8, 60% of initial copper was removed from section S1 and about 20% from S2 in clay with sand pockets specimen and most of the removed copper accumulated in S4. For homogeneous clay, Figure 6.9 shows that appreciable amounts of copper (86%) and (69%) were removed from S1 and S2. Sixteen percent of copper was also removed from S3. All the removed copper precipitated in S4. By comparing Figure 6.5 to Figures 6.6 to 6.9, it is obvious that the copper precipitated near or at acid-base front junction. This is in agreement with earlier results from this study (chapter 5) and previous studies (e.g. Hamed et al., 1991; Acar and Alshawabkeh, 1993; Acar et al., 1994).

The copper removal from the clay with sand pockets and clay-sand layers was not as high as that of the other tests, yet this study shows that electrokinetics can be effective in removing copper from parts of heterogeneous soils. In the clay-sand layers and clay with sand pockets tortuosity can cause faster movement of the dissolution agent (H^+ ions) and consequently less

copper removal. A longer remediation time may be needed to remove substantial amount of heavy metals from heterogeneous soils.

6.2.2 Two-dimensional electrode configuration tests

Tables 6.5 to 6.8 summarize the results for two-dimensional configuration tests (water content, dry soil pH, soil pore fluid electrical conductivity and pH, and copper concentration) along the soil specimens.

6.2.2.1 Applied voltage and electric current

Figures 6.10 and 6.11 show the profile of applied voltage and electric current during the four remediation tests. Figure 6.10 shows the voltage trend with two-dimensional electrode configuration to be identical to that with one-dimensional configuration. In Figure 6.11, the maximum electric currents were 0.55, 0.435, 0.37, and 0.37 A for the homogeneous clay, clay-sand mixture, clay with sand buckets, and clay-sand layer, respectively reported on the first day of the test and the minimum values were 0.29, 0.11, 0.14, and 0.16 A reported on the last day of the test. The higher current values reported in the test with two-dimensional electrode configuration can be attributed to the higher water content compared with the one-dimensional configuration. As shown in Figure 6.11, the decrease in current with time resulted from the decrease in electrical conductivity of the soil as discussed in section 5.3.1.

6.2.2.2 Water content

Figure 6.12 shows the water content after the tests. The water content at 0.1 D/D_o represents the section near the anode (S1), while 0.9 D/D_o represents the section near cathode (S5) (see Figure 4.6). In accordance with electroosmosis, the general trend shows the water content to increase toward the cathode. Figure 6.12 shows that the water content in all sections was higher than the water content in one-dimensional electrodes configuration test (see Figure 6.4). This can be attributed to soil zone with minimum electric field resulted from two-dimensional electrode configuration. As in previous tests, the formation of water at the acid-base front junction influences the trends of the water content.

6.2.2.3 pH

Figure 6.13 shows the pH of the soil along the soil specimen after the tests. The shown pH represents the average pH of the section. The trends of the pH are generally in agreement with the effect of electrolysis reactions at the electrodes with low pH near the anode and high pH at the cathode. For clay-sand layers, the pH profiles for the top and bottom clay layers were acidic (< 3.3) for most of the soil, while the pH of the middle sand layer was basic in all sections except S1. The figure shows that the pH profiles of the homogeneous clay, clay with sand buckets, clay-sand mixture, and the bottom clay layer in the clay-sand layers are almost identical. For inside view, the soil in cell was divided into small specimen (15 per layer) between the electrodes and the pH values for each specimen was measured (see Figures 6.14 to 6.19). In general, the figures show that the pH values of the middle specimens to be lower than the pH values of edge specimens. This is to be expected because the middle specimens were located between the electrodes and therefore were subjected to a higher electric field compared with the edge

specimens. The pH of the specimen where the pair of anodes located was higher than the pH on the subsequent specimen. This is attributed to the fact that the pair of anodes was located 10 mm from the edge of the specimen and therefore part of the specimen was not subjected to the electric field and electrolysis reactions.

Figure 6.20 shows the soil pore fluid pH along the soil specimen after the tests. The figure shows that for the homogeneous clay the pH was acidic up to 0.7 D/D_0 and alkaline for the rest of the sample. The pH profiles for clay with sand pockets and clay-sand layers are almost identical. For clay-sand mixture, the pH values coincided with those of homogeneous clay at 0.3 D/D_0 and the other two cells at 0.5 D/D_0. Figure 6.20 clearly shows that electrokinetics was successful in lowering the pH of the pore fluid from up to 70% of the soil specimen.

6.2.2.4 Copper concentration

Figures 6.21 to 6.24 show the ratio (in percentage) of copper concentration after the remediation (C) to the initial concentration (C_o= 150 mg Cu/kg of dry soil). The concentrations are presented for the total copper in the soil, copper in soil solids, and the copper in pore fluid. The figures clearly show that the power generated by the solar panel for electrokinetic remediation with two-dimensional electrode configuration was in general effective in moving copper from the anode towards the cathode. Figure 6.21 shows that in clay-sand mixture 67% and 73% of the initial copper were removed from S1 and S2. Since the electrodes were placed 10 mm from the edge of the soil the copper concentration on soil behind the anode remained unchanged. This explains the slightly higher concentration of copper in S1. Due to the high pH

value (see Figure 6.13 and Figure 6.20), the amount of copper removed from S3 was somewhat small (10%). Most of the copper removed from S1, S2, and S3 was accumulated at S4. The precipitation of copper at S4 can be attributed to the reaction of the base front with the copper in solution. AT S4 the pH was 8.6, which falls in the range of 8 to 10, in which the solubility of copper hydroxide reaches its minimum, as shown in Figure 2.8. This caused the premature heavy metal precipitation at S4.

In available literature, the researchers tend to report the final copper percentage as a lump sum without differentiating between the amount of copper in soil solids and that on the soil pore fluid. In this research to close this gap, we paid special attention to the percentage of copper existed in pore fluid and in soil solids after the treatment. It worth mentioning that the copper dissolved in the pore fluid is easier to remove from the soil. However, the pHs of the water collected in the cathode compartment during the test were between 10 to 11 for all cells. The soil pore fluid squeezer was used to recover the pore fluid and the copper concentration was obtained. For clay-sand mixture, the amounts of copper in water were zero at S3, S4, and S5, while 5.2% and 8.2% were found at S1 and S2 respectively. Figure 6.22 shows that the percentages of copper removed from clay-sand layers were 32%, 28%, and 17% from S1, S2, and S3, respectively. The copper in water was 13% of the initial copper at S1 and less than 1% for the rest of the soil. Figure 6.23 shows 48%, 40%, and 26% of the initial copper in clay with sand pockets were removed from S1, S2, and S3, respectively. The copper percentage in soil pore fluid was 5.2% of the initial copper in soil at S1 and negligible amounts for the other sections. For homogeneous clay, Figure 6.24 shows that 83% and 86% of initial copper were

removed from S1 and S2, respectively. Forty-eight percent of initial copper was removed from S3. The percentages of copper in pore fluid were 9%, 6%, 1%, 0.2 and 0.03% in S1, S2, S3, S4 and S5, respectively. This is in agreement with dissolution of copper at low pH (see Figure 6.13 and Figure 6.20).

Refer to Appendixes B and C for ICP-OES results.

6.3 CONCLUSIONS

The power generated from solar panels was sufficient for successful electrokinetic remediation with one-and two-dimensional electrode configurations for homogeneous and heterogeneous soils contaminated with 150 mg of copper per kg of dry soil. The electrokinetic remediation with one-dimensional as well as two-dimensional configuration was effective in producing acidic medium near the anode and basic environment at the cathode vicinity. High amount of water was drained from homogeneous clay by electroosmosis compared with that removed from the heterogeneous soils. This further confirms the effectiveness of electrokinetic remediation for fine-grained soils. The pH profiles and the water removal are indicators for the success of electrokinetic remediation treatment with solar energy. Significant amount of copper was removed from soil specimen near the anode in homogeneous and clay-sand mixture tests. For clay-sand layers, one third of the generated electric field was consumed in the sand layer. This may explain the lower percentage of removal in clay-sand layers. The copper removal in the one-dimensional configuration tests was almost similar in clay-sand layer and clay with sand

buckets. The lowest copper removal for two-dimensional configuration tests was reported in clay-sand layer. These encouraging results laid the ground for future research in removing heavy metal from heterogeneous soils.

Table 6.1 Results summary after the test with one-dimensional electrode configuration for the clay-sand mixture.

	Distance from Anode					
	20 mm	60 mm	100 mm	140 mm	180 mm	
	S1	S2	S3	S4	S5	
	Water content (%)					
	16.4	19.2	21.6	25.2	26.2	
	Soil pore fluid pH					
	1.8	3.3	4.6	8.1	11.3	
Anode (+)	Dry soil pH					Cathode (-)
	2.5	3.7	6.6	8.6	8.6	
	Soil pore fluid electrical conductivity (µS/cm)					
	15640	531	1122	162	2040	
	Copper in soil pore fluid (C_f /C_0)*%					
	2.65	0.06	0.41	0.02	0.01	
	Copper in soil solids (C_s/C_0)**%					
	9.89	27.89	201.72	103.98	101.32	
	Total copper in dry soil (C_d/C_0)***%					
	12.54	27.95	202.13	104.0	101.33	

Table 6.2 Results summary after the test with one-dimensional electrode configuration for the clay-sand layers.

	Distance from Anode					
	20 mm	60 mm	100 mm	140 mm	180 mm	
	S1	S2	S3	S4	S5	
	Water content (%)					
	26.3	24.8	28.7	28.6	28.4	
	Soil pore fluid pH					
	6.7	6.8	6.9	8.5	10.1	
Anode	Dry soil pH					Cathode
	3.3	4.4	4.5	6.2	9.0	
(+)	Soil pore fluid electrical conductivity (µS/cm)					(-)
	3280	342	560	467	431	
	Copper in soil pore fluid (C_f /C_0)*%					
	0.04	0.19	0.09	0.01	0.01	
	Copper in soil solids (C_s/C_0)**%					
	42.31	66.69	76.96	102.23	146.47	
	Total copper in dry soil (C_d/C_0)***%					
	42.35	66.88	77.05	102.24	146.48	

*C_0 initial copper concentration in soil sample, C_f Copper concentration in soil pore fluid,

**C_s Copper concentration in soil solids,

***C_d Copper concentration in dry soil.

Table 6.3 Results summary after the test with one-dimensional electrode configuration for the clay with sand pockets.

	Distance from Anode					
	20 mm	60 mm	100 mm	140 mm	180 mm	
	S1	S2	S3	S4	S5	
	Water content (%)					
	22.4	23.4	25.4	32.9	30.5	
	Soil pore fluid pH					
Anode (+)	4.2	4.2	5.9	7.4	10.4	Cathode (-)
	Dry soil pH					
	3.0	4.5	5.9	7.2	8.9	
	Soil pore fluid electrical conductivity (µS/cm)					
	6150	2460	311	576	543	
	Copper in soil pore fluid (C_f /C_0) *%					
	5.49	2.19	0.13	0.03	0.01	
	Copper in soil solids (C_s/C_0)**%					
	33.81	76.86	102.53	132.19	103.26	
	Total copper in dry soil (C_d/C_0)***%					
	39.3	79.05	102.66	132.22	103.27	

Table 6.4 Results summary after the test with one-dimensional electrode configuration for the homogeneous clay.

	Distance from Anode					
	20 mm	60 mm	100 mm	140 mm	180 mm	
	S1	S2	S3	S4	S5	
	Water content (%)					
	18.1	18.1	18.7	24.0	27.3	
	Soil pore fluid pH					
	1.4	3.1	6.6	8.6	11.4	
Anode (+)	Dry soil pH					Cathode (-)
	2.2	2.9	3.3	7.8	8.9	
	Soil pore fluid electrical conductivity (µS/cm)					
	51700	2900	241	893	2560	
	Copper in soil pore fluid (C_f /C_0)*%					
	8.43	1.69	0.04	0.07	0.01	
	Copper in soil solids (C_s/C_0)**%					
	5.37	29.29	84.29	233.28	104.02	
	Total copper in dry soil (C_d/C_0)***%					
	13.8	30.98	84.33	233.35	104.03	

*C_0 initial copper concentration in soil sample, C_f Copper concentration in soil pore fluid,

**C_s Copper concentration in soil solids,

***C_d Copper concentration in dry soil.

Table 6.5 Results summary after the test with two-dimensional electrode configuration for the clay-sand mixture.

Anode (+)	Distance from Anode					Cathode (-)
	20 mm	60 mm	100 mm	140 mm	180 mm	
	S1	S2	S3	S4	S5	
	Water content (%)					
	16.4	19.2	21.6	25.2	26.2	
	Soil pore fluid pH					
	5.1	2.2	6.8	9.7	11.4	
	Dry soil pH					
	4.1	2.7	7.0	8.6	9.0	
	Soil pore fluid electrical conductivity (µS/cm)					
	5520	9920	503	317	3120	
	Copper in soil pore fluid (C_f /C_0)*%					
	5.28	8.16	0.06	0.04	0.04	
	Copper in soil solids (C_s/C_0)**%					
	28.28	19.05	90.23	165.93	124.99	
	Total copper in dry soil (C_d/C_0)***%					
	33.56	27.21	90.29	165.97	125.03	

*C_0 initial copper concentration in soil sample, C_f Copper concentration in soil pore fluid,

**C_s Copper concentration in soil solids,

***C_d Copper concentration in dry soil.

Table 6.6 Results summary after the test with two-dimensional electrode configuration for the clay-sand layers.

	Distance from Anode					
	20 mm	60 mm	100 mm	140 mm	180 mm	
	S1	S2	S3	S4	S5	
	Water content (%)					
	25.8	24.3	27.7	30.6	32.1	
	Soil pore fluid pH					
	3.3	6.0	6.7	7.6	10.7	
	Top clay layer pH					
	3.0	3.0	3.2	3.9	8.8	
Anode	Middle sand layer pH					Cathode
	6.8	8.4	9.1	9.3	9.1	
(+)	Bottom clay layer pH					(-)
	2.4	3.0	3.4	9.2	9.1	
	Soil pore fluid electrical conductivity (μS/cm)					
	5340	1442	388	408	887	
	Copper in soil pore fluid (C_f /C_0)*%					
	12.67	0.08	0.05	0.02	0.04	
	Copper in soil solids (C_s/C_0)**%					
	55.75	72.15	83.51	245.55	114.48	
	Total copper in dry soil (C_d/C_0)***%					
	68.42	72.23	83.56	245.57	114.52	

*C_0 initial copper concentration in soil sample, C_f Copper in soil pore fluid,

**C_s Copper concentration in soil solids,

***C_d Copper concentration in dry soil.

Table 6.7 Results summary after the test with two-dimensional electrode configuration for the clay with sand pockets.

	Distance from Anode					
	20 mm	60 mm	100 mm	140 mm	180 mm	
	S1	S2	S3	S4	S5	
	Water content (%)					
	21.9	27.9	29.9	27.9	40.9	
	Soil pore fluid pH					
Anode (+)	2.5	6.6	6.8	7.4	10.2	Cathode (-)
	Dry soil pH					
	3.4	4.2	7.6	8.3	9.0	
	Soil pore fluid electrical conductivity (µS/cm)					
	2490	635	427	218	368	
	Copper in soil pore fluid (C_f /C_0)* %					
	5.26	0.06	0.04	0.03	0.03	
	Copper in soil solids (C_s/C_0)**%					
	47.65	60.23	74.86	153.06	104.65	
	Total copper in dry soil (C_d/C_0)*** %					
	52.91	60.29	74.90	153.09	104.68	

Table 6.8 Results summary after the test with two-dimensional electrode configuration for the homogeneous clay.

	Distance from Anode					
	20 mm	60 mm	100 mm	140 mm	180 mm	
	S1	S2	S3	S4	S5	
	Water content (%)					
	30.6	24.3	27.6	34.0	34.8	
	Soil pore fluid pH					
	2.6	3.0	3.9	6.6	10.8	
Anode (+)	Dry soil pH					Cathode (-)
	2.9	2.2	4.6	8.2	9.3	
	Soil pore fluid electrical conductivity (µS/cm)					
	8060	2870	992	298	1029	
	Copper in soil pore fluid (C_f /C_0) *%					
	8.91	6.42	1.08	0.26	0.04	
	Copper in soil solids (Cs/C0)**%					
	8.77	8.04	51.28	224.26	122.95	
	Total copper in dry soil (Cd/C0)***%					
	17.68	14.46	52.36	224.52	122.99	

*C_0 initial copper concentration in soil sample, C_f Copper concentration in soil pore fluid,

**C_s Copper concentration in soil solids,

***C_d Copper concentration in dry soil.

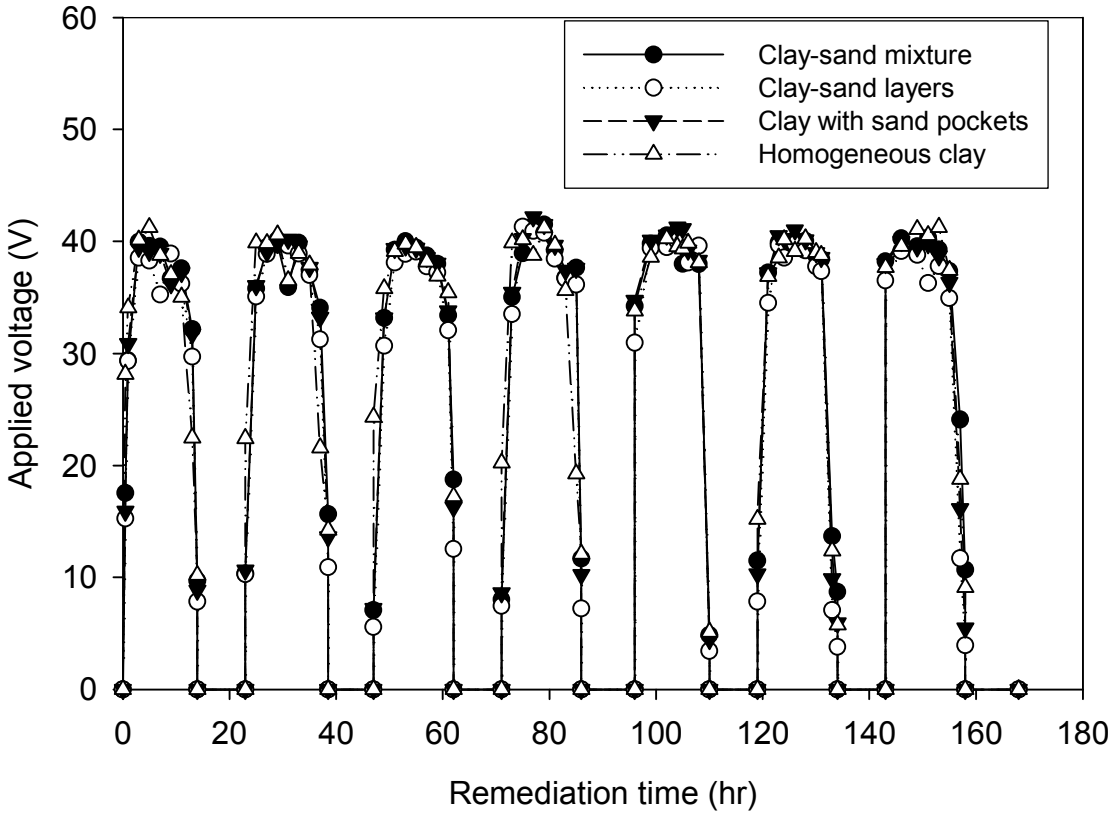

Figure 6.1 Applied voltage during the tests with for one-dimensional electrode configuration.

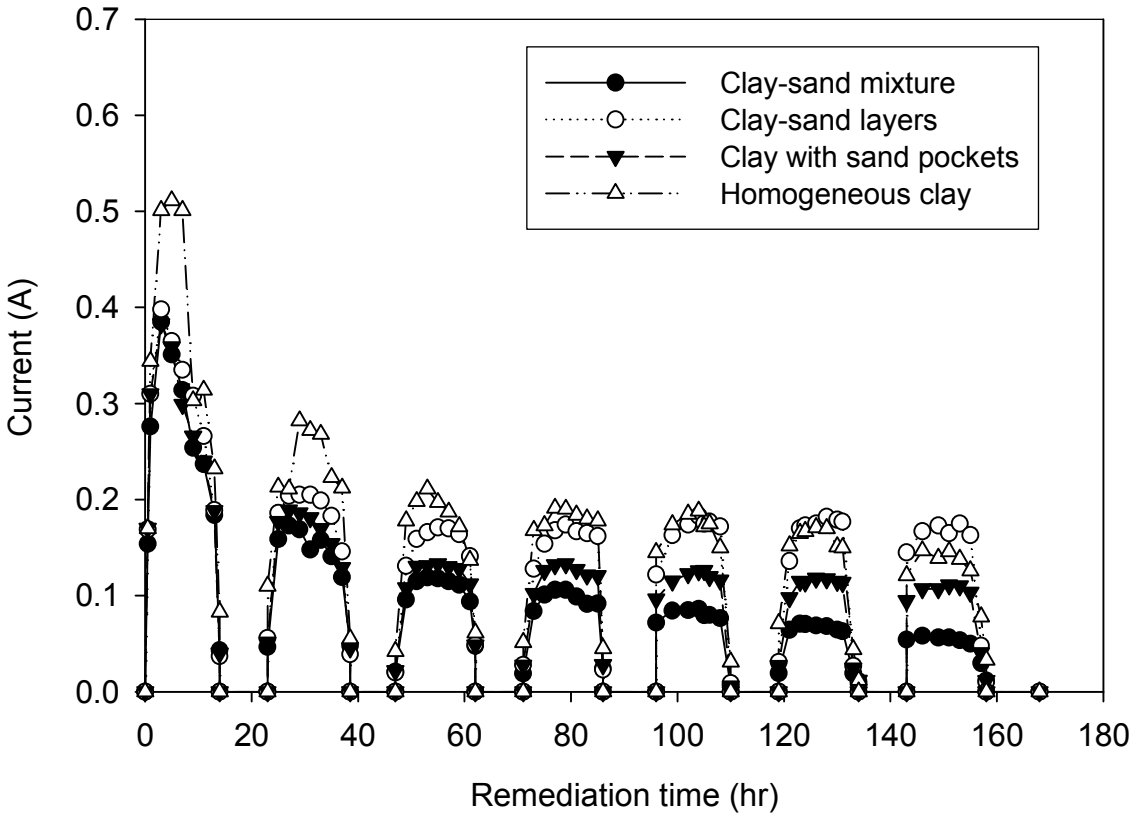

Figure 6.2 Electric current during the tests with one-dimensional electrode configuration.

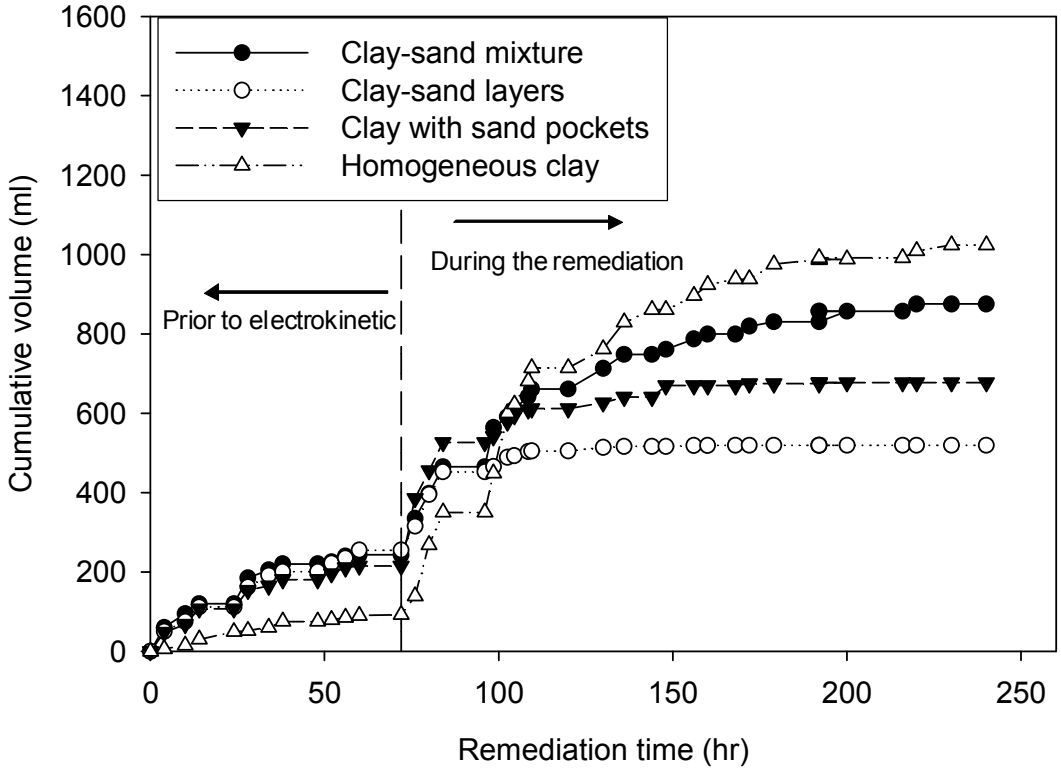

Figure 6.3 Cumulative volume of water collected during the tests with one-dimensional electrode configuration.

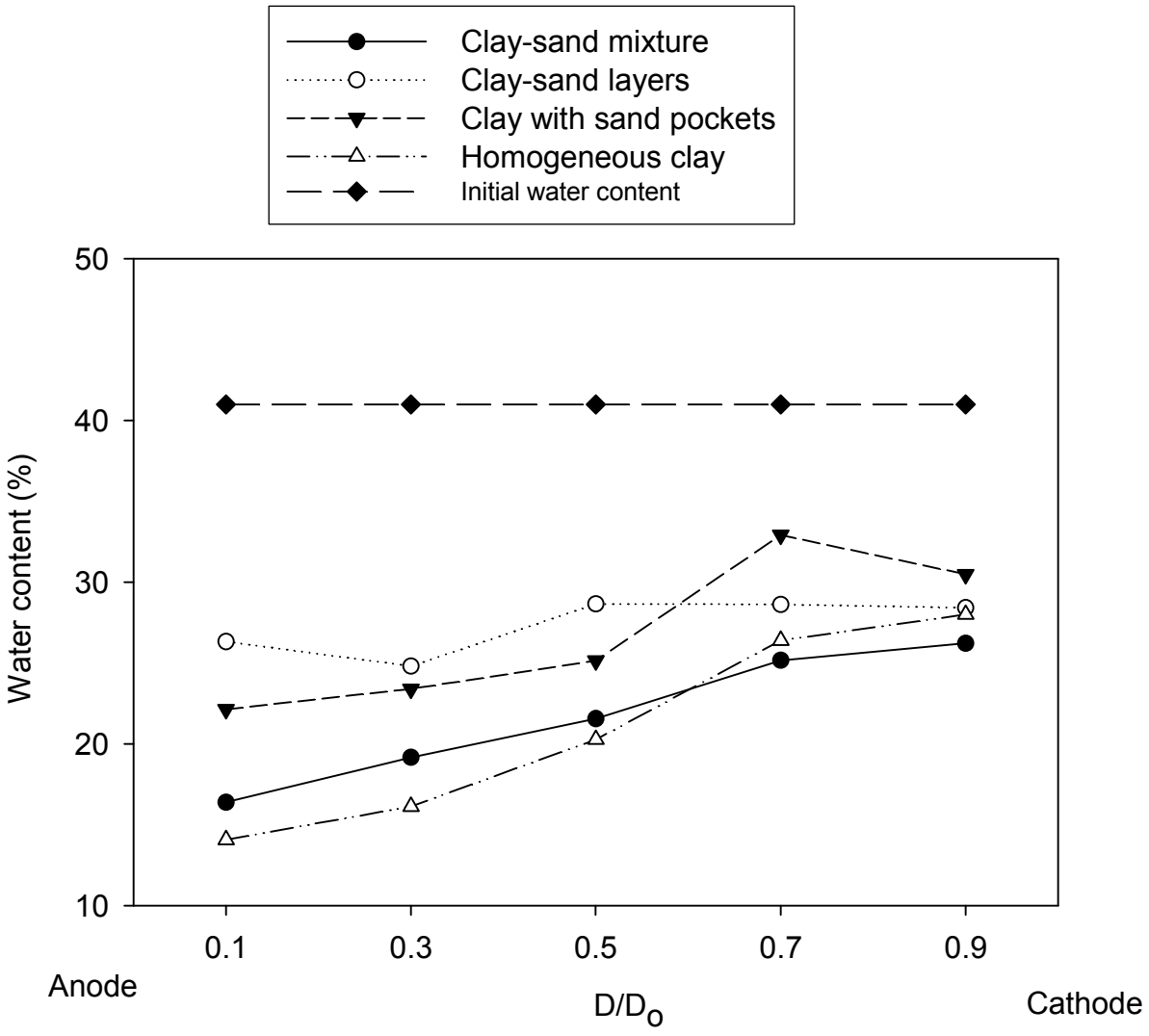

Figure 6.4 Water content vs. normalized distance from the anode for tests with one-dimensional electrode configuration.

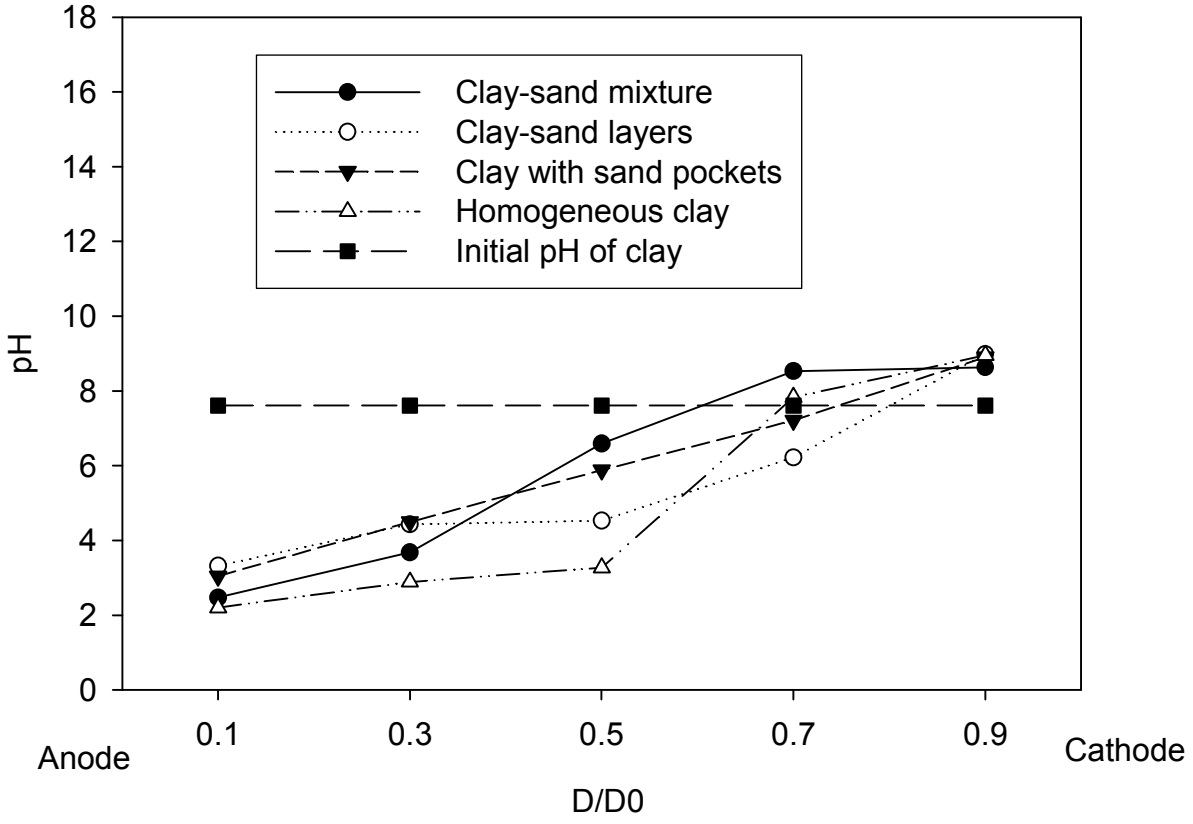

Figure 6.5 pH of the soils after the test vs. normalized distance from the anode for tests with one-dimensional electrode configuration.

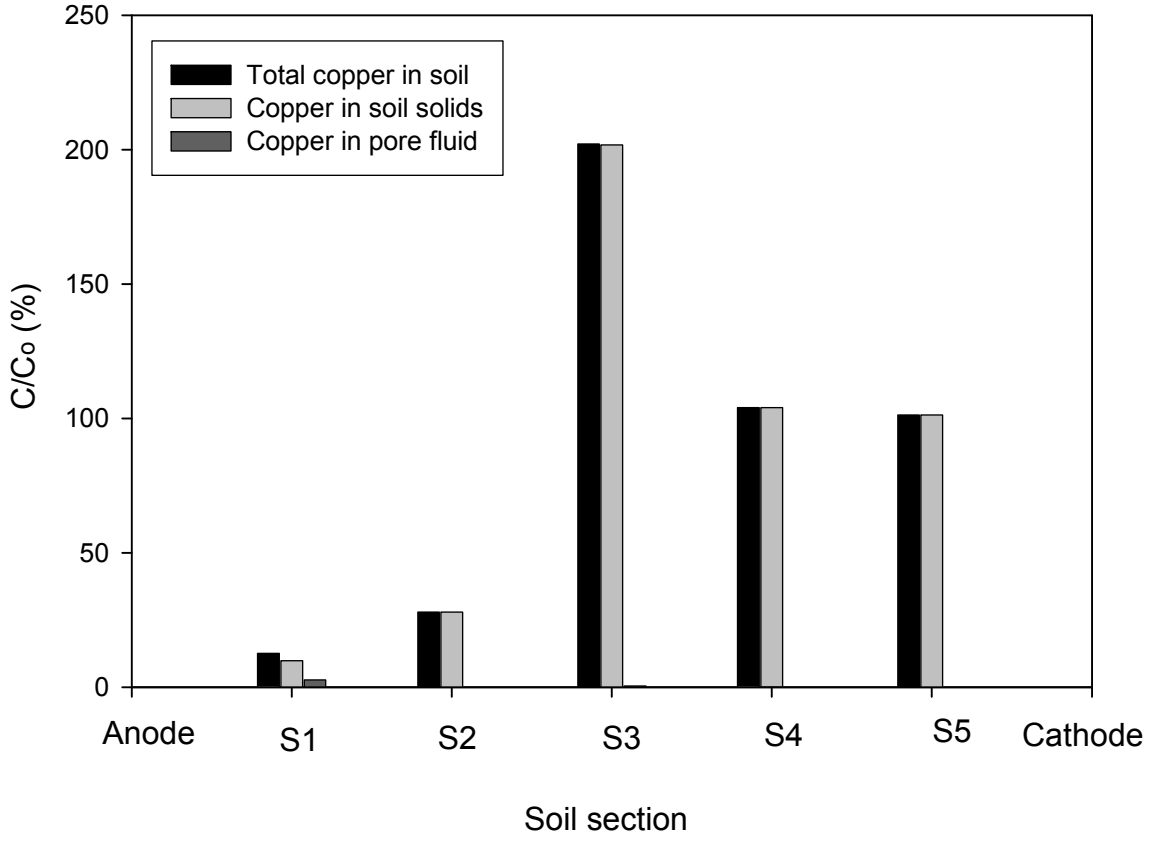

Figure 6.6 Ratio of copper concentration after the test to initial concentration (C/C_o) in sections S1 to S5 for clay-sand mixture tested with one-dimensional electrode configuration.

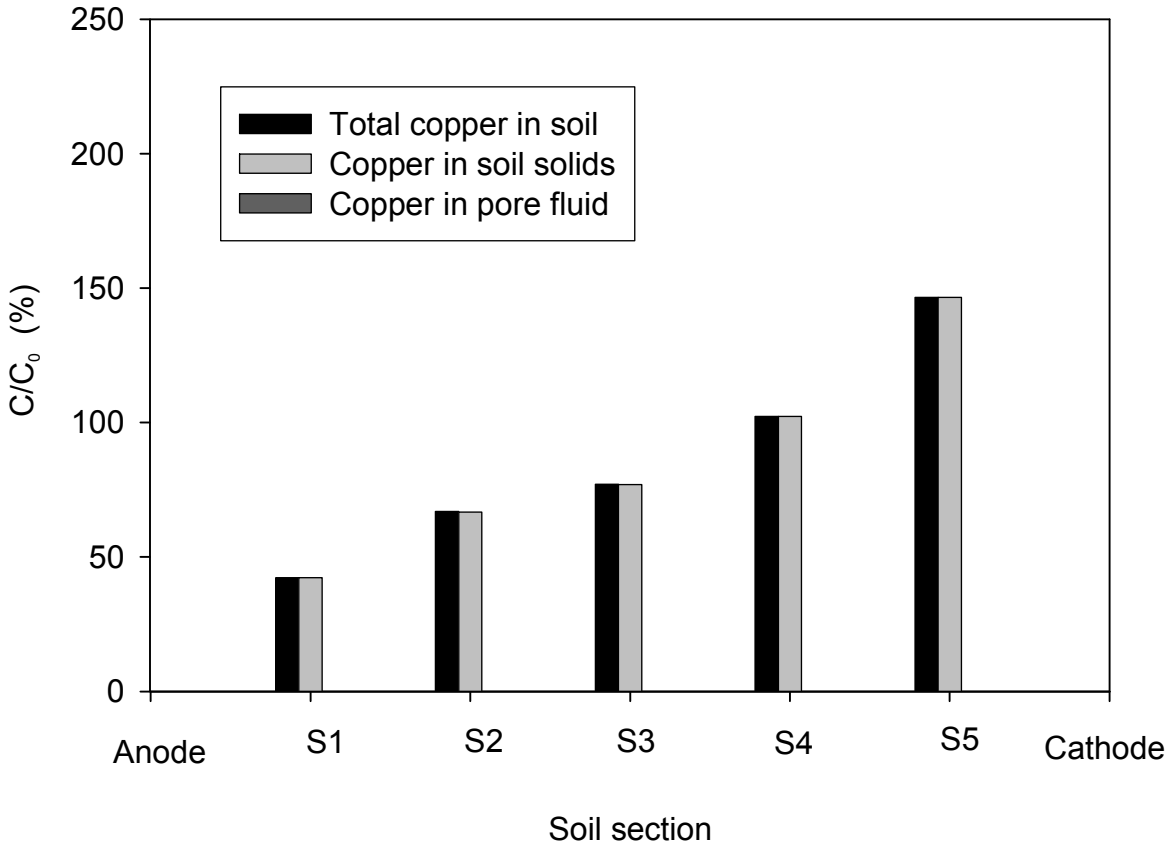

Figure 6.7 Ratio of copper concentration after the test to initial concentration (C/C_o) in sections S1 to S5 for clay-sand layers tested with one-dimensional electrode configuration.

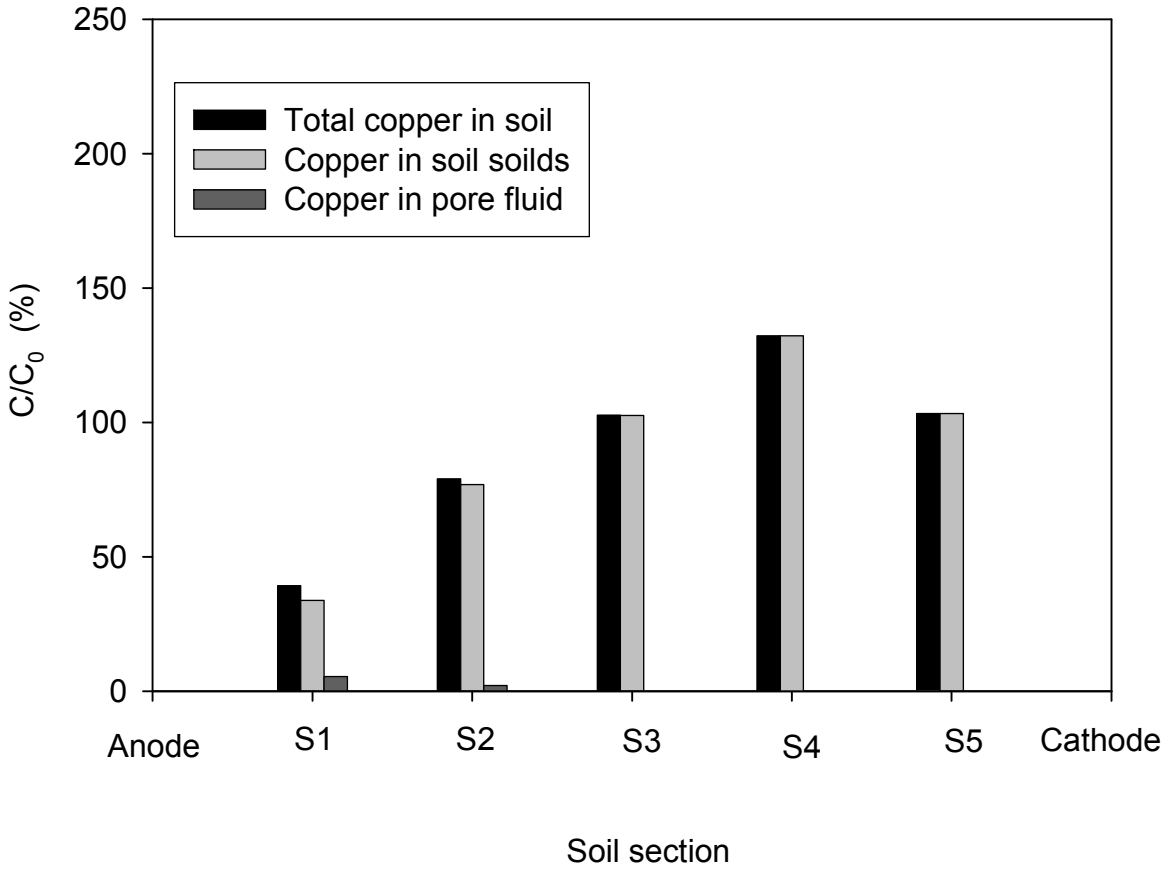

Figure 6.8 Ratio of copper concentration after the test to initial concentration (C/C_o) in sections S1 to S5 for clay with sand pockets tested with one-dimensional electrode configuration.

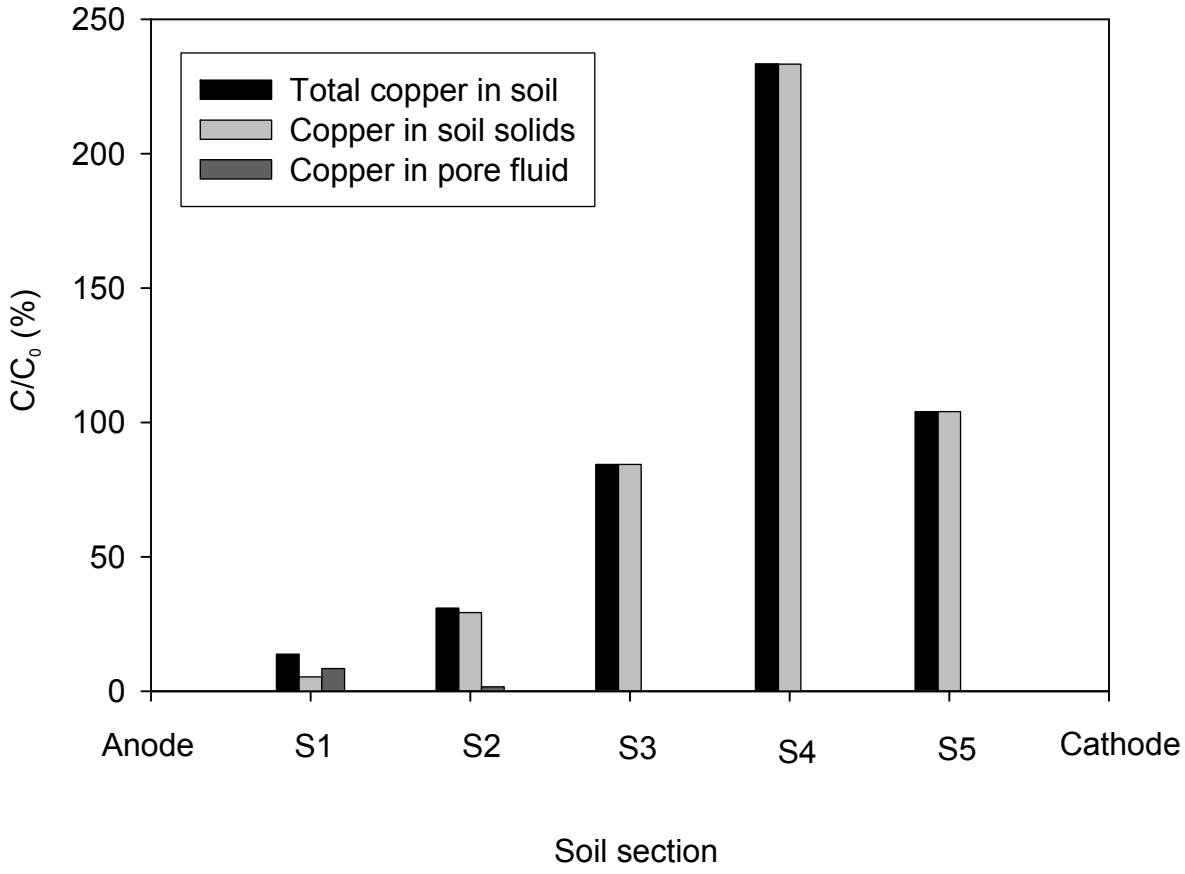

Figure 6.9 Ratio of copper concentration after the test to initial concentration (C/C_o) in sections S1 to S5 for homogeneous clay tested with one-dimensional electrode configuration.

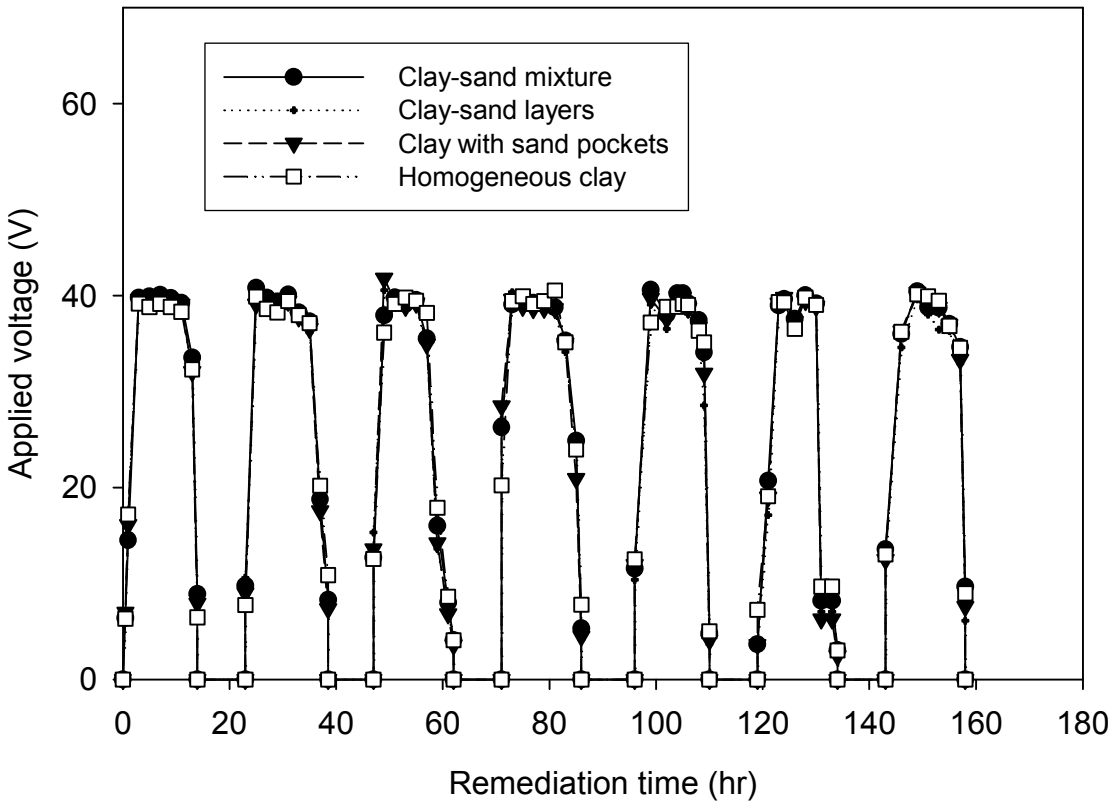

Figure 6.10 Applied voltage during the tests for two-dimensional electrode configuration.

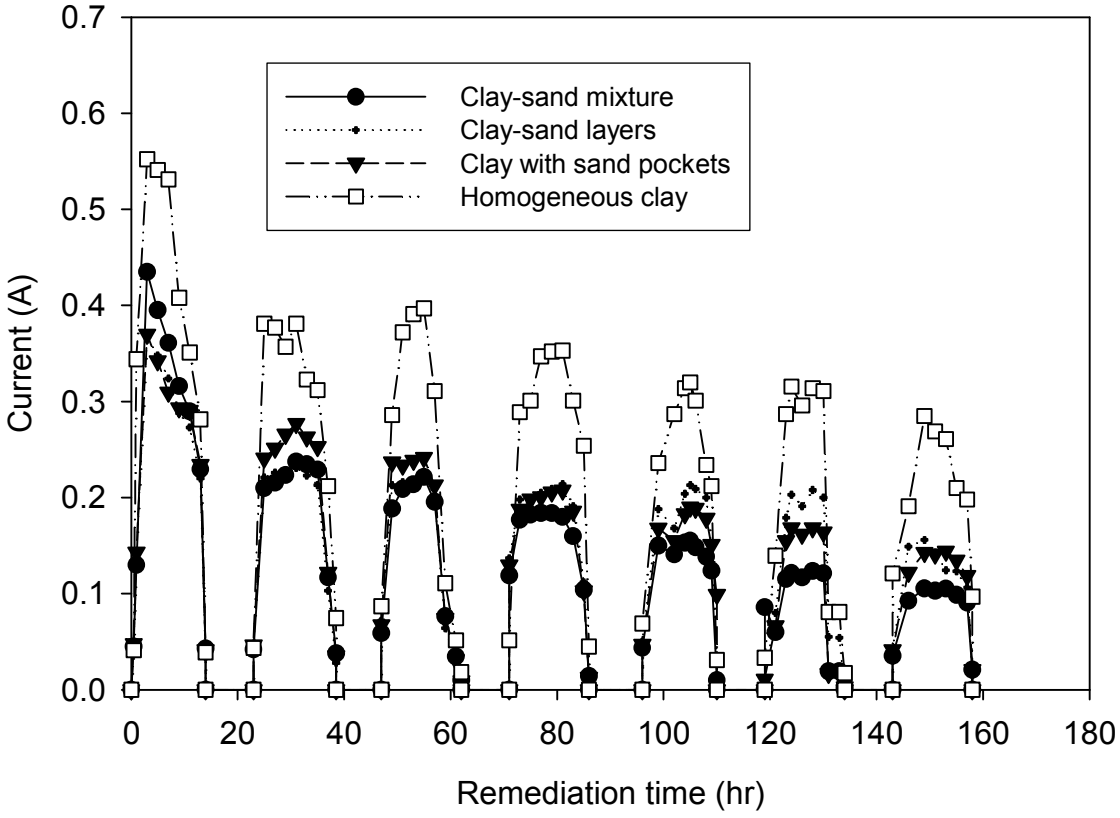

Figure 6.11 Electric current during the tests for two-dimensional electrode configuration.

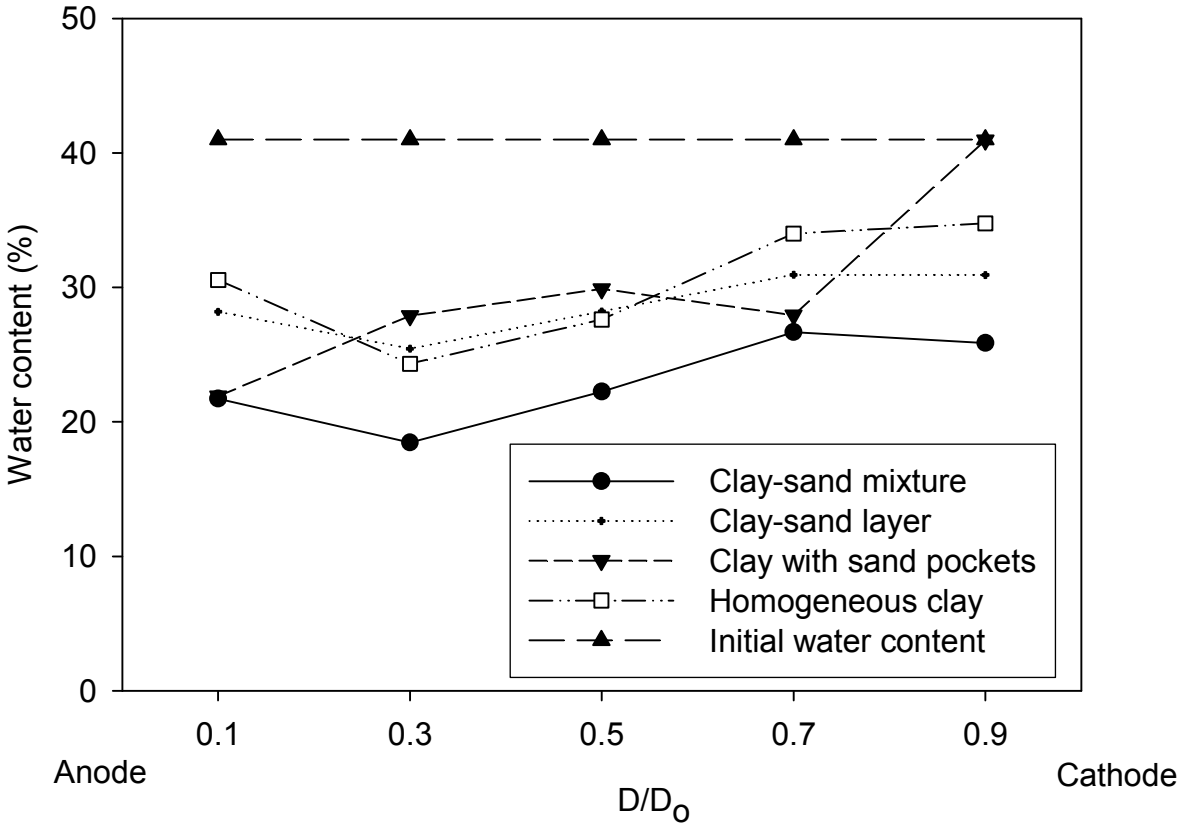

Figure 6.12 Water content vs. normalized distance from the anode for the tests with two-dimensional electrode configuration.

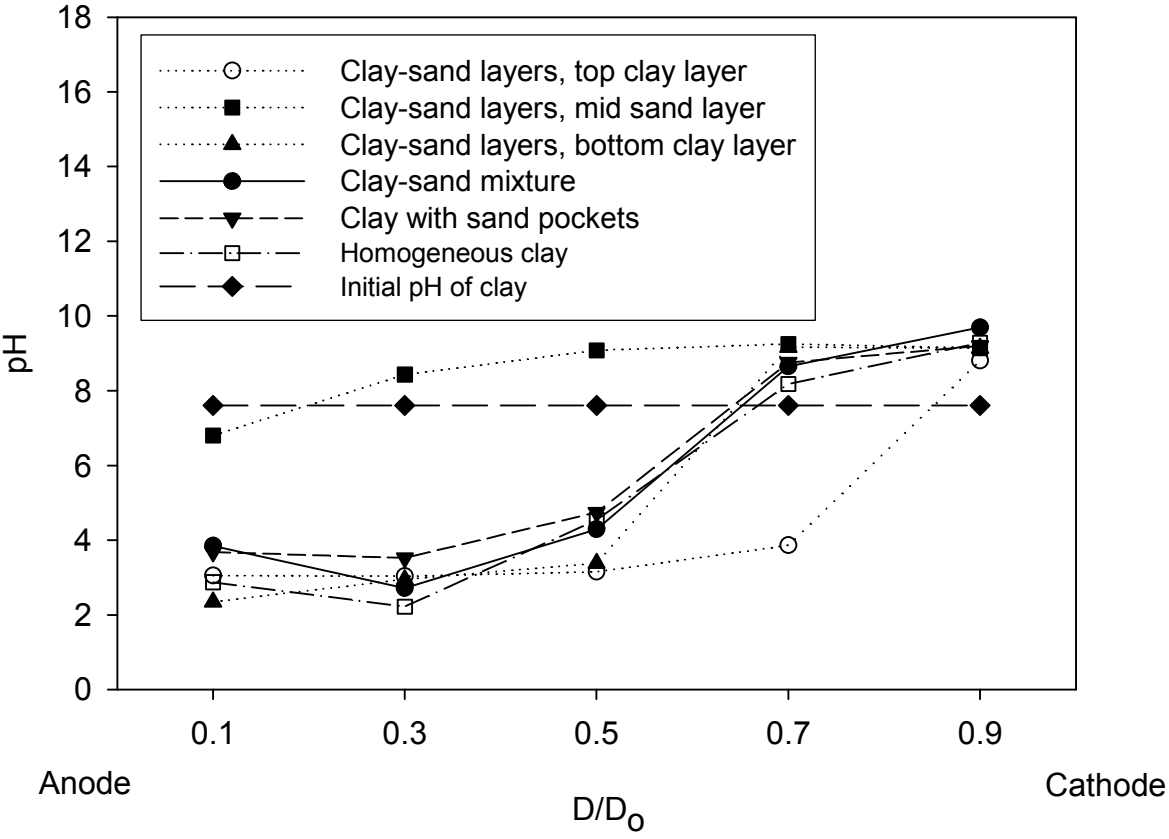

Figure 6.13 Soil pH vs. normalized distance from the anode for tests with two-dimensional electrode configuration.

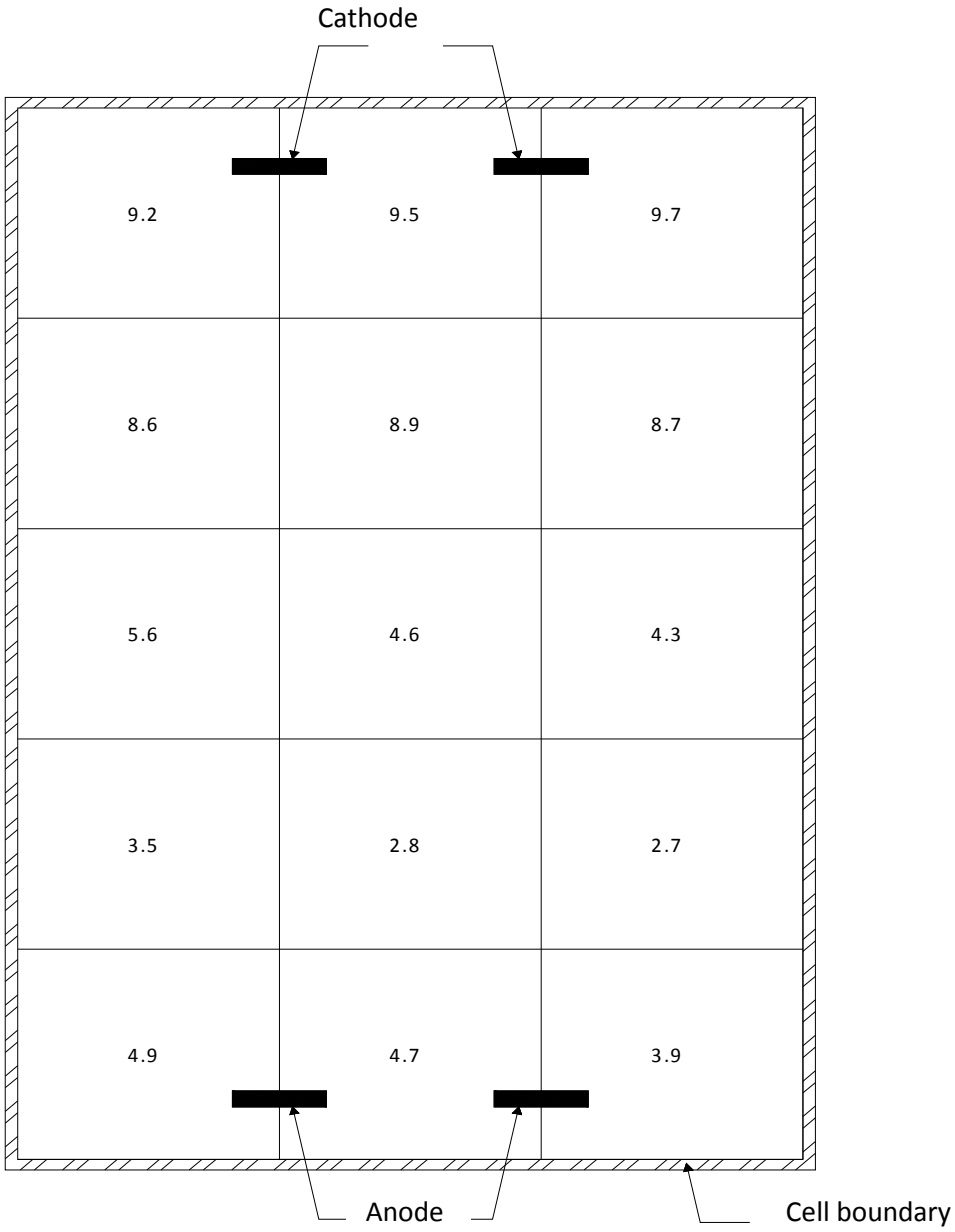

Figure 6.14 Top-view for pH distribution along clay-sand mixture cell tested with two-dimensional electrode configuration.

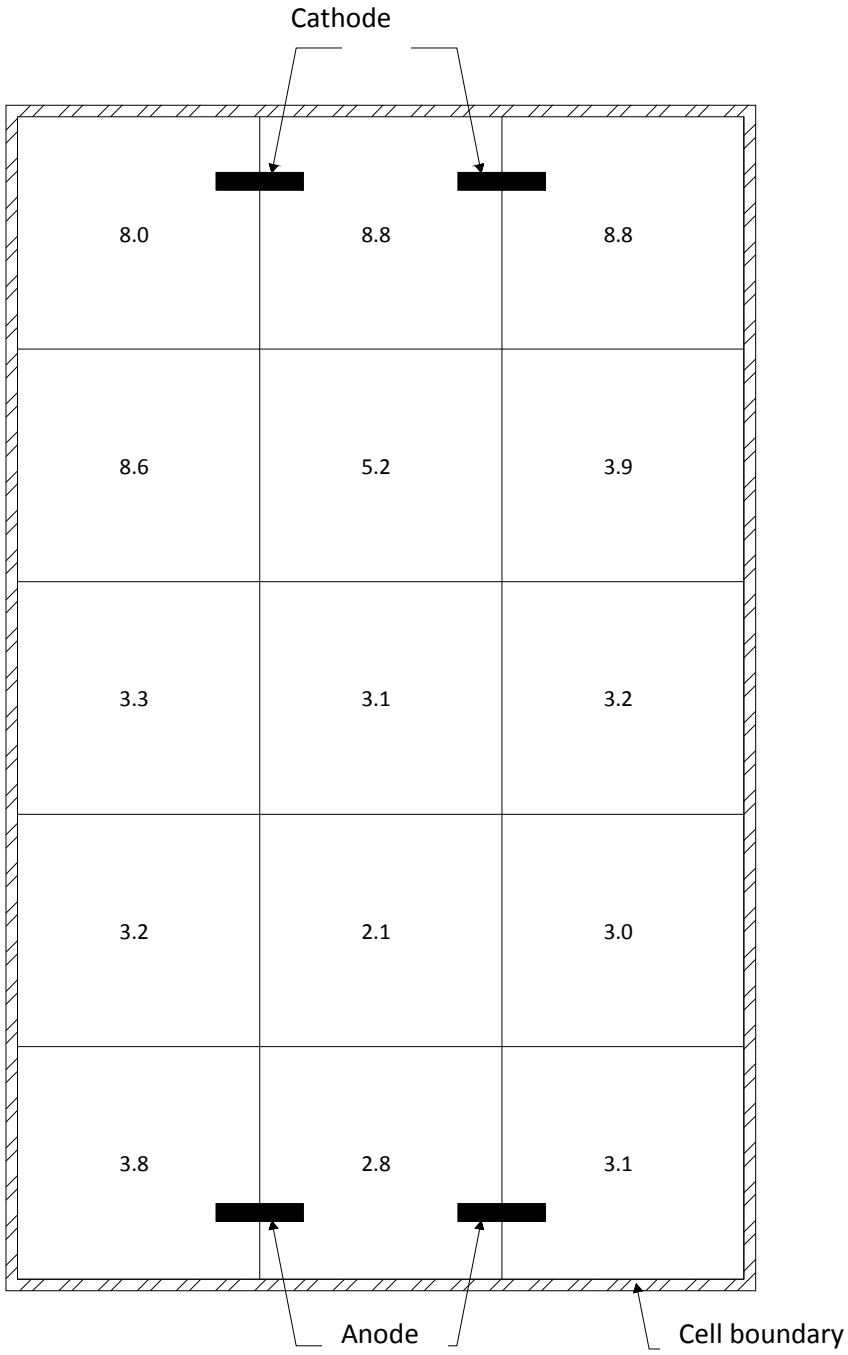

Figure 6.15 Top-view for pH distribution on the top clay layer of the clay-sand layers tested with two-dimensional electrode configuration.

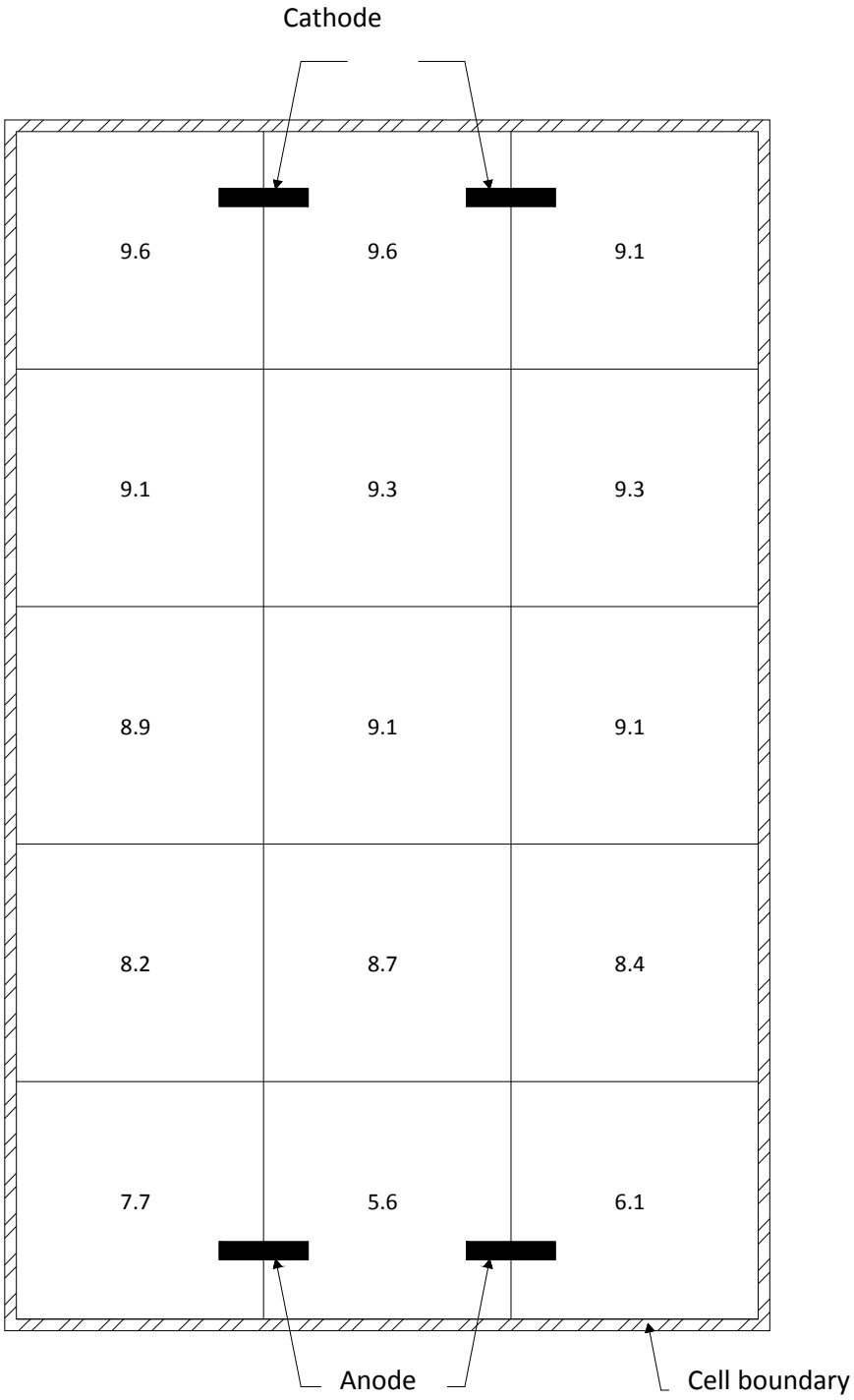

Figure 6.16 Top-view for pH distribution in the sand layer of the clay-sand layers cell tested with two-dimensional electrode configuration.

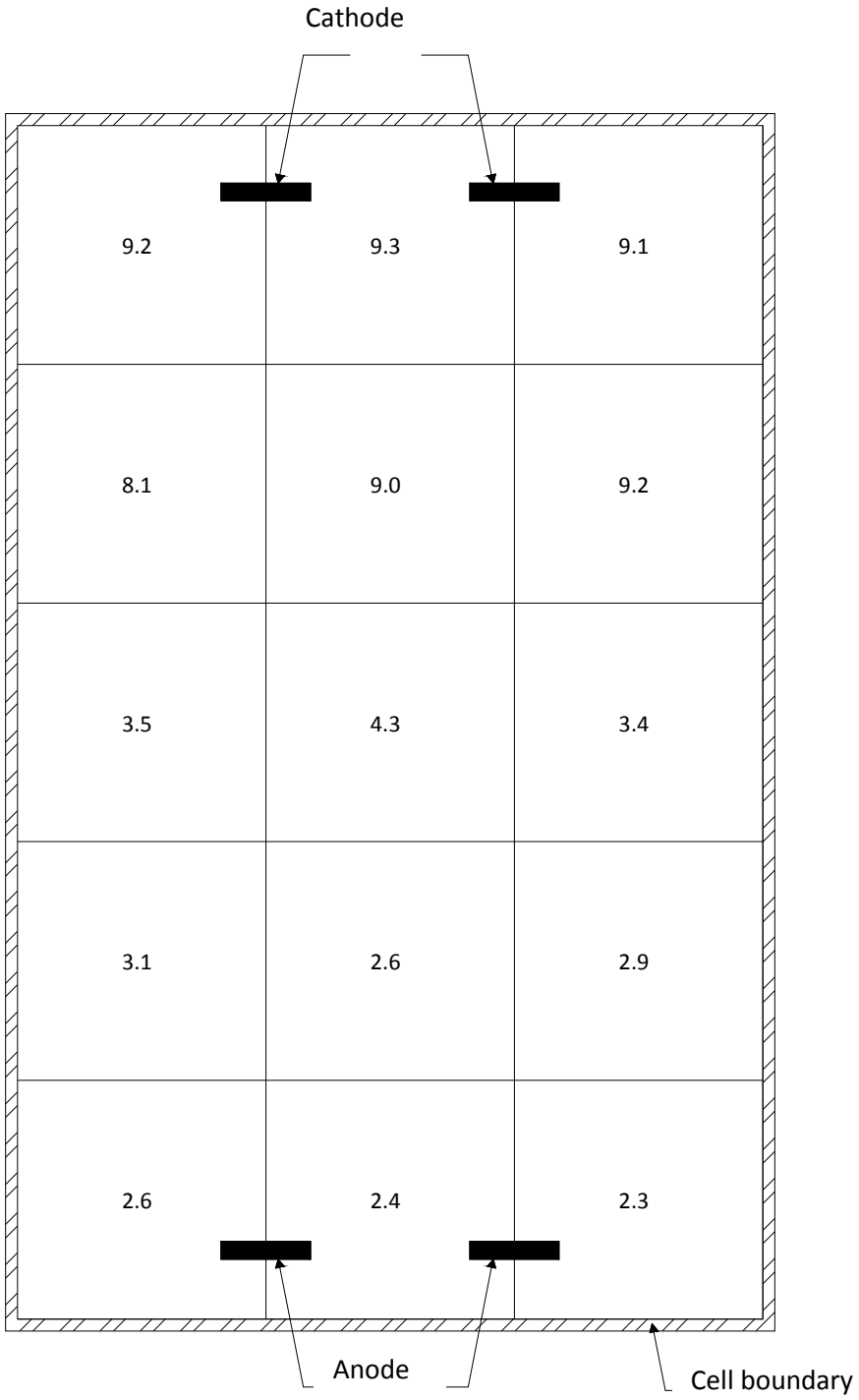

Figure 6.17 Top-view for pH distribution in the bottom clay layer of clay-sand layers cell tested with two-dimensional electrode configuration.

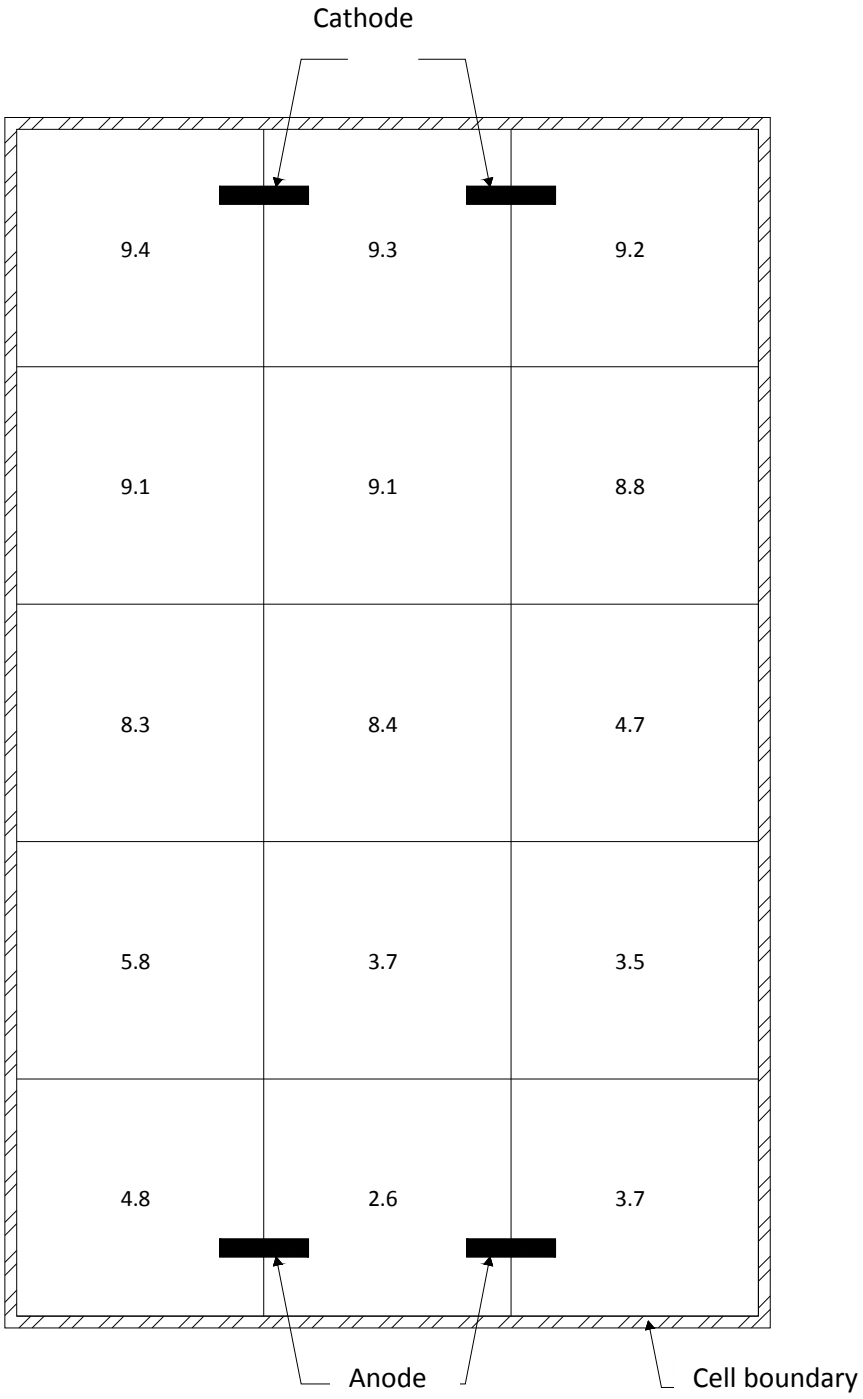

Figure 6.18 Top-view for pH distribution along the clay with sand pockets cell tested with two-dimensional electrode configuration.

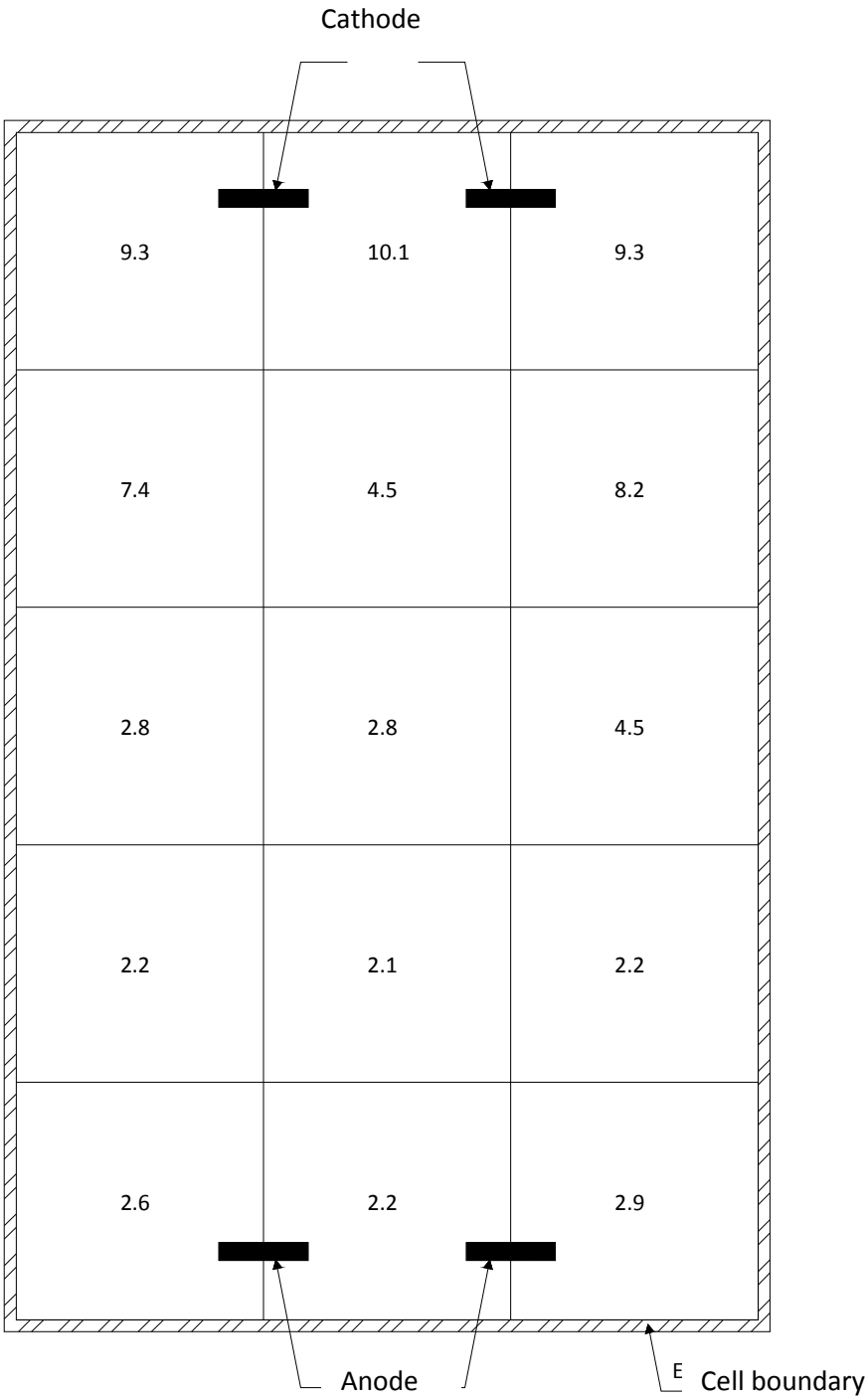

Figure 6.19 Top-view for pH distribution along the homogeneous clay cell tested with two-dimensional electrode configuration.

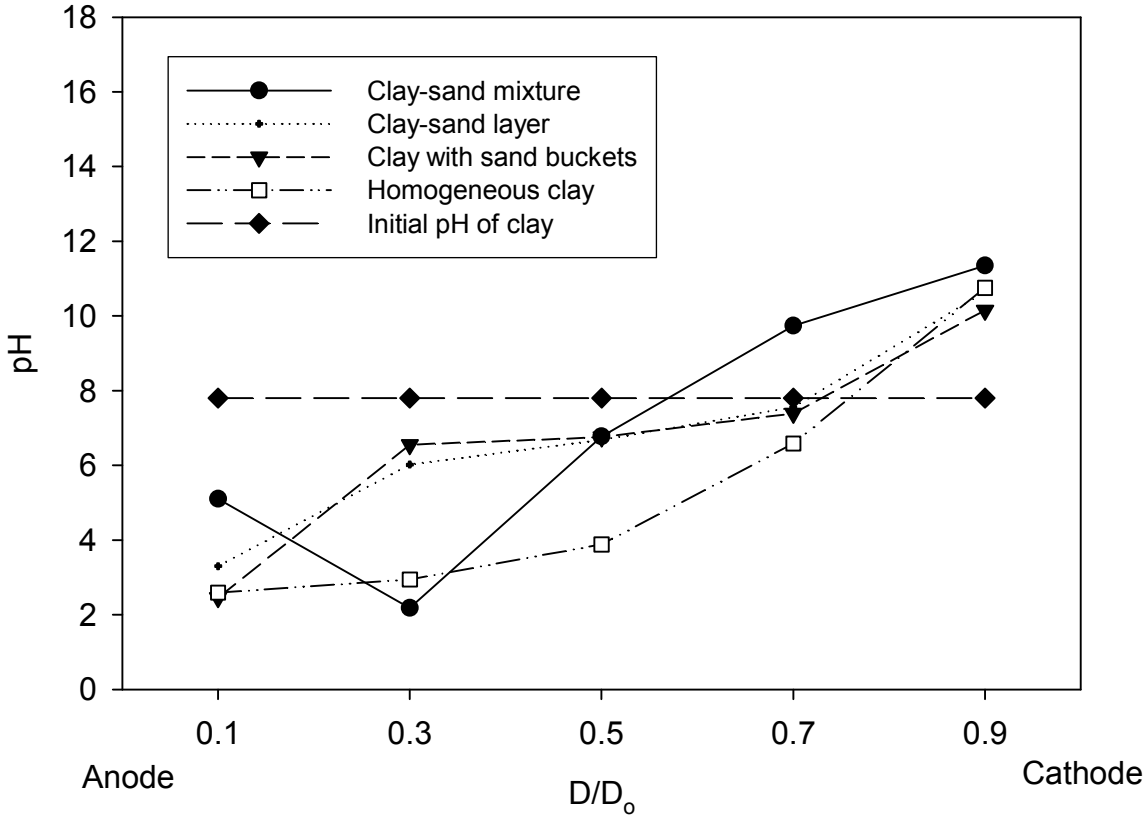

Figure 6.20 Soil pore fluid pH vs. normalized distance from anode for tests with two-dimensional electrode configuration.

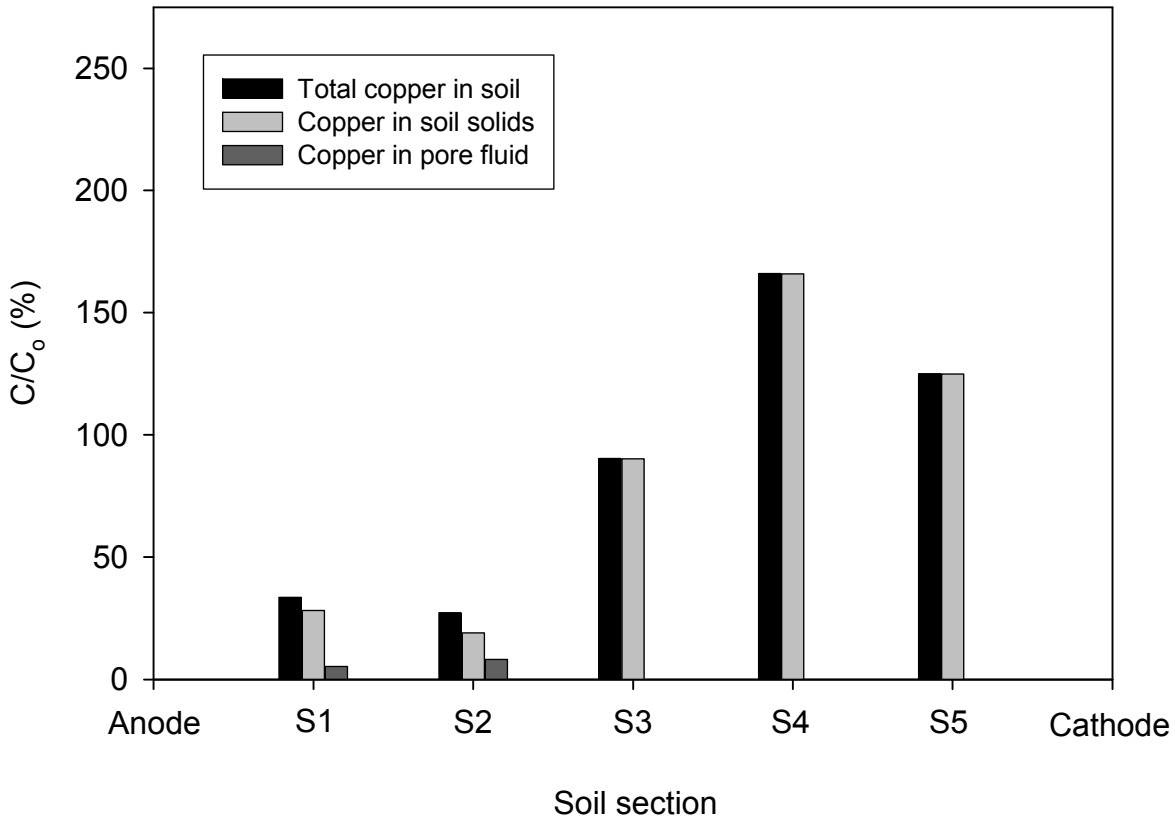

Figure 6.21 Ratio of copper concentration after the test to initial concentration (C/C_o) in sections S1 to S5 for clay-sand mixture tested with two-dimensional electrode configuration.

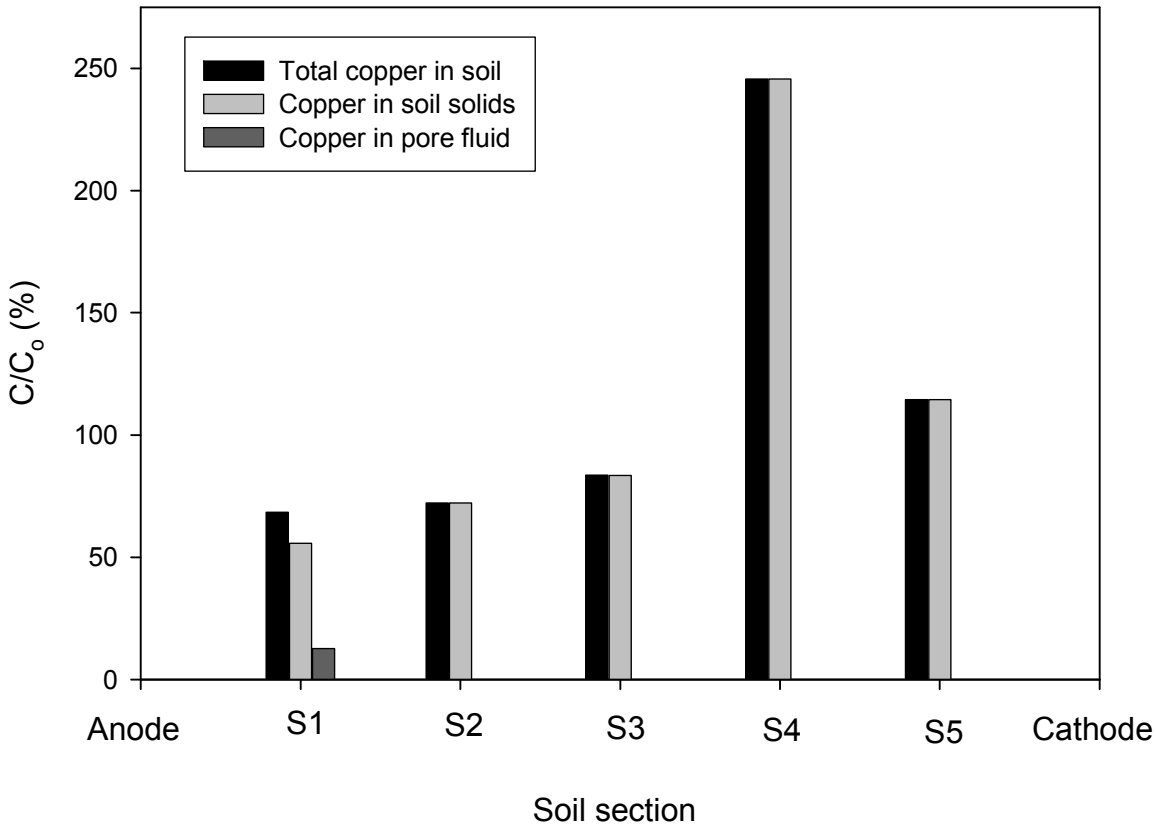

Figure 6.22 Ratio of copper concentration after the test to initial concentration (C/C_o) in sections S1 to S5 for clay-sand layers tested with two-dimensional electrode configuration.

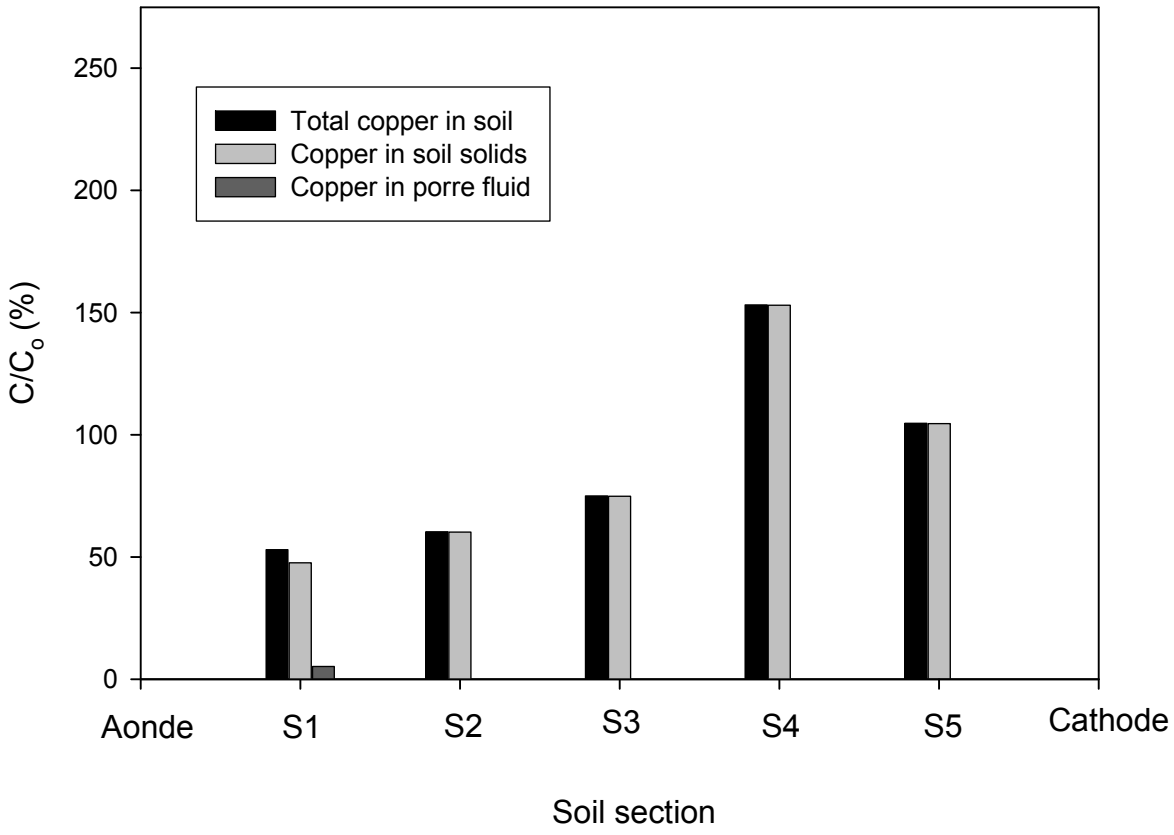

Figure 6.23 Ratio of copper concentration after the test to initial concentration (C/C_o) in sections S1 to S5 for clay with sand buckets tested with two-dimensional electrode configuration.

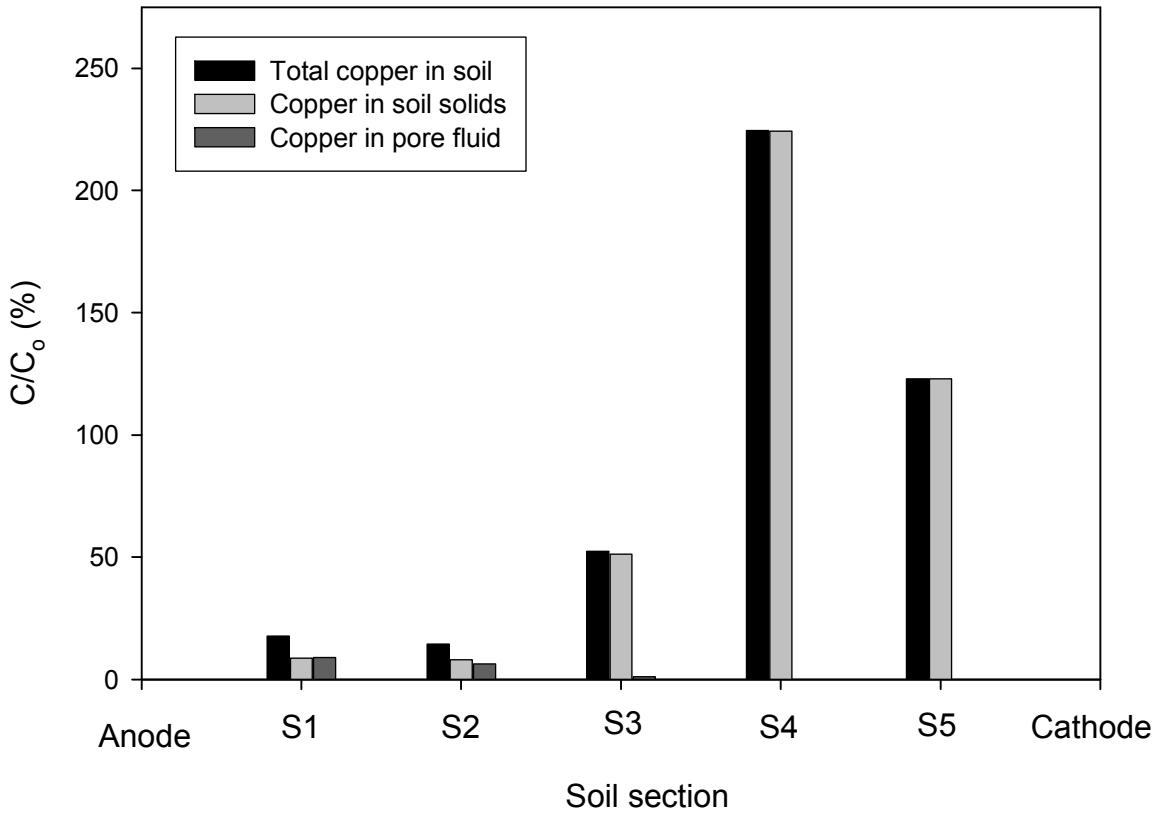

Figure 6.24 Ratio of copper concentration after the test to initial concentration (C/C_o) in sections S1 to S5 for homogeneous clay tested with two-dimensional electrodes configuration.

CHAPTER SEVEN

NOVEL ELECTRODE CONFIGURATION TECHNIQUE

7.0 INTRODUCTION

During the electrokinetic remediation for soils used in this research, the acid front (generated at the anode) travels towards the cathode by electromigration and electroosmosis fluxes, while the base front (produced at the cathode) moves towards the anode by electromigration. As discussed in chapters 5 and 6, the acid front meets the base front at a distance closer to the cathode. The base front reacts with the cations in the soil pore fluid causing premature precipitation of the heavy metals, a major drawback for electrokinetic remediation. Numerous attempts, conventional and innovative, have been carried out to hinder the base front advancement and the subsequent premature precipitation of ionic species. The conventional approaches rely solely on the addition of chemical compounds to prevent the base front advancement. In innovative techniques, such as Stepwise Moving Anode and polarity reversal, electrodes and electric field re-configuration are used to hinder the base front movement.

This chapter will discuss our proposed novel approach, Two Anodes Technique (TAT), to combat the advancement of the base front and enhance electrokinetic remediation of soil without using chemical compounds. In TAT configuration, a primary anode and a cathode are placed at the boundaries of the soil with a secondary anode placed between them in close proximity to the cathode (see Figure 4.8). The role of the secondary anode is to generate H^+ ions, which

travel by electroosmosis and electromigration towards the cathode and meet the OH^- ions at distance closer to the cathode (see Figure 4.11). Thus, the H^+ ions generated by the secondary anode hinder the advancement of the base front. Moreover, the H^+ ions will form a second zone of low pH near the cathode. The additional low pH zone near the cathode means most of the soil becomes acidic, which facilitate the dissociation of heavy metals form the soil. As per the current published literature, this research illustrates the first application of TAT in electrokinetic remediation.

This chapter discusses electrokinetic remediation tests conducted with three configurations, including Stepwise Moving Anode (SMA), Conventional Anode-Cathode (CAC), and the novel Two Anodes Technique (TAT). The power consumption during the remediation was kept constant for comparison in the three tests. The results of the electrokinetic remediation with TAT were compared with the results from CAC and SMA. The tests procedure is discussed in section 7.1. The results and discussion are presented in section 7.2.

7.1 TEST PROCEDURE

Three identical electrokinetic cells were used to perform the tests (see Figure 4.1). For the three cells, the anode compartment was filled with water to maintain the supply of water at the anode. The water at the anode compartment increases electroosmosis flow and consequently the acid front travels farther causing desorption of copper from the soil. The cathode compartment was filled with water to the level of the anode compartment to ensure that the

flow through the soil was due to electroosmosis alone. Homogeneous clay soil contaminated with 355 mg of copper per kg of dry soil was used in the tests.

The procedure described in section 4.2.1 was followed for sample preparation. Two-dimensional electrode configuration (as described in section 4.2.4) was used in the tests. The tests were carried out between October and December 2010 using four solar cell panels. The solar panels setup is discussed in section 4.1.3. As shown in Figure 7.1, two solar panels were connected to the graphite electrodes in the electrokinetic testing cell with TAT (see section 4.3.1 and Figure 4.8). The third solar cell was connected to the pairs of graphite electrodes in Cell-SMA (Stepwise Moving Anode) and the fourth solar cell was used in Cell-CAC (Conventional Anode-Cathode). The treatment in each of the three cells was terminated at power consumption of 500 Whr. In Cell-SMA, the pair of anodes was moved towards the pair of cathodes in four steps (see Figure 7.2). At the start of the test the pair of anodes was placed at X1 (200 mm from the cathode) and then moved to X2 (150 mm from the cathode), X3 (100 mm from the cathode), and X4 (50 mm from the cathode) at power consumptions of 200, 350, and 450 Whr, respectively. At the end of the three tests, the soil was extruded from cell and divided into 4 equal sections S1, S2, S3, and S4 (see Figure 4.7). For data collection and soil sampling, the procedure described in section 4.2.5 was followed. For ICP-OES analysis, 5 mL of each copper solution was diluted by adding 40 mL of deionized water.

7.2 RESULTS AND DISCUSSION

Table 7.1 to 7.3 summarize the tests results (water content, soil pore fluid pH and electrical conductivity, dry soil pH, copper concentration) for the Cell-SMA, Cell-CAC, and Cell-TA, respectively. Section 7.2.1 presents the voltage and current results during the test. Section 7.2.2 discusses the water content. Section 7.2.3 presents the dry soil and soil pore fluid pH results. Section 7.2.4 presents and discusses copper concentration after the tests.

7.2.1 Applied voltage and electric current

Figure 7.3 shows the voltage distribution across Cell-SMA during the four steps. Figures 7.4 and 7.5 show the voltage distribution across Cell-CAC and Cell-TAT during the first day of remediation. For Cell-SMA, it is obvious that the voltage gradient increased as the anode moved closer to the cathode. The steep voltage gradient along Cell-SMA resulted in high electrical current. Figure 7.6 shows the peak electric current for Cell-SMA in steps 1, 2, 3, and 4 to be 0.54, 0.3, 0.5, 1.28 A, respectively. High current value can be a major obstacle for field applications of SMA because it poses high risk to personnel. Figure 7.4 shows a constant voltage gradient throughout the soil in Cell-CAC. Figure 7.7 shows the current for Cell-CAC to be between 0.42 A at the start of the test and 0.23 A at the end of the test. In the test with TAT the secondary electric circuit current was kept at around 0.09 A by regular adjustment (every three to four hours) of the voltage at the secondary anode. Therefore, the introduction of the secondary anode resulted in low voltage gradient for the soil specimen between the primary and secondary anodes and relatively higher voltage gradient between the secondary anode and the cathode (see Figure 7.5). The current for the outer circuit was also affected by the

secondary anode and found to be lower than the current in the Cell-CAC (see Figures 7.7 and 7.8).

7.2.2 Water content

Figure 7.9 shows the water content along the cells after the tests. D is the horizontal distance from the anode and D_o is the total length of the soil samples. Thus, the water content at 0-0.25 D/D_o represents the soil section near the anode (S1) while 0.75-1 D/D_o represents the section near cathode (S4) (see Figure 4.7). Although electroosmosis flow was responsible for dewatering the cells, the movement of H^+ and OH^- ions towards the oppositely charged electrode also affects the water content of the soil. For Cell-CAC, Figure 7.9 shows low water content in S2 and high water content in S1, S3, and S4. The higher water content in S1 can be attributed to water transfer from the adjacent water compartment. Cell-CAC was run for longer time compared with Cell-TAT and Cell-SMA. Due to the secondary electric circuit, Cell-TAT consumed the predetermined power of 500 Whr faster than Cell-CAC, while Cell-SMA consumed more power as the anode moved towards the cathode due to the increase in current (power consumption is equal to the product of electric current, applied voltage, and time). The water formation at H^+ and OH^- ions junction could explain the high water content in Cell-CAC at S3 and S4. For Cell-TAT, the water content was high in S3 and low in S1, S2, and S4. The noticeable difference in water content between S3 and S4 suggested that S4 was drained by electroosmosis (enhanced by the effect of secondary electric circuit current) and no water was formed at S3 and S4. For Cell-SMA, the water content was high in S1 and S4 and low at S2 and S3. Low water content was observed in S3 compare to the two other methods. The high water

content in S4 was either due to the formation of water by H^+ and OH^- ions, or due to short time and consequently low power consumed (50 Whr) when the anode placed at X4 (see Figure 7.6).

7.2.3 pH

Figure 7.10 shows the pH of the pore fluid along the soil specimens after the tests. The initial pH of the soil pore fluid was 7.6. The figure shows that for Cell-CAC, the pH was < 4 from the anode to 0.75 D/D_0 and > 4 for the rest of the soil specimen. The pH values at S1, S2, and S4 for Cell-SMA and Cell-CAC were almost identical. However, the pH at S3 was lower for the former. The pH values for Cell-TAT were lower than in the previous two tests through the entire soil. Cell-TAT obviously was successful in lowering the pH to acidic values even near the cathode with a highest pH of 3. The SMA technique requires the advancement of the anode towards the cathode in steps. In the field application this means more labour work, additional excavation cost, and the risk of electrode damage each time the electrode pulled out or pushed into the ground. TAT requires less effort and consequently less cost compared with SMA technique. Moreover, the pH profile of the pore fluid in Cell-TAT was acidic throughout the soil specimen, which promotes copper desorption. The acidic pH values prevent the base front advancement as well as the premature heavy metals precipitation.

Figure 7.11 shows the pH of the soil along the specimen after the tests. The initial pH of the soil specimen was 7.6. The figure shows that for Cell-CAC, the pH was < 5 from the anode to 0.75 D/Do and 10 for the rest of the soil. For Cell-SMA, the pH values at S1 and S4 were 2.3 and 9.5, respectively. The pH profile for Cell-TAT shows that the pH values were around 2.2 at S1 and S2

and lower than the other two tests for the rest of the soil. The pH profiles of the dry soil show higher values than the corresponding pH values obtained from the soil pore fluid. Nevertheless, Cell-TAT obviously was successful in lowering the dry soil pH in sections S1, S2, S3, and most of S4 except for small portion near the cathode where the pH was 7.6. It is clear that TAT had significantly lowered the pH of the soil and prevented the base front advancement. The water content at S4 for Cell-TAT as shown in Figure 7.9 was lower compared with other tests. This confirms the cessation of base front advancement by TAT. Thus, the TAT with lesser effort than SMA had generated environment that prevent or minimize the premature precipitation of copper in most of the soil specimen.

7.2.4 Copper concentration

Figures 7.12 to 7.14 show the ratio (in percentage) of the copper concentration after the test (C) to the initial copper concentration (C_o = 355 mg of copper per kg of dry soil). The concentrations are presented for the total copper in the soil, the copper in pore fluid and copper in soil solids. The results represent the entire sections S1, S2, S3, and S4 (see Figure 4.7). Figures 7.12 to 7.14 clearly show that the power generated by solar cell panel for electrokinetic remediation was in general effective in moving copper from the anode towards the cathode.

Figure 7.12 shows the copper removal in Cell-SMA was uneven (e.g. copper removed from S2 (58%) > copper removed from S1 (36%)). This was to be expected as S1 was subjected to shorter remediation time than S2. The copper removed from S3 was 19%. The percentages of copper in pore fluid were 0.1%, 16%, 14%, and 14% in S1, S2, S3, and S4, respectively. For Cell-

CAC, Figure 7.13 shows that 65% and 60% of initial copper were removed from S1 and S2, respectively. Considerable amount of copper however, precipitated prematurely in S3. The percentages of copper in pore fluid were 4%, 5%, 6%, and 1.5% at S1, S2, S3, and S4, respectively. For Cell-TAT, Figure 7.14 shows that 80% and 67% of copper were removed from S1 and S2, respectively. Interestingly, 21% of total copper in S4 was in found in the pore fluid meaning it was readily available to be removed by slightly extending the remediation time. Therefore, TAT was successful in removing significant amount of copper from S1, S2, and S3 and dissolution of 21% of copper in S4.

Refer to Appendix D for ICP-OES results.

7.3 CONCLUSIONS

In this chapter the novel Two Anodes Technique (TAT) was implemented to remediate homogeneous clay soil contaminated with 355 mg of copper per kg of dry soil. The tests were carried out to investigate the effectiveness of TAT in suppressing the advancement of the base front. For comparison, Stepwise Moving Anode (SMA) and the Conventional Anode Cathode (CAC) methods were also used to remove copper from identical specimens. For Cell-SMA and Cell-CAC, the pH profiles of the pore fluid and dry soil show that the electrolysis reactions resulted in a low pH near the anode and a high pH near the cathode. For SMA, the high copper concentration in water at S4 can be attributed to formation of hydrogen ions and the fact that at high pHs values the cations forms negative complexes that dissolve in water (see figure 2.9). For Cell-TAT, the pH was acidic throughout the soil even near the cathode the pH was 3. The

water content in the soil specimens S3 and S4 after completion of the test in Cell-CAC was high. This confirms the formation of water at the point where acid front meets base front. In Cell-TAT, lower water content was reported in S4 indicating that no water formation took place. Therefore, the base front was successfully suppressed by Cell-TAT. Significant amount of copper (80%) was removed from S1 of Cell-TAT. From desorption test section 3.2.2.2.2, the maximum amount of copper desorbed at pH value 2 was about 81% (see Figure 3.7), which exactly coincides with the removal from S1. This indicates that the implementation of TAT can significantly increase the heavy metal removal by electrokinetic remediation.

Table 7.1 Results summary after the test of the test with Stepwise Moving Anode (SMA) configuration.

Anode (+)	Distance from Anode				Cathode (-)
	0-50 mm	50-100 mm	100-150 mm	150-200 mm	
	Water content (%)				
	34.5	28.8	26.9	31.5	
	Soil pore fluid pH				
	1.7	1.5	2.0	11.5	
	Dry soil pH				
	2.3	2.1	6.5	9.5	
	Soil pore fluid electrical conductivity (µS/cm)				
	17800	23300	2420	1320	
	Copper in soil pore fluid (C_f /C_0)*%				
	0.04	16.11	14.02	13.80	
	Copper in soil solids (C_s/C_0)**%				
	63.45	25.46	66.85	138.09	
	Total copper in dry soil (C_d/C_0) ***%				
	63.49	41.57	80.87	151.89	

Table 7.2 Results summary after the test of the test with Conventional Anode Cathode (CAC) configuration.

Anode (+)	Distance from Anode				Cathode (-)
	0-50 mm	50-100 mm	100-150 mm	150-200 mm	
	Water content (%)				
	31.9	25.5	31.6	32.3	
	Soil pore fluid pH				
	1.6	1.9	4.2	11.9	
	Dry soil pH				
	1.7	2.5	4.7	9.6	
	Soil pore fluid electrical conductivity (µS/cm)				
	28000	7810	416	3090	
	Copper in soil pore fluid (C_f /C_0)*%				
	4.21	5.56	6.3	1.44	
	Copper in soil solids (C_s/C_0)**%				
	31.07	34.20	145.34	127.13	
	Total copper in dry soil (C_d/C_0)***%				
	35.28	39.76	151.64	128.57	

*C_0 initial copper concentration in soil sample, and C_f Copper concentration in soil pore fluid

**C_s Copper concentration in soil solids

***C_d Copper concentration in dry soil

Table 7.3 Results summary after the test of the test with Two Anodes Technique (TAT) configuration.

Anode (+)	Distance from Anode				Cathode (-)
	0-50 mm	50-100 mm	100-150 mm	150-200 mm	
	Water content (%)				
	29.4	27.5	34.7	29.9	
	Soil pore fluid pH				
	1.1	1.2	1.7	3.0	
	Dry soil pH				
	2.3	2.3	3.1	7.7	
	Soil pore fluid electrical conductivity (µS/cm)				
	54000	50200	15640	1390	
	Copper in soil pore fluid (C_f /C_0)*%				
	0.13	0.64	13.69	20.72	
	Copper in soil solids (C_s/C_0)**%				
	19.19	131.79	93.63	196.72	
	Total copper in dry soil (C_d/C_0)***%				
	19.31	32.43	107.32	217.44	

*C_0 initial copper concentration in soil sample, and C_f Copper concentration in soil pore fluid

**C_s Copper concentration in soil solids

***C_d Copper concentration in dry soil

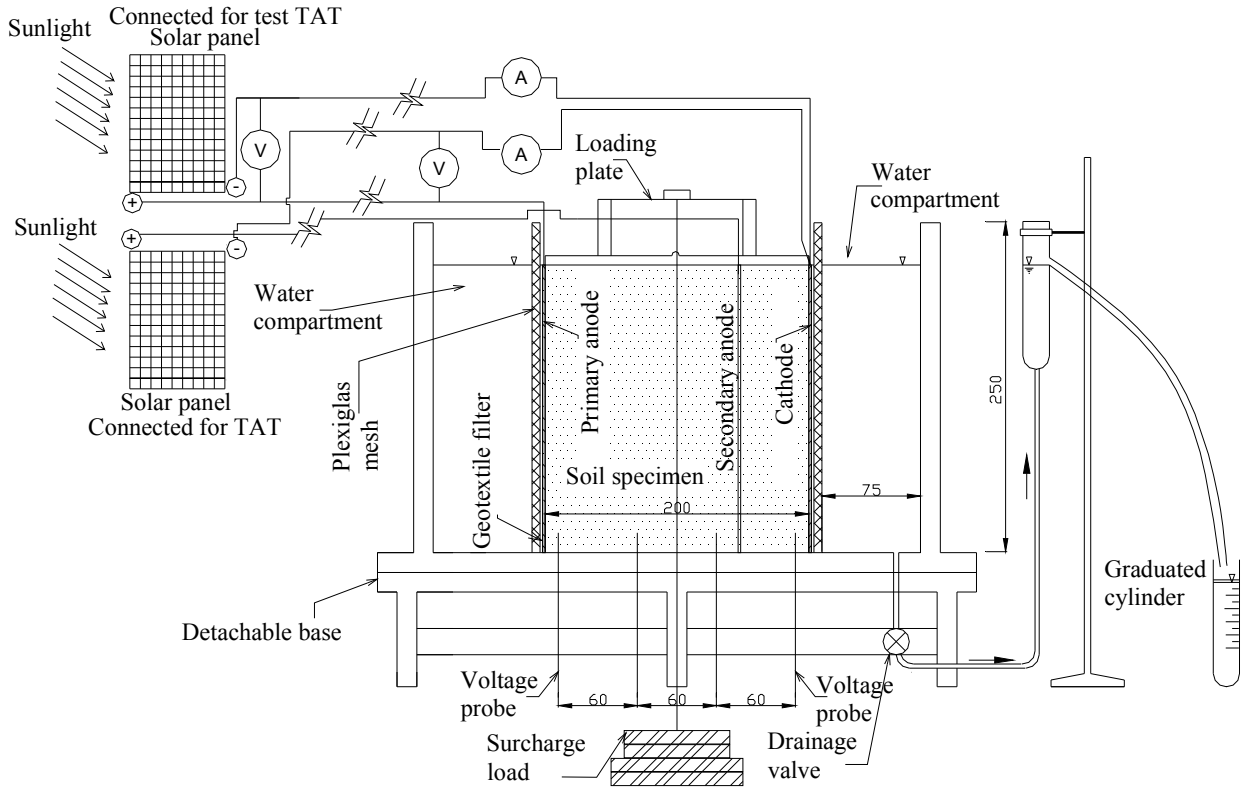

Figure 7.1 Sectional elevation view of electrokinetic cell with Two Anodes Technique.

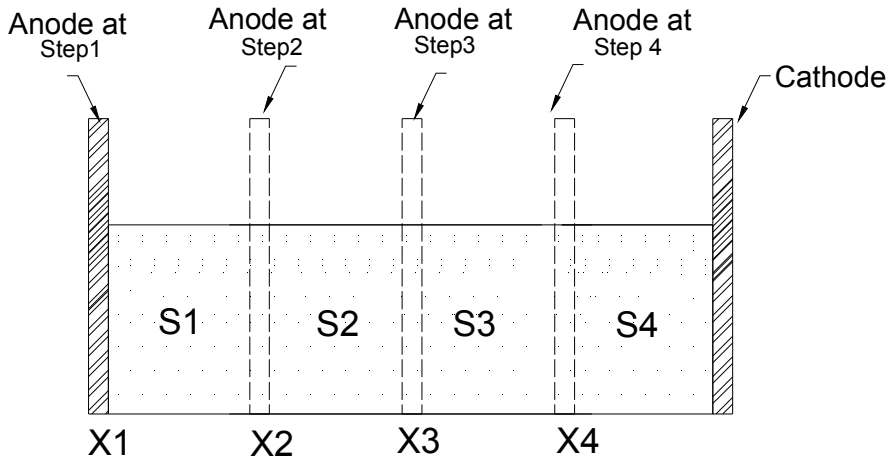

Figure 7.2 Anode steps in Cell-SMA.

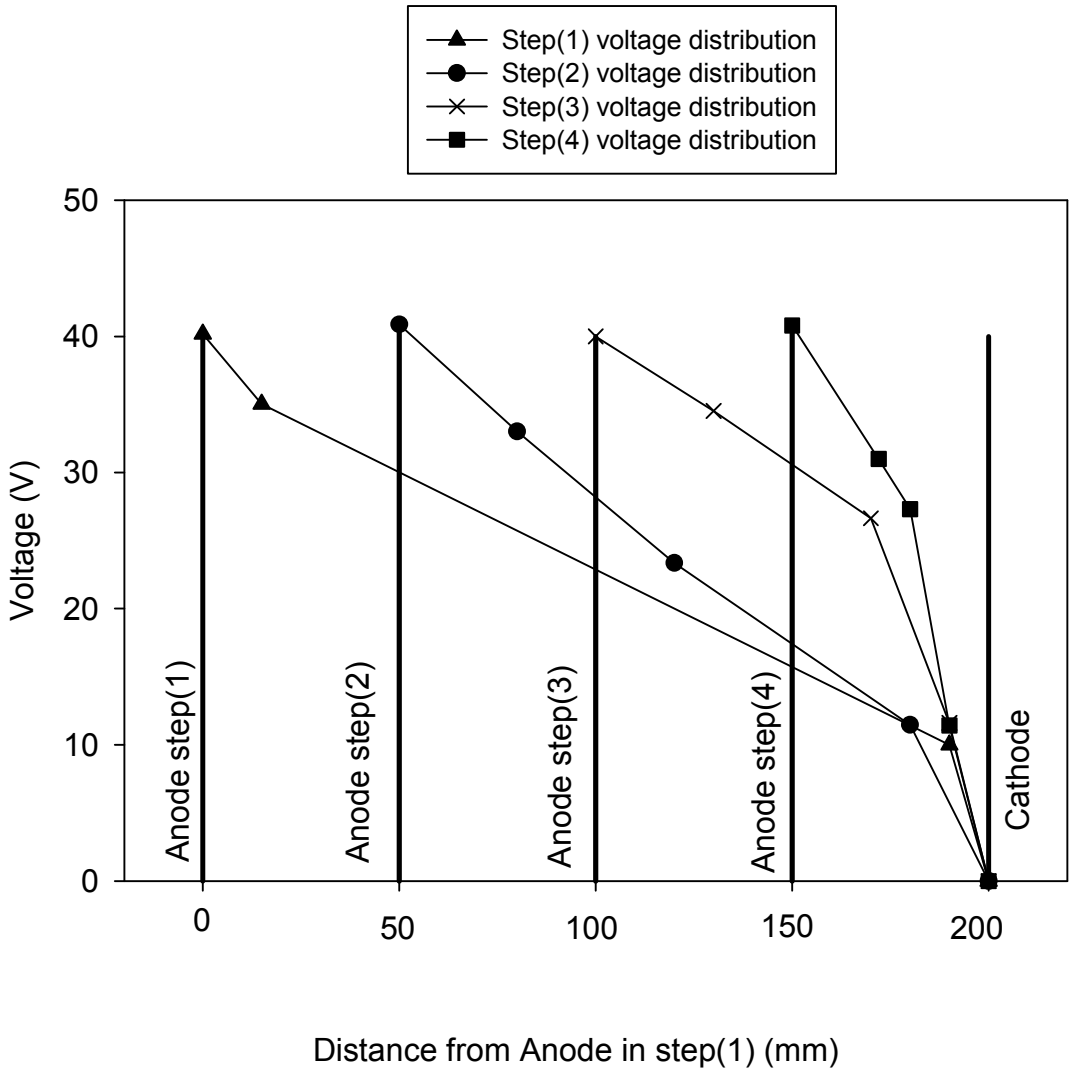

Figure 7.3 Voltage distribution for the first day of remediation along Cell-SMA for applied voltage (41 V).

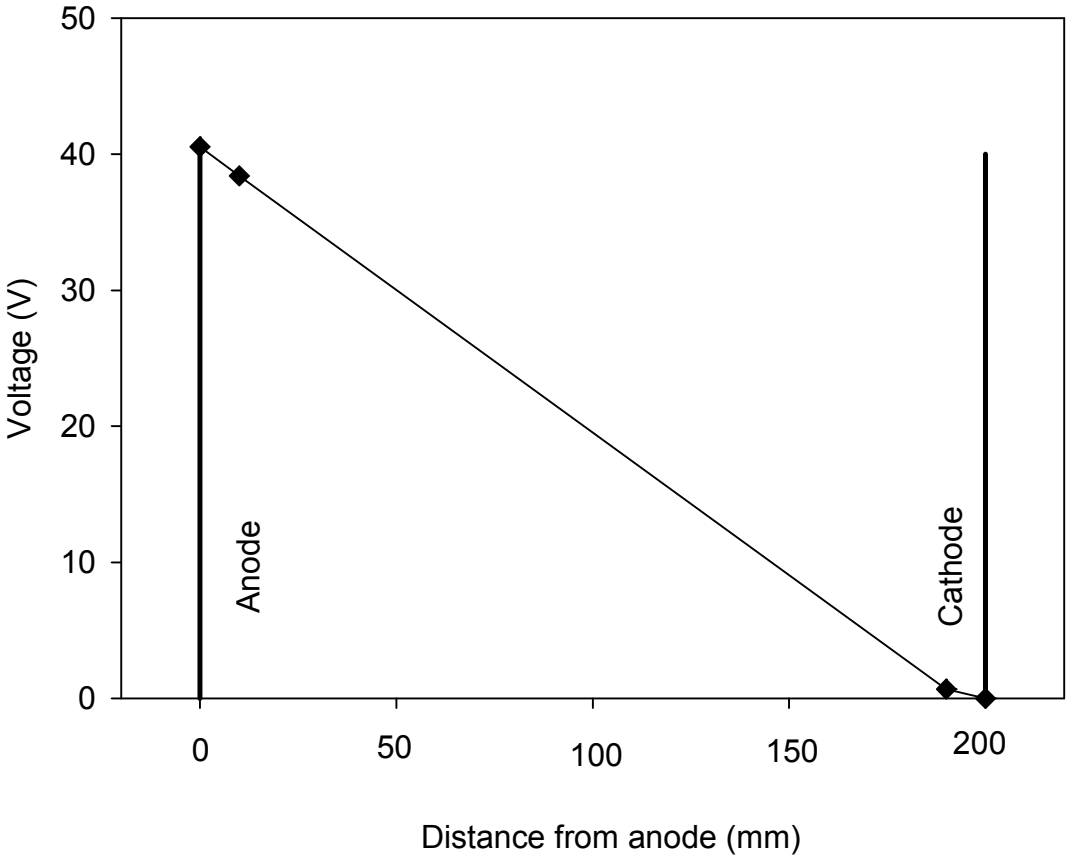

Figure 7.4 Voltage distribution for the first day of remediation along Cell-CAC for applied voltage (41 V).

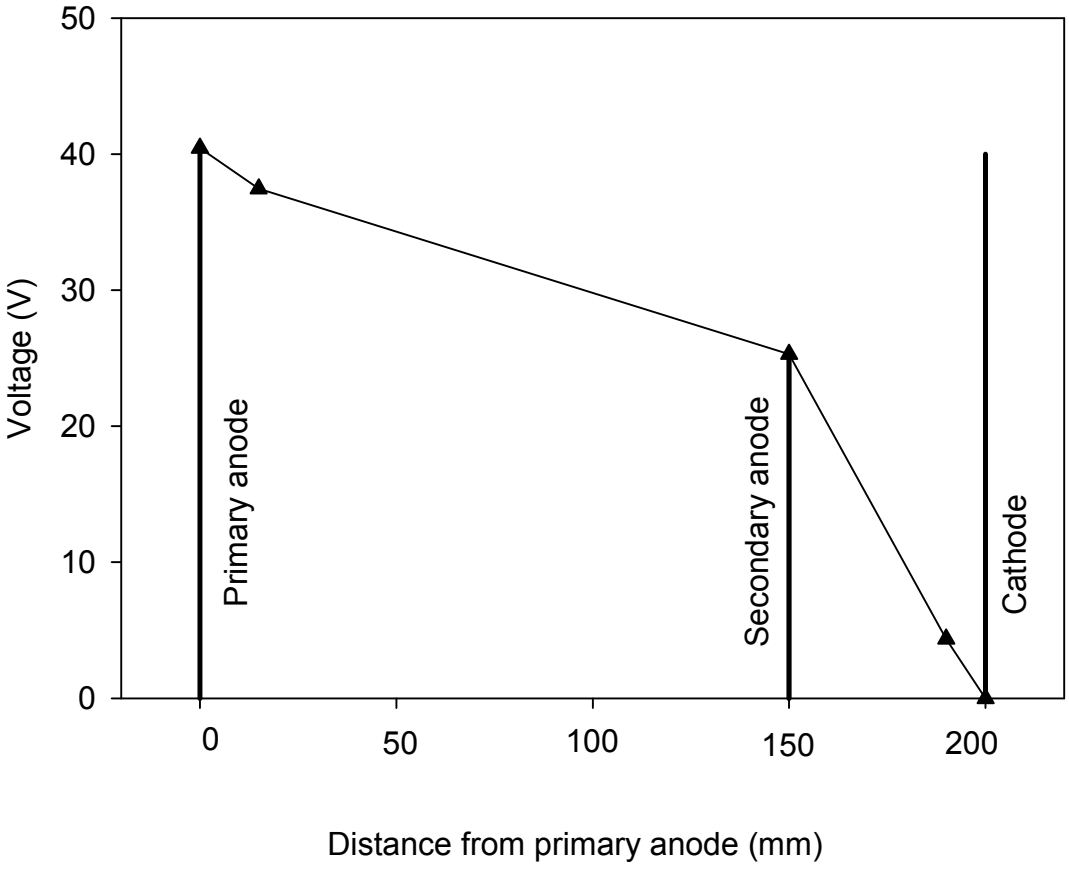

Figure 7.5 Voltage distribution along Cell-TAT for main electric circuit applied voltage (41 V).

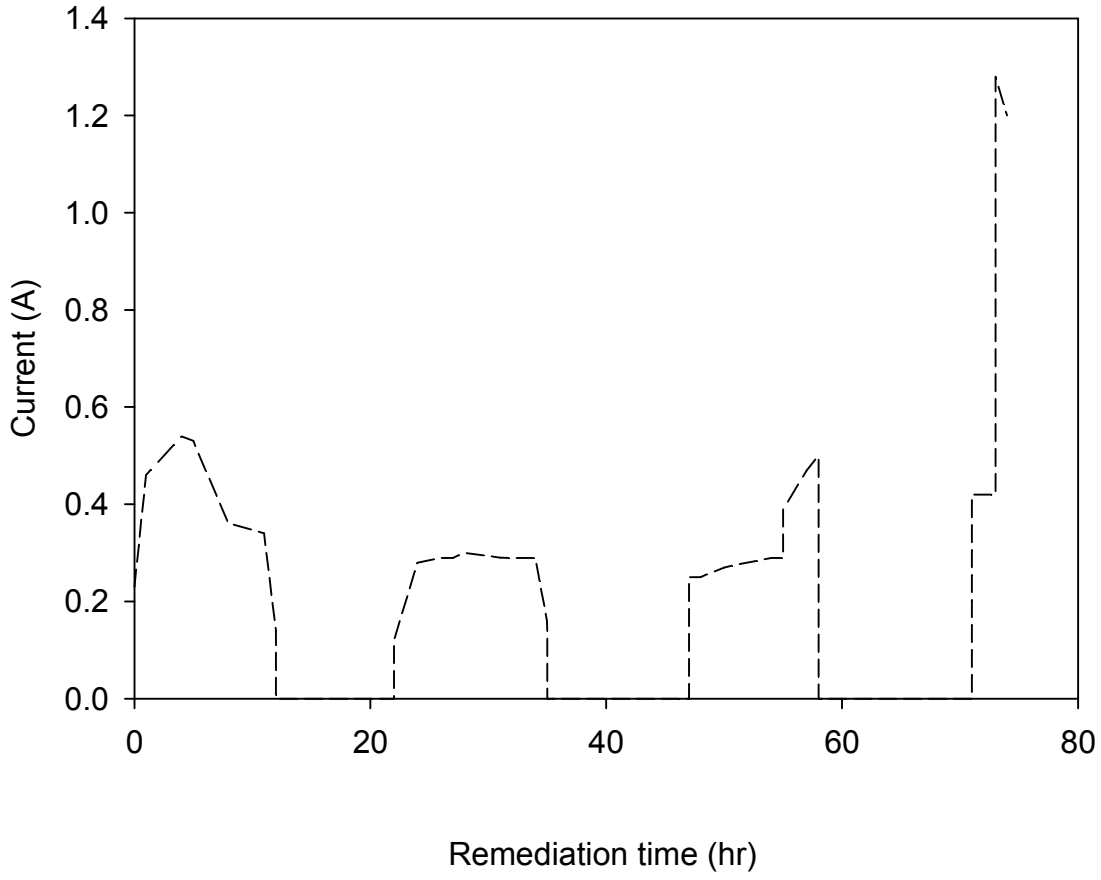

Figure 7.6 Electric current vs. time in Cell-SMA.

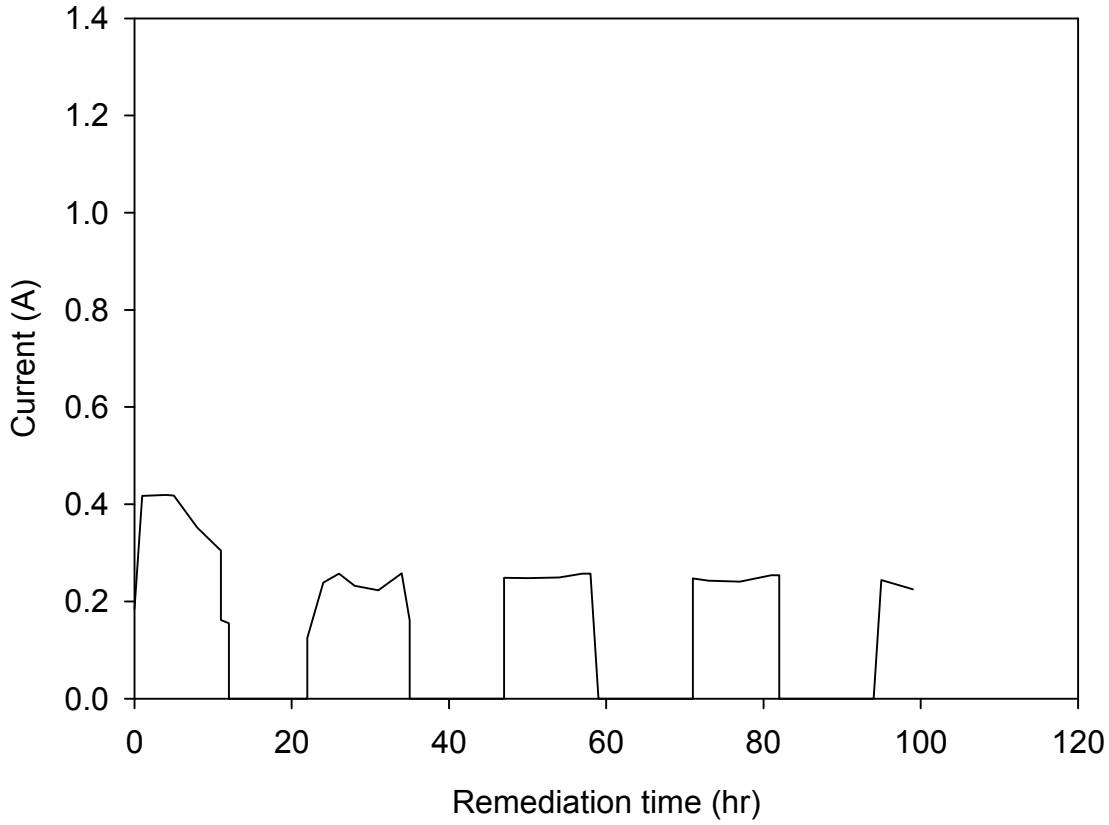

Figure 7.7 Electric current vs. time in Cell-CAC.

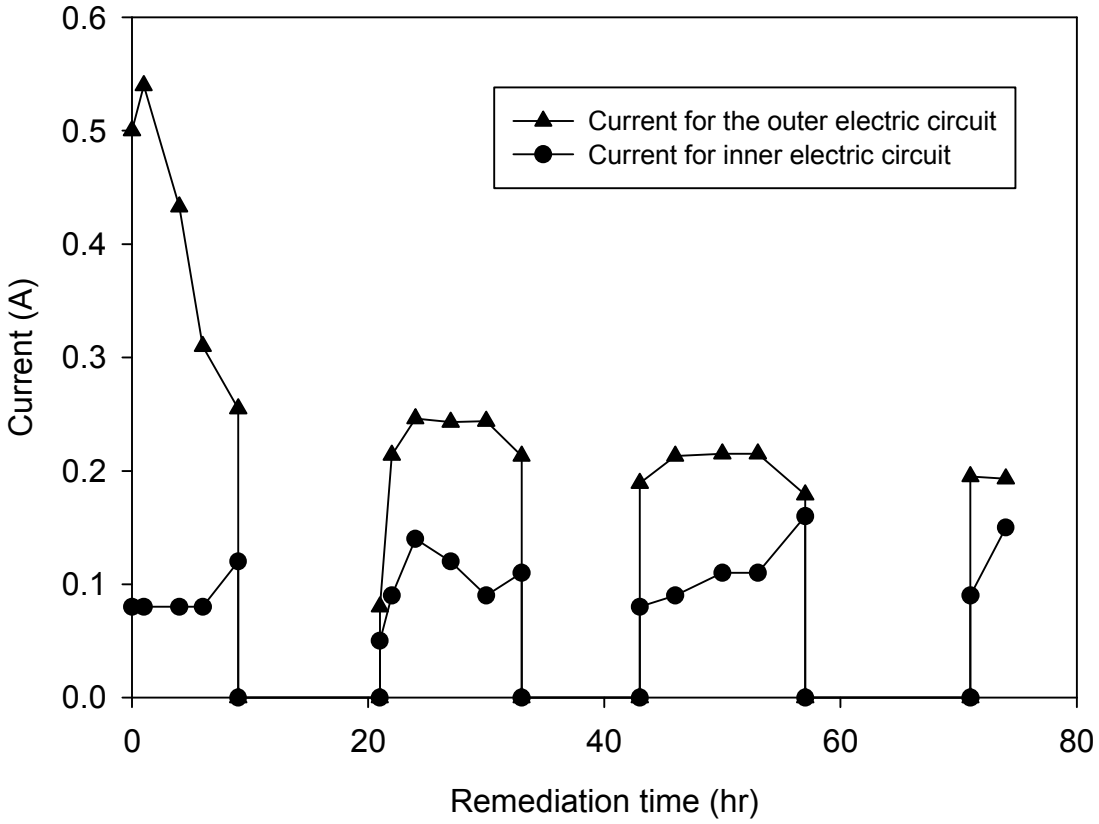

Figure 7.8 Electric current vs. time in Cell-TAT.

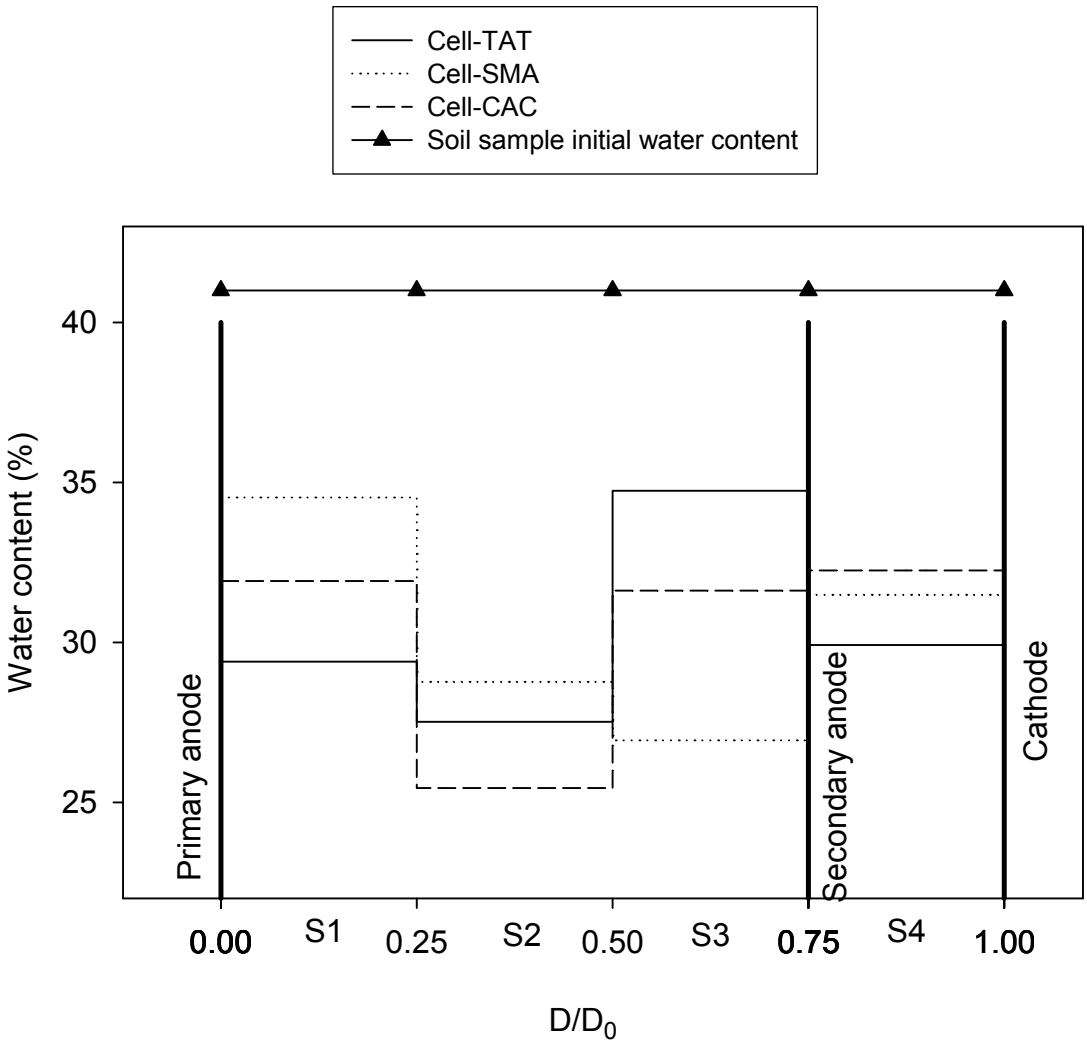

Figure 7.9 Water content along the cells after the test.

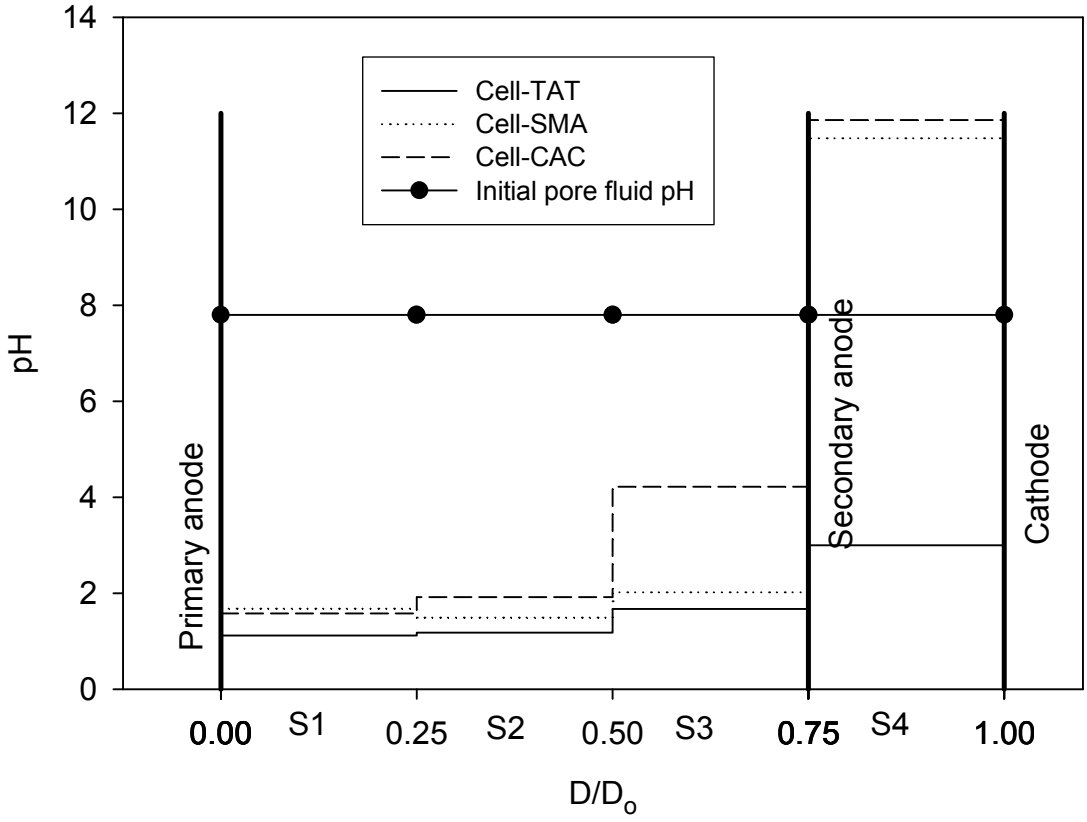

Figure 7.10 pH of the soil pore fluid along the cells after the test.

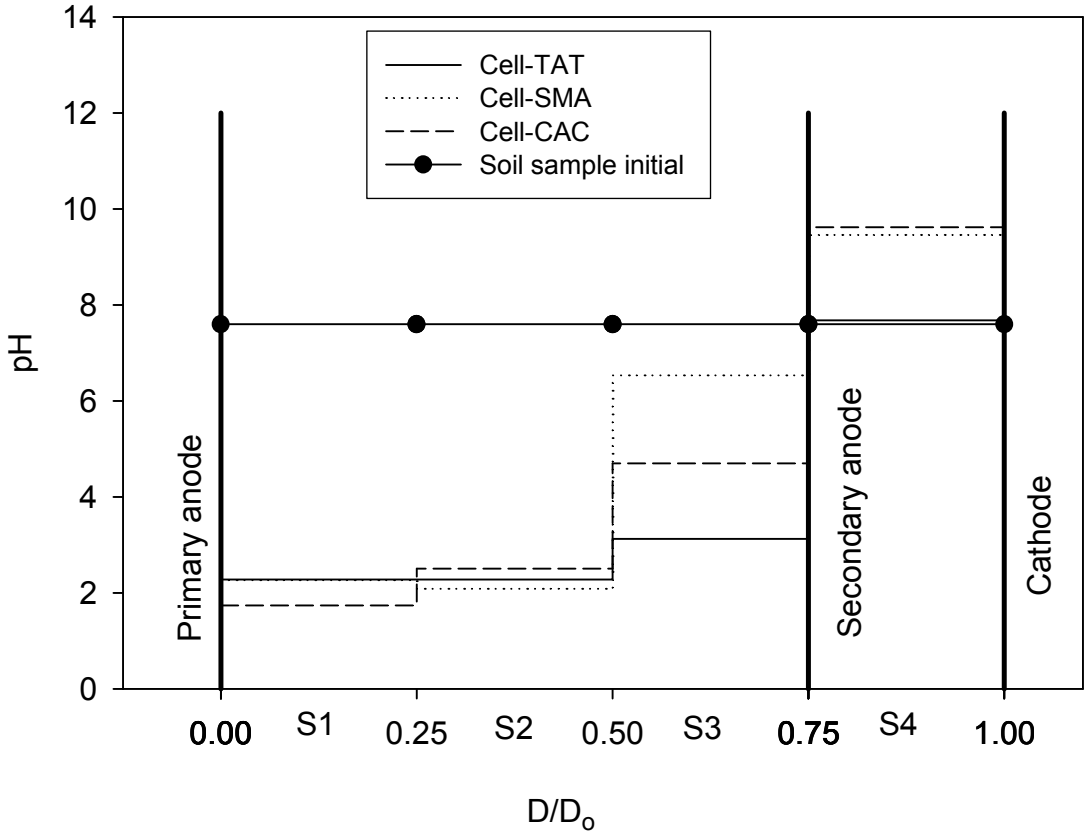

Figure 7.11 pH of the soil along the cells after the test.

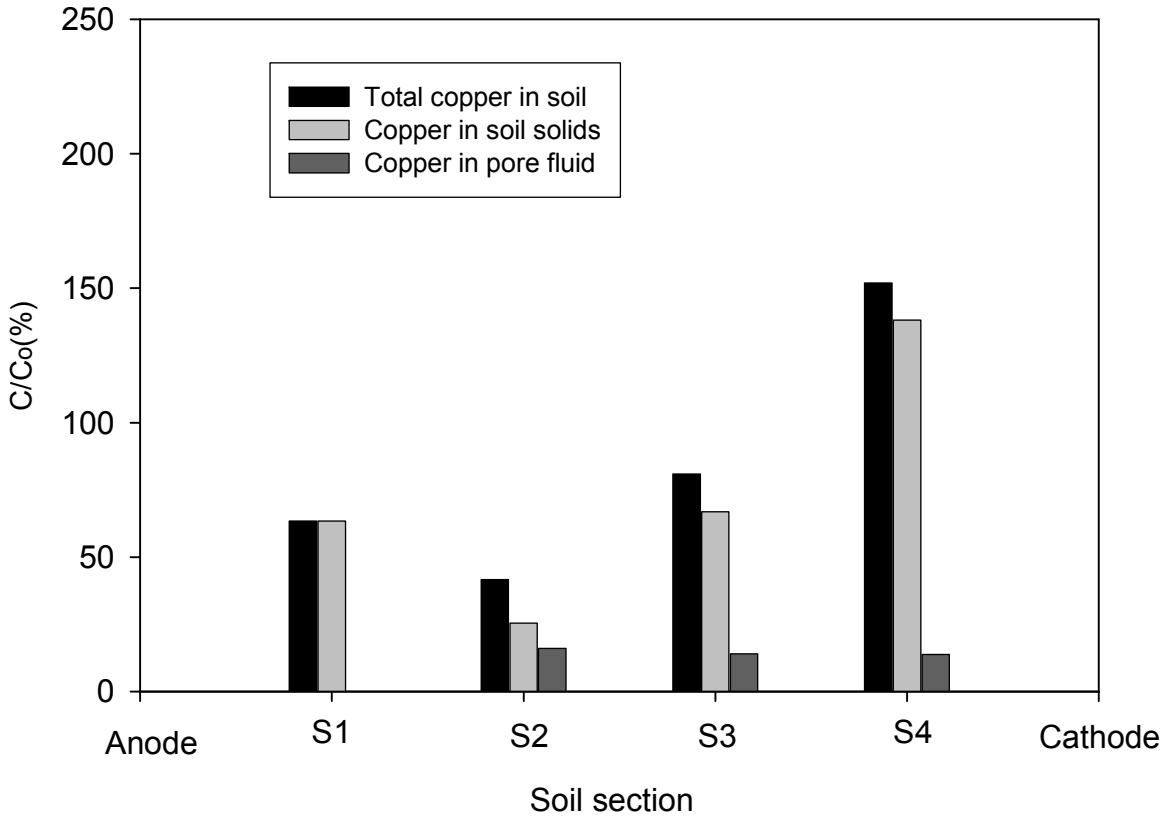

Figure 7.12 Ratio of copper concentration after the tests to initial concentration (C/C_o) in sections S1 to S4 of Cell-SMA.

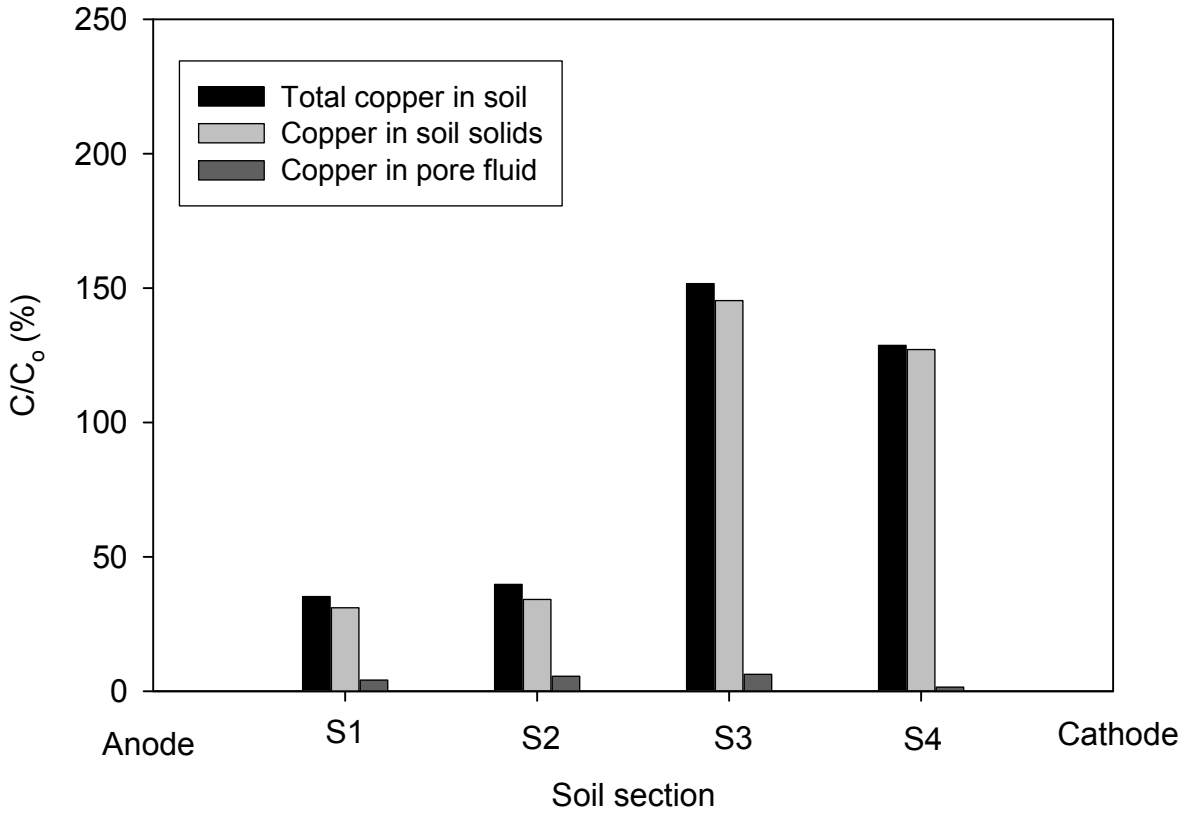

Figure 7.13 Ratio of copper concentration after the tests to initial concentration (C/C_o) in sections S1 to S4 of Cell-CAC.

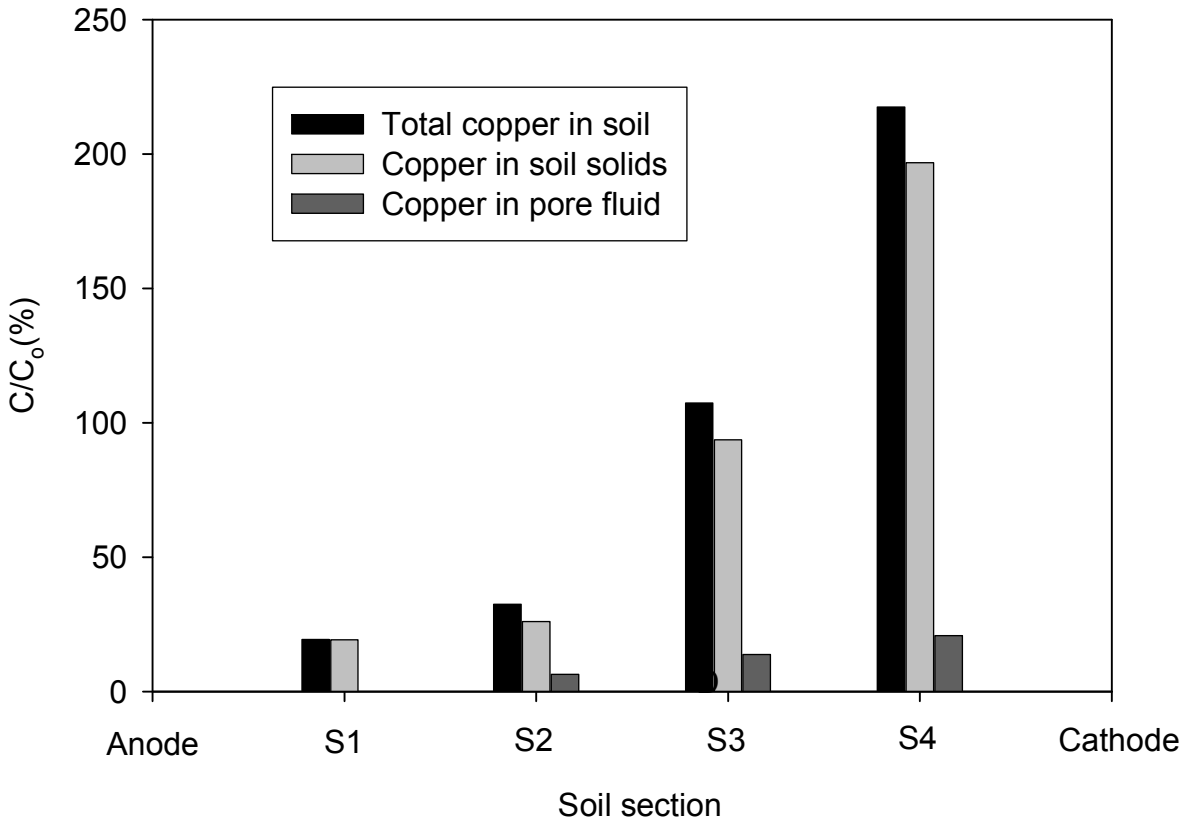

Figure 7. 14 Ratio of copper concentration after the tests to initial concentration (C/C_o) in sections S1 to S4 of Cell-TAT

CHAPTER EIGHT

OPTIMIZATION OF THE NOVEL TWO ANODES TECHNIQUE

8.0 INTRODUCTION

This chapter explores the effects of current intermittence and location of the secondary anode on the effectiveness of electrokinetic remediation with the novel Two Anodes Technique (TAT). In the chapter, a total of 16 electrokinetic remediation tests were conducted. The first eight tests were performed to compare the effect of intermittent current with continuous current in the effectiveness of electrokinetic remediation with TAT. The second set of four tests was carried out to investigate the effect of the location of the secondary anode in electrokinetic remediation with TAT. The remaining four tests were conducted with a Conventional Anode-Cathode (CAC) approach for comparison. The power consumption during the remediation was used as the reference for comparison. The experiments were conducted in sets of four tests with power consumptions of 500, 750, 1000, and 1250 Whr.

8.1 TEST PROCEDURE

The electrokinetic cell described in section 4.1.1 was used for the tests. The soil, homogeneous clay, was artificially contaminated with 355 mg copper per kg of dry soil. The procedure described in section 4.2.1 was followed for sample preparation and placement. Two-dimensional electrode configuration as presented in section 4.2.4 was used in the tests. The procedure described in section 4.2.5 was followed for data collection and samples analysis. For

ICP-OES analysis, 5 mL of each copper solution was diluted by adding 40 mL of deionized water. Three sets of tests were carried out. In the first set, eight TAT tests were performed with the secondary anode at 50 mm from the cathode. Four tests were conducted with current intermittence of 3 min on and 1 min off for the main and secondary circuits (see Figure 4.9). The other four tests were performed with continuous current. In the second set, four tests were performed with current intermittence of 3 min on and 1 min off for both circuits with the secondary anode at 15 mm from the cathode. The third set consisted of four tests carried out with the Conventional Anode-Cathode (CAC) and continuous electric current. The power consumptions in the four tests were 500, 750, 1000, and 1250 Whr.

8.2 RESULTS AND DISCUSSION

In the following sections, the results of the three sets of tests are presented. The optimum results from the first set are compared with the results of the second set. The superior results are compared with the results of the third set. Section 8.2.1 discusses the current during the remediation time. Section 8.2.2 presents the water content of the soil after the tests. The dry soil and pore fluid pH results are discussed in section 8.2.3. Copper concentration after the tests is presented in section 8.2.4.

8.2.1 Electric current

Figure 8.1 shows the three electric currents (i.e. current in main circuit, current in secondary circuit, and total current in the secondary circuit) for the TAT test with continuous current and the secondary anode at 50 mm from the cathode. The figure shows that the main electric

circuit current was 0.55 A on the first day of remediation and decreased to 0.35 A at the end of the day. The main electric circuit current values were between 0.2 and 0.1 A during the rest of the test.

Figure 8.2 shows the three electric currents (current in main circuit, current in secondary circuit, and total electric current in the secondary circuit) for the TAT test with intermittent current and the secondary anode at 50 mm from the cathode. The figure shows that the current in the main electric circuit was 0.57 A on the first day of remediation and decreased to 0.4 A at the end of the day. The values of the current in the main electric circuit were between 0.3 and 0.2 A for the following three days of the test and then fluctuated between 0.2 and 0.1 A for the rest of the test. By comparing Figures 8.1 and 8.2, the current of the main circuit in TAT test with intermittent current was in general higher than in the test with continuous current.

Figure 8.3 shows the three electric currents in TAT test with intermittent current and the secondary anode at 15 mm from the cathode. The figure shows that the current in the main electric circuit current was 0.62 A on the first day of the test and decreased to 0.45 A at the end of the day. The values of the current in the main electric circuit were between 0.4 and 0.3 A for the second and third day of the test. The figure shows that the values of the current in the main electric circuit were between 0.3 and 0.2 A during the fourth and fifth day of the test, and between 0.2 and 0.1 A during the rest of the test. Figures 8.2 and 8.3 show that the location of the secondary anode influences the electric current in the main circuit. The high current was reported in the test with the secondary anode at 15 mm from the cathode.

Figure 8.4 shows the electric current during the remediation for the test with CAC. The figure shows that at the start, the electric current was 0.59 A. An abrupt decrease in the current to 0.3 A occurred during the first day of the test. Figure 8.4 shows that for all days of the test, the current was high at the early hours of the day and decreases during the day. The figure shows that the current decreased with each passing day of remediation. The lowest current was 0.13 A reported during the last day of the test. Figures 8.1 to 8.4 show a general decrease in current with time. The decrease resulted from the change in the electrical conductivity of the soil as discussed in section 5.3.1.

By comparing Figure 8.3 and 8.4, the current of the main circuit in test with TAT was higher than the current in the CAC test at the start and during most of the test and lower at the end of the test. The off time in the test with intermittent current allows more time for the H^+ ions to dissolve the cations from the contaminated soil. This results in increase in the cations concentration in the pore fluid and consequently increases the electrical conductivity. Therefore, the high current values at the start of the test with TAT can be attributed to the effect of the current intermittence. The lower current values at the end of TAT test can be attributed to the introduction of secondary anode that changes the voltage distribution between the primary anode and the secondary anode (see Figures 4.10 and 7.5). The secondary electric circuit current values fluctuated between 0.15 and 0.09 A for the first five days of the test and between 0.07 and 0.01 A for the rest of the test. The total current in the secondary electric circuit is the summation of the main and secondary electric circuit currents. The highest value of the total current was 0.7 A recorded on the first day of the test, which gradually

decreased to 0.5 A at the end of the first day. The total current values were 0.5 to 0.4 A for the second to fourth day of the test, between 0.4 to 0.2 A form fifth to the eighth day of the test, and between 0.2 to .015 for the remaining of the test. The lowest values recorded was 0.13 A on the last day of remediation.

8.2.2 Water content

Figures 8.5 to 8.8 present the water content in soil specimen after the first set (TAT with intermittent and continuous currents). No consistent trend of water content can be concluded from the tests. The water content in S1 was slightly higher than in S2 as a result of the water permeation through the Plexiglas mesh and the geotextile filter from the adjacent water compartment. In the continuous current tests, the water content in S3 compared with that in S4 was higher at power consumption of 500 Whr, lower at power consumptions of 750 and 1000 Whr, and the same at power consumption of 1250 Whr. In the intermittent current tests, the water content in S3 was lower than in S4 for all tests, except for test with power consumption of 1250 Whr where they were equal. In most tests, the water content in S3 was lower than in S4. This is contrary to the results of the tests discussed in chapter six (6.3.1.2 and 6.3.2.2) conducted with CAC. The lower water content in S3 indicates that TAT successfully hindered the movement of the base front. For the range of power consumption tested, the water content in the tests carried out with intermittent current were lower than the in the tests with continuous current. Thus, the current intermittence was more effective than the continuous current in dewatering the cells. This is in agreement with previous researches that showed intermittent current is superior to continuous current in moving water in the soil pores (e.g., Rabie et al., 1994; Mohamedelhassan and Shang, 2001).

Figures 8.9 to 8.12 show the water content results of TAT with intermittent current tests from the first set (secondary anode at 50 mm from the cathode) and from the second set (secondary anode at 15 mm from the cathode). As discussed before, the water content in S1 was higher than that in S2. Similar to the first set, in most tests the water content in S3 was found to be lower than that in S4. For all power consumptions, the water content of the second set of tests was lower than from the first set of tests except for S1 and S2 at power consumption of 1250 Whr. This indicates that no water formation takes place near the cathode for the second set of tests. Therefore, it was concluded that the results obtained from the second set of tests (secondary anode at 15 mm from cathode) are superior to the first set (secondary anode at 50 mm from the cathode) in terms of hindering the advancement of the base front.

Figures 8.13 to 8.16 show the water content of the third set of tests and the second set of tests. At all sections, for all power consumptions, the water content of the second set of tests is lower than for the third set of tests, except in S2 for power consumption of 1000 Whr and S1 for power consumption of 1250 Whr. For sections S3 and S4, the comparison revealed that the low water content in S3 and S4 for the second set of tests indicates no water formation occurred. On the other hand, for third set of tests the higher water content in S3 and S4 implies high probability of water formation.

8.2.3 pH of soil and soil pore fluid

Figures 8.17 to 8.20 show the dry soil pH of the first set of tests. The figures show that the pH values at S1 in all tests were the same. At power consumption of 500 Whr, Figure 8.17 shows

that at S2, S3, and S4, the pH of the test with intermittent current were slightly higher than in the tests with continuous current. For power consumption of 750 Whr, Figure 8.16 shows at S2 and S4 the pH were higher for the tests with intermittent current, and at S3 pH was lower for the test with intermittent current. Figure 8.19 shows the pH for test with intermittent current at S2 to be similar to that with continuous current, at S3 to be lower for test with intermittent current, and higher pH at S4 was recorded for the cell with intermittent, and to be higher at S4 compare with continuous current.

Figures 8.21 to 8.24 show the pH of the soil pore fluid for the first set tests. Figure 8.21 shows that at all sections, the pH values were slightly higher for the test with intermittent current. For power consumption of 750 Whr, Figure 8.22 shows that the pH values were equal or slightly higher in the test with intermittent current. Similar trend was observed in the test with 1000 Whr shown in Figure 8.23. For power consumption of 1250 Whr, Figure 8.24 shows that the pH values in all sections of tests with intermittent current to be slightly lower or equal to pH of the with continuous current. Thus, as the power consumption increased, the pH decreased throughout the soil in the tests with intermittent currents.

Figures 8.25 to 8.28 show the pH of dry soil for the second set of tests (TAT tests with intermittent current and secondary anode at 15 mm from the cathode) and the pH of TAT tests with intermittent current for the first set (the secondary anode at 50 mm from the cathode). The figures show that pH at S1 and S2 were similar for both set of tests at most power consumptions. Figure 8.25 shows that pH values were higher at S3 and S4 for the second set of

tests. For power consumption of 750 Whr, Figure 8.26 shows that pH values were lower at S3 for the second set of tests and equal for both tests at S4. For power consumption of 1000 Whr, Figure 8.27 shows that pH values at S3 and S4 were higher for the second set of tests. Figure 8.28 shows that the pH values were equal at S4 for both tests and lower at S3 for the second set of tests. Thus, in general the pH values in the second series were similar to or smaller than that of the first series. Lower pH values promote more dissolution of copper and subsequently enhance its removal by electrokinetics.

Figures 8.29 to 8.32 show the pH of the pore fluid for the second set of tests (TAT tests with intermittent current and the secondary anode at 15 mm from the cathode) and for the first set of tests with intermittent current (TAT tests with intermittent current and the secondary anode at 50 mm from the cathode). At all power consumptions, the pH values were approximately the same at S1 and S2 for both tests. Figure 8.29 shows that pH values were lower at S3 and S4 for second set of tests. For power consumption 750 Whr, Figure 8.30 shows that pH at S3 was lower for the second set of tests. Figure 8.31 shows that pH values were almost equal at S3 for both cells and lower at S4 for the second set of tests. Figure 8.32 shows that the increase in power from 1000 to 1250 Whr slightly changes the pH profile. Similar to the pH of the clay soil, pH values of the soil pore fluid in the second series were in general lower than or equal to the values in the first set of tests.

Figures 8.33 to 8.36 show the dry soil pH of the third set of the tests (Conventional Anode-Cathode (CAC)) and the second set of tests (TAT intermittent current tests with secondary

anode placed at 15 mm from the cathode). Figure 8.33 shows that pH values were higher at S1 and S3 for the second set of tests, similar at S2, and lower at S4 for second set of tests. For power consumption of 750 Whr, Figure 8.34 shows that the pH values were lower in all sections for the second set of tests except S4. Figure 8.35 shows identical pH values for both tests at S1 and S4 and lower pH values at S2 and S3 for the second set of tests. For power consumption of 1250 Whr, Figure 8.36 shows higher pH at S1 for second set of tests, identical values at S2, lower pH values for second set of tests at S3 and S4.

Figures 8.37 to 8.40 show the pH of the pore fluid for the third set of tests (CAC) and the second set of tests (TAT intermittent current tests with secondary anode at 15 mm from the cathode). Figure 8.37 shows that pH values were similar for both set of tests at S1 and lower for all other sections for the second set of tests. For power consumption of 750 Whr, Figure 8.38 shows that the pH values were lower at all sections for second set of tests. Figure 8.39 shows that pH values were fairly similar at S1 and lower for the rest of the soil specimen for second set of tests. For power consumption of 1250 Whr, Figure 8.40 shows that pH values were equal at S1 and S2 and lower at S3 and S4 for the second set of tests. In general, Figures 8.37 to 8.40 show the pH of pore fluid in the test with TAT to be lower than in the CAC test. The discussion and the results above clearly demonstrate the superiority of the second set of tests over the third set of tests.

8.2.4 Copper concentration

Figures 8.41 to 8.52 show ratio (in percentage) of copper concentration after the test (C) to the initial concentration (C_o= 355 mg Cu/kg dry soil) at sections S1 to S4 (see Figure 4.7). Figures 8.41 to 8.44 show copper ratio for the tests with continuous current in first set of tests. For power consumption of 500 Whr, Figure 8.41 shows that 80% and 68% of the initial copper was removed from S1 and S2. For power consumption of 750 Whr, Figure 8.42 shows that 90% and 83% of the initial copper was removed from S1 and S2. This means increasing power consumption by 50% increased the removal by 10-15%. For power consumption of 1000 Whr, Figure 8.43 shows that 93% and 86% of the initial copper was removed from S1 and S2. Figure 8.44 shows that 95% and 88% of initial copper was removed from S1 and S2 with power consumption of 1250 Whr. This suggests that increasing the power consumption by 66% (from 750 to 1250 Whr) increased the copper removal by 5% only. As the power consumption increased from 500 to 1250 Whr, the pH at S4 increased from 3 to 6. This may explain the lower copper concentration in the pore fluid at S4.

Figures 8.45 to 8.48 show the ratio of copper concentration (C/C_o) in S1 to S4 for the test with intermittent current in first set of tests. For power consumption of 500 Whr, Figure 8.45 shows that 84% and 60% of initial copper was removed from S1 and S2. For power consumption 750 Whr, Figure 8.46 shows that 88%, 73%, and 50% of initial copper was removed from S1, S2, and S3 respectively. This means increasing the power consumption by 50% in the test with intermittent current not only increases the percentage of copper removal but also removes 50% of the initial copper from S3. For power consumption 1000 Whr, Figure 8.47 shows that 90%, 83%, and 65% of the initial copper was removed from S1, S2, and S3, respectively. Figure

8.48 shows that increasing the power consumption by 25% (i.e. from 1000 to 1250) increased the copper removal by 2%, 8%, and 10% for S1, S2, and S3, respectively. Comparison of the results of the first set of tests shows that the amount of copper removed by the test with intermittent current is significantly higher than the copper removed by the test with continuous current.

Figures 8.49 to 8.52 show the ratio of copper concentration (C/C_o) in S1 to S4 for the third set of tests (CAC) and the second set of tests (TAT tests with intermittent current and the secondary anode at 15 mm from the cathode). For easy comparison, each figure shows the results of the two sets, CAC and TAT, for one power consumption. Figure 8.49 shows that 64% and 59% of the initial copper was removed from S1 and S2 of the CAC test, while 79% and 62% of initial copper removed from S1 and S2 of the TAT test. Figure 8.50 shows that increasing the power consumption by 50% (from 500 to 750 Whr) increased the copper removal by 25-30% at S1 and S2 for CAC test, while the concentration at S3 remain the same. For TAT at 750 Whr, 38% of initial copper was removed from S3 (62% compare to 180% at 500 Whr) and the copper removal increased by 10-16% at S1 and S2. Figure 8.51 shows that for S1 and S2, increasing the power consumption to 1000 Whr increased the copper removal in both tests by 3-10%. Figure 8.51 shows that for test with CAC the copper removed from S1 and S2 accumulated at S3 and S4, but for the test with TAT 20% increase in the copper removal was reported at S3. Figure 8.52 shows that for S1 and S2, increasing power consumption to 1250 Whr slightly increased the copper removal for both tests. As shown in Figure 8.52, no significant removals of copper from S3 in test CAC. However, increasing power consumption to 1250 Whr increased the

copper removal at S3 of the TAT by 23% as shown in Figure 8.52. The copper removed from S1, S2, and S3 of the test with TAT accumulated at S4. Therefore it can be concluded that the copper removal in the second set (TAT) of tests is superior to the removal in the third set of tests (CAC).

The comparison between the copper removal in TAT tests with intermittent current and the secondary anode at 15 mm from the cathode and the CAC tests shows clearly the superiority of the TAT tests, as significant amount of copper was removed from 75% of the soil.

Refer to Appendixes E, F, G, and H for ICP-OES results.

8.3 EFFECT OF ACIDIFICATION IN SOIL FERTILITY

Further tests were carried out to compare the acidification due to electrolysis reactions with that caused by addition of acidic chemical compounds. These tests were designed to lower the pH of the soil to around 2 to 2.5 by adding one of the following acids: hydrochloric, citric, and nitric acids. Three soil samples contaminated at 355 mg of copper per kg of dry soil were acidified using the acids. The acidified soil samples along with soil sample from section S1 in the electrokinetic test with intermittent current, TAT and secondary anode at 15 mm from the cathode, and power consumption of 1250 Whr were analyzed at the Forest Recourse and Soil Testing (FoReST) Laboratory, Lakehead University to examine the effect of acidification on fertility of the soil.

The results are shown in Table 8.1. For a soil with high acidity to be suitable for plant growth, ground limestone is added to raise the pH of the soil. Ontario Ministry of Agriculture, Food and Rural Affairs, OMAFRA, fertilizer recommendations chart to optimize plant growth was used to obtain the amount of lime required for the soil. The results shows that according to OMAFRA fertilizer recommendations chart, 2, 2, and 1.9 kg of limestone per m^2 should be added to the soil acidified with electrokinetic, hydrochloric, and nitric acids, respectively. The soil acidified with citric acid needs significantly high amount of lime. Further, the results showed that the amount of phosphorus on the soil treated with electrokinetics is 11.7 μg/g compared with 3.5 and 6.6 μg/g hydrochloric acid, and nitric acid, respectively. A highly phosphorous content is beneficial for soil fertility and plant growth. Despite the higher amount of phosphorus in soil acidified with citric acid (14.4 μg/g), substantial amount of lime is required for the soil to achieve the optimum pH required for plant growth. The low amount of K, Mg, Na, and Ca in the soil treated with TAT can be attributed to the electroosmosis and electromigration. The soil samples treated with acids have high concentration cations because the acids were used to lower the pH of the soil and there was no movement of the cation by any mean. It worth mentioning that there was no copper removal from the soil samples treated with acids. Therefore, it can be concluded that the soil treated with TAT is likely to regain more of its fertility characteristics compared to the soil samples treated with acids.

8.4 CONCLUSIONS

The purpose of the conducted tests was to further investigate and enhance the efficiency of the novel Two Anodes Technique (TAT). Current intermittence proved to enhance the effectiveness

of electrokinetic treatment by TAT. The tests performed using continuous current showed higher pH values at sections S2 and S3 when compared with the tests conducted using intermittent current. The tests conducted with intermittent current and the secondary anode at 15 mm from the cathode showed minor changes in pH values in S1, S2, and S3, whereas other tests showed considerable variation in pH values at S1, S2, and S3. In addition, the water contents of specimens after the tests were higher in the tests with continuous current. This indicates that the intermittent current was effective in dewatering the soil sample when compared with continuous current. The copper removal from sections S1 and S2 was remarkably higher in the case when the current intermittence was used with TAT. This is in agreement with the published literature, where the current intermittence positively contributes to the observed enhancement of electrokinetic remediation as discussed in previous sections.

The position of secondary anode was found to influence the outcome of electrokinetic treatment by TAT. It was found that in TAT tests with the secondary anode at 15 mm from the cathode, the pH values were lower than the values of TAT tests with secondary anode at 50 mm from the cathode. High copper removal was reported in S1, S2, and S3 in TAT tests with the secondary anode at 15 mm from the cathode. All other tests showed lower or no copper removal from section S3. Therefore, Two Anodes Technique with intermittent current and the secondary anode placed at 15 mm is superior to all other tests in the power consumption range tested.

Novel TAT configuration is a significant contribution to improve the effectiveness of electrokinetic remediation. The optimization of TAT had improved the removal of copper from the 75% of the soil under treatment.

Table 8.1 Factors affecting soil fertility and plant growth

				Olsen P(µg/g)	Ammonium Acetate Extractable (µg/g)			
Soil treated by	pH	Buffer pH	Limestone (kg/m^2)	P	K	Mg	Na	Ca
Hydrochloric acid	2	4.7	20	3.5	156.9	487.7	193.8	875
Citric acid	2.3	3.1	∞	14.4	164.3	400.9	153.8	718
Nitric acid	2.5	5.4	19	6.6	163.4	470.1	188.4	855
Electrokinetics	2	5	20	11.7	70.4	40.4	20.9	139

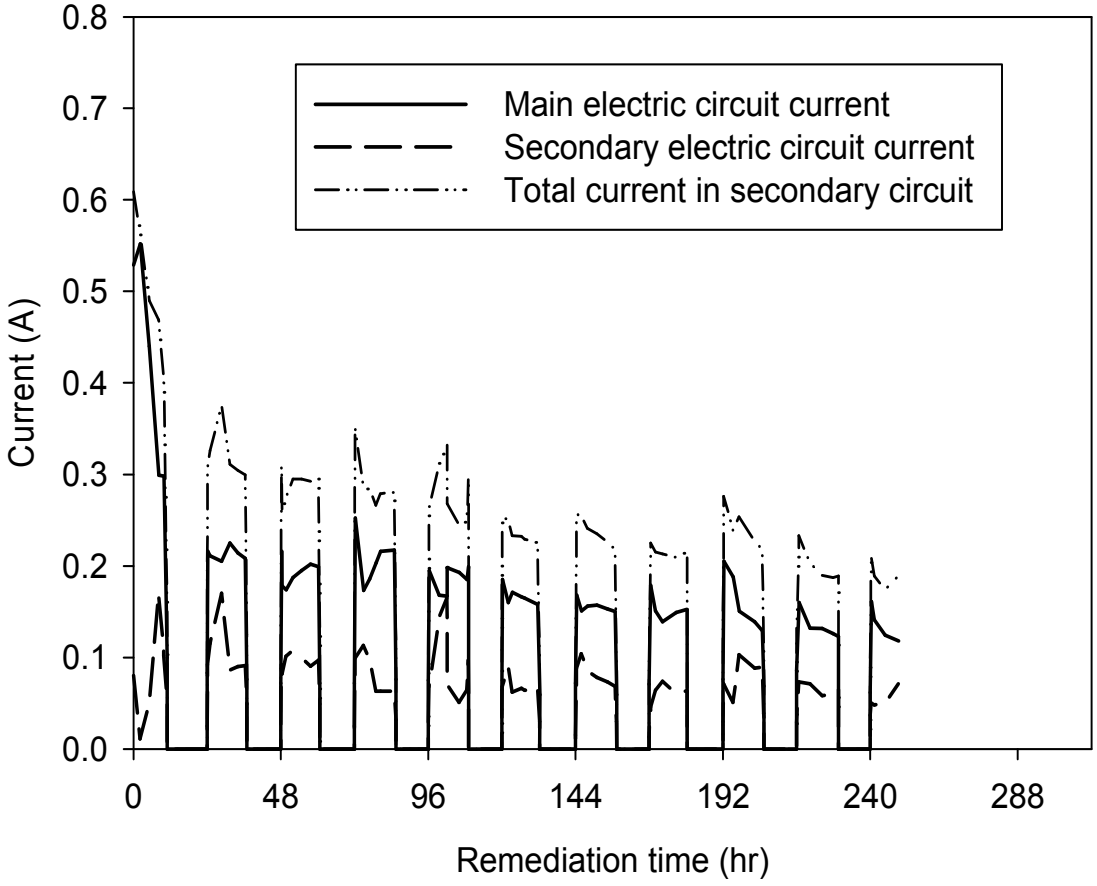

Figure 8.1 Electric current during TAT test with continuous current and secondary anode at 50 mm from the cathode for power consumption 1250 Whr.

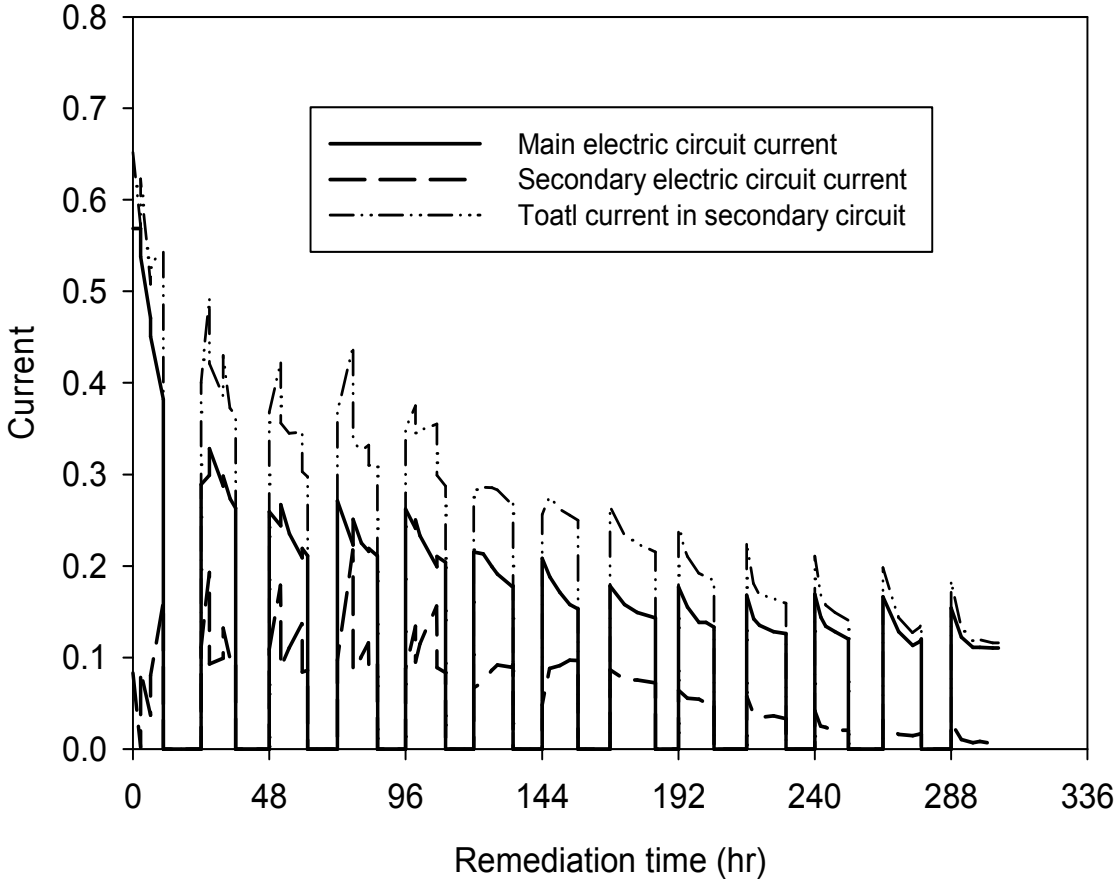

Figure 8.2 Electric current during TAT test with intermittent current and secondary anode at 50 mm from the cathode for power consumption 1250 Whr.

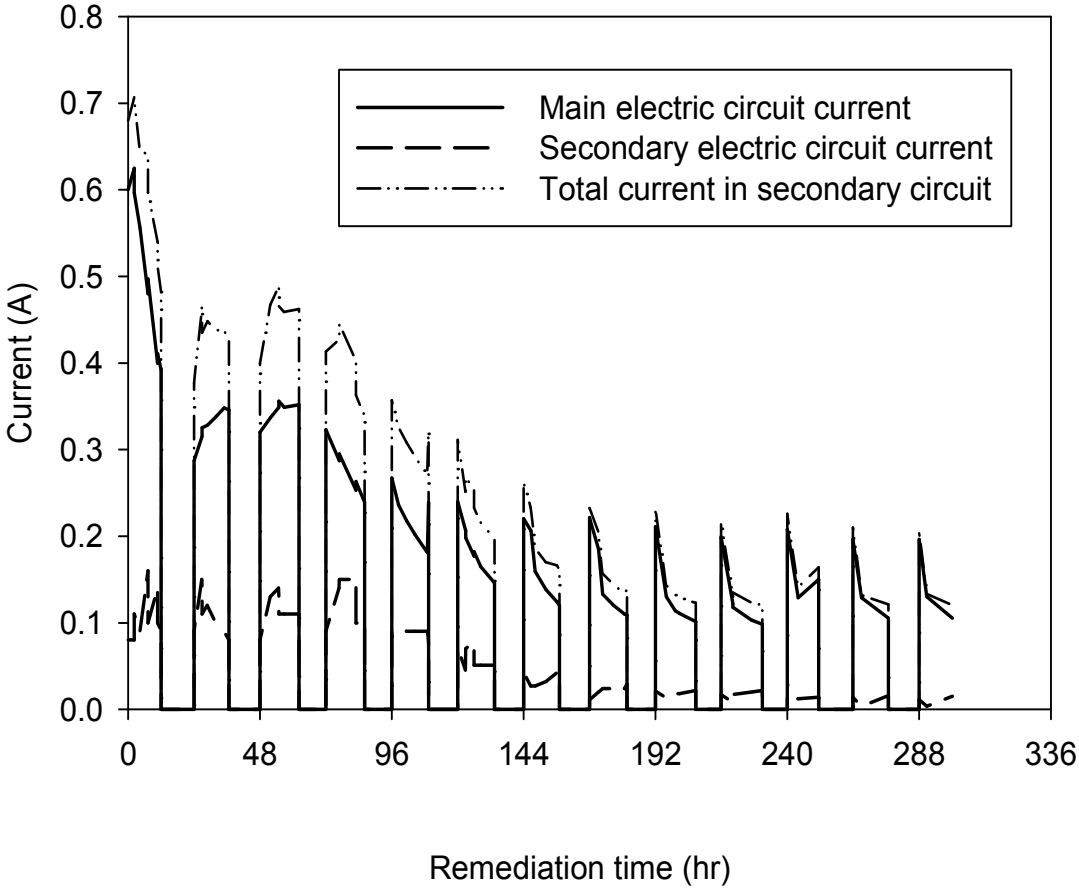

Figure 8.3 Electric current during TAT test with intermittent current and secondary anode at 15 mm from the cathode for power consumption 1250 Whr.

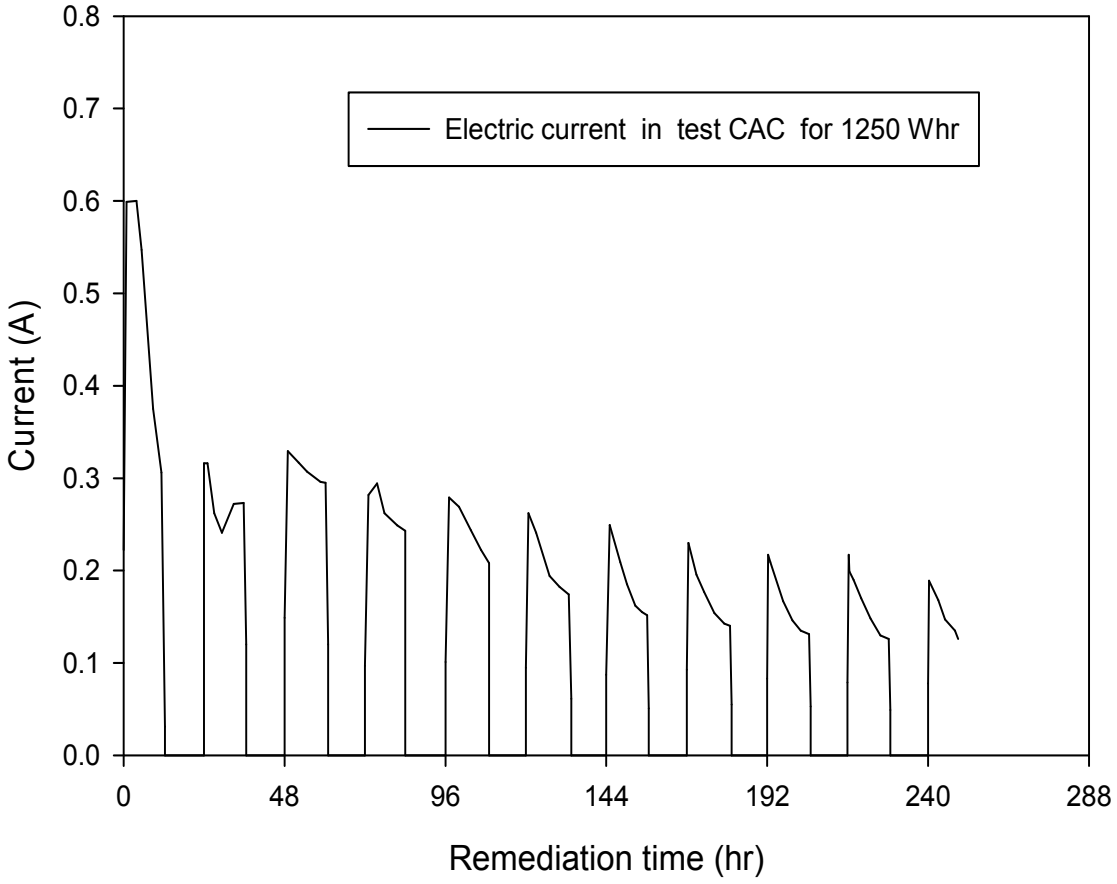

Figure 8.4 Electric current during CAC test for power consumption 1250 Whr.

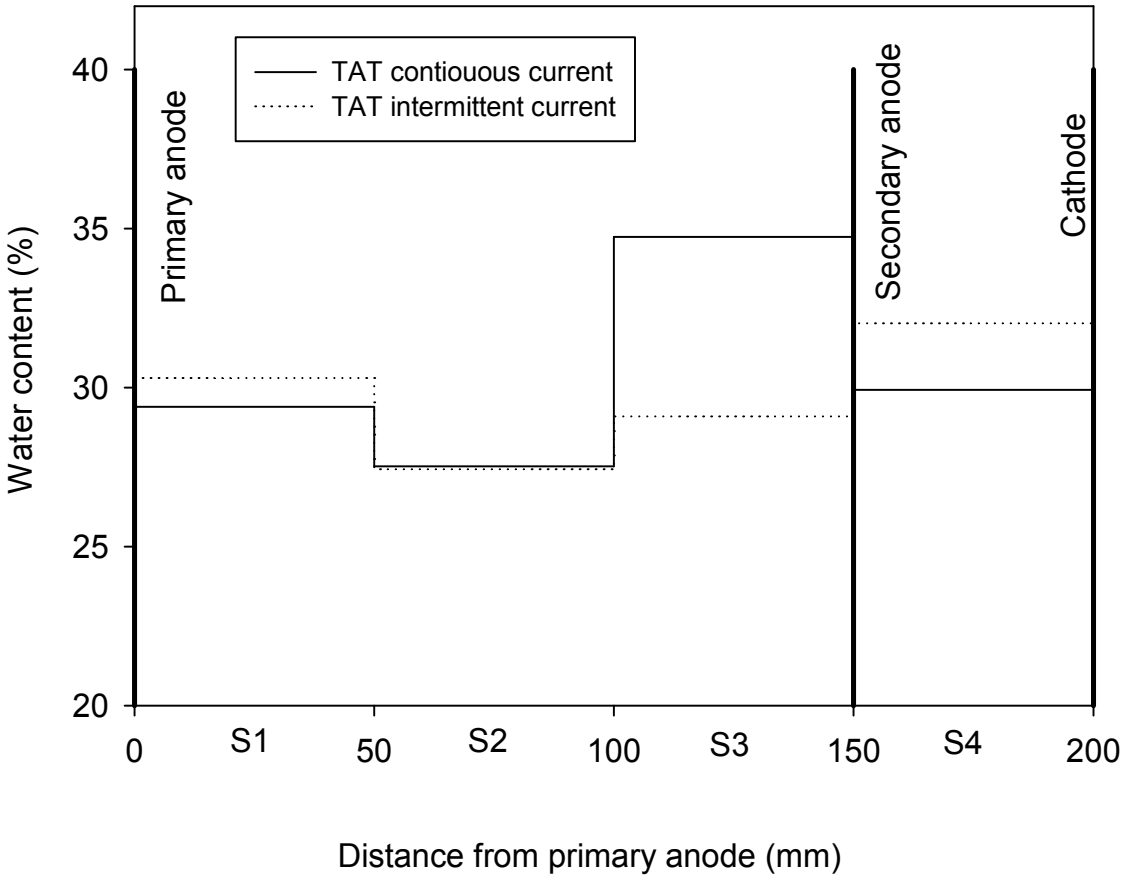

Figure 8.5 Water content after TAT tests with intermittent current and continuous current for power consumption 500 Whr.

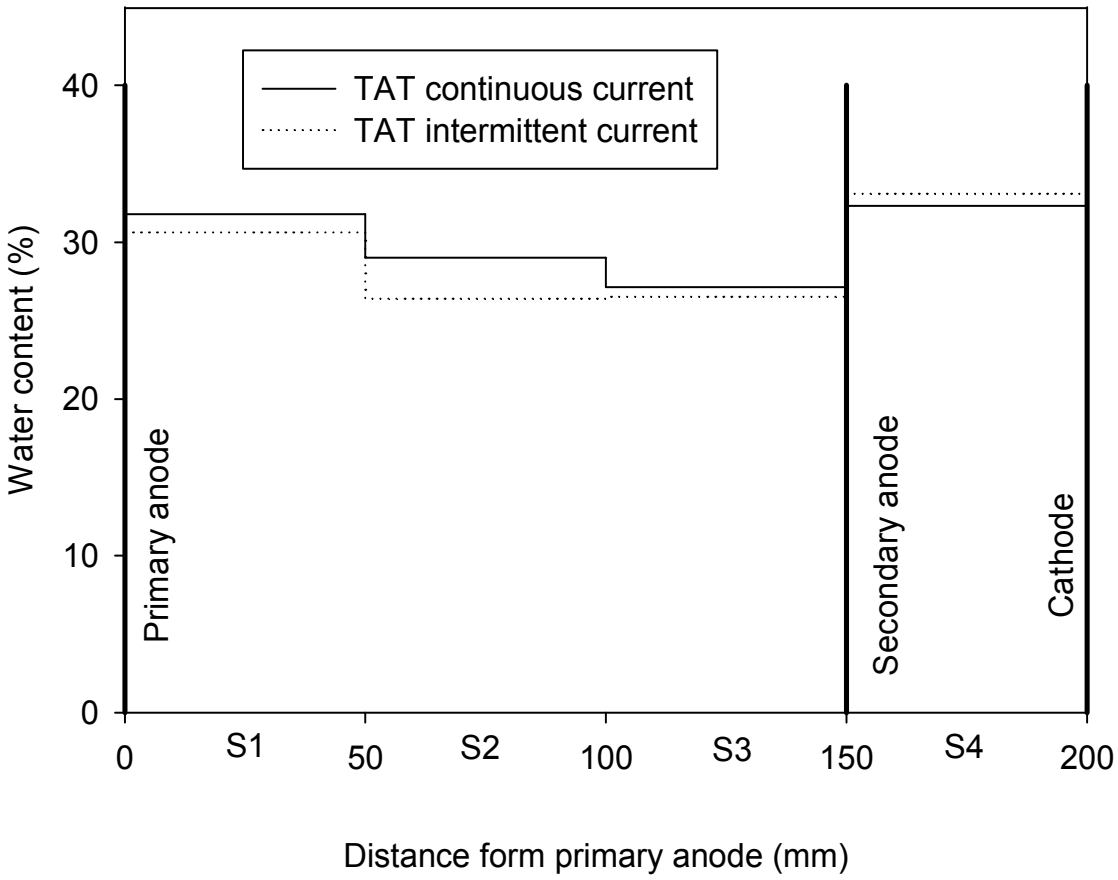

Figure 8.6 Water content after TAT tests with intermittent current and continuous current for power consumption 750 Whr.

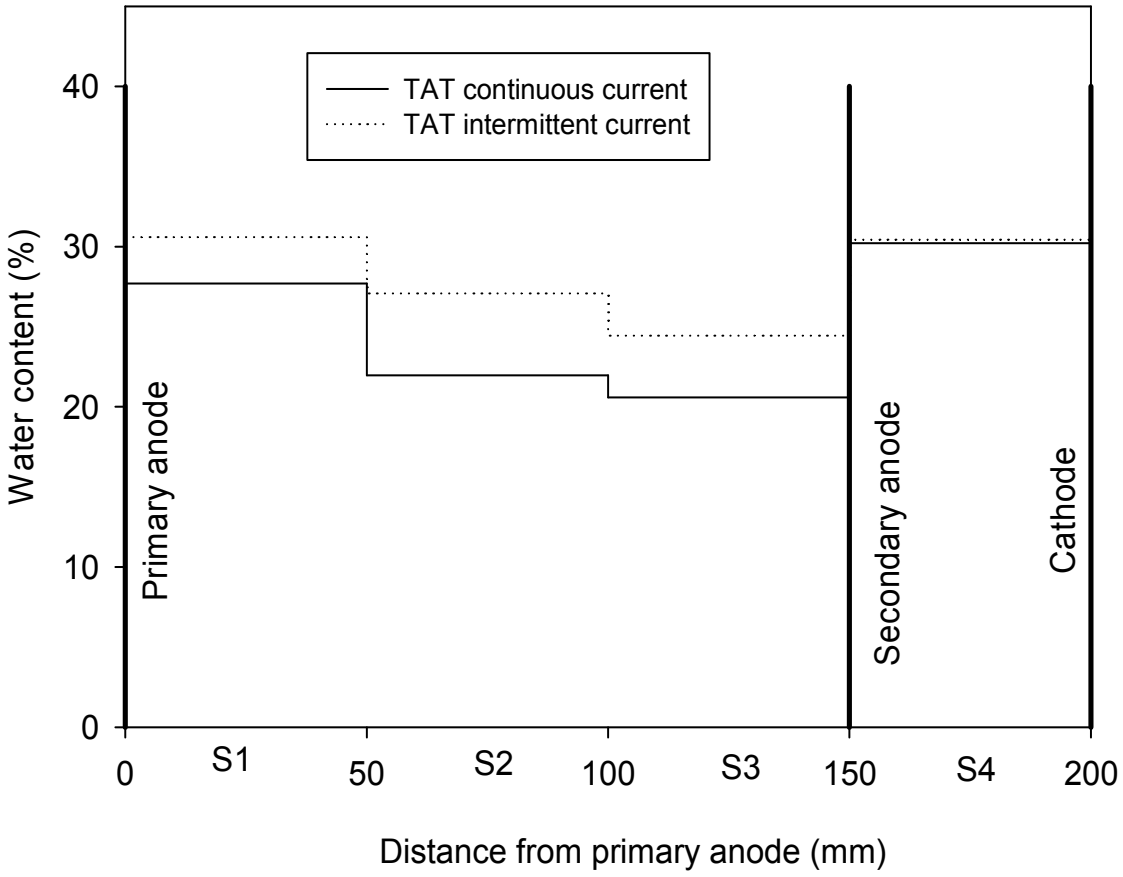

Figure 8.7 Water content after TAT tests with intermittent current and continuous current for power consumption 1000 Whr.

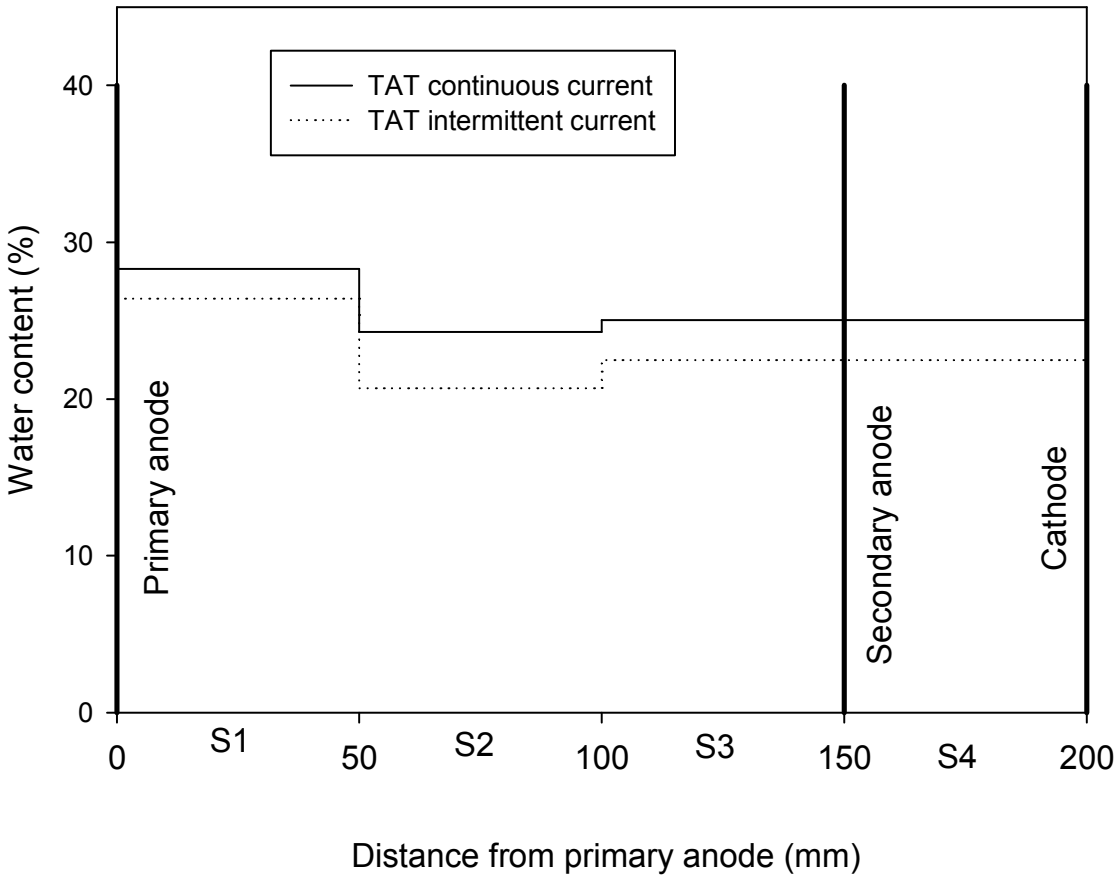

Figure 8.8 Water content after TAT tests with intermittent current and continuous current for power consumption 1250 Whr.

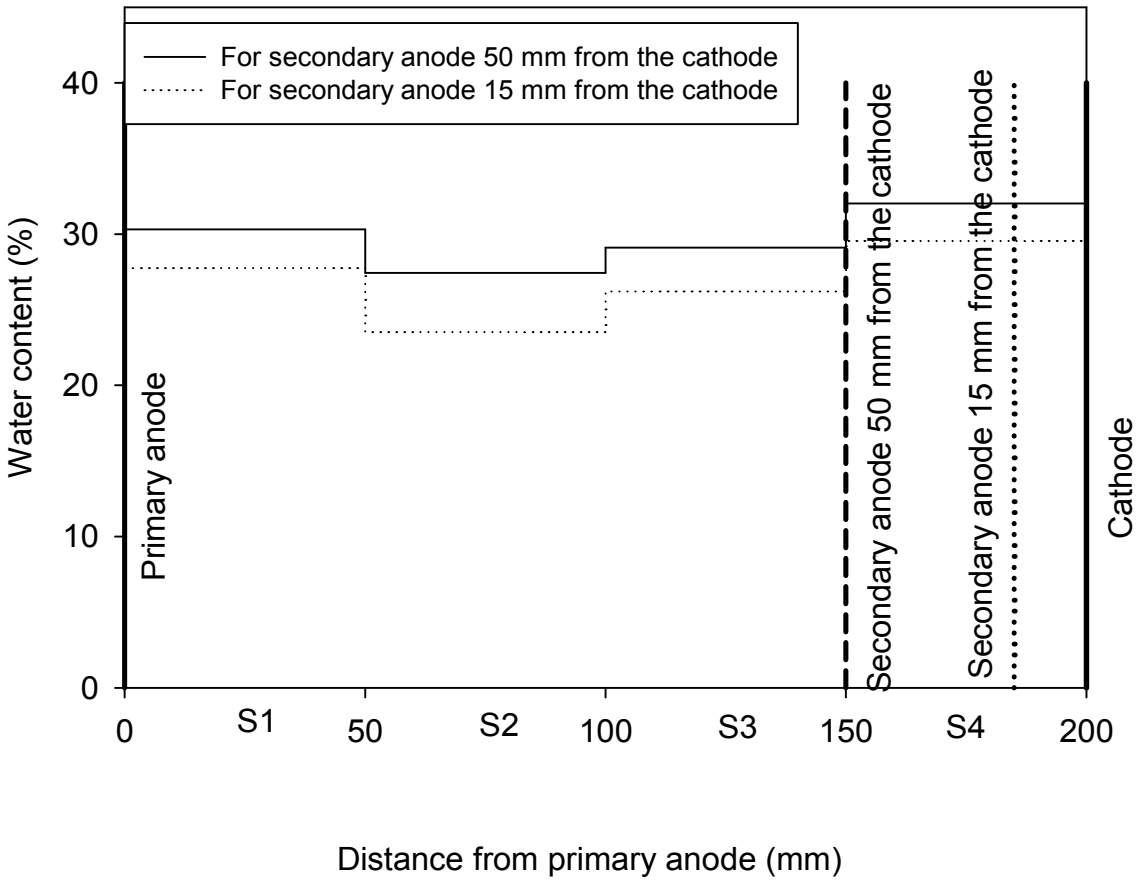

Figure 8.9 Water content after TAT tests with intermittent current and the secondary anode at 50 mm and 15 mm from the cathode and power consumption 500 Whr.

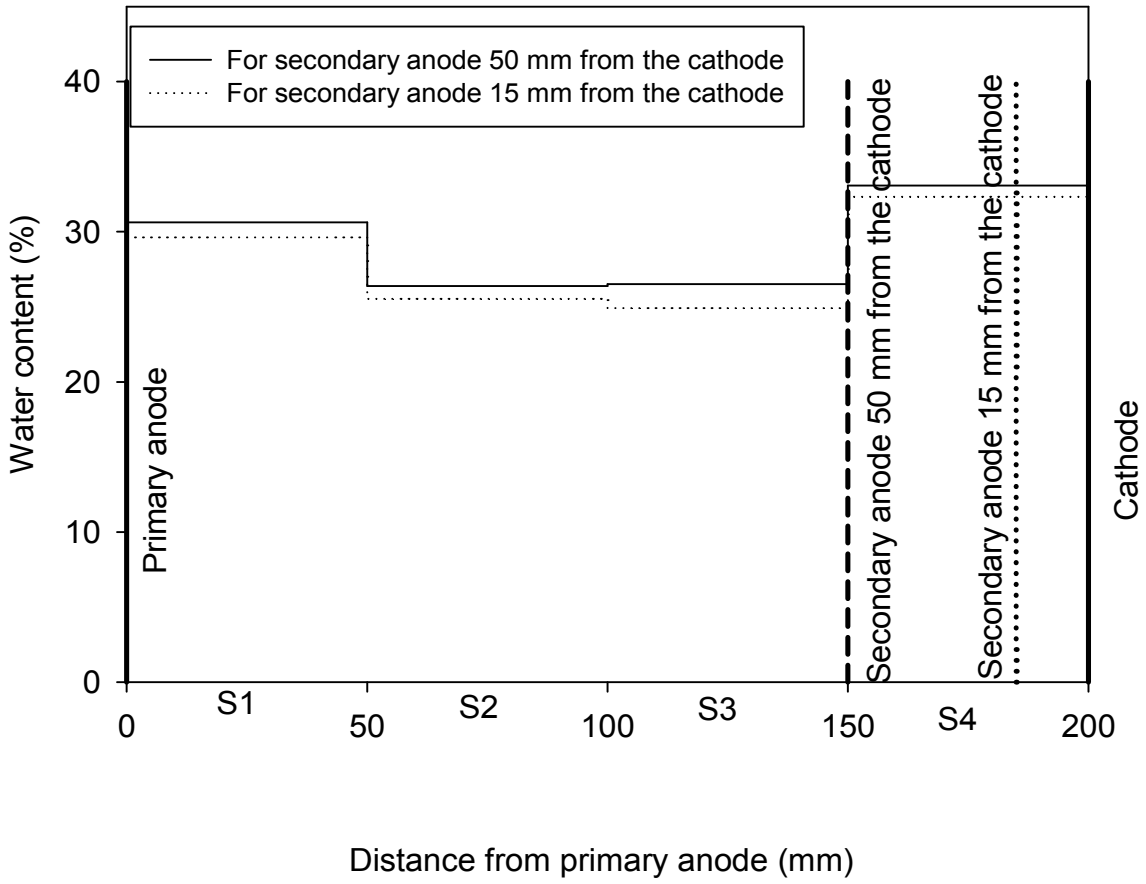

Figure 8.10 Water content after TAT tests with intermittent current and the secondary anode at 50 mm and 15 mm from the cathode and power consumption 750 Whr.

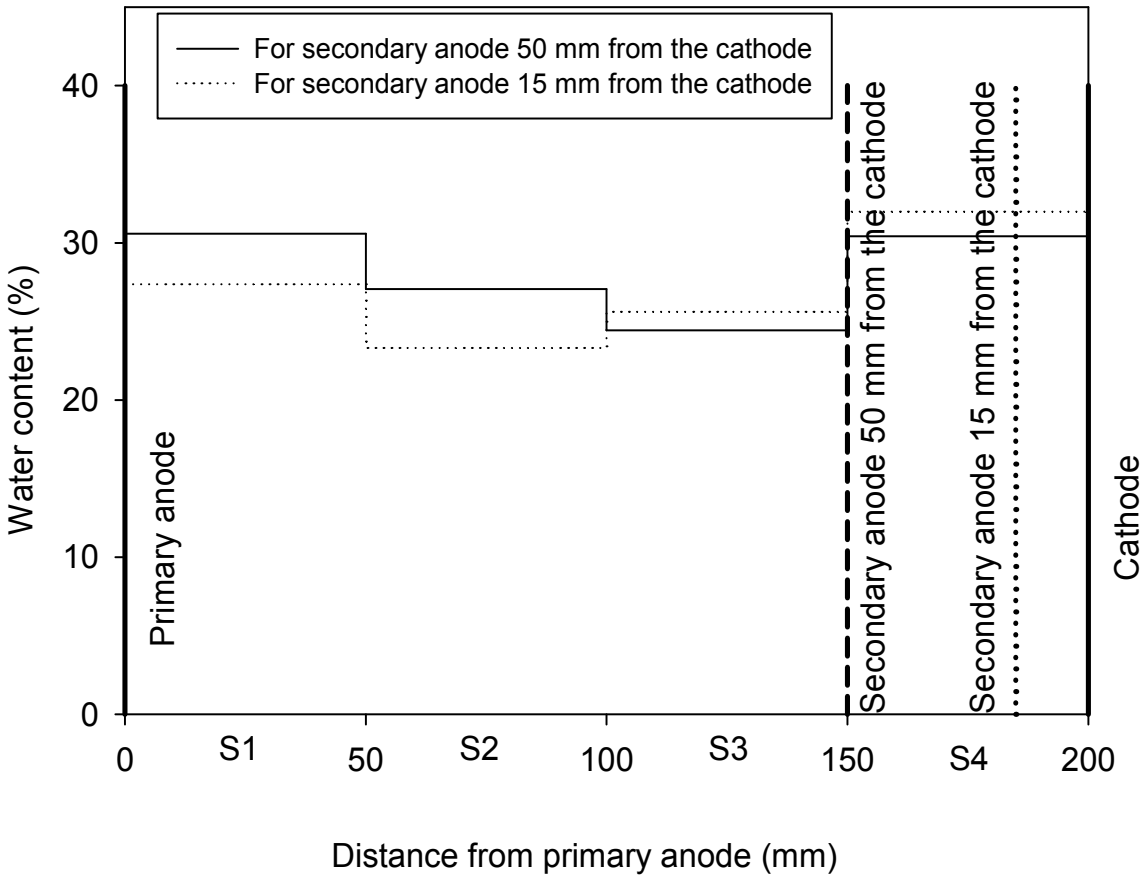

Figure 8.11 Water content after TAT tests with intermittent current and the secondary anode at 50 mm and 15 mm from the cathode and power consumption 1000 Whr.

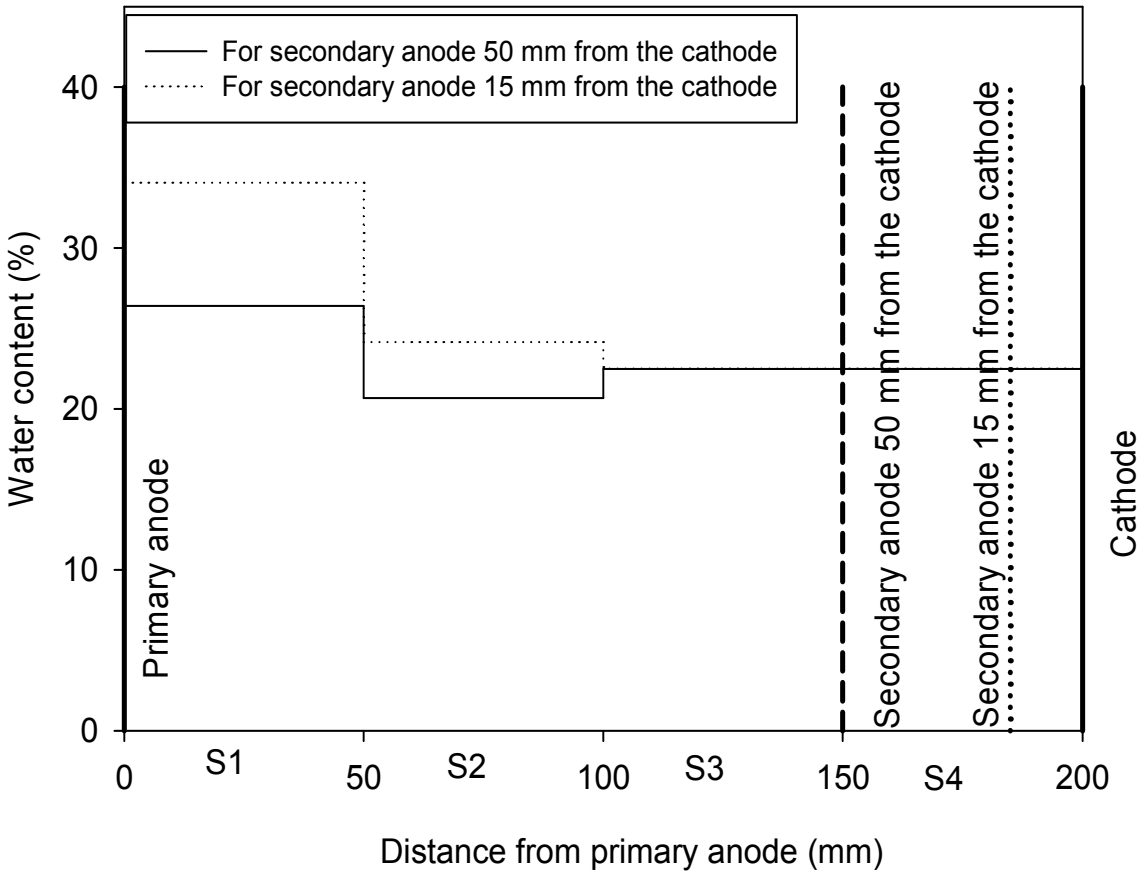

Figure 8.12 Water content after TAT tests with intermittent current and the secondary anode at 50 mm and 15 mm from the cathode and power consumption 1250 Whr.

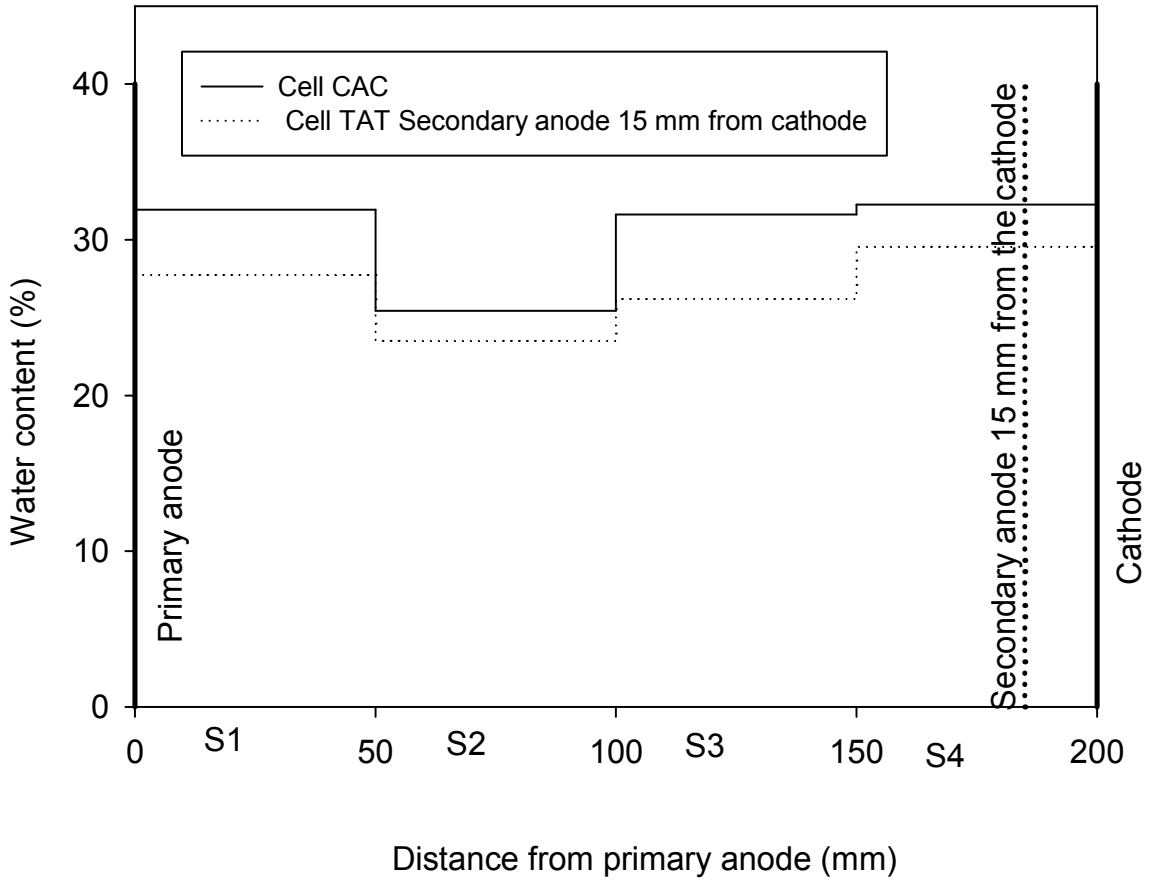

Figure 8.13 Water content after the TAT test with intermittent current and secondary anode at 15 mm from the cathode and CAC test for power consumption 500 Whr.

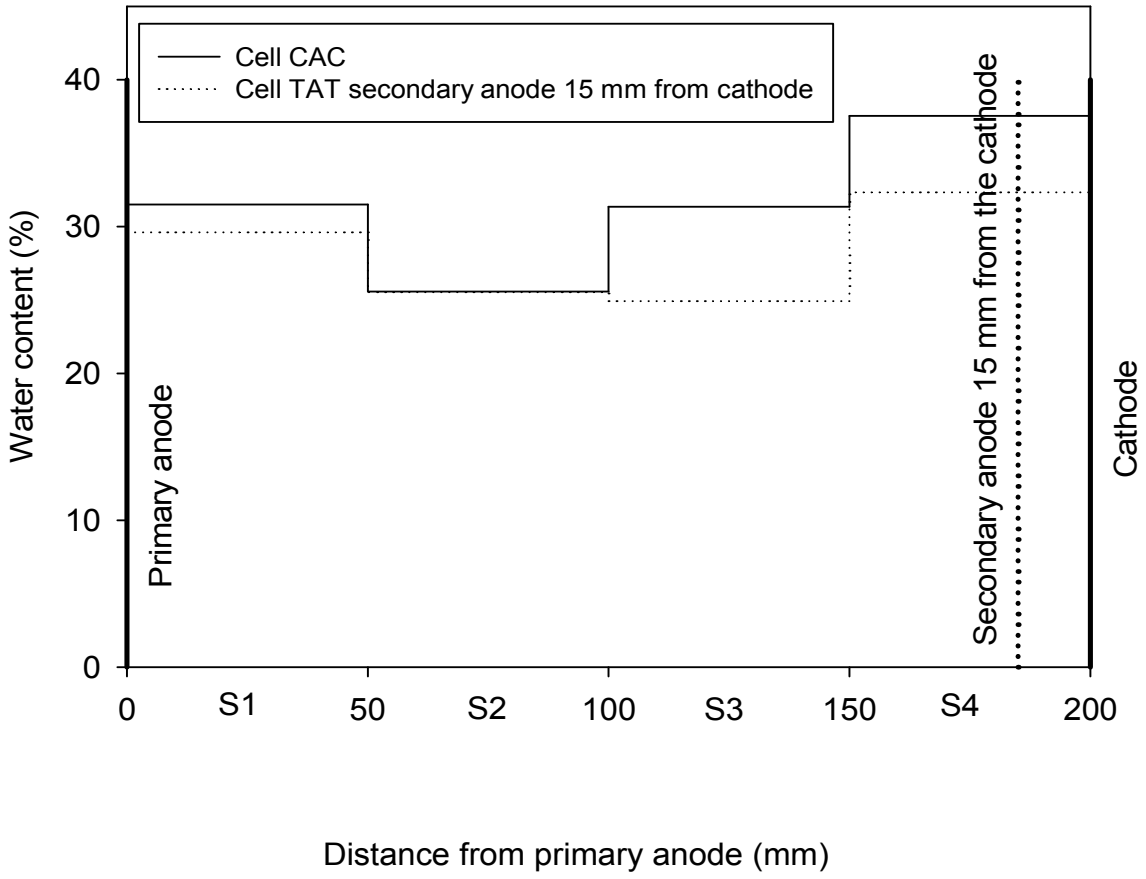

Figure 8.14 Water content after the TAT test with intermittent current and secondary anode at 15 mm from the cathode and CAC test for power consumption 750 Whr.

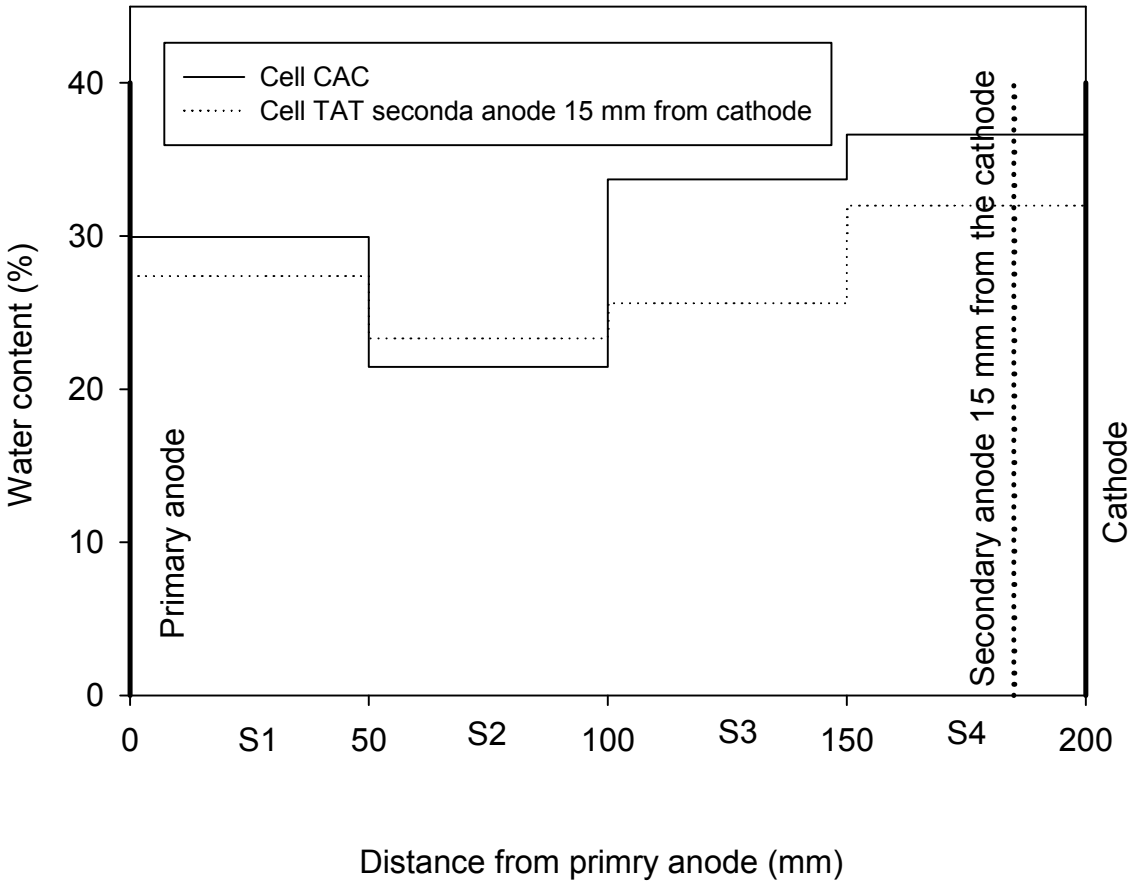

Figure 8.15 Water content after the TAT test with intermittent current and secondary anode at 15 mm from the cathode and CAC test for power consumption 1000 Whr.

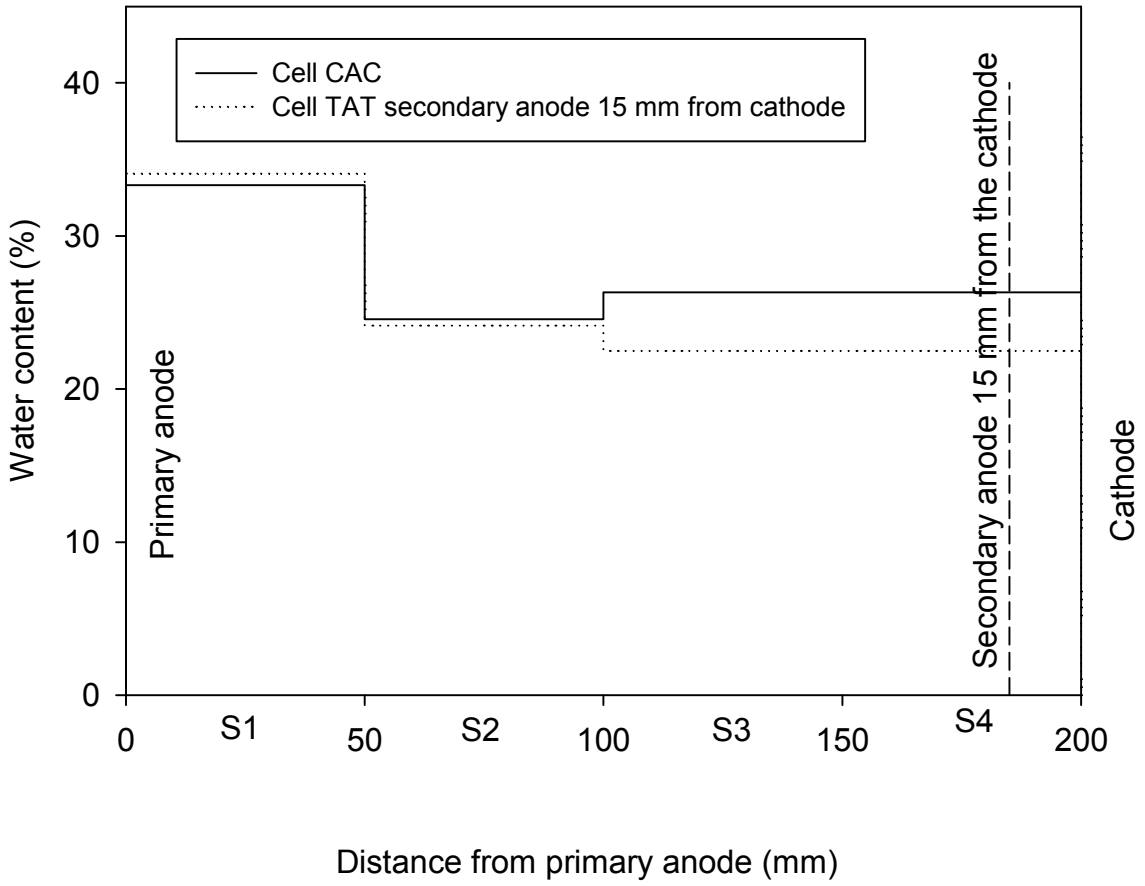

Figure 8.16 Water content after the TAT test with intermittent current and secondary anode at 15 mm from the cathode and CAC test for power consumption 1250 Whr.

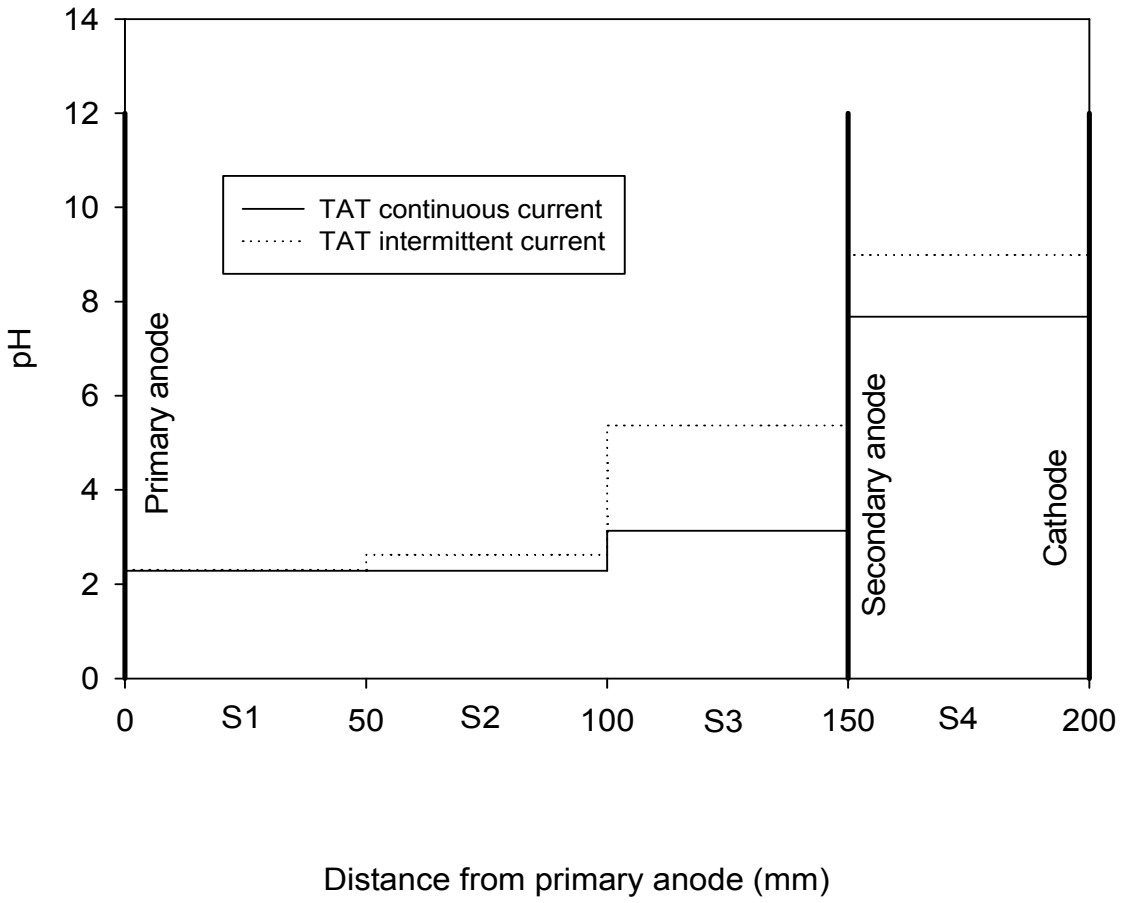

Figure 8.17 Dry soil pH after the TAT tests with intermittent current and continuous current and the secondary anode at 50 mm from the cathode for power consumption 500 Whr.

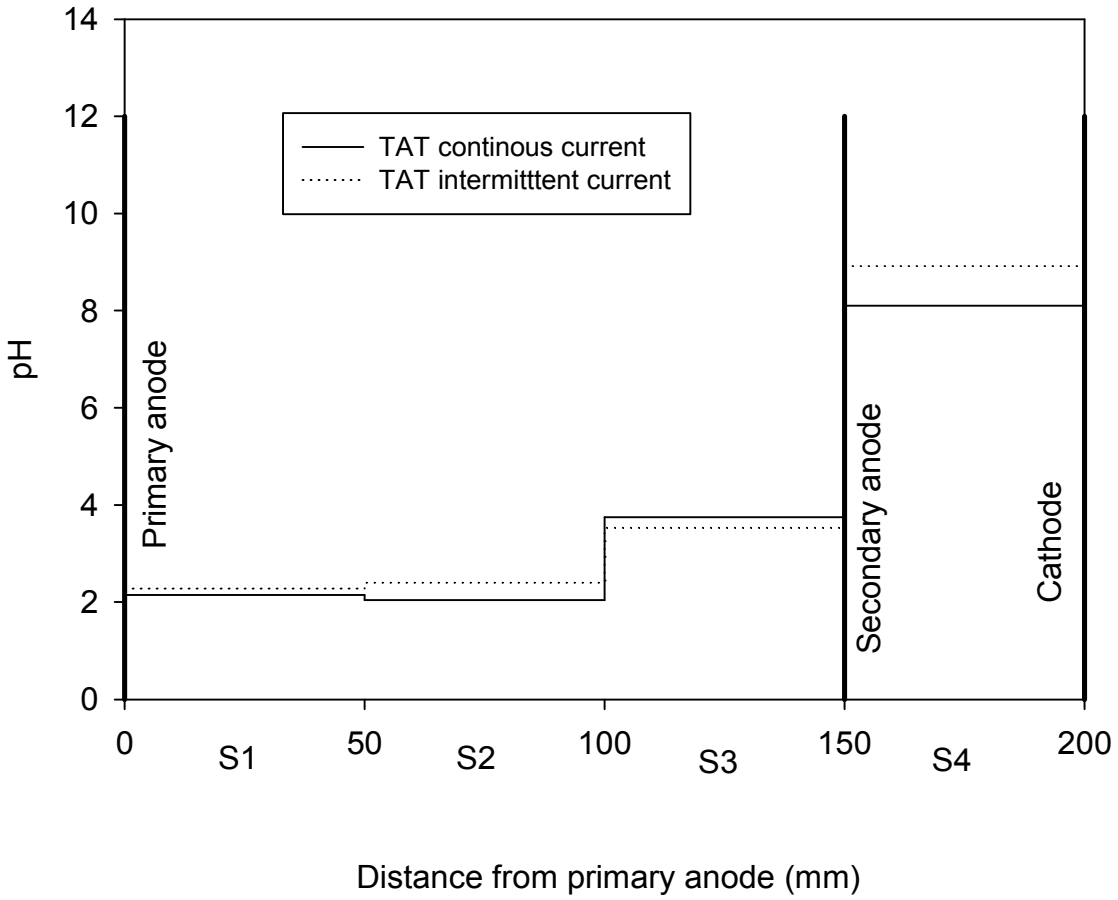

Figure 8.18 Dry soil pH after the TAT tests with intermittent current and continuous current and the secondary anode at 50 mm from the cathode for power consumption 750 Whr.

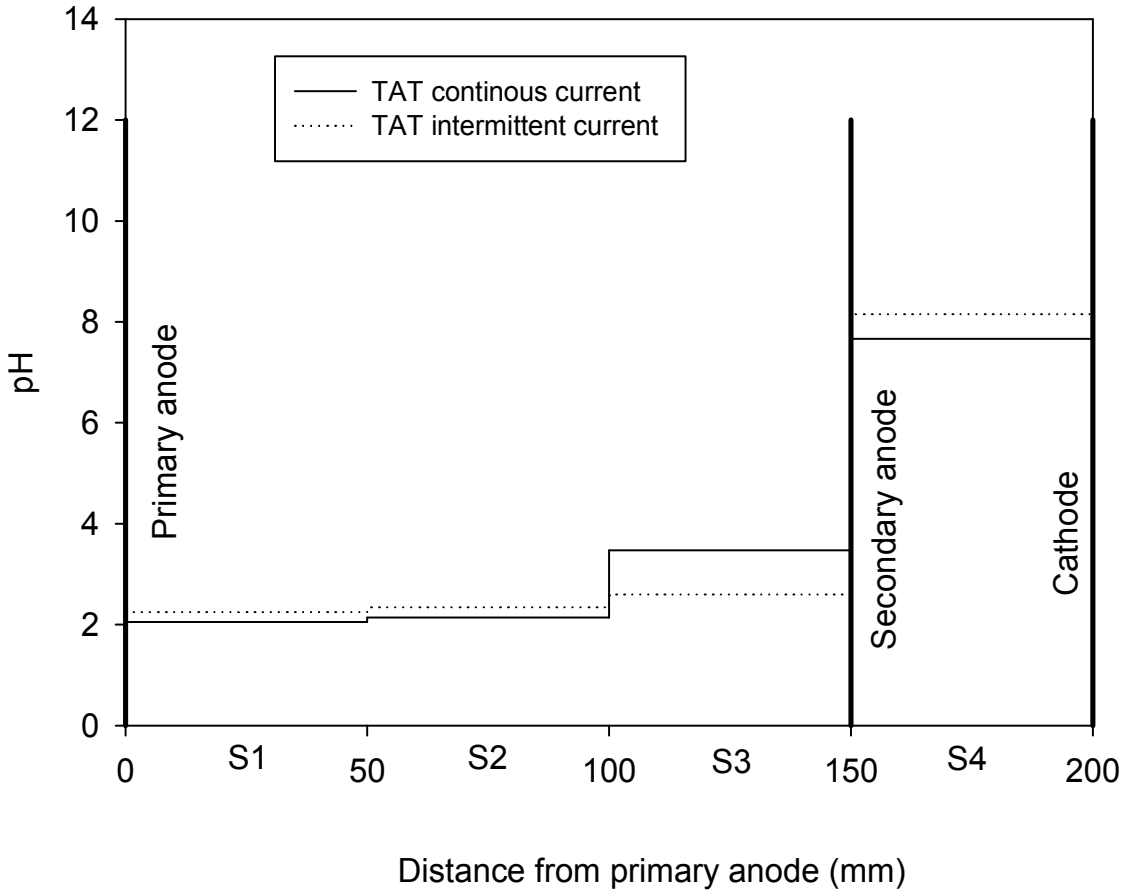

Figure 8.19 Dry soil pH after the TAT tests with intermittent current and continuous current and the secondary anode at 50 mm from the cathode for power consumption 1000 Whr.

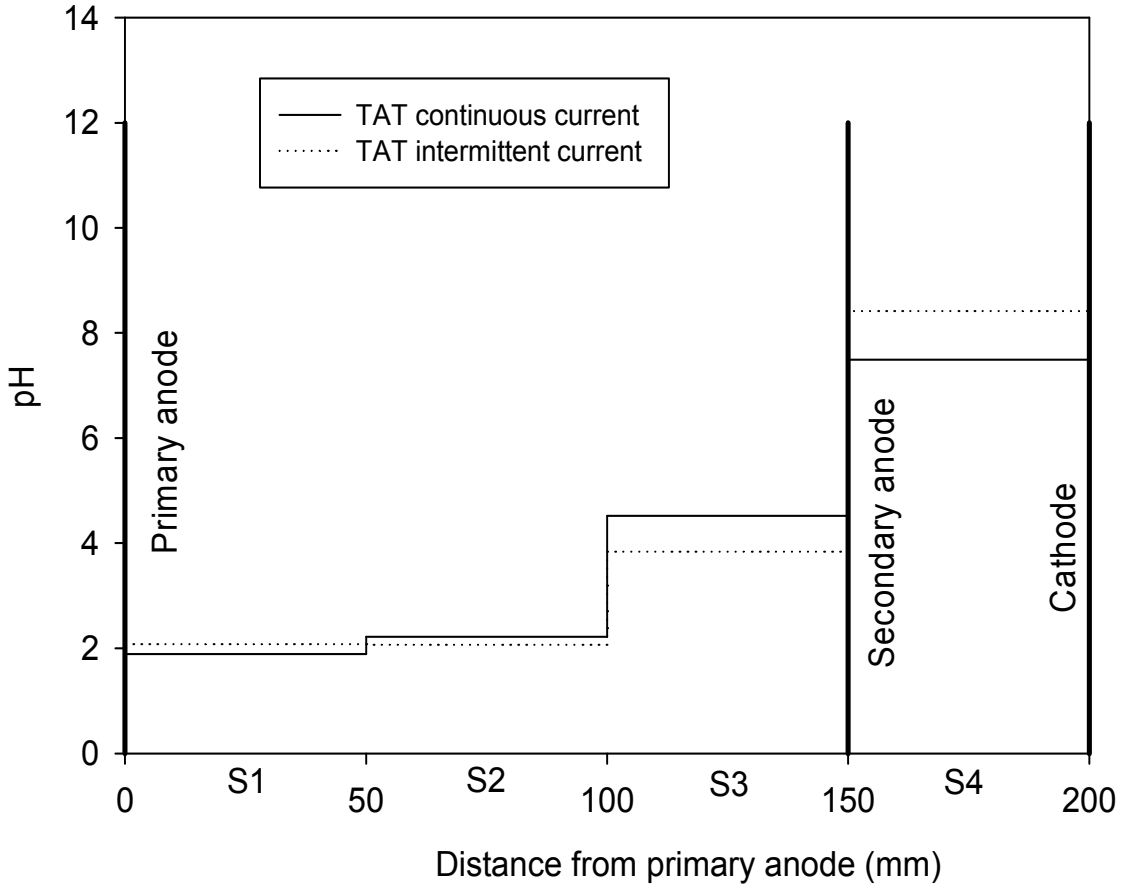

Figure 8.20 Dry soil pH after the TAT tests with intermittent current and continuous current and the secondary anode at 50 mm from the cathode for power consumption 1250 Whr.

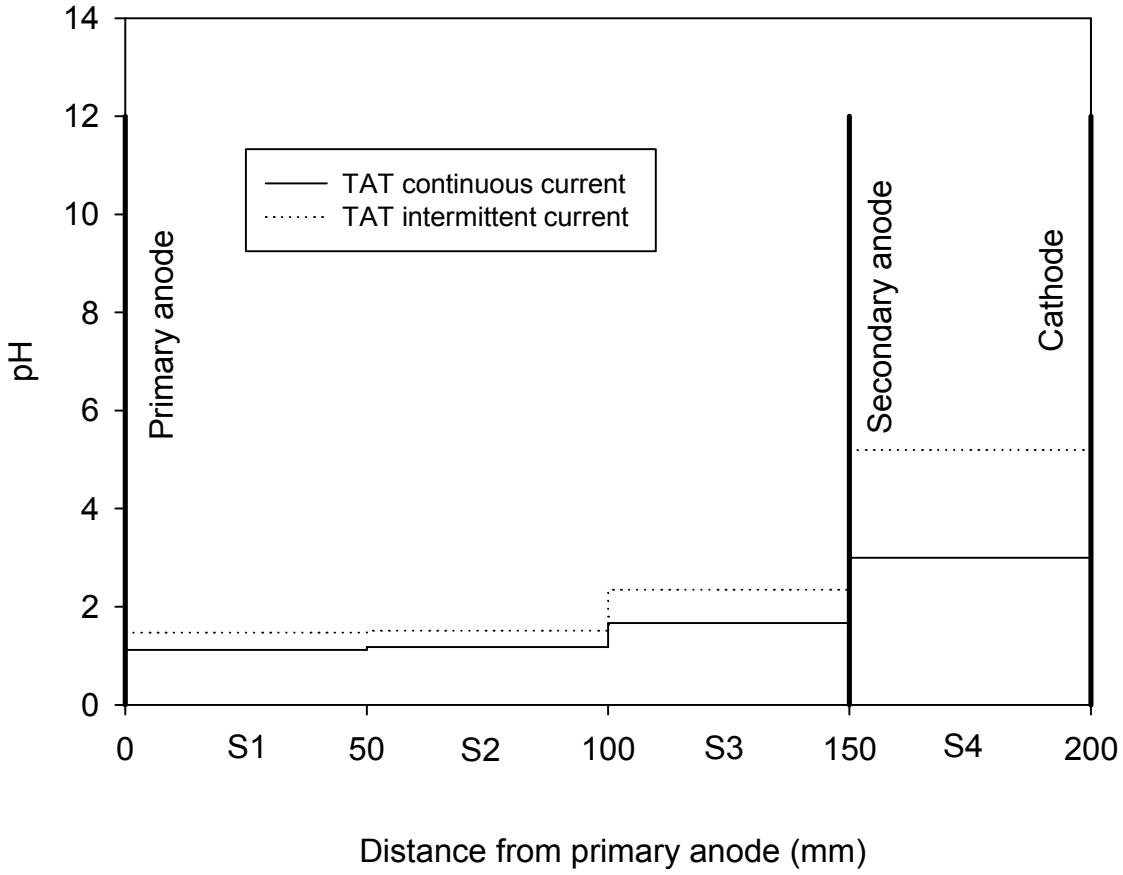

Figure 8.21 Pore fluid pH after TAT tests with intermittent current and continuous current for power consumption 500 Whr.

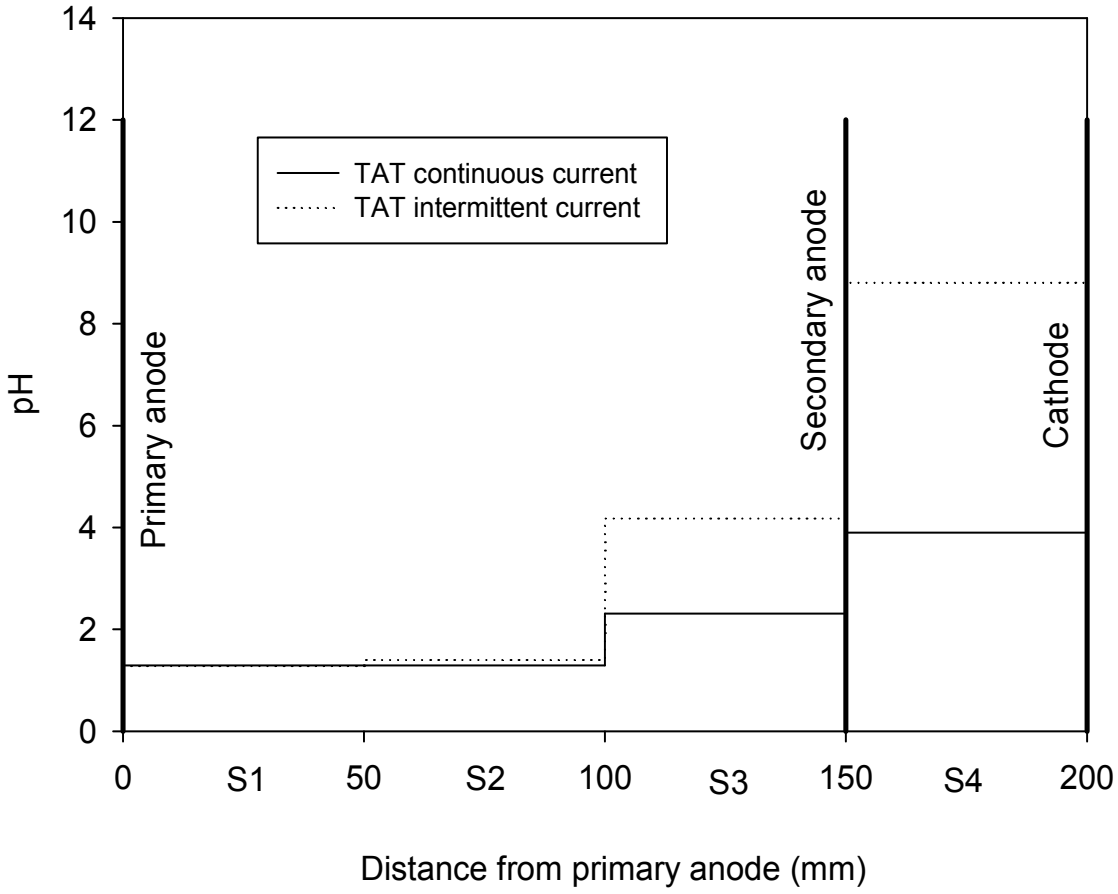

Figure 8.22 Pore fluid pH after TAT tests with intermittent current and continuous current for power consumption 750 Whr.

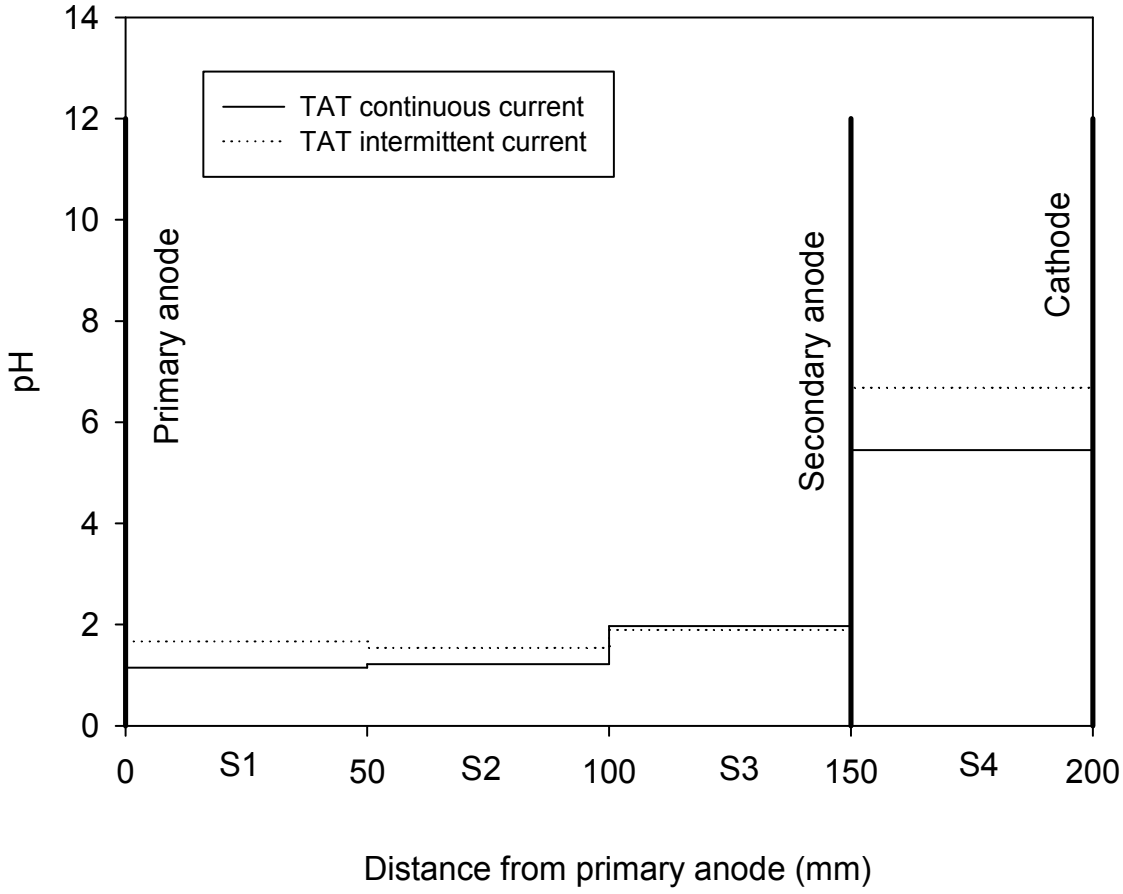

Figure 8.23 Pore fluid pH after TAT tests with intermittent current and continuous current for power consumption 1000 Whr.

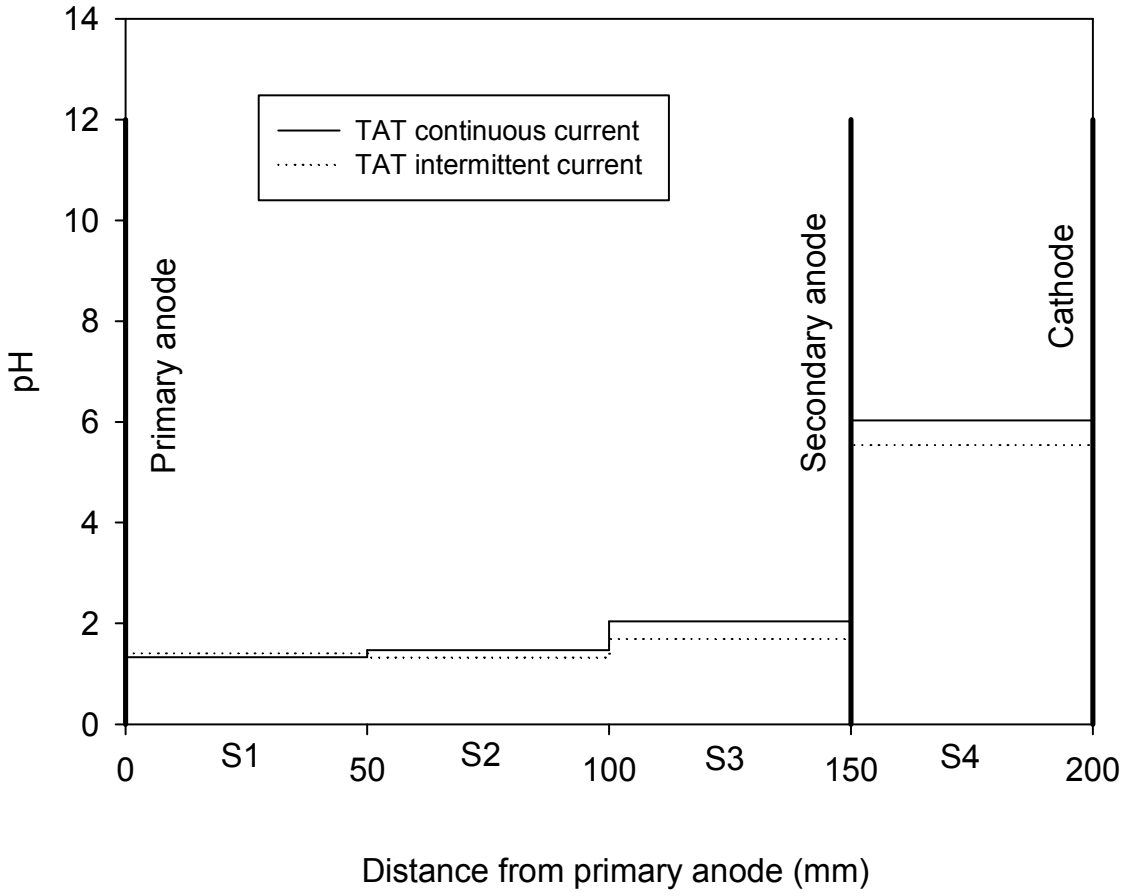

Figure 8. 24 Pore fluid pH after TAT tests with intermittent current and continuous current for power consumption 1250 Whr.

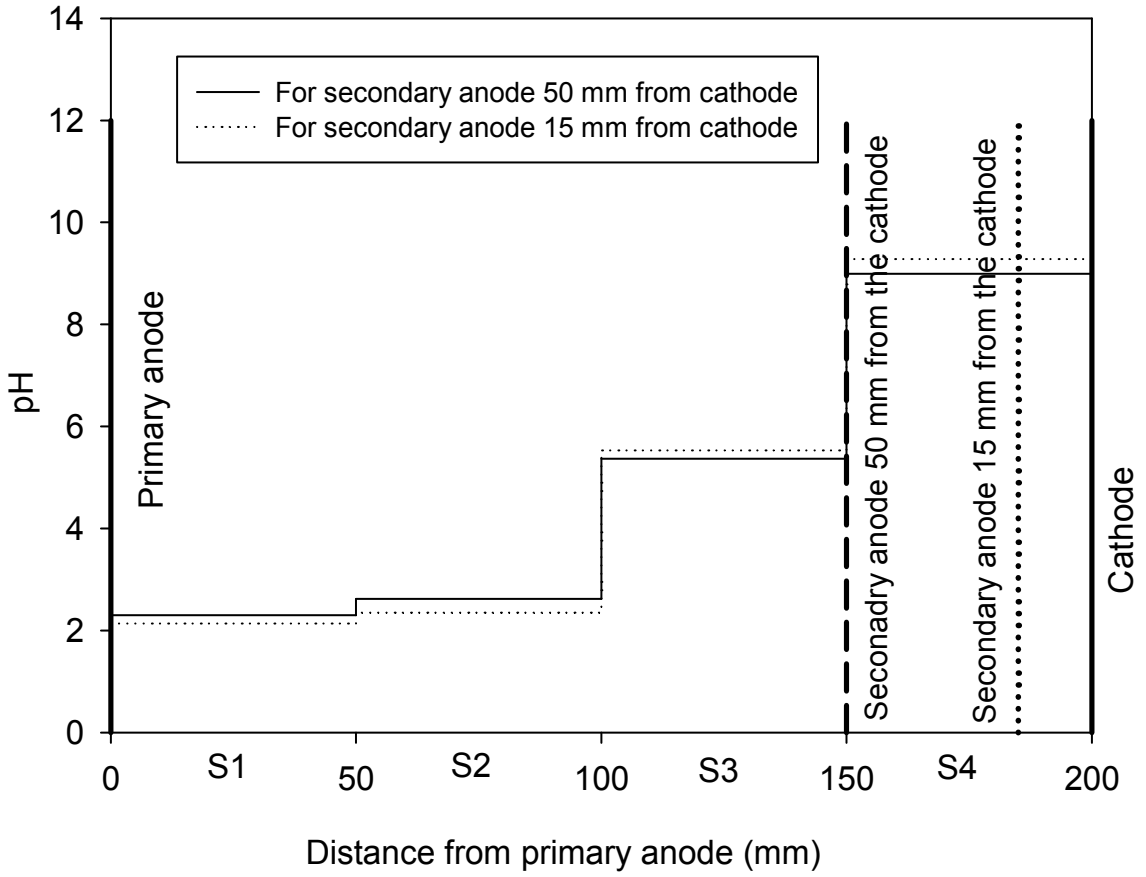

Figure 8.25 Dry soil pH after TAT tests with intermittent current and secondary anode at 50 mm and 15 mm from the cathode and power consumption 500 Whr.

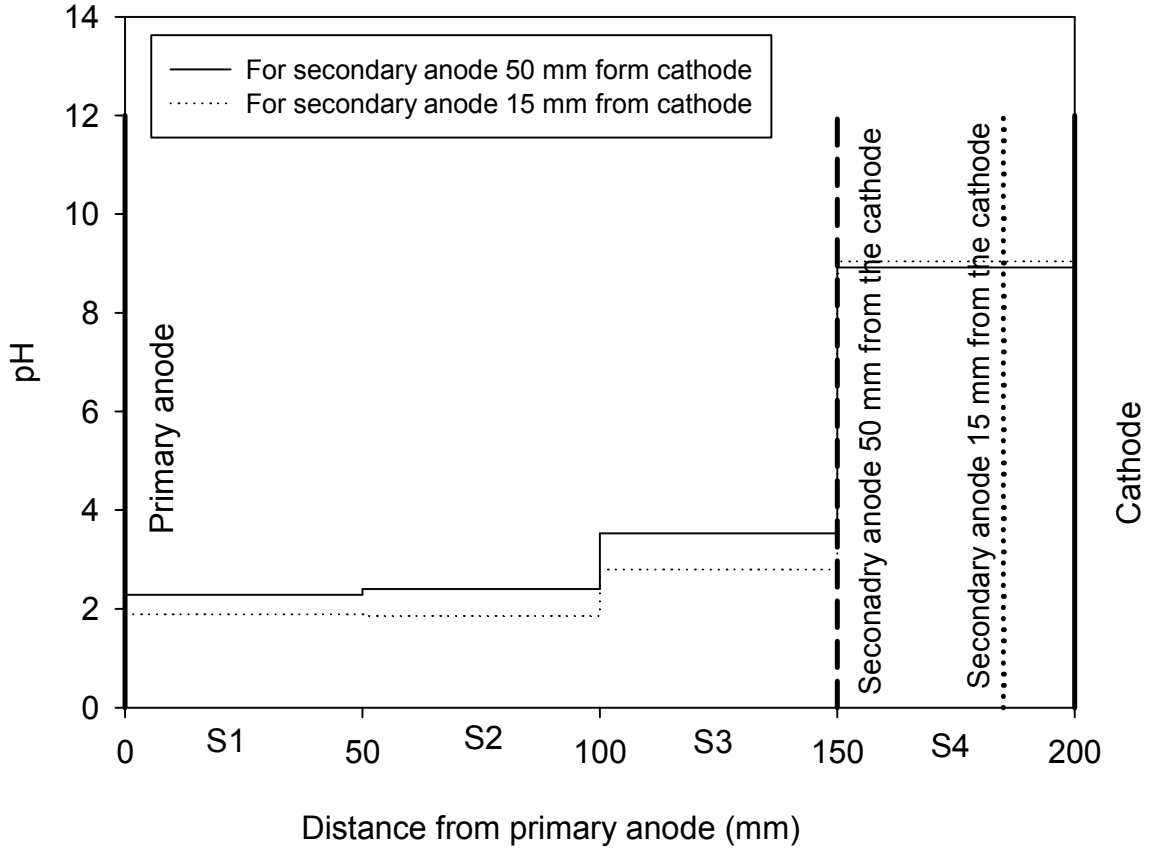

Figure 8.26 Dry soil pH after TAT tests with intermittent current and secondary anode place at 50 mm and 15 mm from the cathode and power consumption 750 Whr.

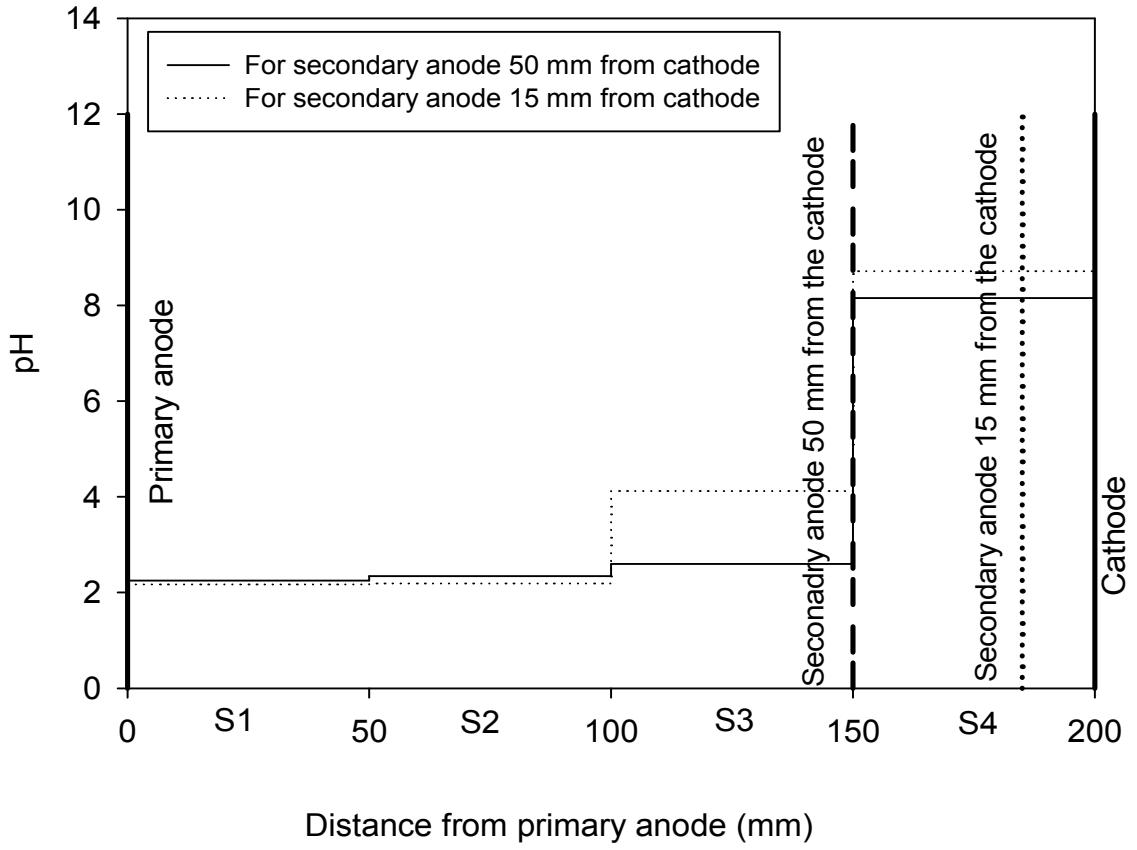

Figure 8.27 Dry soil pH after TAT tests with intermittent current and secondary anode place at 50 mm and 15 mm from the cathode and power consumption 1000 Whr.

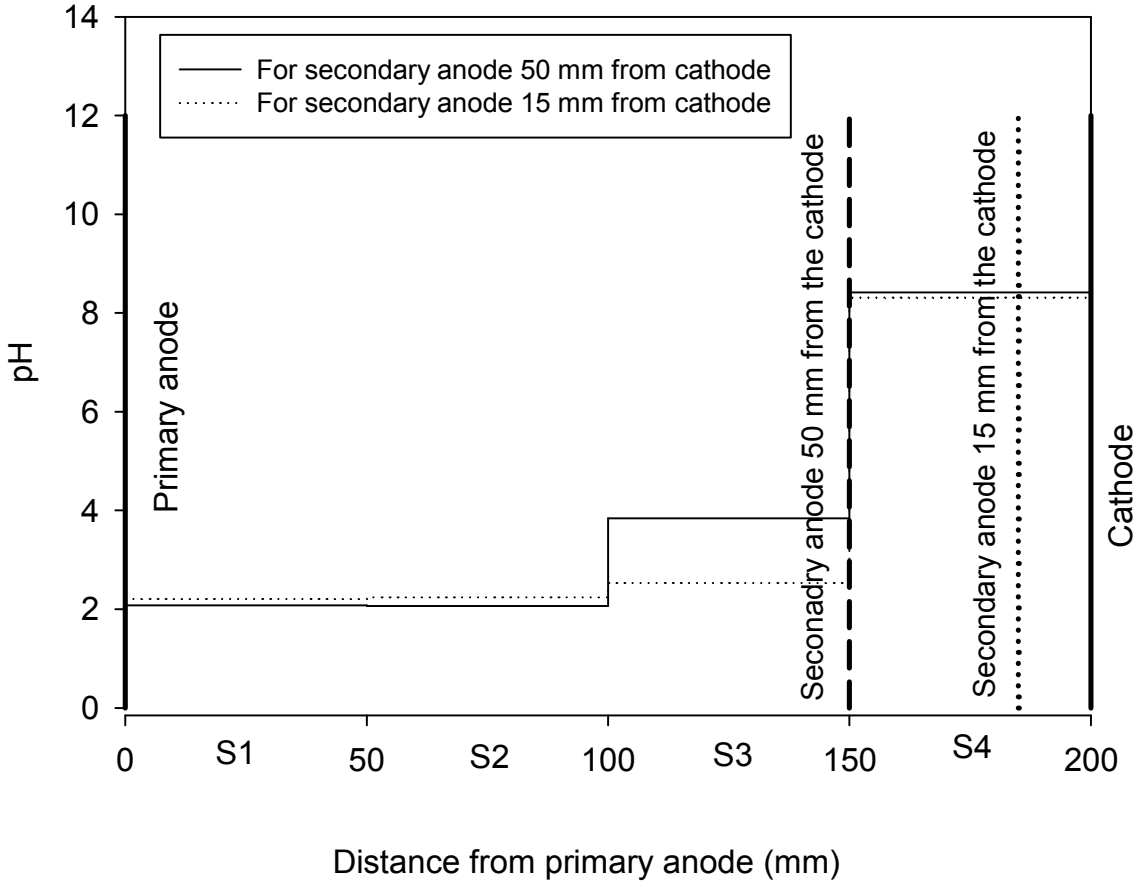

Figure 8.28 Dry soil pH after TAT tests with intermittent current and secondary anode place at 50 mm and 15 mm from the cathode and power consumption 1250 Whr.

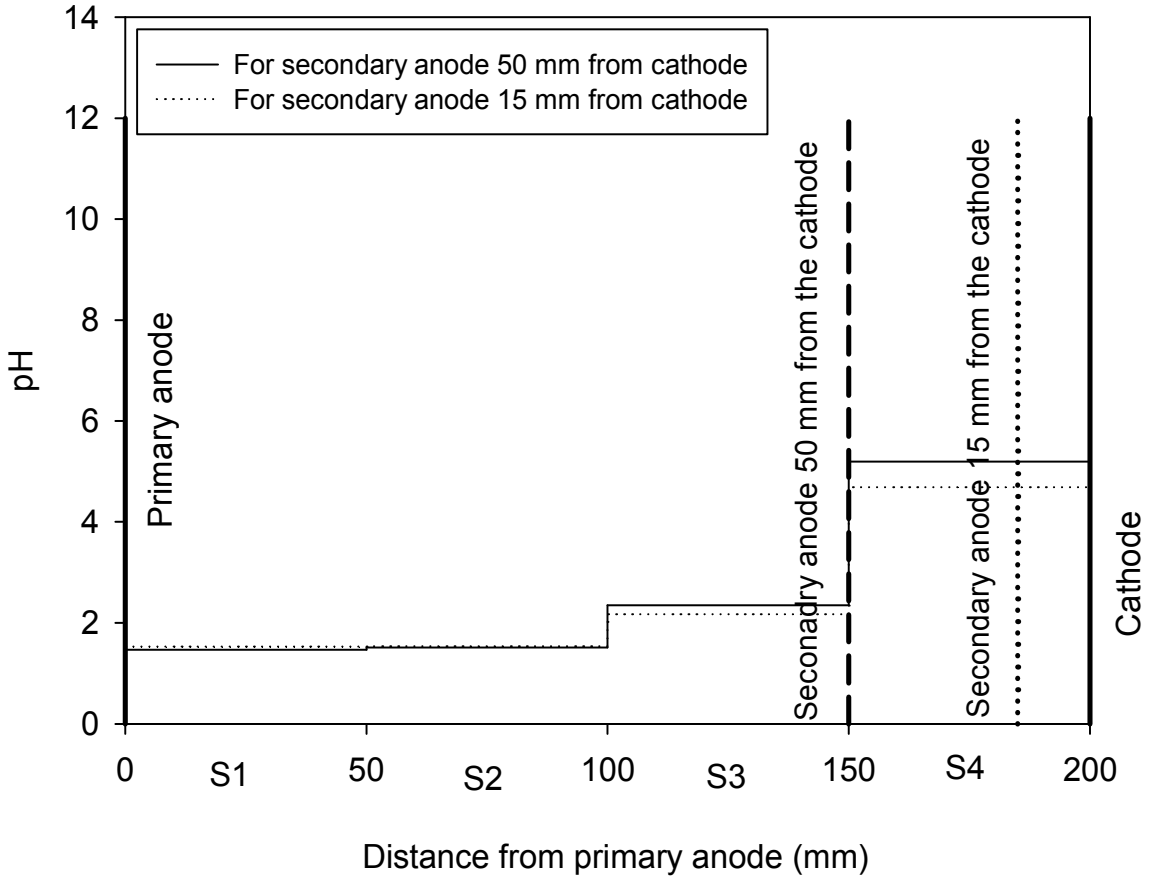

Figure 8.29 Pore fluid pH after TAT tests with intermittent current and the secondary anode at 50 mm and 15 mm from the cathode and power consumption 500 Whr.

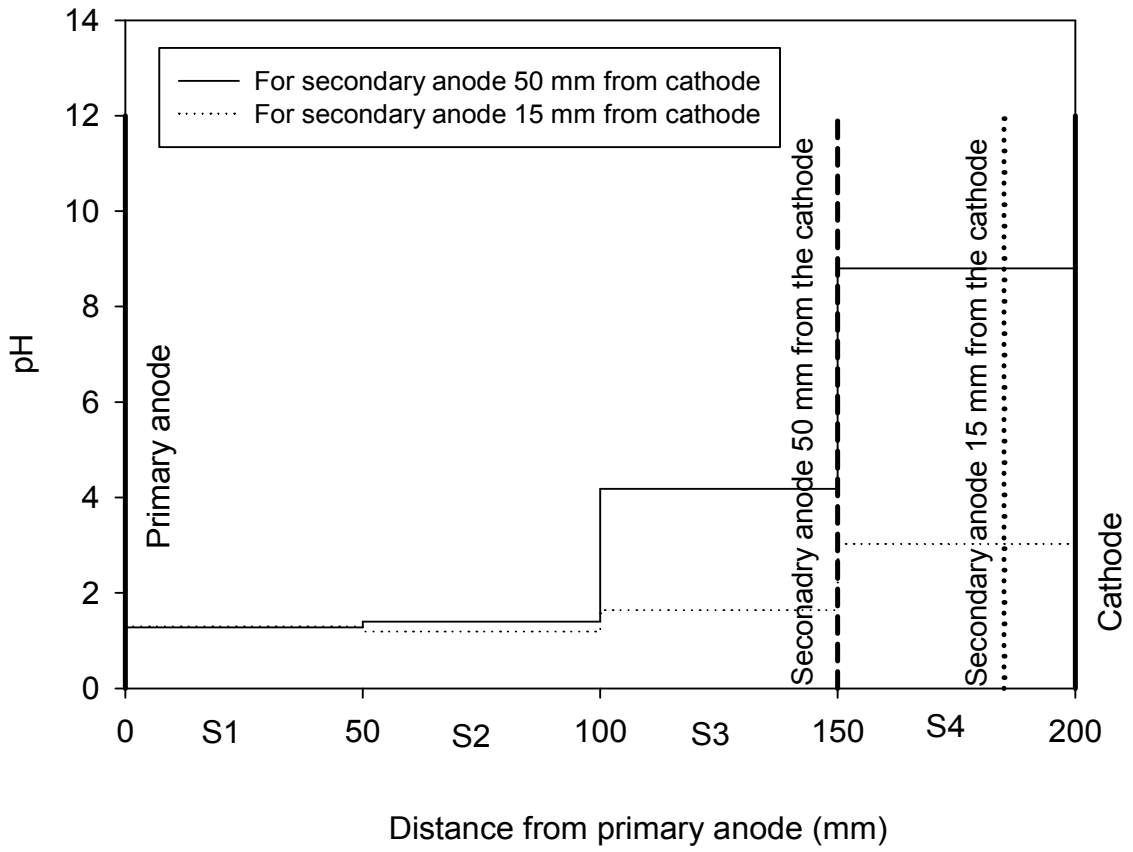

Figure 8.30 Pore fluid pH after TAT tests with intermittent current and the secondary anode at 50 mm and 15 mm from the cathode and power consumption 750 Whr.

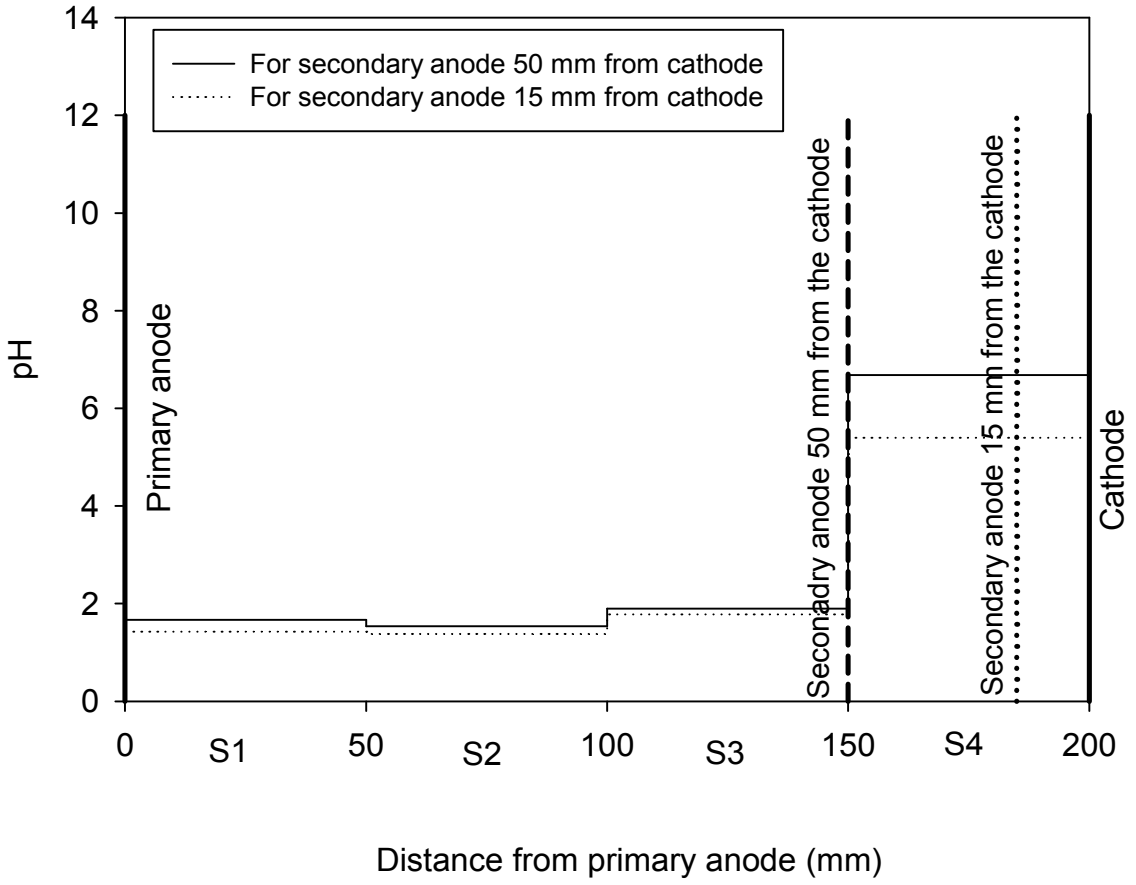

Figure 8.31 Pore fluid pH after TAT tests with intermittent current and the secondary anode at 50 mm and 15 mm from the cathode and power consumption 1000 Whr.

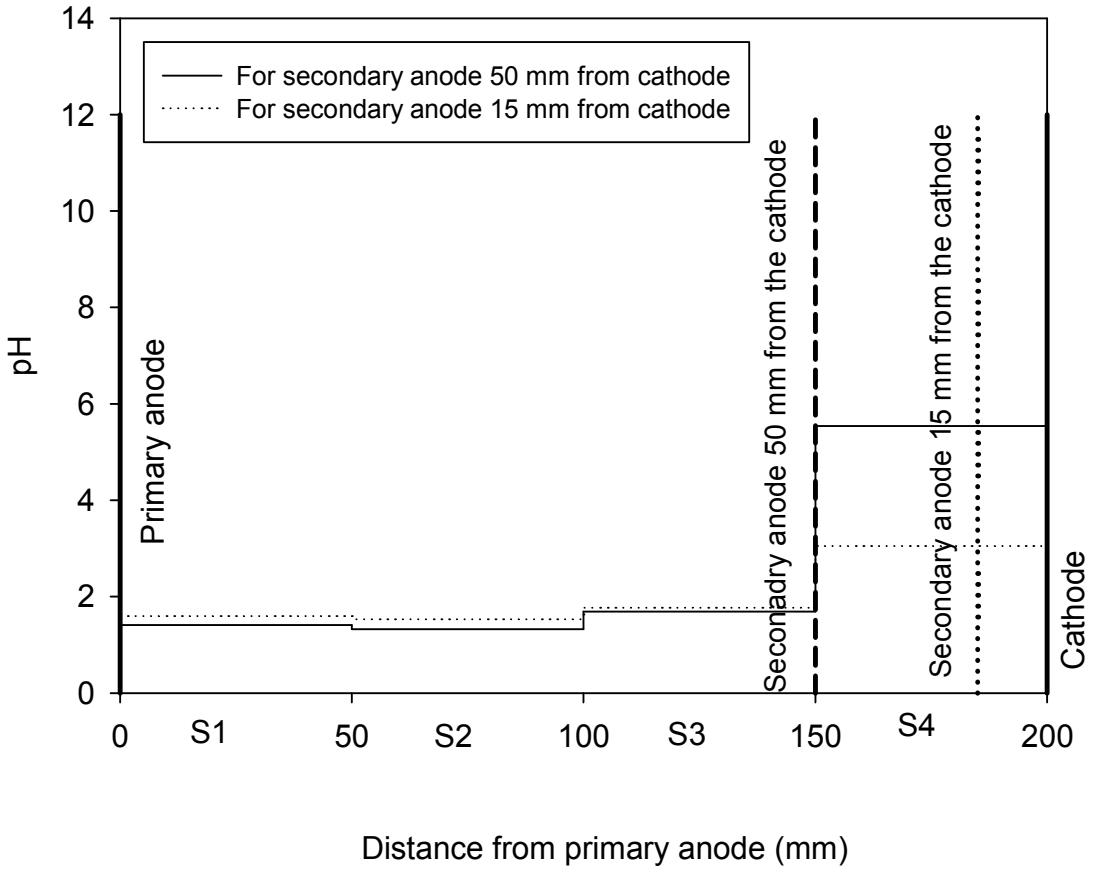

Figure 8.32 Pore fluid pH after TAT tests with intermittent current and the secondary anode at 50 mm and 15 mm from the cathode and power consumption 1250 Whr.

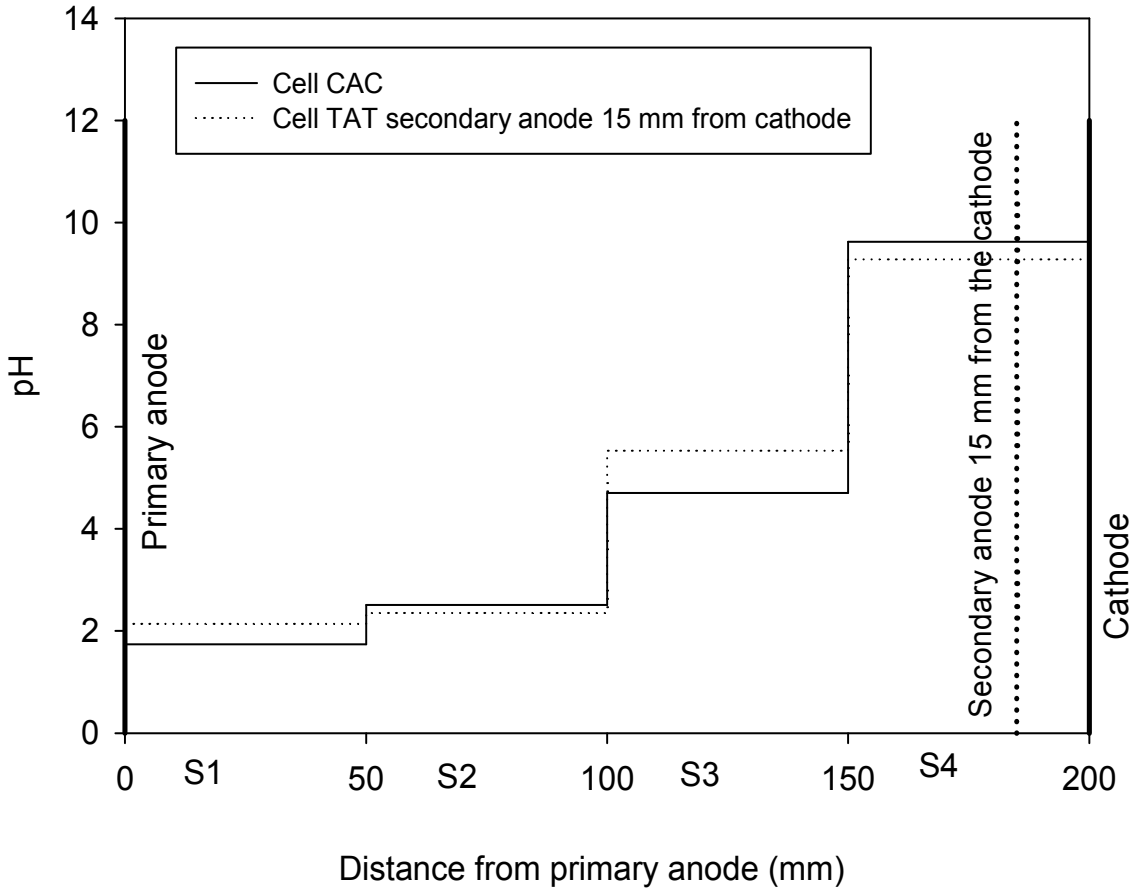

Figure 8.33 Dry soil pH after the TAT test with intermittent current and secondary anode at 15 mm from the cathode and CAC test for power consumption 500 Whr.

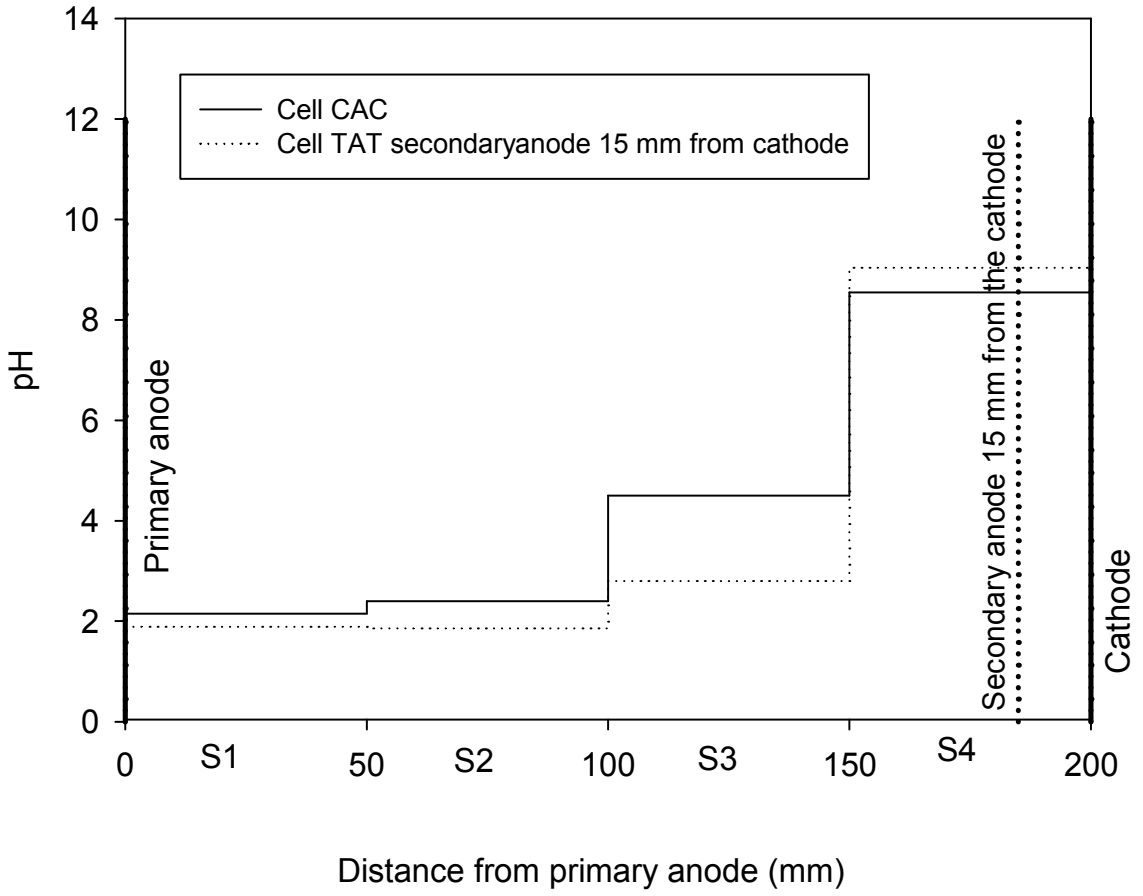

Figure 8.34 Dry soil pH after the TAT test with intermittent current and secondary anode at 15 mm from the cathode and CAC test for power consumption 750 Whr.

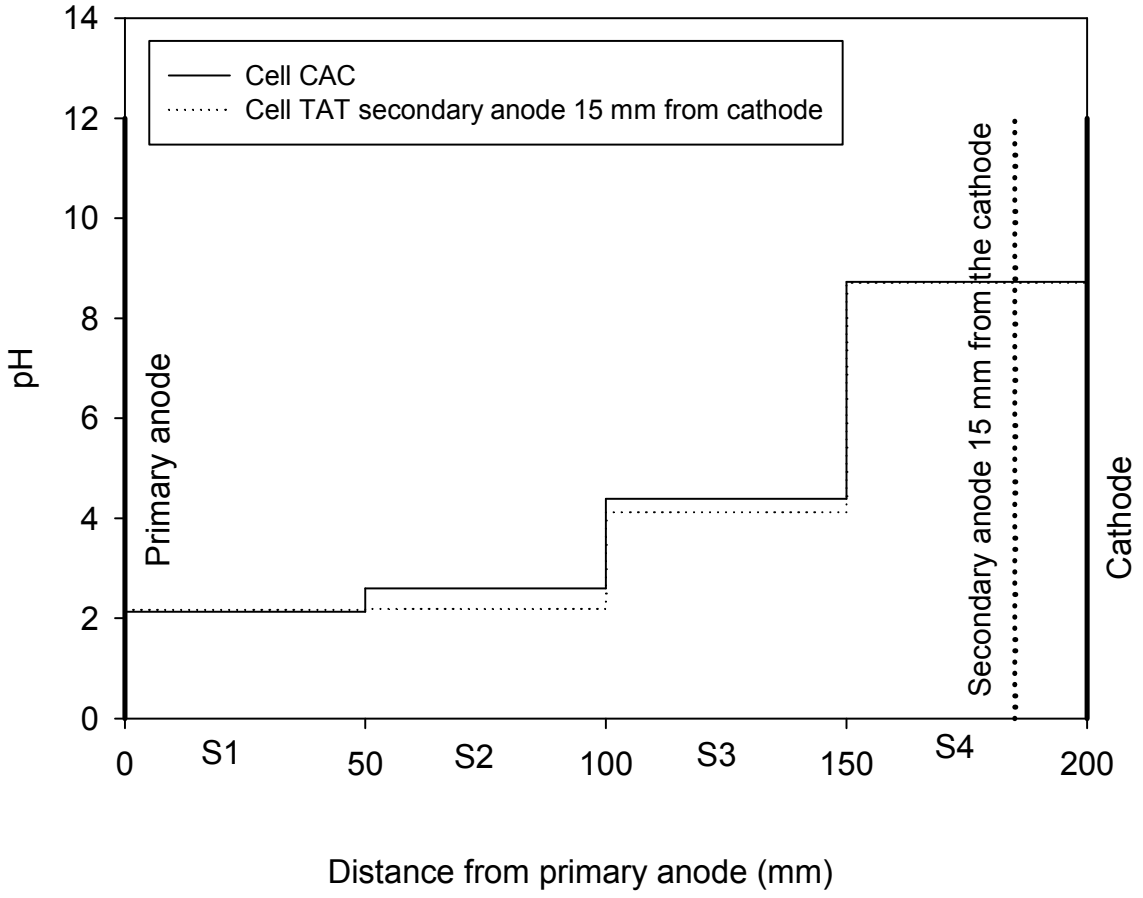

Figure 8.35 Dry soil pH after the TAT test with intermittent current and secondary anode at 15 mm from the cathode and CAC test for power consumption 1000 Whr.

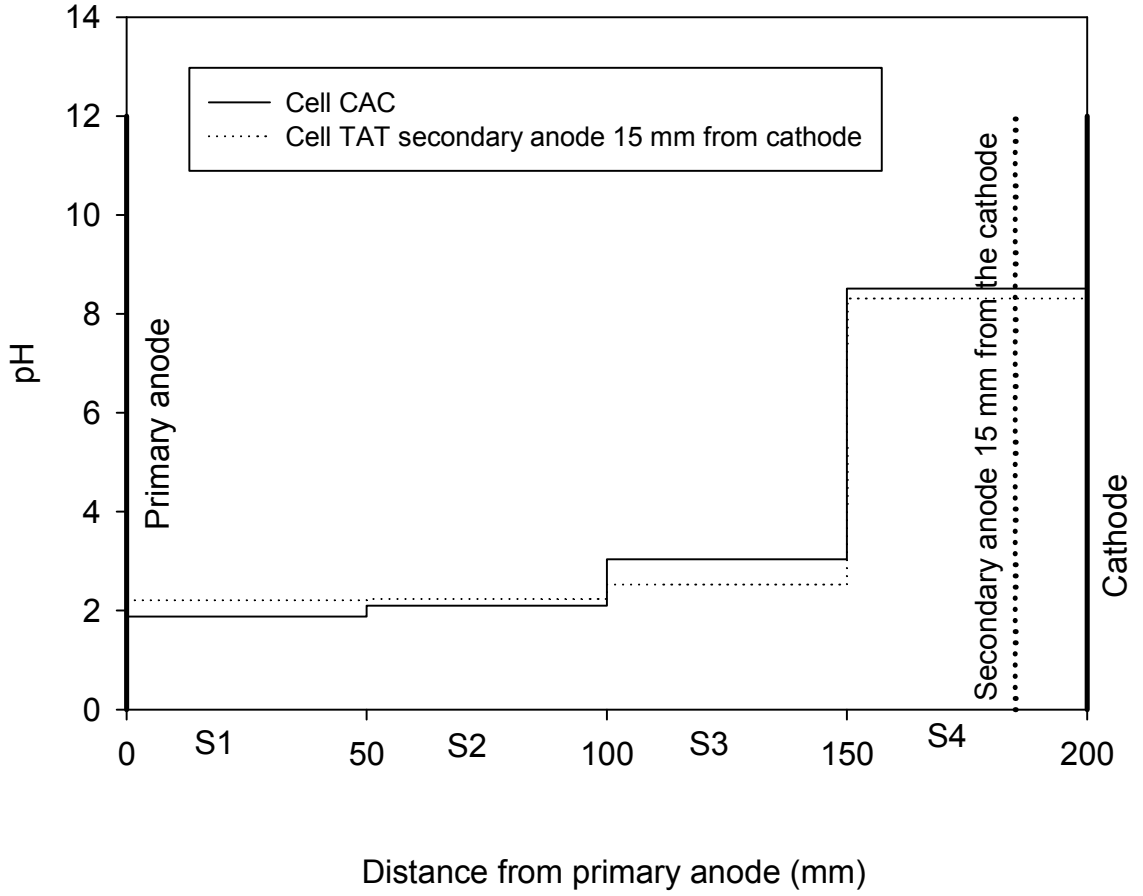

Figure 8.36 Dry soil pH after the TAT test with intermittent current and secondary anode at 15 mm from the cathode and CAC test for power consumption 1250 Whr.

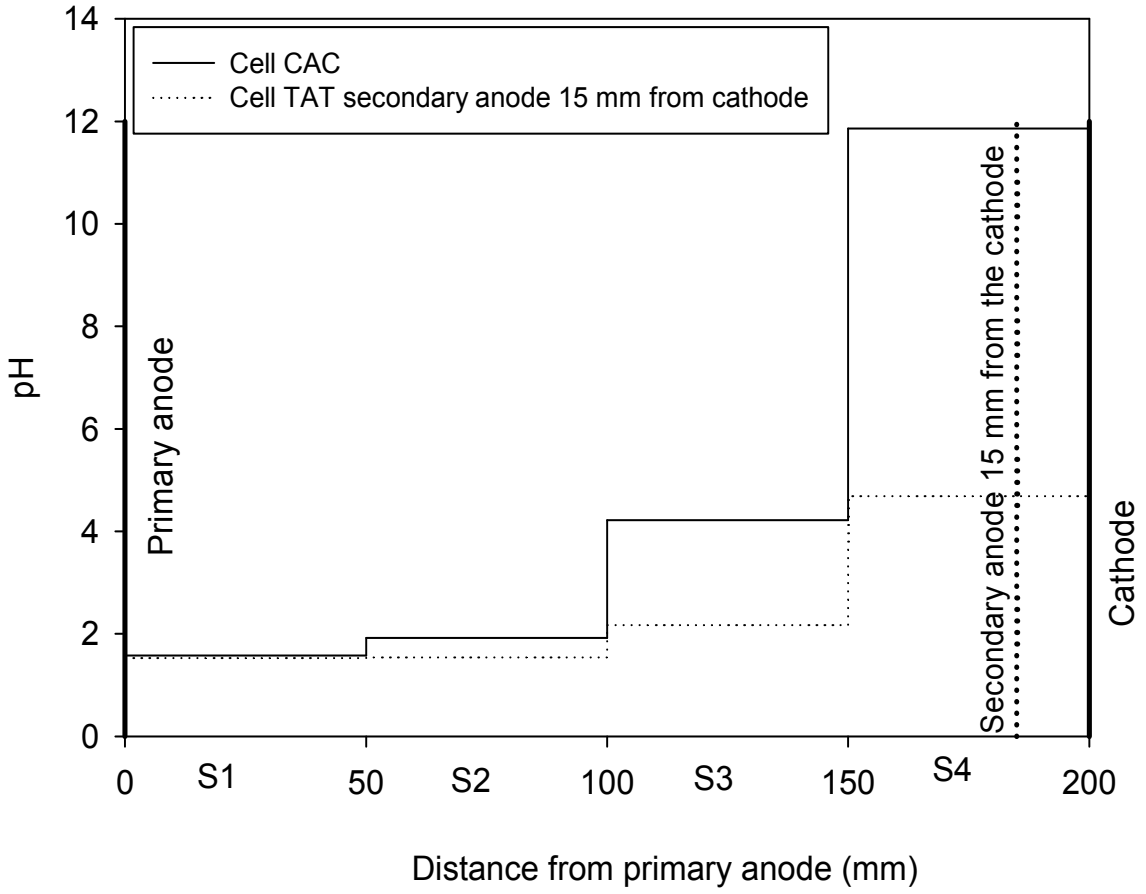

Figure 8.37 Pore fluid pH after the TAT test with intermittent current and secondary anode at 15 mm from the cathode and CAC test for power consumption 500 Whr.

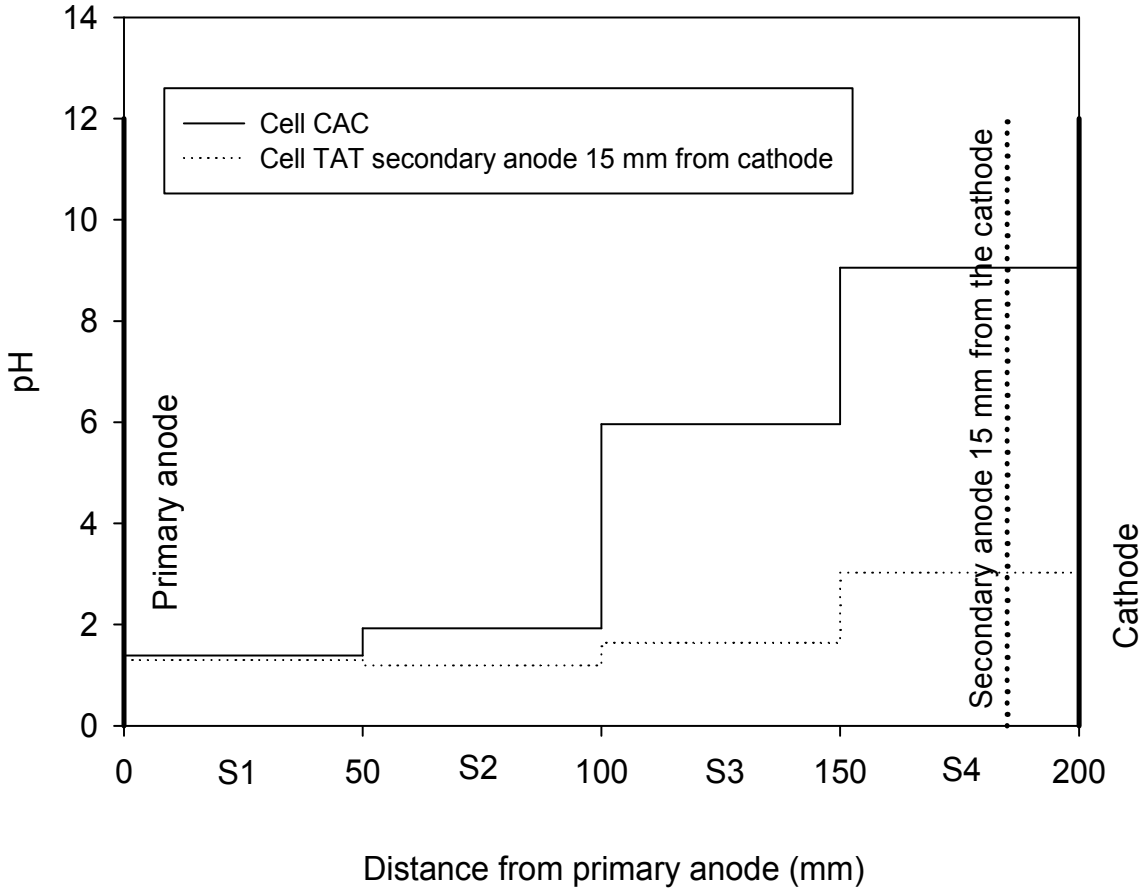

Figure 8.38 Pore fluid pH after the TAT test with intermittent current and secondary anode at 15 mm from the cathode and CAC test for power consumption 750 Whr.

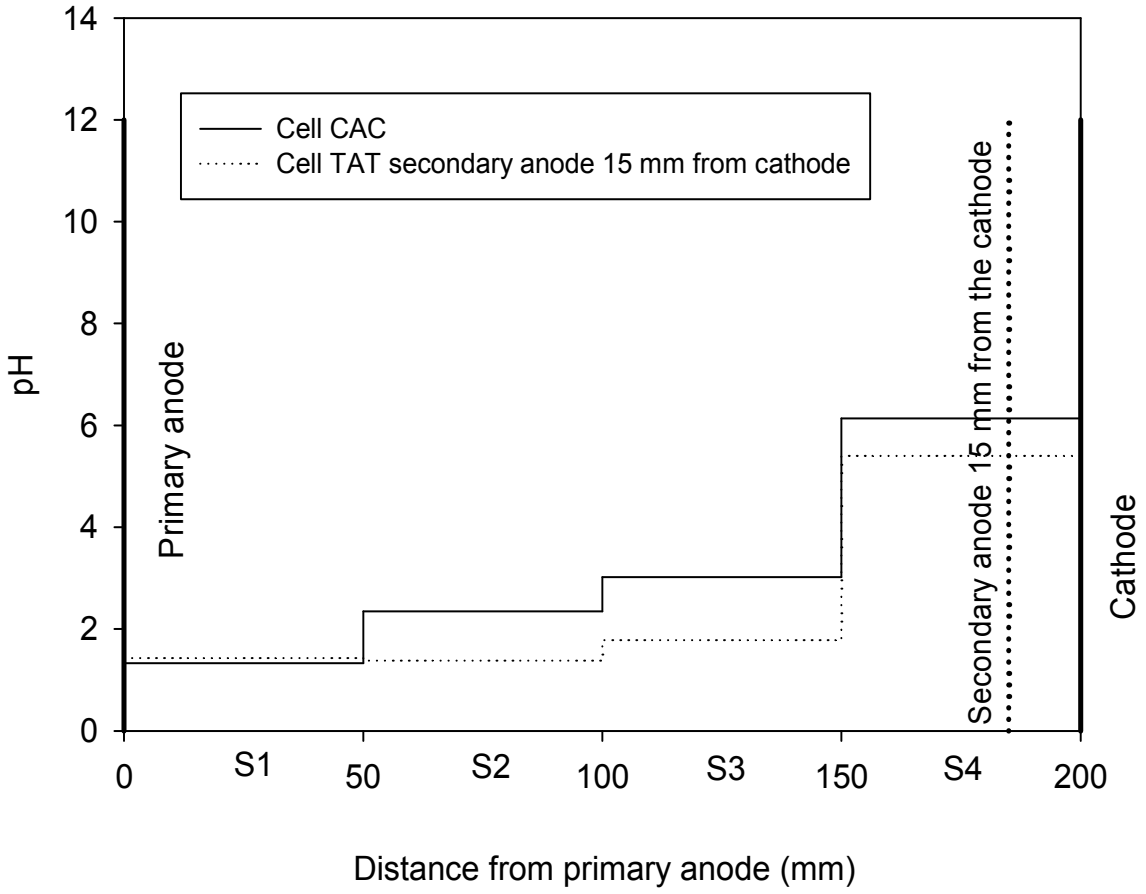

Figure 8.39 Pore fluid pH after the TAT test with intermittent current and secondary anode at 15 mm from the cathode and CAC test for power consumption 1000 Whr.

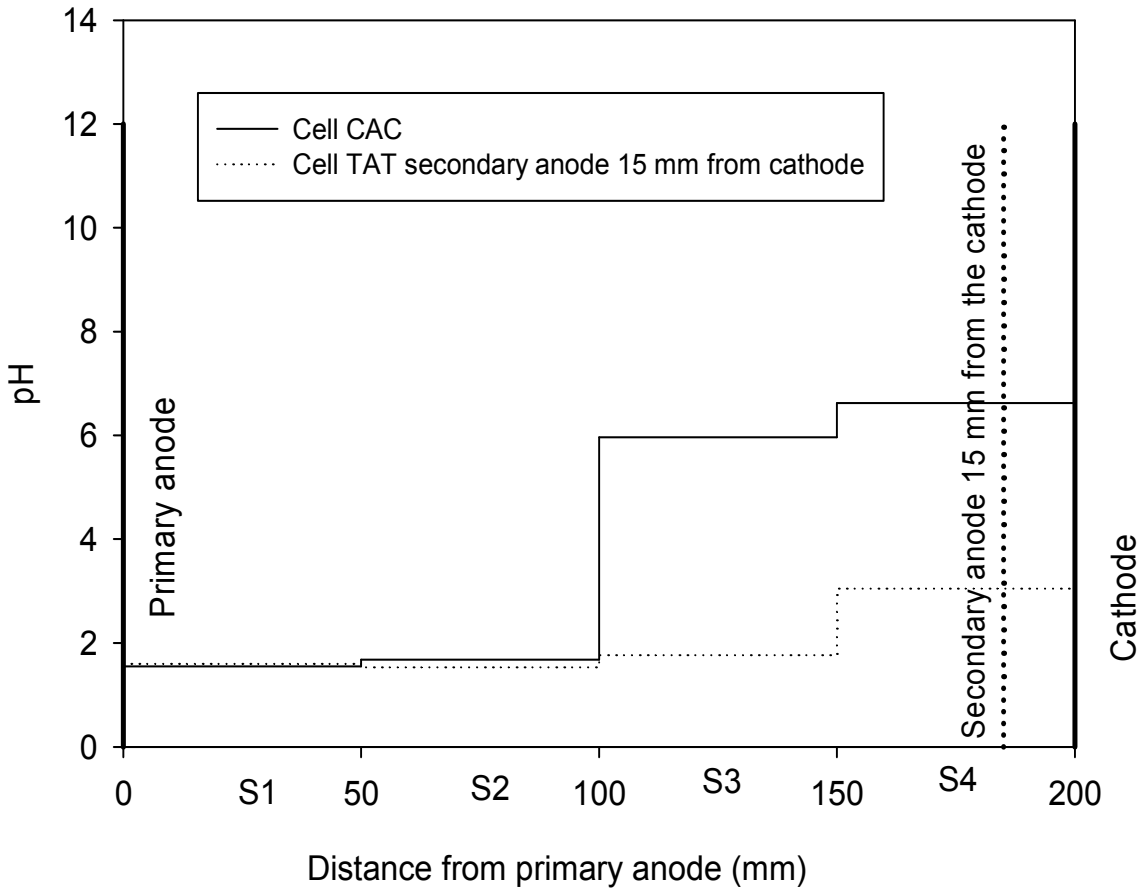

Figure 8.40 Pore fluid pH after the TAT test with intermittent current and secondary anode at 15 mm from the cathode and CAC test for power consumption 1250 Whr.

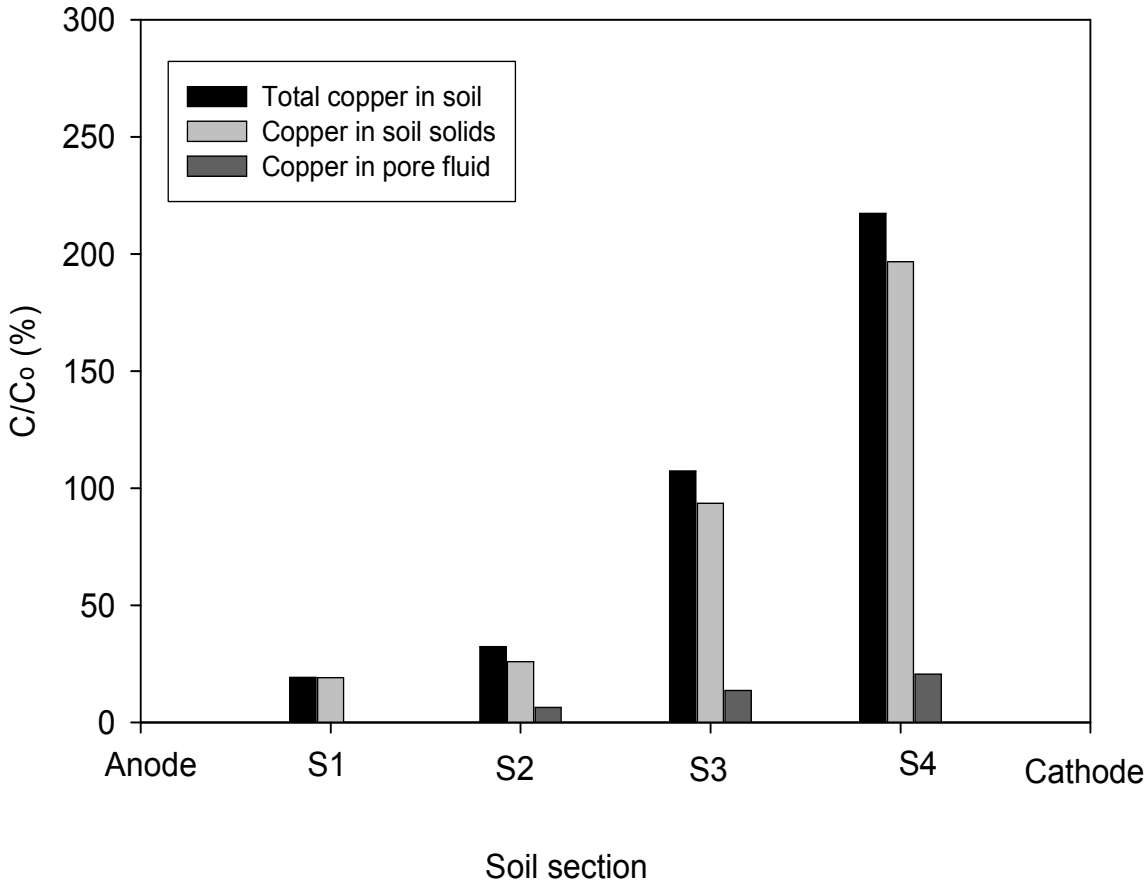

Figure 8.41 Copper concentration after TAT test with continuous current and secondary anode at 50 mm from cathode and power consumption 500 Whr.

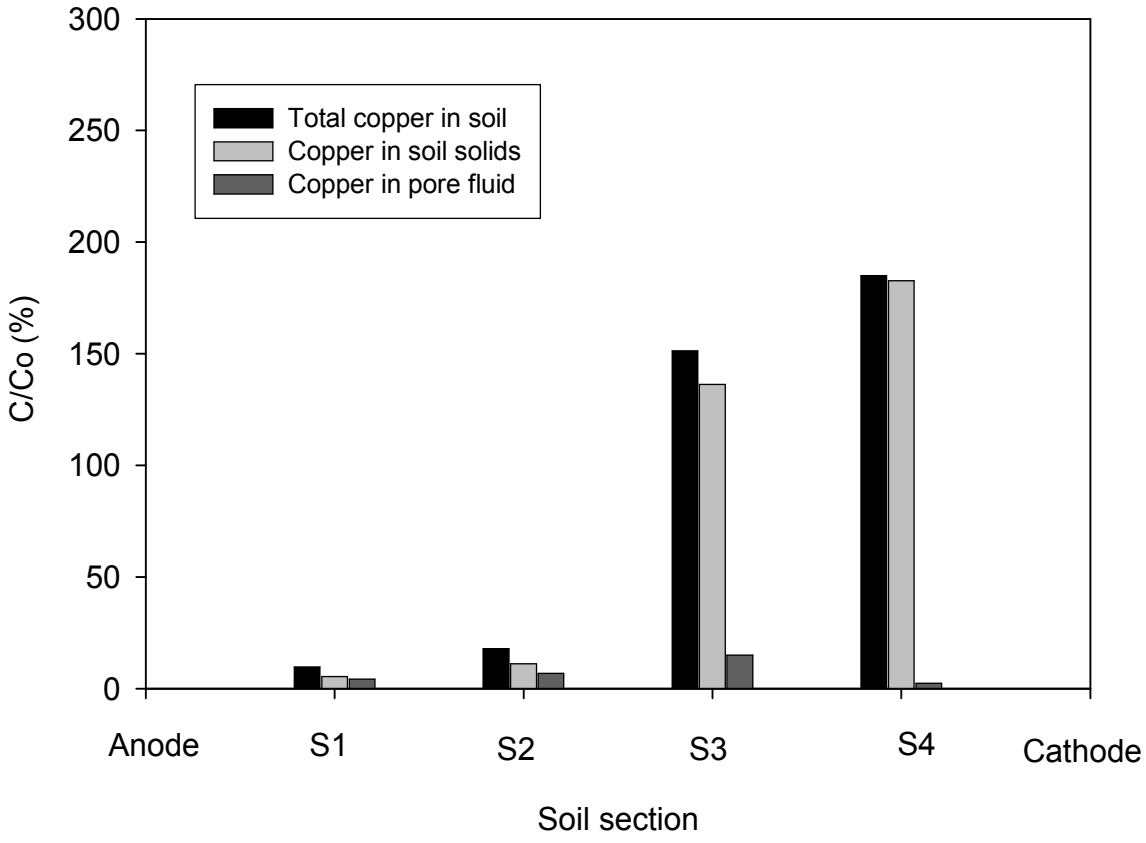

Figure 8.42 Copper concentration after TAT test with continuous current and secondary anode at 50 mm from cathode and power consumption 750 Whr.

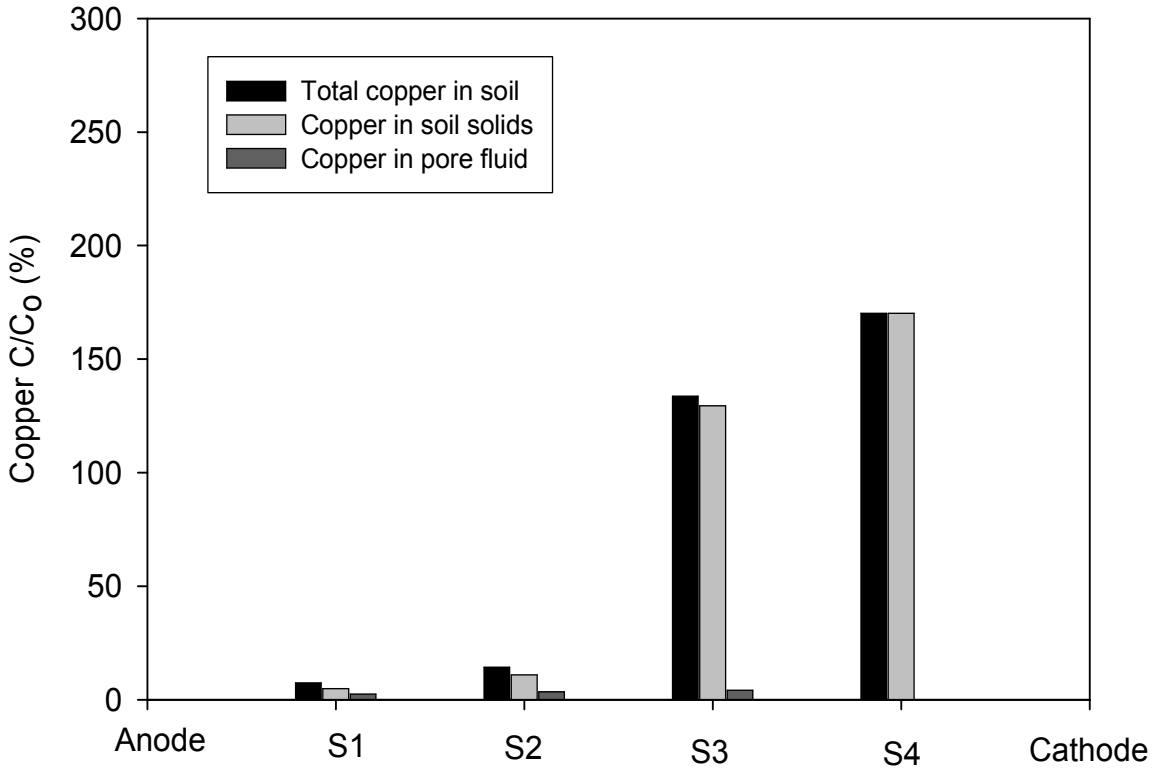

Figure 8.43 Copper concentration after TAT test with continuous current and secondary anode at 50 mm from cathode and power consumption 1000 Whr.

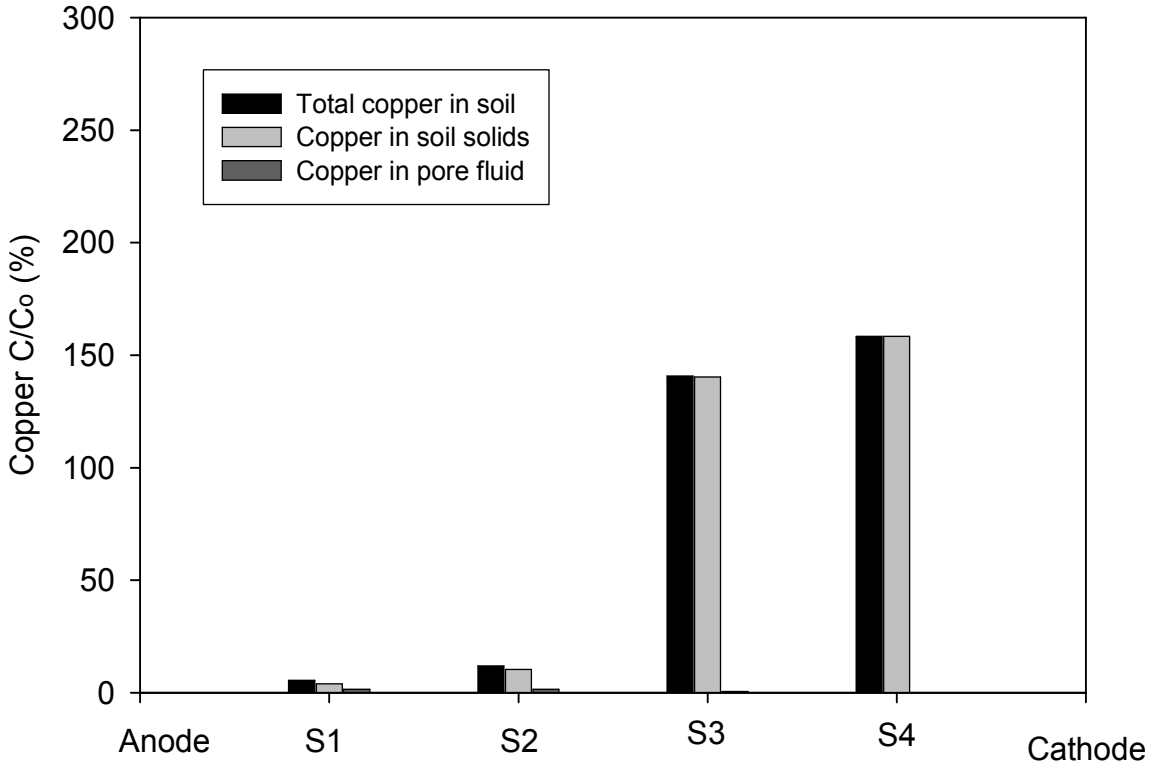

Figure 8.44 Copper concentration after TAT test with continuous current and secondary anode at 50 mm from cathode and power consumption 1250 Whr.

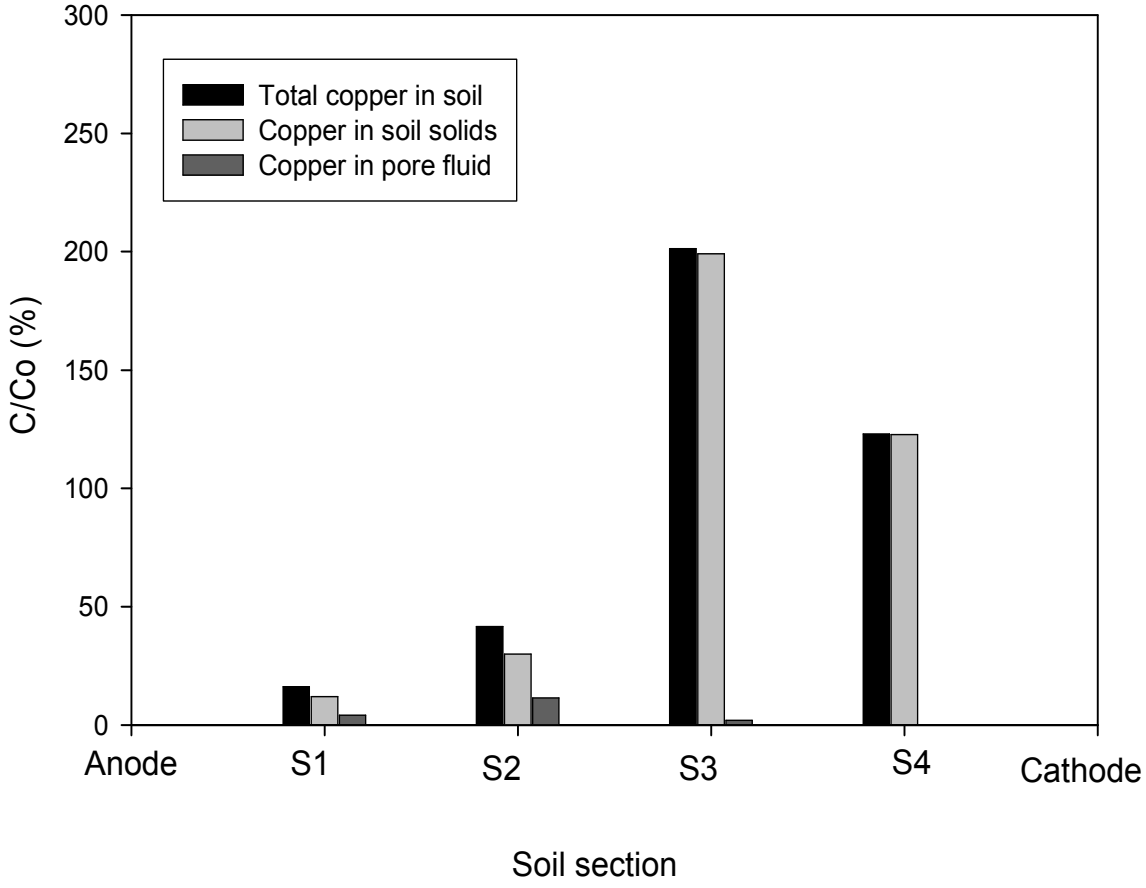

Figure 8.45 Copper concentration after TAT test with intermittent current and secondary anode at 50 mm from cathode and power consumption 500 Whr.

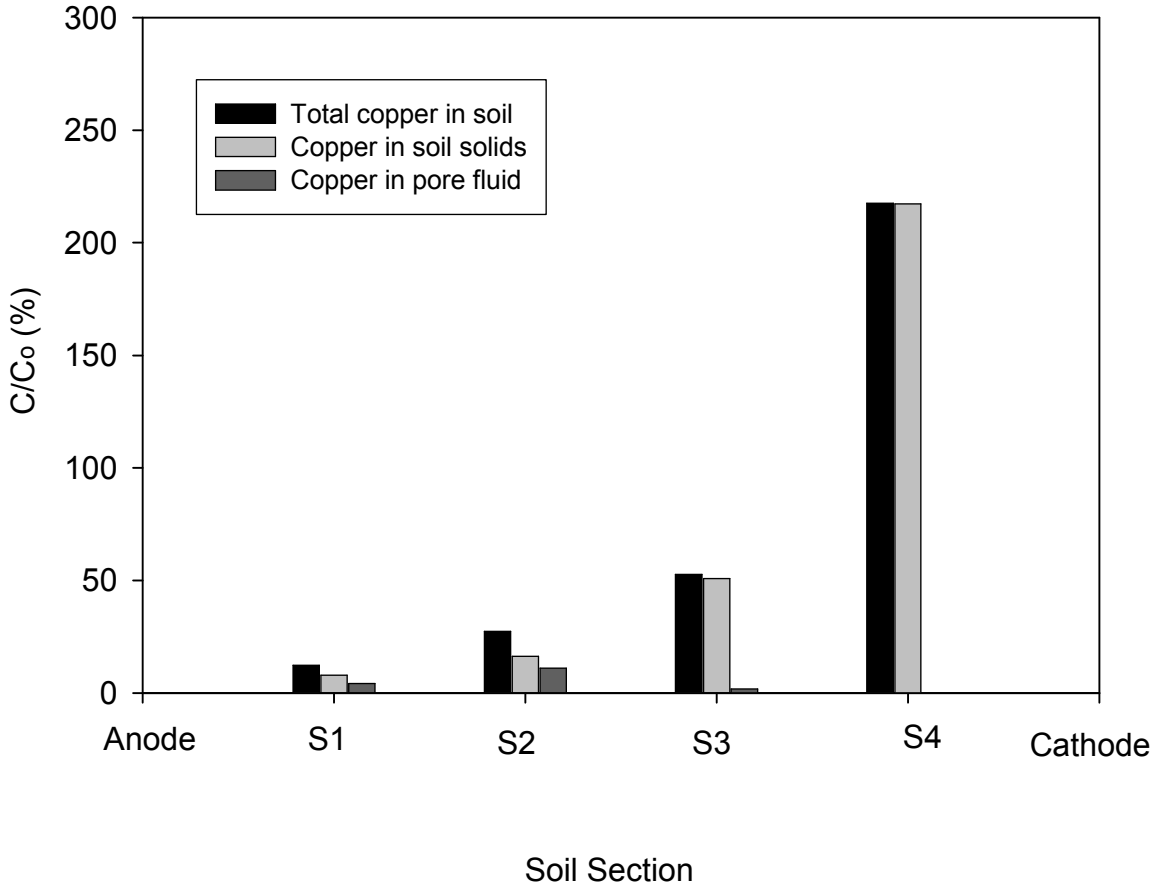

Figure 8.46 Copper concentration after TAT test with intermittent current and secondary anode at 50 mm from cathode and power consumption 750 Whr.

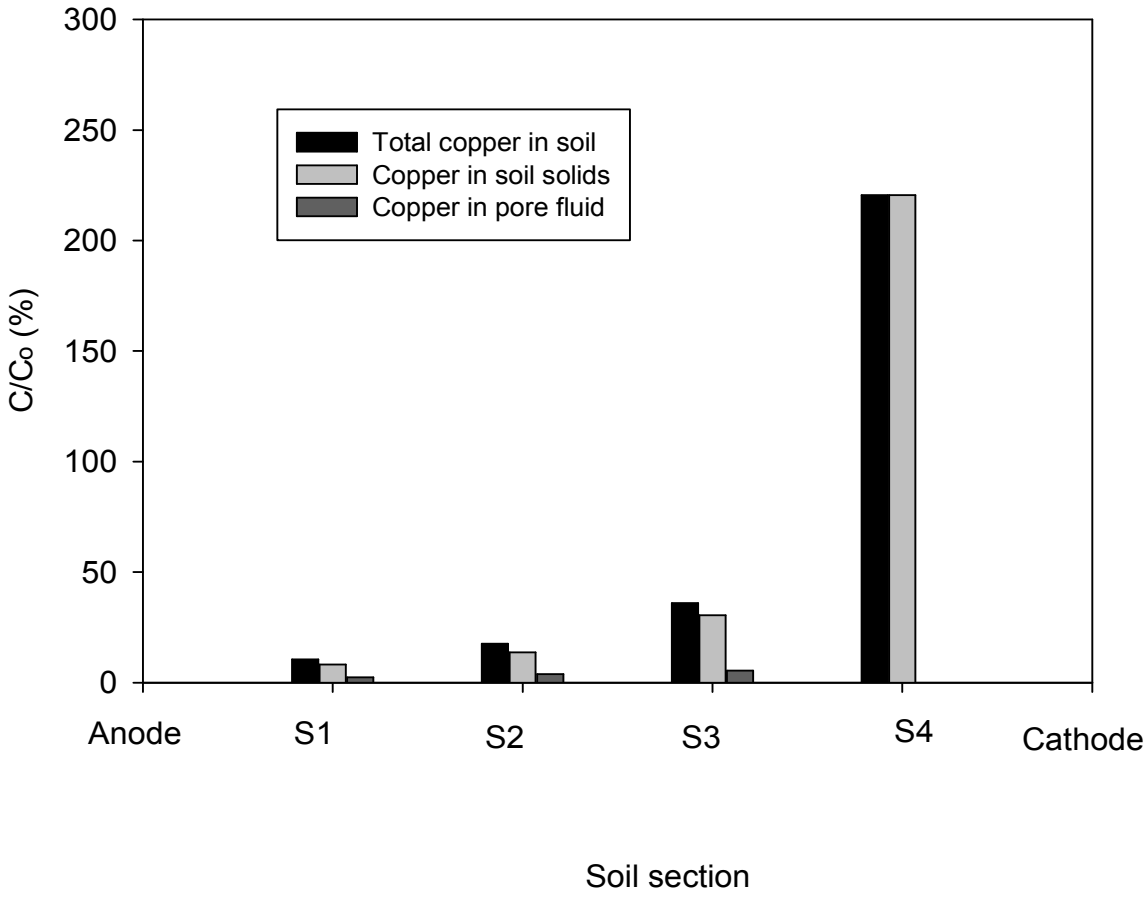

Figure 8.47 Copper concentration after TAT test with intermittent current and secondary anode at 50 mm from cathode and power consumption 1000 Whr.

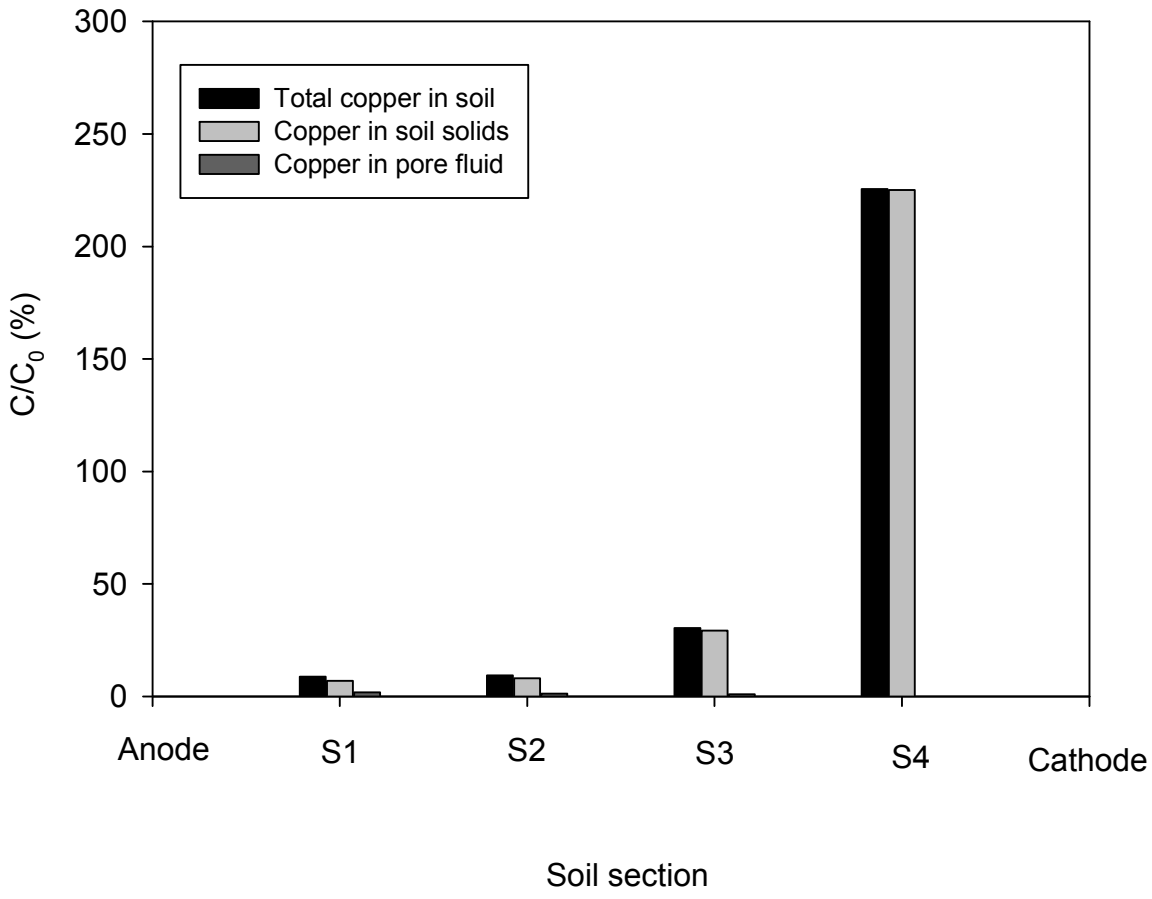

Figure 8.48 Copper concentration after TAT test with intermittent current and secondary anode at 50 mm from cathode and power consumption 1250 Whr.

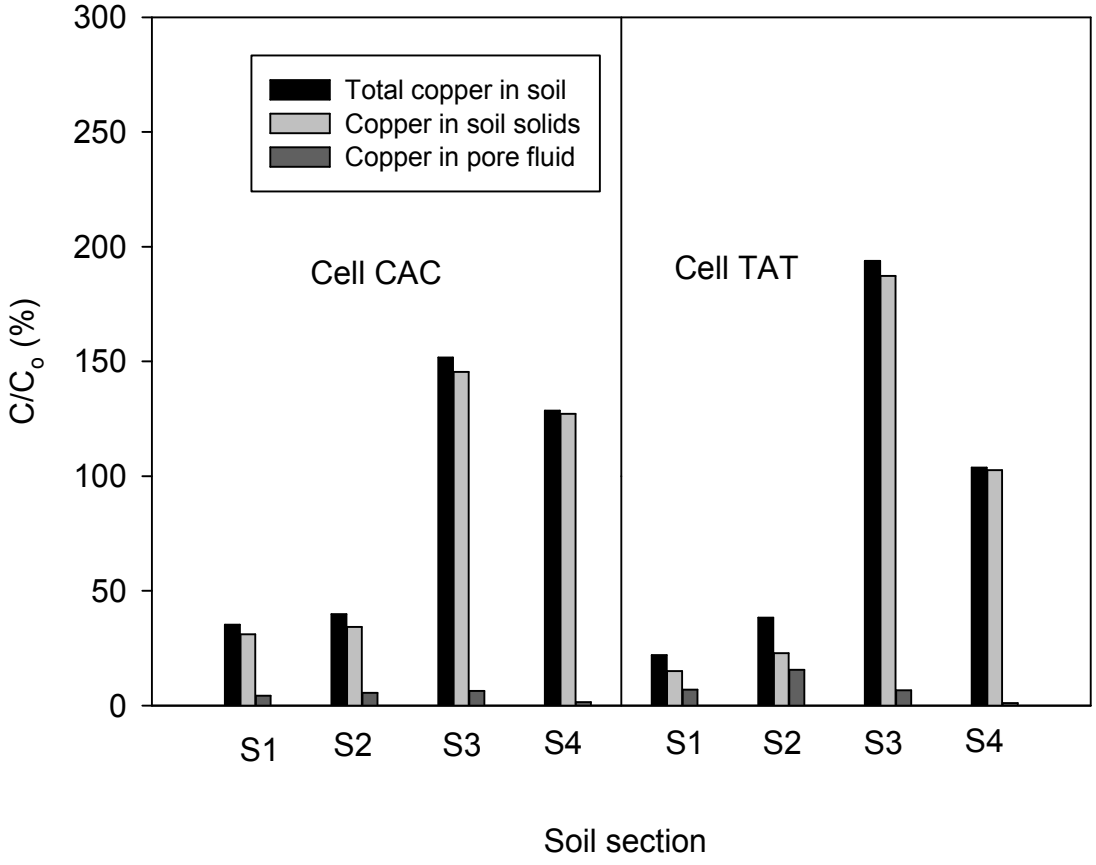

Figure 8.49 Copper concentration after tests of CAC and TAT with intermittent current with secondary anode at 15 mm from the cathode for power consumption 500 Whr.

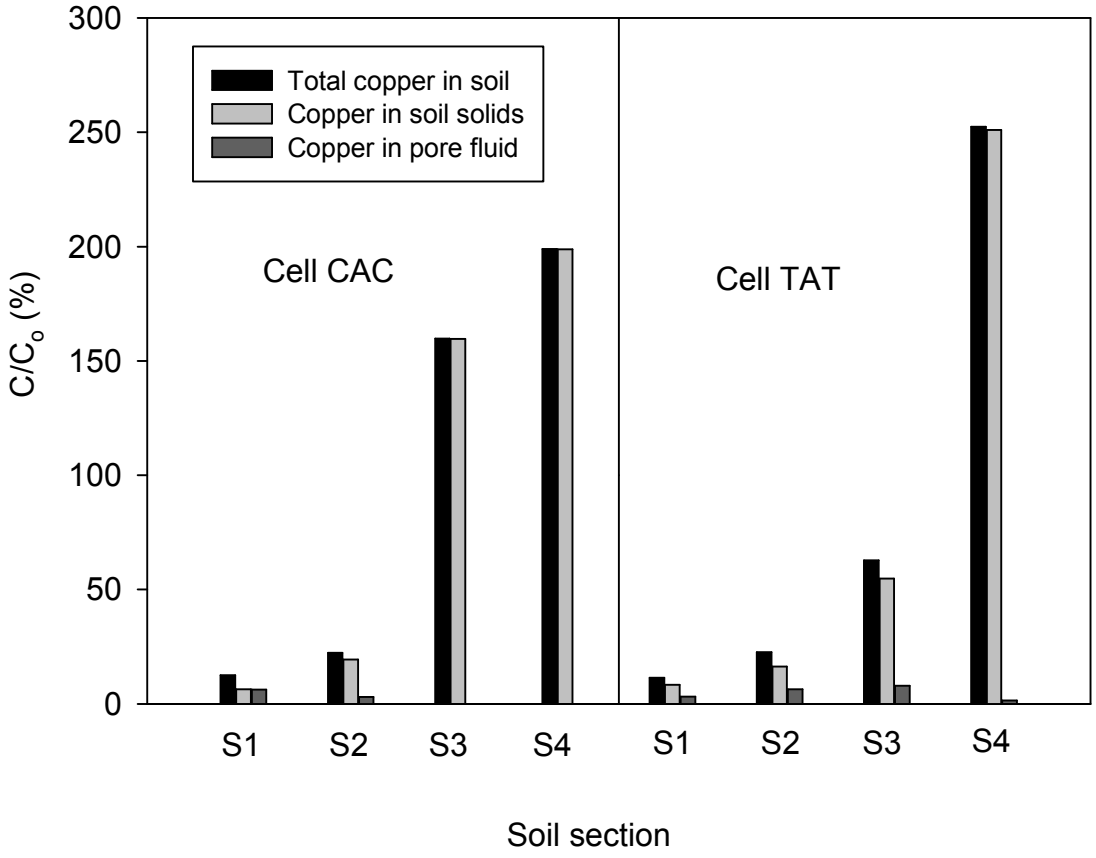

Figure 8.50 Copper concentration after tests of CAC and TAT of intermittent current with secondary anode at 15 mm from the cathode for power consumption 750 Whr.

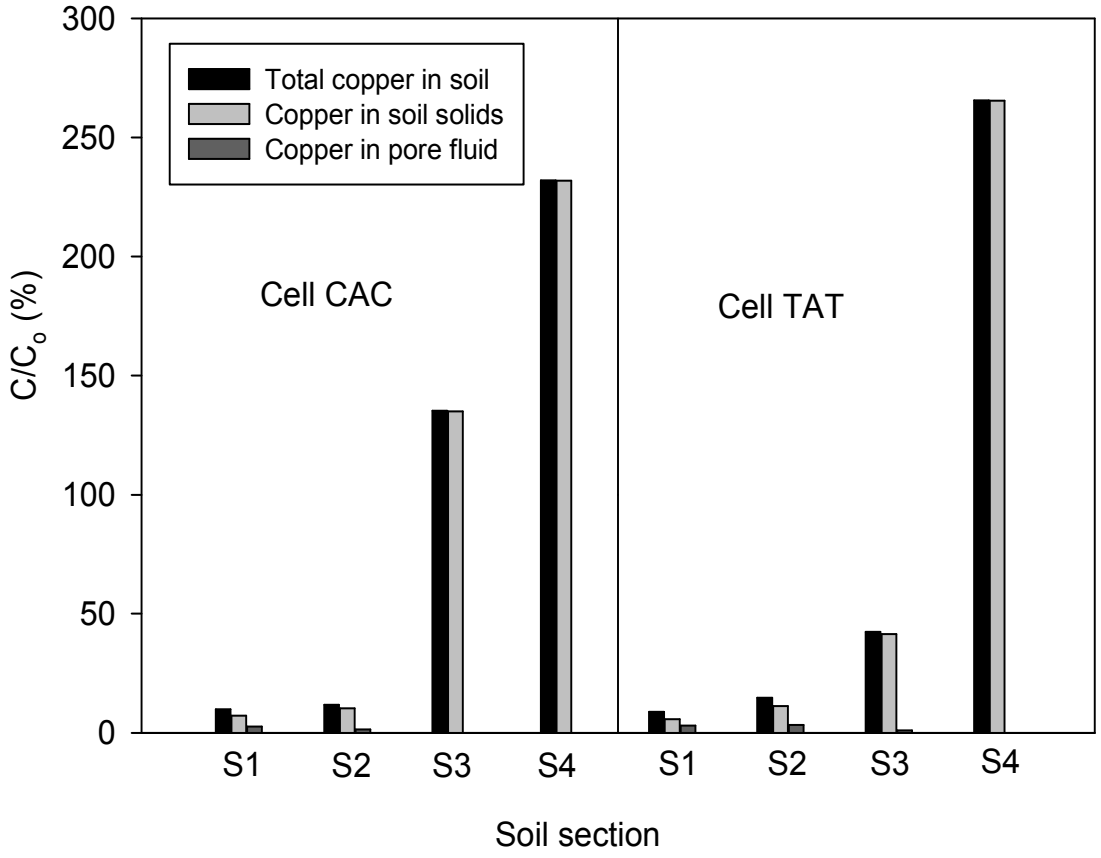

Figure 8.51 Copper concentration after tests of CAC and TAT with intermittent current with secondary anode at 15 mm from the cathode for power consumption 1000 Whr.

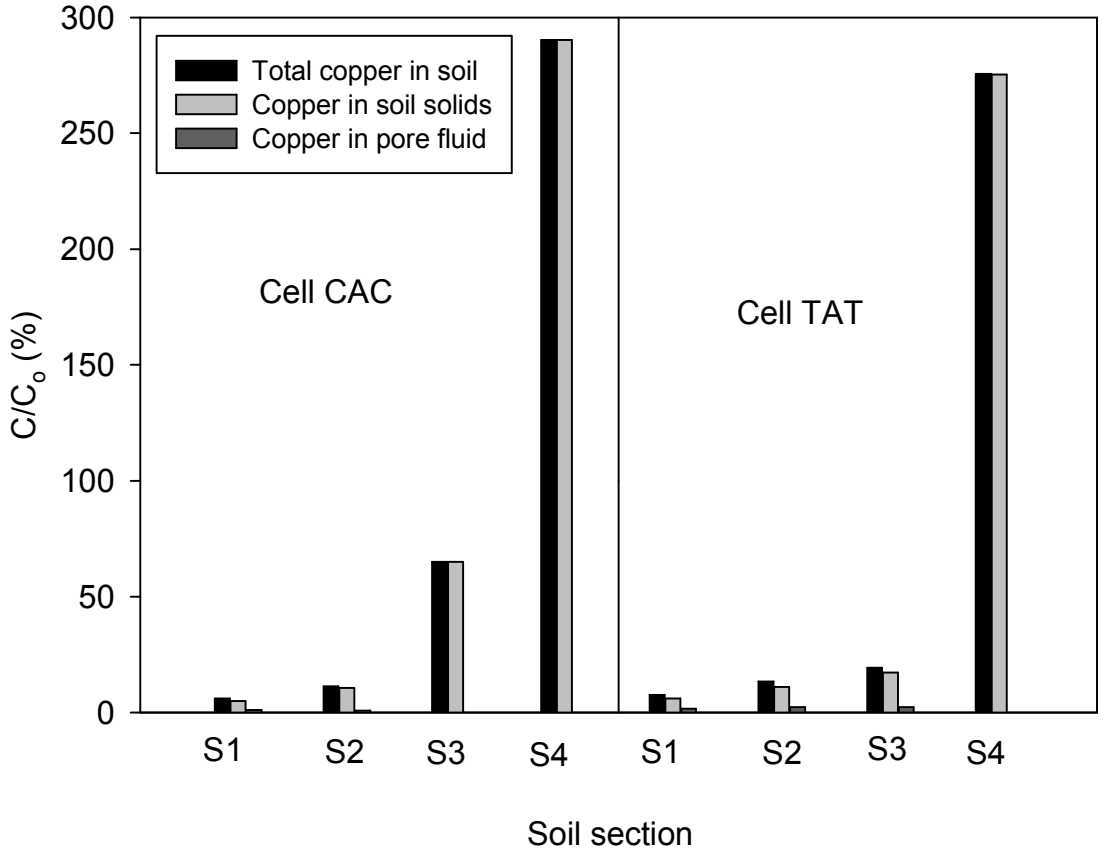

Figure 8.52 Copper concentration after tests of CAC and TAT with intermittent current with secondary anode at 15 mm from the cathode for power consumption 1250 Whr.

CHAPTER NINE

SUMMARY, CONCLUSIONS, AND RECOMMENDATIONS FOR FUTURE RESEARCH

9.0 SUMMARY AND CONCLUSIONS

A comprehensive study was carried out on electrokinetic remediation of homogeneous and heterogeneous soils contaminated with copper. The investigations were performed with one- and two-dimensional electrode configurations. An electrokinetic testing cell, 385×125×250 mm (length × width × height), and soil pore fluid squeezer were specifically designed and manufactured for this study. In addition, three solar cell panels provided the DC electric power for the tests. The study was conducted in three phases. Phase 1 investigated the effects of the power generated by solar panel in electrokinetic remediation. Phase 2 focused on soil heterogeneity and electrokinetic remediation. In phase 3 a novel technique to retard the movement of the base front was proposed, rigorously tested, compared, and optimized.

In phase 1 varying voltages generated by solar cell panels with one-dimensional electrode configuration were investigated and evaluated. The investigations demonstrated that the power generated by solar panel is sufficient for successful electrokinetic remediation. The results showed that the copper removal from the soil increased with the applied voltage. The optimum applied voltage was 41 V.

The optimum voltage from phase 1 was used in phase 2. The tests in phase 2 were conducted using three heterogeneous soils, including clay-sand mixture, clay-sand layers, and clay with sand pockets along with a homogeneous clay. One- and two-dimensional electrode configurations were used. The water content, pH, and copper removal were determined for the soils. The results showed that electrokinetic remediation was successful in dewatering and changing the pH profile of the heterogeneous soils in similar manner to the homogeneous soil. The highest copper removal near the anode in the heterogeneous soils reported in the tests with clay-sand mixture followed by clay with sand pockets, and the clay-sand layers.

Phase 3 was carried out to investigate the proposed novel Two Anodes Technique (TAT). The results were compared with results from tests with Conventional Anode Cathode (CAC) and Stepwise Moving Anode (SMA). The comparison showed that higher copper removal near the anode was achieved by TAT. The effect of current intermittence on TAT was investigated. The tests conducted with intermittent current showed higher copper removal than tests with continuous current. To optimize the position of the TAT secondary anode, tests were carried out with the anode at varying distances from the cathode. The results showed that, the tests with intermittent current and the secondary anode placed at a distance of 15 mm from the cathode is superior to other tests.

TAT has the potential to enhance the outcome of the electrokinetic remediation by targeting its main drawback, namely; the advancement of base front. The electrolysis reactions at the secondary anode generate an acid front which subsequently lowers the pH of the soil. The acid

front meets the base front at a distance closer to the cathode. The secondary electric circuit causes an increase in the voltage at the secondary anode position. The increase in voltage has two main advantages. First, it maintains a relatively low electric gradient between the primary and secondary anodes. This results in slower movement of the hydrogen ions between the primary and secondary anode. The hydrogen ions are recognized as the heavy metal dissolving agent. Therefore, the longer interaction time between the dissolving agent and the soil will result in higher copper desorption. Second, the high voltage at the secondary anode increases the voltage gradient and therefore exploited electromigration and electroosmosis between the secondary anode and the cathode. As a result, the dissolved copper was moved further towards the cathode via the combined effect of electroosmosis and electromigration. An important advantage of TAT is the high degree of control of the enhancement process by switching on and off the secondary electric circuit. That is because during the process the secondary electric circuit can be turned off. Table 9.1 provides a comparison between TAT, the addition of chemical compounds, Step Moving Anode, and polarity exchange.

9.1 RECOMMENDATIONS FOR FUTURE RESEARCH

The following are recommendation for future research:

- The maximum voltage generated by the solar cell panel in this study was 41 V. Further studies should investigate the effects of higher voltages.
- Further investigations on the effect of soil heterogeneity in electrokinetic remediation should be conducted with the aid of water within the anode compartment.

Consideration should also be given to the implementation of enhanced techniques such as TAT.

- Further studies to optimize the location of the secondary anode in TAT and the intensity of the electric current in secondary electric circuit in TAT. This should be followed by geometrical and transport modelling and analysis on electrokinetic remediation by TAT.
- Large scale study to evaluate the effect of scaling.
- Further investigation to compare the effect of acidity by electrolysis reactions and by the addition of chemical compounds in the soil fertility.

Table 9. 1 Comparison between different enhancement techniques

Method	Two Anodes Technique (TAT)	Step Moving Anode (SMA)	Polarity Exchange	Addition of Chemical Compounds
Capital Cost	Initial setup (anode and cathode) plus the secondary electrode	Initial setup(anode cathode) plus the anode steps cost(extra excavation, and labour charges), and cation-exchange membrane	Initial setup (anode cathode) plus pH monitoring cost(labour charges and instruments)	Initial setup (anode cathode) plus the cost of chemicals compounds, and pH monitoring
Field work during treatment		Need frequent field attendance to relocate the anodes	Need to monitor the pH, change the setup many times, required high quality control	Need to add chemical compounds, control the pH
Operational management	High degree of control: At any time the enhancement process (secondary electric circuit) can be stopped	High degree of control: The step length and duration are controllable	Less degree of control: Reverse electroosmosis and electromigration can occurs	Uncontrollable: After the addition of chemicals to the soil it is impossible to stop the reactions
Potential difficulties	-	Additional cost: Relocating the anode involved high risk of electrode damage each time the anode pull out or push into the soil. Generation of high electric current. Maintenance for the cation-exchange membrane	Adverse effect: The possibility of the heavy metals movement towards the anode	Adverse effect: Excessive acidification for the soil, formation of by-products which increase the contamination problem(chlorine gas), formation of strong complexes(EDTA), aggravate the contamination problem

REFERENCES

Acar, Y. B. and A. N. Alshawabkeh (1993). "Principles of Electrokinetic Remediation." Environmental Science & Technology 27(13): 2638-+.

Acar, Y. B. and A. N. Alshawabkeh (1996). "Electrokinetic remediation .1. Pilot-scale tests with lead-spiked kaolinite." Journal of Geotechnical Engineering-Asce 122(3): 173-185.

Acar, Y. B. and R. J. gale, Electrokinetic Decontamination of Soils and Slurries, US Patent No. 5, 137, 608, Commissioner of Patents and Trademarks, Washington, DC, August 11, 1992.

Acar, Y. B., R. J. Gale, A. N. Alshawabkeh, R. E. Marks, S. Puppala, M. Bricka and R. Parker (1995). "Electrokinetic Remediation - Basics and Technology Status." Journal of Hazardous Materials 40(2): 117-137.

Acar, Y. B., J. T. Hamed, A. N. Alshawabkeh and R. J. Gale (1994). "Removal of Cadmium (Ii) from Saturated Kaolinite by the Application of Electrical-Current." Geotechnique 44(2): 239-254

Alshawabkeh, A. N. and Y. B. Acar (1994). "Electrokinetic Remediation - Pilot-Scale Test-Results." Abstracts of Papers of the American Chemical Society 207: 114-ENVR.

Alshawabkeh, A. N., S. K. Puppala, Y. B. Acar, R. J. Gale and M. Bricka (1997). "Effect of solubility on enhanced electrokinetic extraction of metals." In Situ Remediation of the Geoenvironment(71): 532-544.

American Water Works, A. (1990). Water quality and treatment : a handbook of community water supplies / American Water Works Association.

American Society for Testing and Materials (ASTM) D422 - 63, 2007. Standard Test Method for Particle-Size Analysis of Soils. ASTM International, West Conshohocken, PA.

American Society for Testing and Materials (ASTM) D854 - 06, 2006. Standard Test Method for Specific Gravity of Soil by Water Pycnometer. ASTM International, West Conshohocken, PA.

American Society for Testing and Materials (ASTM) D4318 - 05, 2005. Standard Test Method for Liquid Limit, Plastic Limit, and Plasticity Index of Soils. ASTM International, West Conshohocken, PA.

American Society for Testing and Materials (ASTM) G 57 - 95a, 2001. Standard Test Method for Field Measurement of Soil Resistivity Using the Wenner Four-Electrode Method. ASTM International, West Conshohocken, PA.

Atanassova, I. and M. Okazaki (1997). "Adsorption-desorption characteristics of high levels of copper in soil clay fractions." Water Air and Soil Pollution 98(3-4): 213-228.

Buchireddy, P. R., R. M. Bricka and D. B. Gent (2009). "Electrokinetic remediation of wood preservative contaminated soil containing copper, chromium, and arsenic." Journal of Hazardous Materials 162(1): 490-497.

Casagrande, L. (1952) Electro-osmotic stabilization of soils. Journal of the Boston society of civil engineers Volume 39, January 1952, Pages 51-83.

Chen, X. J., Z. M. Shen, T. Yuan, S. S. Zheng, B. X. Ju and W. H. Wang (2006). "Enhancing electrokinetic remediation of cadmium-contaminated soils with stepwise moving anode method." Journal of Environmental Science and Health Part a-Toxic/Hazardous Substances & Environmental Engineering 41(11): 2517-2530.

Denisov, G., R. E. Hicks and R. F. Probstein (1996). "On the kinetics of charged contaminant removal from soils using electric fields." Journal of Colloid and Interface Science 178(1): 309-323.

Evangelou, V. P. (1998). Environmental soil and water chemistry : principles and applications / V.P. Evangelou.

Eykholt, G. R. and D. E. Daniel (1994). "Impact of System Chemistry on Electroosmosis in Contaminated Soil." Journal of Geotechnical Engineering-Asce 120(5): 797-815.

Ferguson, J. F. and P. Nelson (1986) Migration of inorganic contaminants in groundwater under the influence of an electric field in :Proceedings of the Workshop on Electrokinetic Treatment of Hazardous Wastes Remediation, University of Washington, Seattle, Washington, DC, USA.

Gary, D. H. and J. K. Mitchell (1967). Fundamental aspects of electro-osmosis in soils. Journal of the soil Mechanics and Foundations Division, ASCE, Vol. 93 No. SM6, pp. 209-235; Closure Discussion, (1969):Vol. 95, No. SM3, pp.875-879.

Gary, D. H. and H. W. Olsen (1986) Physics and chemistry of electrokinetic process, in: Proceedings of the Workshop on Electrokinetic Treatment of Hazardous Wastes Remediation, University of Washington, Seattle, Washington, DC, USA.

Giannis, A. and E. Gidarakos (2005). "Washing enhanced electrokinetic remediation for removal cadmium from real contaminated soil." Journal of Hazardous Materials 123(1-3): 165-175.

Gibbs, H. J. (1966). ''Research on electroreclamation of saline-alkali soils.'' Trans. Am. Soc. Agricultural Eng., 9(2), 164-169.

Hamed, J., Y. B. Acar and R. J. Gale (1991). "Pb(Ii) Removal from Kaolinite by Electrokinetics." Journal of Geotechnical Engineering-Asce 117(2): 241-271.

Hansen, H. K., L. M. Ottosen, B. K. Kliem and A. Villumsen (1997). "Electrodialytic remediation of soils polluted with Cu, Cr, Hg, Pb and Zn." Journal of Chemical Technology and Biotechnology 70(1): 67-73.

Hansen, H. K. and A. Rojo (2007). "Testing pulsed electric fields in electroremediation of copper mine tailings." Electrochimica Acta 52(10): 3399-3405.

Hicks, R. E. and S. Tondorf (1994). "Electrorestoration of Metal-Contaminated Soils." Environmental Science & Technology 28(12): 2203-2210.

Hunter, R. J. and M. James (1992). "Charge reversal of kaolinite by hydrolyzable metal ions; an electroacoustic study." Clays and Clay Minerals 40(6): 644-649.

James, R. O. and T. W. Healy (1972) Adsorption of Hydrolysable Metal ions at the Oxide-Water Interface II Charge reversals of SiO2 and TiO2 colloids by adsorbed Co(II), La(III), and Th(IV) as model systems. Colloid and Interface Science, Vol 40, No. 1. pp: 53-64.

Karim, M. A. and L. I. Khan (2001). "Removal of heavy metals from sandy soil using CEHIXM process." Journal of Hazardous Materials 81(1-2): 83-102.

Koryta, J. (1982). "Theory and Applications of Ion-Selective Electrodes .4a." Analytica Chimica Acta 139(Jul): 1-51.

Lageman, R., W. Pool and G. Seffinga (1989). "Electro-Reclamation - Theory and Practice." Chemistry & Industry(18): 585-590.

Lee, H. H. and J. W. Yang (2000). "A new method to control electrolytes pH by circulation system in electrokinetic soil remediation." Journal of Hazardous Materials 77(1-3): 227-240.

Li, R. S. and L. Y. Li (2000). "Enhancement of electrokinetic extraction from lead-spiked soils." Journal of Environmental Engineering-Asce 126(9): 849-857.

Li, Z. M., J. W. Yu and I. Neretnieks (1997). "Removal of Pb(II), Cd(II) and Cr(III) from sand by electromigration." Journal of Hazardous Materials 55(1-3): 295-304.

Li, Z. M., J. W. Yu and I. Neretnieks (1998). "Electroremediation: Removal of heavy metals from soils by using cation selective membrane." Environmental Science & Technology 32(3): 394-397.

Lockhart, N. C. (1983). "Electroosmotic Dewatering of Clays .1. Influence of Voltage." Colloids and Surfaces 6(3): 229-238.

Lockhart, N. C. and G. H. Hart (1988). "ELECTRO-OSMOTIC DEWATERING OF FINE SUSPENSIONS: THE EFFICACY OF CURRENT INTERRUPTIONS." Drying Technology 6(3): 415-423.

Mitchell, J. K., and K. Soga, (2005). Fundemental of soil behavior. 3rd Edition, John & Sons, New York.

Mohamedelhassan, E., I. Mohamed Ahmed and A. Mahmoud (2010). Electrokinetic remediation of soft clay soil contaminated with heavy metals, *63rd Canadian Geotechnical Conference & 6th Canadian Permafrost Conference 2010*, Canadian Geotechnical Society, Calgary, Canada, 1192-1196.

Mohamedelhassan, E. and J. Q. Shang (2001). "Effects of electrode materials and current intermittence in electro-osmosis." Ground Improvement 5(1): 3-11.

Oren, A. H. and A. Kaya (2006). "Factors affecting adsorption characteristics of Zn2+ on two natural zeolites." Journal of Hazardous Materials 131(1-3): 59-65.

Ottosen, L. M., I. V. Kristensen, A. J. Pedersen, H. K. Hansen, A. Villumsem and A. B. Ribeiro (2003). "Electrodialytic removal of heavy metals from different solid waste products." Separation Science and Technology 38(6): 1269-1289.

Page, M. M. and C. L. Page (2002). "Electroremediation of contaminated soils." Journal of Environmental Engineering-Asce 128(3): 208-219.

Pazos, M., M. A. Sanroman and C. Cameselle (2006). "Improvement in electrokinetic remediation of heavy metal spiked kaolin with the polarity exchange technique." Chemosphere 62(5): 817-822.

Phillips, I. R., D. T. Lamb, D. W. Hawker and E. D. Burton (2004). "Effects of pH and salinity on copper, lead, and zinc sorption rates in sediments from Moreton Bay, Australia." Bulletin of Environmental Contamination and Toxicology 73(6): 1041-1048.

Probstein, R. F. and R. E. Hicks (1993). "Removal of Contaminants from Soils by Electric-Fields." Science 260(5107): 498-503.

Probstein, R. F., M. Z. Sengun and T. C. Tseng (1994). "Bimodal Model of Concentrated Suspension Viscosity for Distributed Particle Sizes." Journal of Rheology 38(4): 811-829.

Puppala, S. K., A. N. Alshawabkeh, Y. B. Acar, R. J. Gale and M. Bricka (1997). "Enhanced electrokinetic remediation of high sorption capacity soil." Journal of Hazardous Materials 55(1-3): 203-220.

Puri, A. N., and B. Anand (1936). ''Reclamation of alkali soils by electrodialysis.'' Soil Sci., 42, 23-27.

Reddy, K. R. and C. Cameselle (2009). Electrochemical remediation technologies for polluted soils, sediments and groundwater / edited by Krishna R. Reddy, Claudio Cameselle.

Reddy, K. R. and U. S. Parupudi (1997). "Removal of chromium, nickel and cadmium from clays by in-situ electrokinetic remediation." Journal of Soil Contamination 6(4): 391-407.

Reddy, K. R., U. S. Parupudi, S. N. Devulapalli and C. Y. Xu (1997). "Effects of soil composition on the removal of chromium by electrokinetics." Journal of Hazardous Materials 55(1-3): 135-158.

Reed, B. E., M. T. Berg, J. C. Thompson and J. H. Hatfield (1995). "Chemical Conditioning of Electrode Reservoirs during Electrokinetic Soil Flushing of Pb-Contaminated Silt Loam." Journal of Environmental Engineering-Asce 121(11): 805-815.

Ribeiro, A. B. and J. T. Mexia (1997). "A dynamic model for the electrokinetic removal of copper from a polluted soil." Journal of Hazardous Materials 56(3): 257-271.

Sah, J. G. and J. Y. Che (1998). "Study of the electrokinetic process on Cd and Pb spiked soils." Journal of Hazardous Materials 58(1-3): 301-315.

Saichek, R. E. and K. R. Reddy (2003). "Effect of pH control at the anode for the electrokinetic removal of phenanthrene from kaolin soil." Chemosphere 51(4): 273-287.

Saichek, R. E. and K. R. Reddy (2005). "Surfactant-enhanced electrokinetic remediation of polycyclic aromatic hydrocarbons in heterogeneous subsurface environments." Journal of Environmental Engineering and Science 4(5): 327-339.

Segall, B. A. and C. J. Bruell (1992). "Electroosmotic contaminant-removal processes." Journal of Environmental Engineering 118(1): 84-100.

Segall, B. A., C. E. Obannon and J. A. Matthias (1980). "Elctroosmosis Chemistry and Water-Quality." Journal of the Geotechnical Engineering Division-Asce 106(10): 1148-1152.

Shang, J. Q. (1997). "Electrokinetic dewatering of clay slurries as engineered soil covers." Canadian Geotechnical Journal 34(1): 78-86.

Shang, J. Q., K. Y. Lo and K. M. Huang (1996). On factors influencing in electro-osmotic consolidation. Journal of Geotechnical Engineering, South East Asia Geotechnical Socity, Vol. 27, No.4, pp. 23-26.

Shapiro, A. P. and R. F. Probstein (1993). "Removal of Contaminants from Saturated Clay by Electroosmosis." Environmental Science & Technology 27(2): 283-291.

Sprute, R. H. and D. J. Kelsh (1974). "LABORATORY EXPERIMENTS IN ELECTROKINETIC DENSIFICATION OF MILL TAILINGS - 2. APPLICATION TO VARIOUS TYPES AND CLASSIFICATIONS OF TAILINGS." Report of Investigations - United States, Bureau of Mines(7900).

Sprute, R. H. and D. J. Kelsh (1976). "DEWATERING AND DENSIFICATION OF COAL WASTE BY DIRECT CURRENT - LABORATORY TESTS." Report of Investigations - United States, Bureau of Mines(8197).

Vadyunina, A. F. (1968). '' Meliorative effect of direct electric current on leaching solonchakous Solonetz.'' Proc., Trans of the 9th Int. Congress of Soil Science, Adelaide, Australia, 455-463.

Vane, L. M. and G. M. Zang (1997). "Effect of aqueous phase properties on clay particle zeta potential and electro-osmotic permeability: Implications for electro-kinetic soil remediation processes." Journal of Hazardous Materials 55(1-3): 1-22.

Virkutyte, J., M. Sillanpaa and P. Latostenmaa (2002). "Electrokinetic soil remediation - critical overview." Science of the Total Environment 289(1-3): 97-121.

West, L. J. and D. I. Stewart (1995). "Effect of zeta potential on soil electrokinesis." Geoenvironment 2000: Characterization, Containment, Remediation, and Performance in Environmental Geotechnics, Vols 1 and 2(46): 1535-1549.

Wong, J. S. H., R. E. Hicks and R. F. Probstein (1997). "EDTA-enhanced electroremediation of metal-contaminated soils." Journal of Hazardous Materials 55(1-3): 61-79.

Yankovskii A. A., Y. Y. Khrustalev, Y. Yu and N. A. Zavialova (1989) ''Experimental investigations of electro-osmosis in peat at impulse electric field.'' Torphovaya Promyshlenost (Peat Industry), 7, 10-12.

Yang, G. C. C. and S. L. Lin (1998). "Removal of lead from a silt loam soil by electrokinetic remediation." Journal of Hazardous Materials 58(1-3): 285-299.

Yeung, A. T. (1994). "Electrokinetic flow processes in porous media and their applications." Advances in Porous Media 2: 309-395.

Yuan, S. H., Z. M. Xi, Y. Jiang, J. Z. Wan, C. Wu, Z. H. Zheng and X. H. Lu (2007). "Desorption of copper and cadmium from soils enhanced by organic acids." Chemosphere 68(7): 1289-1297.

Yuan, S. H., Z. H. Zheng, J. Chen and X. H. Lu (2009). "Use of solar cell in electrokinetic remediation of cadmium-contaminated soil." Journal of Hazardous Materials 162(2-3): 1583-1587.

APPENDIX A

Soil section	Cell A 13.5 V		Cell B 27 V		Cell C 41 V	
	Cu in soil ppm	Cu in pore fluid ppm	Cu in soil ppm	Cu in pore fluid ppm	Cu in soil ppm	Cu in pore fluid ppm
S1	5.29	82.92	2.06	33.95	1.035	69.80
S2	5.6	6.53	4.03	3.34	2.32	13.98
S3	5.91	0.24	9.58	0.56	6.32	0.32
S4	10.15	0.11	11.51	0.15	17.5	0.46
S5	6.05	0.39	6.24	0.13	7.81	0.07

APPENDIX B

One-dimensional electrode configuration

Soil section	Clay-sand mixture		Clay-sand layers		Clay with sand pockets		Homogeneous Clay	
	Cu in soil (ppm)	Cu in pore fluid (ppm)	Cu in soil (ppm)	Cu in pore fluid (ppm)	Cu in soil (ppm)	Cu in pore fluid (ppm)	Cu in soil (ppm)	Cu in pore fluid(ppm)
S1	0.94	19.88	3.18	15.46	2.94	37.2	1.03	69.80
S2	2.09	0.45	5.02	0.28	5.92	14.04	2.32	13.98
S3	15.15	3.08	5.78	1.82	7.69	0.75	6.32	0.32
S4	7.8	0.15	7.67	0.06	9.91	0.14	17.5	0.46
S5	7.59	0.08	10.98	0.04	7.74	0.04	7.81	0.07

APPENDIX C

Two-dimensional electrode configuration

Soil section	Clay-sand mixture		Clay-sand layers		Clay with sand pockets		Homogeneous Clay	
	Cu in soil (ppm)	Cu in pore fluid (ppm)	Cu in soil (ppm)	Cu in pore fluid (ppm)	Cu in soil (ppm)	Cu in pore fluid (ppm)	Cu in soil (ppm)	Cu in pore fluid (ppm)
S1	2.52	36.48	5.13	67.43	3.97	36.02	1.33	43.72
S2	2.04	66.32	5.41	0.48	4.5	0.34	1.0	39.64
S3	6.77	0.39	6.27	0.24	5.62	0.18	3.93	5.88
S4	12.45	0.21	18.42	0.11	11.48	0.17	16.84	1.17
S5	9.38	0.21	8.59	0.17	7.85	0.13	9.22	0.17

APPENDIX D

Soil section	SMA		CAC		TAT	
	Cu in soil (ppm)	Cu in pore fluid (ppm)	Cu in soil (ppm)	Cu in pore fluid (ppm)	Cu in soil (ppm)	Cu in pore fluid (ppm)
S1	5.037	0.4587	2.799	47.1	1.532	1.532
S2	3.298	199.9	3.154	78	2.573	82.92
S3	6.416	185.8	12.03	71.11	8.514	140.7
S4	12.05	156.5	10.2	15.89	17.25	247.2

APPENDIX E

TAT with continuous current and secondary anode at 50 mm from cathode

Soil section	TAT 500 Whr		TAT 750 Whr		TAT 1000 Whr		TAT 1250 Whr	
	Cu in soil (ppm)	Cu in pore fluid (ppm)	Cu in soil (ppm)	Cu in pore fluid (ppm)	Cu in soil (ppm)	Cu in pore fluid (ppm)	Cu in soil (ppm)	Cu in pore fluid (ppm)
S1	1.532	1.532	0.7665	47.88	0.5816	27.87	0.4432	20.37
S2	2.573	82.92	1.418	83.44	1.132	41.22	0.9467	22.51
S3	8.514	140.7	12.0	197.1	10.6	54.58	11.17	8.03
S4	17.25	247.2	14.67	25.63	13.5	0.6809	12.57	0.4773

APPENDIX F

TAT with intermittent current and secondary anode at 50 mm from cathode

	TAT 500 Whr		TAT 750 Whr		TAT 1000 Whr		TAT 1250 Whr	
	Cu in soil (ppm)	Cu in pore fluid (ppm)	Cu in soil (ppm)	Cu in pore fluid (ppm)	Cu in soil (ppm)	Cu in pore fluid (ppm)	Cu in soil (ppm)	Cu in pore fluid (ppm)
S1	1.286	50.01	0.9754	50.01	0.8344	27.87	0.6994	26.3
S2	3.3	150.3	2.174	150.3	1.393	50.25	0.747	22.67
S3	15.96	25.18	4.182	25.18	2.849	80.34	2.41	17.09
S4	9.763	2.956	17.26	2.956	17.5	0.5921	17.19	3.262

APPENDIX G

CAC with continuous current and secondary anode at 50 mm from cathode

	CAC 500 Whr		CAC 750 Whr		CAC 1000 Whr		CAC 1250 Whr	
	Cu in soil (ppm)	Cu in pore fluid (ppm)	Cu in soil (ppm)	Cu in pore fluid (ppm)	Cu in soil (ppm)	Cu in pore fluid (ppm)	Cu in soil (ppm)	Cu in pore fluid (ppm)
S1	2.799	47.1	0.9892	69.32	0.7889	34.4	0.4785	11.44
S2	3.154	78	1.772	41.65	0.9353	23.77	0.8941	10.09
S3	12.03	71.11	12.67	1.569	10.73	5.895	5.159	0.2828
S4	10.2	15.89	15.78	0.2197	18.4	0.4877	23.03	0.1685

APPENDIX H

TAT with intermittent current and secondary anode at 15 mm from cathode

	CAC 500 Whr		CAC 750 Whr		CAC 1000 Whr		CAC 1250 Whr	
	Cu in soil (ppm)	Cu in pore fluid (ppm)	Cu in soil (ppm)	Cu in pore fluid (ppm)	Cu in soil (ppm)	Cu in pore fluid (ppm)	Cu in soil (ppm)	Cu in pore fluid (ppm)
S1	1.745	89.31	0.9035	36.91	0.6945	40.05	0.6036	16.48
S2	3.043	236.4	1.789	88.01	1.165	51.4	1.058	34.47
S3	15.37	89.63	4.973	113.1	3.366	13.06	1.537	35.35
S4	7.748	13.1	20.02	15.5	21.095	0.6764	21.87	4.054